PROTEOMICS IN COPD

by

HELEN MARIE STONE

A thesis submitted to the University of Birmingham for the degree of DOCTOR OF MEDICINE

School of Clinical and Experimental Medicine

College of Medical and Dental Sciences

The University of Birmingham

May 2016

ABSTRACT

In alpha-1-antitrypsin deficiency (A1ATD) there is excess neutrophil elastase activity, resulting in proteolytic destruction of the lung parenchyma. I hypothesised that the peptide fragments of proteins present in the lung might be detectable in plasma by mass spectrometry and that they might be useful biomarkers of disease activity and treatment efficacy.

Calcium ionophore, neutrophil elastase and proteinase 3 were added to plasma from patients with A1ATD to create an *in vitro* model of the destructive processes. MALDI-based peptide profiling of plasma from patients pre and post treatment with intravenous A1AT was undertaken and MS/MS performed to identify differences. Plasma was also depleted of abundant plasma proteins, labelled with isobaric tags and analysed by shotgun proteomics.

The readily detectible components of the plasma proteome remained unchanged with intravenous A1AT. Addition of ionophore, elastase and proteinase 3 to patient blood generated predominantly fragments of fibrinogen. In patients treated with intravenous A1AT, fragments of A1AT increased significantly with treatment: – 2 of these were fragments of a short C-terminal segment of the A1AT protein and were also present in healthy subjects. The shotgun experiments did not identify any robust biomarkers and illustrate the challenging nature of plasma proteomics.

DEDICATION

To my family, friends and colleagues

ACKNOWLEDGEMENTS AND STATEMENT OF CONTRIBUTORSHIP

I would firstly like to thank Professor Stockley and all of the team at the ADAPT programme at the Queen Elizabeth Hospital in Birmingham, especially Becky and Anita, for giving me the opportunity to undertake the research presented in this thesis. I would also like to thank my 2 supervisors – Professor Stockley and Dr Douglas Ward for all of their help and guidance - coming up with the title of my thesis, ideas for possible experiments, proof reading my thesis, and to Doug particularly for teaching me how to work in a laboratory, and how to operate a mass spectrometer.

Finally I would like to thank the patients whose samples have been analysed in the work in this thesis. The work presented here and my time as a Clinical Research Fellow was funded by an unrestricted educational grant from Grifols (previously Talecris Biotherapeutic).

I was involved in conducting the ECLIPSE A1ATD study, including the drawing up and administration of the intravenous A1AT, and taking the clinical samples. I consented patients and control subjects, as well as taking samples, for the enzyme work. I performed all of the laboratory work and statistical analyses presented in this thesis, with statistical advice on the complex datasets generated from Dr Peter Nightingale.

TABLE OF CONTENTS

LIST OF FIGURES

Chapter 5

Chapter 6

LIST OF TABLES

LIST OF ABBREVIATIONS

A1AT	Alpha 1 antitrypsin
A1ATD	Alpha 1 antitrypsin deficiency
ABC	Ammonium bicarbonate
ACN	Acetonitrile
ADAPT	Antitrypsin Deficiency Assessment and Programme for Treatment
ANOVA	Analysis of variance
BALF	Bronchoalveolar lavage fluid
BCA	Bicinochoninic Acid (protein assay)
BODE Index	Multidimensional index used in assessing the impact of COPD, using BMI, FEV_1, dyspnoea score and 6 minute walk distance
BSA	Bovine serum albumin
CC-16	Club cell protein 16
CHAPS	3-[(3-Cholamidopropyl)dimethylammonio]-1 propanesulfonate
CHCA	α-cyano-4-hydroxy-cinnaminic acid
CID	Collision induced dissociation
COPD	Chronic obstructive pulmonary disease
CRP	C-reactive protein
CT PET	Computed tomography positron emission tomography
CT	Computed tomography
$CuS0_4$	Copper sulphate
CV	Coefficient of variance
Da	Daltons
DMSO	Dimethyl sulfoxide
EBC	Exhaled breath condensate
EGFR	Epidermal growth factor
ELF	Epithelial lining fluid
ELISA	Enzyme-linked immunosorbent assay
ESI	Electrospray ionisation
FASP Digest	Filter aided sample preparation digest

FDA	Food and drug administration
FDR	False discovery rate
FEV_1 % predicted	Forced expiratory volume in 1 second expressed as a percentage of that expected for age, sex and height
FEV_1	Forced expiratory volume in 1 second
HDL	High density lipoprotein
HPLC	High performance liquid chromatography
IgA	Immunoglobulin A
IgG	Immunoglobulin G
IgM	Immunoglobulin M
IL6	Interleukin 6
IL8	Interleukin 8
IMAC	Immobilised Metal Affinity Chip
IPF	Idiopathic pulmonary fibrosis
iTRAQ	Isobaric tag for relative and absolute quantification
KCO	Gas transfer corrected for alveolar volume
LC	Liquid chromatography
LC-MALDI	Liquid chromatography matrix enhanced laser desorption/ionisation
LDL	Low density lipoprotein
LTB4	Leukotriene B4
m/z	Mass to charge ratio
MALDI	Matrix enhanced laser desorption/ionisation
MMP	Matrix metalloproteinases
MOWSE score	Molecular weight search score
MPO	Myeloperoxidase
MS	Mass spectrum
MS/MS	Tandem mass spectrometry
MZ	Heterozygote for alpha-1-antitrypsin deficiency
NE	Neutrophil elastase
NSCLC	Non-small cell lung cancer
PBS	Phosphate buffered saline
PDE4	Phosphodiesterase type 4
PEDF	Pigment epithelial derived factor
PET CT	Positron emission tomography - computed tomography

PIGR	Polymeric immunoglobulin receptor
PiZZ	Homozygous for protease inhibitor Z
PR3	Proteinase 3
SAA	Serum amyloid alpha
SELDI	Surface enhanced laser desorption/ionisation
SEM	Standard error of mean
SILAC	Stable isotope labelling with amino acids in cell culture
SPA	Sinapinic acid
SP-A	Surfactant protein A
SPAAT	Short peptide of alpha-1 antitrypsin
SP-D	Surfactant protein D
SPE	Solid phase extraction
sRAGE	Soluble receptor for advanced glycation end-products
TEAB	Triethylammonium bicarbonate
TFA	Trifluoroacetic acid
TIMP	Tissue inhibitor of metalloproteinase
TKI	Tyrosine kinase inhibitor
TLC	Total lung capacity
TLCO	Diffusion capacity for carbon monoxide
TMT	Tandem mass tags
TNF α	Tumour necrosis factor alpha
VEGF	Vascular endothelial growth factor
WCX	Weak cation exchange

CHAPTER 1 INTRODUCTION

1.1 COPD Definition and Epidemiology

Chronic obstructive pulmonary disease (COPD) is a multi-system inflammatory condition, characterised by airflow obstruction which is not fully reversible, according to the ATS/ERS joint COPD guideline in 2004 (Celli et al., 2004). It is a common condition, diagnosed in around 1 million people in the UK alone, although this may be a gross underestimation of the actual number of people with this disease, which may be closer to 3 million (National Clinical Guideline Centre 2010). It is not only a health issue in the UK; globally the prevalence of COPD is increasing, particularly in less developed countries, and it has become the third leading cause of death worldwide (Lozano et al., 2012). Globally, it is estimated that there are over 200 million people who have COPD (Lopez et al., 2006). In the UK, around 25,000 people per year die from COPD, and the estimated health care costs exceed £800 million per year (National Clinical Guideline Centre 2010). There is a need for newer therapies for this common, progressive and debilitating condition, yet there have been few new classes of therapies introduced into routine patient care in recent years, and no specific therapies have shown a reduction in mortality, other than long term oxygen therapy (Stuart-Harris et al., 1981 and the NOTT Trial Group, 1980) and smoking cessation (Godtfredson et al., 2008).

The definition of COPD is based on airflow obstruction, diagnosed with post bronchodilator lung function parameters, (according to the ATS/ERS guidelines) therefore patients have to undergo spirometry in order to have a correct diagnosis. In the past, COPD was regarded as a condition which affected only the lungs. It is now

widely regarded as a multi-system inflammatory condition with extra pulmonary manifestations. Patients with COPD have an increased risk of ischaemic heart disease (Sin et al, 2003), depression (Wagena et al, 2001), lung cancer (Noruma et al, 1991) and osteoporosis (Agusti 2005). In addition, COPD is a term which encompasses several phenotypes, with similar spirometry, which were traditionally separated into the 2 phenotypes of chronic bronchitis and emphysema. More phenotypes are now recognised, and can differ on the parameter used in the definition, whether it is based on physiology, radiology or symptoms including sputum production and exacerbations. It is possible that future treatments for COPD may vary according to these different phenotypes, as was the case with roflumilast, a phosphodiesterase type 4 (PDE4) inhibitor, which is effective in patients with a chronic bronchitic phenotype, who experience recurrent exacerbations despite maximal other therapies (Rennard et al., 2011).

1.2 Causes of COPD

The main cause of COPD globally is tobacco smoking. However, only around 20% of people who smoke go on to develop COPD. (Doll et al., 1991 and Tashkin et al., 1984) Clearly the relationship between smoking and COPD is far more complex than simple cause and effect, and it has been hypothesised that there is a genetic link between smoking, the development of COPD and the environment (Sandford et al., Silverman 2002). Familial clustering of cases adds further evidence to support the genetic hypothesis link (Marciniak et al., 2008), and first degree relatives of COPD patients have a higher incidence of airflow obstruction when compared with the general population. (Larson et al., 1970) A genome wide association study by Pillai and colleagues in 2009 identified 2 single nucleotide polymorphisms (SNPs) – of the α-

nicotinic acetylcholine receptor (CHRNA 3/5) which were significantly associated with COPD, and a further SNP of the hedgehog interacting protein on chromosome 4 which was associated, but did not reach genome-wide significance, with the development of COPD (Pillai et al., 2009).

Amongst the other recognised causes of COPD are occupational exposures, air pollution, both outdoor and indoor (for example burning of biomass fuels in poorly ventilated housing in less developed countries (Bruce et al., 2000)), passive smoking and the genetic condition of alpha-1-antitrypsin deficiency (A1ATD).

1.3 Alpha-1-Antitrypsin

Alpha-1-antitrypsin (A1AT) is one of the most abundant plasma proteins. It is a member of the serine proteinase inhibitor family, which also includes C1 esterase inhibitor, α-1 antichymotrypsin and antithrombin III. It is 52kDa glycoprotein, consisting of 394 amino acids and is produced predominantly in the liver by the hepatocytes, although it is made in much smaller amounts by monocytes and lung airway epithelial cells (Lomas 2000). It has a plasma half-life of 4 to 5 days (Fregonese et al, 2007). Its function is to inhibit the actions of a number of serine proteases, but its main target is an enzyme released from neutrophils – neutrophil elastase (NE), and to a lesser extent the enzymes cathepsin G and proteinase 3 (PR3). In common with other members of the serpin family, A1AT is made of 3 β sheets and 9 α helices. The most important part of the A1AT molecule is the reactive site; this is a mobile loop, which presents a 'pseudosubstrate' for neutrophil elastase (although this could be one of the other proteases such as cathepsin G or PR3). Once the elastase has covalently bound, it becomes inactivated and this complex of A1AT and protease is taken up from the

plasma by the liver and cleared (Mast et al., 1991).

A1AT binds to NE in an irreversible manner, at a molar ratio of 1:1, and thus once it has bound, complexes of A1AT/NE can be found in the bloodstream prior to their removal by the liver. Free NE is not usually detectable in the bloodstream. NE is responsible for proteolytic damage to the lung alveoli, which may result in the development of emphysema, a finding which also has been found in animal models whereby the instillation of NE results in changes typical of emphysema (Fukada et al., 1989).

A1AT is an acute phase protein, which means that its production, and subsequent release into the bloodstream, is increased in response to stimuli such as IL6 during intercurrent infection or inflammation. This is a protective mechanism; neutrophils travel to sites of infection and inflammation, and increasing the production of A1AT can help to enhance the inhibition of destructive enzymes released from the neutrophils during degranulation once their physiological role is complete. The lung is the main site requiring the presence of A1AT, which enters the airways by passive diffusion. The normal plasma level of A1AT in a healthy adult is 1.1-1.9g/L (20-48μM), but may rise up to four fold in the bloodstream in response to systemic infection/inflammation (Grimstein et al., 2011 and Brantly, 2002).

In addition to its inhibitory effects on the proteases outlined above, A1AT has a number of other anti-inflammatory and immunomodulatory effects such as regulation of the expression of several cytokines, which include TNF α, IL6 and IL8 IL 10 and interleukin 1beta (Janciauskiene et al., 2007).

1.3.1 Alpha-1-Antitrypsin Deficiency

Alpha-1-antitrypsin deficiency (A1ATD) is one of the most common genetic deficiencies in the UK. Its clinical manifestations include emphysema, cirrhosis of the liver and panniculitis. In 1963 the association of a deficiency of A1AT and emphysema was first recognised by Laurell and Erikson, who noticed the lack of a serum protein in association with severe emphysema in patients in their 40s, and much has been learnt about this condition since this time.

1.3.2 Genetics and Epidemiology of A1ATD

A1ATD is an autosomal co-dominant condition; each of the 2 copies of the gene is responsible for production of 50% of the body's production of A1AT, and does so independently of the other (Luisetti et al., 2004). The gene is located on chromosome 14, (14.q32.1) (Luisetti et al., 2004) and is part of the Serpin supergene cluster (Luisetti et al., 2004). There are over 100 mutations of the A1AT gene which have been identified to date (Fregonese at al., 2007). The most common of these are the Z and S mutations. The nomenclature of these deficiencies was originally classified by a system which named the proteins by their mobility during starch gel electrophoresis. Thus, the normal protein is denoted by the letter M, as the proteins had medium migratory velocity, S for slow, Z for very slow and F for fast moving (Luisetti et al., 2004). Thus a normal person is denoted as PiMM (protease inhibitor MM), and the most deficient patients PiZZ, although there are a small number of null genes, which produce no A1AT at all (Luisetti et al., 2004).

The Z protein arises as a result of a change in the amino acid sequence from glutamic

acid to lysine, at position 342, which causes polymerisation of the protein. Around 3-4% of northern Europeans carry this genetic mutation (Luisetti et al., 2004). The structure of the Z molecule is altered, allowing the reactive loop of one molecule of A1AT to lock into the β sheet of another, leading to lengthening chains of the molecules, which accumulate in the rough endoplasmic reticulum of the liver (Lomas et al., 2004). Large polymers cannot be released from the liver and thus only around 10 – 15% of the A1AT made by each Z allele enters the systemic circulation. This (in ZZ individuals) results in a plasma level of about 10 – 15% of normal. Besides patients who have null genes, the PiZZ patients are the individuals who are most at risk of developing disease, both of the lung and liver, as a result of their deficiency. The polymerised chains of proteins accumulate in the liver and may, over time, result in cirrhosis of the liver.

The S protein is due to a different point mutation; at position 264 valine is substituted for glutamic acid, which results in some mis-folding of the A1AT protein. Patients who are homozygous with the S gene have A1AT levels of around 60% of normal. The S mutation is found in around 6% of people of northern European descent and originated in the Mediterranean (Luisetti et al., 2004). This milder form of deficiency is not thought to predispose to emphysema, even in S homozygotes (Mulgrew et al., 2007).

1.3.3 Clinical Manifestations of A1ATD

The clinical manifestations of A1ATD are most strongly associated with the ZZ genotype, and include primarily lung disease, liver disease and rarer associations such as the skin condition panniculitis and systemic vasculitis. The lung manifestations may include emphysema, (which is predominantly basal), a degree of bronchodilator

reversibility, chronic bronchitis and bronchiectasis. Thus the condition is heterogeneous, as seen in usual COPD, and there may be asymptomatic individuals who are diagnosed only as a result of family screening, at one end of the spectrum, with patients with end-stage lung disease (some of whom will progress and may require lung transplantation) at the other. Active smoking is the most significant risk factor for the development of emphysema and accelerates the decline in lung function (Needham et al., 2004). Recurrent exacerbations have also been shown to result in more rapid decline, due to the increased levels of inflammation at these times, but air pollution can also play a role (Wood et al., 2009).

A proportion of PiZZ A1ATD patients develop chronic liver disease; the incidence of cirrhosis is higher in men than women and the risk of developing cirrhosis increases with age (Needham et al., 2004). Panniculitis is another, rarer manifestation, in which patients develop necrotic and suppurating lesions of the skin, which can be present almost anywhere in the body, but occur particularly over the anterior tibial region, in the gluteal region or on the arms. These can be treated with dapsone, and in some instances intravenous replacement of A1AT can produce rapid resolution of necrotising lesions (O'Riordan et al., 1997).

1.3.4 Treatment of A1ATD

Patients with A1ATD who develop COPD are treated in the same way as patients with usual (non A1ATD) COPD, with inhaled therapies, smoking cessation strategies, pulmonary rehabilitation, oxygen therapy where appropriate and adequate treatment of exacerbations and co-morbidities. Furthermore, for patients with end stage disease who are deemed suitable, lung transplantation may be considered, especially as patients with

A1ATD at this end of the spectrum are usually younger than those with non A1ATD COPD. In addition to this conventional treatment, in some countries, such as the US (but not in others such as the UK), intravenous augmentation therapy is licensed for patients with A1ATD.

1.3.5 Role of Intravenous Augmentation Therapy

A1AT can be purified from human plasma from blood donors and given intravenously to augment the low levels in deficient patients. This has been available in the US since the early 1980s when Gadek et al undertook a study to determine the feasibility of replacing A1AT, and were able to demonstrate significantly elevated levels of A1AT in epithelial lining fluid of the lungs followed intravenous replacement (Gadek et al., 1981).

Wewers et al in 1987 continued the work which showed that using a regimen of 60mg/kg bolus weekly is able to produce a trough level in the airways within the 'safe' level 6 days post infusion. This regimen is the currently licensed by the FDA, and thus accepted and utilised in countries where treatment with augmentation therapy is available (Wewers et al., 1987). Clearly, the need for a weekly infusion has a patient acceptance issue as well as significant cost and time implications, therefore Hubbard and co-workers have investigated the use of 2 weekly and monthly infusions, of much higher doses of A1AT, of up to 250mg/kg per month, and have been able to demonstrate that plasma levels greater than 11μM can be generated for most of the time. This is important as the threshold of 11μM has been termed the 'protective threshold' below which the lungs are vulnerable to damage from proteolytic enzymes normally controlled by A1AT (Hubbard et al., 1988). However, these alternative regimens are

not approved by the FDA.

Dirksen et al (1999) performed a randomised study of 55 patients with the PiZZ genotype of A1ATD. Calculations from this data, using $FEV1_1$ decline as the primary study endpoint, indicated that 550 patients would need to be included in each arm of an interventional augmentation trial to see a significant reduction in the rate of decline in FEV_1 if this was the end-point measured. The study also showed that CT densitometry measurements were more sensitive than lung function parameters, and thus offered the use of an alternative endpoint in monitoring emphysema progression in patients with A1ATD and any benefit from treatment (Dirksen et al., 1999).

Augmentation therapy at 60mg/kg over a short term study by Stockley et al demonstrated a rise in serum and sputum A1AT levels, a reduction in sputum elastase and leukotriene B4 (LTB4) activity, both of which were significant, and a non-significant reduction in IL8 and myeloperoxidase (MPO) (Stockley et al., 2002). This demonstrated that intravenous replacement therapy can reduce bronchial inflammation in A1ATD and hence potentially halt the destructive progression of the disease.

The EXACTLE trial conducted between 2003 and 2005 was a randomised controlled trial of 77 patients receiving augmentation therapy or placebo for a follow up period of 2 to 2.5 years. Its primary endpoint was a change in lung densitometry measured on CT scans. The study confirmed that CT densitometry was a more sensitive measure of emphysema progression than either health status or lung physiology, and an overall trend towards a reduction in the rate of progression of emphysema with augmentation therapy was found (Dirksen et al., 2009). Combining the raw data from this study and

from the previous Dutch-Danish Study (Dirksen et al., 1999) provided robust evidence that the progression of emphysema as measured by CT density, can be reduced by augmentation therapy at the dose of 60mk/kg weekly (Stockley et al., 2010).

However, there still remains controversy regarding the efficacy of augmentation therapy, as a recent Cochrane review concluded that there was not sufficient evidence to support its use (Gotzsche et al, 2010). This review ignored the wealth of data from observational studies, which have shown a reduction in the number of exacerbations whilst on treatment and differences in the rate of decline in FEV_1 (Stockley et al., 2010).

In addition to the cost implication of augmentation therapy, there is the theoretical risk of transmission of infection. The protein given to patients is purified from human donor blood, and theoretically, although rigorously screened, still carries the potential risk of infection. However, to date, no cases of transmission of hepatitis A, B or C, or HIV have been reported as a result of augmentation therapy (Tirado-Conde et al., 2008). Overall, the administration of intravenous therapy has been shown to be safe and well tolerated by patients. The infusions of purified A1AT contain 70-80% A1AT protein, whilst the remainder is made of common plasma proteins, including $alpha_2$-plasmin inhibitor, $alpha_1$-antichymotrypsin, C_1-esterase inhibitor, haptoglobin, antithrombin III, $alpha_1$-lipoprotein, albumin and IgA. The A1AT protein once purified and infused remains around 75% active (Wewers et al., 1987).

1.3.6 Role of Nebulised Replacement Therapy

An alternative approach to intravenous infusions of A1AT is the use of nebulised A1AT. Patients with chronic lung diseases are used to receiving inhaled treatment, and

theoretically, by nebulising the A1AT, the protein is delivered to the site from which its absence is deemed most critical. In order for this to be beneficial, the protein which is nebulised needs to be able to diffuse into the lung interstitium, which is the opposite direction of movement than normal. Work by Hubbard in 1989 showed that intact A1AT of the normal M variant could be found in the plasma and hence the epithelial lining fluid of patients with the PiZZ genotype of A1ATD post-delivery via the aerosolised route (Hubbard et al., 1989). However, direct sampling of levels in A1AT in the lung interstitium is much more difficult without undertaking invasive procedures, which is prohibitive in large numbers of patients. In addition, using the nebulised route removes the need for intravenous access with its' inherent complications, and allows patients to administer their own treatment. Currently, clinical trials are ongoing to investigate any benefit of nebulised therapy in this patient cohort.

1.3.7 Liver Transplantation

A proportion of patients with A1ATD develop clinical liver disease instead of or in addition to lung disease. In some patients, this progresses into end stage liver disease and hepatic failure. In this instance, it is possible for patients to undergo liver transplantation if organs are available and the patient does not have other co-morbidities which may make them unsuitable. This results in the normalisation of the circulating plasma A1AT level, as nearly always the donor has the MM genotype and hence the transplanted liver will produce and release normal A1AT. This is clearly only an option available to patients with severe end stage liver disease, and not a treatment that could be offered to all patients with A1ATD, due to the morbidity and mortality of the surgery and post-operative immunosuppression, with its inherent risks, but also due to a lack of available donor livers which are needed for other conditions besides A1ATD.

1.4 Clinical Trial End-Points in COPD

Lung function parameters, especially the forced expiratory volume in 1 second (FEV_1), have formed the basis of outcome of clinical trials of therapy in patients with COPD. The FEV_1 is easy to measure and record but is effort dependant and hence can be a variable measurement, even for patients in the stable state. The measurement also shows variable progression with time and in some cases FEV_1 may remain stable; (Agusti et al., 2013 on behalf of the ECLIPSE investigators) this means that clinical trials require large numbers of patients, with lengthy follow up periods, in order to detect a significant change in the decline of this measurement whereas short term improvement with bronchodilator therapy is easier to detect.

Furthermore, the measurement of an abnormal FEV_1 alone does not make a diagnosis of COPD, is not specific to COPD, and does not always provide a measurable change with treatment – for example treatment with long term oxygen therapy (LTOT) which has been proven to improve survival (Stuart-Harris et al., 1981 and the NOTT Trial Group, 1980) has no effect on the FEV_1 decline. In addition, FEV_1 alone does not provide comprehensive information on the COPD phenotype, and composite measures are being used as alternatives to the FEV_1, such as the BODE index which is described below (Celli et al., 2004).

There is, therefore, a need for other markers for both usual COPD and that caused by A1ATD, and its' phenotypes to predict response to treatment, particularly in phase II and proof of concept studies, in order to reduce the numbers of patients needed to be recruited and the duration of follow up.

1.5 Biomarkers Studied to Date in Usual COPD and A1ATD COPD

A number of different markers have been studied to date as potential biomarkers in COPD. A biomarker should fulfil one or more of a number of key roles, which include:-

- Being central to the disease process (disease specific)
- Varying with progression of disease
- Predicting progression
- Stratifying individual patient risk
- Being sufficiently sensitive to detect changes resulting from effective interventions or treatments (Stockley, 2007)

Any measurable parameter including physiological measures such as the FEV_1 may fulfil some or all of these criteria; however the following review and the remainder of this thesis will be focused on proteins. Proteins carry out many essential physiological functions, including those within cell structural integrity, through actions as enzymes, hormones, transport and storage molecules, and antibodies. Therefore, many potential candidate markers studied to date in both usual COPD and COPD secondary to A1ATD have been proteins.

A literature review was performed in 2010, before the start of the work presented in this thesis, using the Embase, Pubmed and Web of Science databases and using the search terms ‘alpha 1 antitrypsin deficiency, biomarkers and augmentation therapy’. This search did not identify any relevant published work. The search was repeated using the same search terms in 2017 and identified a number of recent studies of desmosine and isodesmosine in A1ATD (although there is a wealth of data describing its role in usual COPD eg Rabinovich et al., on behalf of the ECLIPSE investigators, 2016), data

on exhaled breath condensate analysed using mass spectrometry which is discussed in more detail in section 1.7.5 (Fumigalli et al., 2008 and 2012) and 2 studies on a fibrinogen fragment termed Aαval 360, that met these criteria.

The first study measured desmosine and isodesmosine in the serum of patients receiving A1AT augmentation therapy for A1ATD as part of the RAPID study, and demonstrated a significant reduction in patients on active drug, and this was associated with a reduction in decline in CT densitometry (Ma et al., 2017). The second by Ma and colleagues (2013) measured desmosine and isodesmosine in plasma, BALF and urine in patients with A1ATD pre and post augmentation therapy. These were significantly reduced following active treatment but not placebo (Ma et al., 2013). This is in contrast to work by Gottlieb and co-workers in 2000 who measured urinary desmosine in 12 patients with A1ATD at the start and end of 8 weeks of augmentation therapy, and found that there was no significant reduction (Gottlieb et al., 2000). A further desmosine paper analysed desmosine in urine and plasma samples from patients with A1ATD over a 14 month period; the authors concluded that plasma samples were more robust than urine samples, and that higher levels were likely to be the result of continued elastin degradation (Fregonese et al., 2011). However, this paper did not include samples from patients following treatment with augmentation therapy.

The study of desmosine and isodesmosine began before the studies discussed above. Initially comparisons were made between patients with A1ATD, healthy smokers and healthy controls and patients with usual COPD (Viglio et al., 1998). Patients with A1ATD had higher urinary desmosine levels than seen in the other groups, including

usual COPD groups with exacerbations. In addition, techniques to quantify desmosine and isodesmosine have improved considerably, from ELISAs to radioimmunoassay to the widespread use of mass spectrometry to increase the sensitivity of detection (Viglio et al., 2007). However, there have been only a small number of recent studies, discussed here, which measure desmosine and isodesmosine before and after augmentation therapy in patients with A1ATD. Desmosine and isodesmosine show promise as possible future end-points in clinical trials, but need to be more rigorously tested, and validated against CT densitometry data, before they could be routinely utilised.

Aα-val 360 is a marker of pre-inhibition activity of NE and has been studied as a potential biomarker in both usual COPD and in patients with A1ATD. It has been shown, by Carter et al, to be elevated in patients with A1ATD compared to healthy control subjects, to increase further during acute exacerbations, and to decrease following treatment with augmentation therapy. In patients in the EXACTLE trial (Dirksen et al., 2009) who received intravenous A1AT, there was a significant decrease in this signal, whereas in patients receiving placebo infusions rather than active drug, there was no change in this signal at the end of the 6 months (Carter et al., 2011).

There were no other potential biomarkers in A1ATD identified through this literature search. Besides augmentation therapy, the evidence for treatment for patients with COPD secondary to A1ATD is extrapolated from that for usual COPD, and because the literature review of biomarkers in A1ATD is sparse, a review of biomarkers in usual COPD is presented below.

There is no biomarker at present in usual COPD which meets all of the above listed

criteria for a biomarker. In COPD, potential biomarkers may be measured a variety of clinical samples, including, blood (plasma or serum), sputum, tissue, exhaled breath condensate (EBC) and broncho-alveolar lavage fluid (BALF). The advantages and disadvantages of each of these sample types are shown in table 1.1.

Sample	Advantages	Disadvantages
Blood	Hold great potential – every tissue in the body requires a blood supply Could be collected pre and post intervention Easy to create standard operating procedure for sample collection and handling All patients, irrespective of disease severity, can have samples taken.	Wide dynamic range of protein concentrations No mass spectrometer can overcome this dynamic range Attempts to remove abundant proteins may remove other information (albumin acts as a co-transporter for other proteins which may also be removed) Information may relate to a co-morbidity rather than COPD
BALF	Samples epithelial lining fluid, giving information close to the site of the inflammatory process	Samples conventionally taken from right middle/lower lobes, emphysema typically affects upper lobes Some patients cannot tolerate procedure Repeat sampling more difficult. Saline used to harvest samples interferes with mass spectrometry, therefore samples need more preparation steps. Dilutional factor present which is difficult to quantify – inter-operator variability occurs
Tissue	Information about architecture in addition to protein content	Invasive – follow up data difficult to obtain

	Samples taken from site of inflammatory process.	If taken endobronchially, multiple samples from different sites needed as the inflammation may be patchy in COPD Patients with severe disease may not be able to provide samples.
Spontaneous or Induced Sputum	Minimally invasive Gives information from closer to the site of the inflammatory process. Could be repeated pre and post intervention (not on consecutive days if induced sputum used).	Not all COPD patients produce spontaneous sputum – this selects a subset of COPD patients with the chronic bronchitis phenotype. Contamination of sample from oropharynx when expectorated. Unlikely to represent disease in small airways/alveoli Healthy control population difficult for comparison as healthy people do not produce sputum. Repeat sampling of induced sputum cannot occur on consecutive days Induced sputum sampling is pro-inflammatory and may alter inflammatory burden of the lower airways Saline may interfere with mass spectrometry, and samples need more preparation steps.

Table 1.1 Advantages and disadvantages of each of the different samples which may be utilised in biomarker investigation in COPD.

Some of the most clinically relevant/studied potential markers studied to date in each

of these sample types in patients with usual COPD will be discussed below.

1.5.1 Serum and Plasma Biomarkers

Fibrinogen is one of the most widely investigated candidate markers in COPD and on the strength of the evidence in COPD, has been recommended for review by the Food and Drug Administration (FDA) in the United States as a prognostic marker. It is a positive acute phase protein which is increased in concentration in the plasma in response to production of IL6 by the liver (Gabay et al., 1999). It is associated with mortality in patients with COPD (both COPD related and unrelated), disease progression, and increased risk of exacerbations and is discussed in depth in chapter 5 (Manino et al., 2012, and Danesh et al., 2005).

C reactive protein (CRP) is a protein synthesised mainly in the liver, in response to IL6, which has been investigated in patients with COPD. It has been shown to predict mortality in patients with mild to moderate COPD (Man et al., 2006), although not in moderate to severe disease (de Torres et al., 2008). In addition, IL6 levels have also been demonstrated to be higher in the plasma of patients with COPD when compared to healthy control subjects (Yende et al., 2006). Neither CRP nor IL6 are specific markers for COPD, and can be raised in many other infectious and inflammatory states, which reduces the potential usefulness as biomarkers for COPD.

Tumour necrosis factor α (TNFα) is a cytokine which has a role in systemic inflammation. In COPD it has been shown that patients have an elevated level of both TNFα and its soluble receptor detectable in the bloodstream (Takabatake et al., 2000). It has also been demonstrated that levels of TNFα correlate with disease severity (von

Haehling et al., 2009), and that levels are elevated following exacerbations compared to the stable state (Kardag et al., 2008).

Surfactant protein D (SP-D) is a protein that's expression is almost unique to type II pneumocytes and Clara cells in the lungs, where it plays a role in surfactant homeostasis and immunity. Therefore, this has the potential to be a more 'lung specific' marker of disease. In COPD patients, serum levels are higher than those measured in healthy controls, yet lower in lavage fluid, and it has been hypothesised that this results from leakage of the protein from the lungs into the bloodstream as a result of inflammation, rather than a problem with its production or integrity. Furthermore, its concentration correlates with health status and over a 3-month period can predict risk of exacerbations (Sin et al., 2007 and Sin et al., 2008). Furthermore, it is sensitive to steroid therapy, although the mechanism has yet to be determined (Lomas et al., 2009).

Club Cell Secretory Protein 16 (CC-16) is produced predominantly in the lungs, but detectable in serum, and it is thought to have anti-inflammatory effects within the airways and reducing the burden of oxidative stress (Broeckaert et al., 2000). It was decreased in the serum of 4724 patients in the Lung Health Study and related to decline in lung function (FEV_1) over a 9 year period (Park et al., 2013). However although the relationship was statistically significant the variance related to CC16 levels was weak (Stockley, 2013). In the ECLIPSE patient cohort, CC-16 was measured in the serum of 2083 COPD patients, and levels were lower than in either non-smoking subjects or smoking controls who did not have evidence of airflow obstruction (Lomas et al., 2008).

The receptor for advanced glycation end-products (RAGE) is a member of the immunoglobulin superfamily, and is a transmembrane receptor, and interactions between RAGE and its ligands initiates a pro-inflammatory cascade (Smith et al., 2011). The soluble receptor for advanced glycation end-products (sRAGE) binds to RAGE and it therefore protective against the inflammatory cascade (Smith et al., 2011). sRage was significantly lower in the plasma of the 61 COPD patients when compared to 42 healthy controls, and correlated with FEV_1 percent predicted (Smith et al., 2011). Miniati and colleagues measured sRAGE in 200 COPD patients and 201 control subjects. They found that sRAGE concentrations were significantly lower in the group of patients with COPD compared to the healthy control group. When further analyses were performed on the COPD patient group, there were significant differences between patients with and without cor pulmonale (lower in the group with cor pulmonale) and amongst those with emphysema on CT scan (those with severe emphysema having lower levels than those with mild emphysema) (Miniati et al., 2011).

Adiponectin is a 244 amino acid protein which is made almost entirely by adipocytes in humans and as body mass increases, the circulating levels of adiponectin decrease (Yoon et al., 2012). Levels of adiponectin were measured in patients participating in the Lung Health Study, and Yoon et al were able to demonstrate that in patients with higher plasma levels were less likely to be hospitalised or die from coronary artery disease (hazard ratios 0.73 and 0.83 respectively) (Yoon et al., 2012). They also showed that higher levels were associated with an increased risk of respiratory death from respiratory disease (hazard ratio 2.09), and decline in lung function (Yoon et al., 2012) Leptin, which is part of a common pathway with adiponectin, and has a role in energy regulation through its actions on the hypothalamus, was investigated by Creutzberg and

colleagues and they described an association between elevated leptin levels in patients with COPD during acute exacerbations and disturbances in energy regulation (Creutzberg et al., 1999).

A number of the markers described so far were combined and analysed in 1755 patients from the ECLIPSE cohort. Markers included peripheral white blood cell count, CRP, IL6, IL8, fibrinogen and TNFα. Patients who had evidence of systemic inflammation at baseline (based on values for each of the 6 parameters) had significantly higher exacerbation rates per year and increased risk of mortality compared to those without and therefore the authors concluded that this may represent a further phenotype of patients with a systemic inflammatory response (Agusti et al., 2012). Investigators from the Copenhagen General Population Study and City Heart Study analysed 3 of these markers together (CRP, fibrinogen and peripheral blood leucocyte count) and demonstrated that in patients where all 3 were high, there was an increased likelihood of having an exacerbation of their airways disease, even amongst patients who were not previously frequent exacerbators (Thomsen et al., 2013).

1.5.2 BALF Biomarkers

Broncho-alveolar lavage fluid is collected at bronchoscopy by the instillation of saline and is conventionally sampled from the right middle and lower lobes. One potential problem with this technique is that emphysema in usual COPD is often present only in the upper lobes. In addition, there is operator dependent technique in sample collection. A study by Lofdahl and colleagues conducted in patients with COPD and compared BAL recovery rates to those from healthy control subjects and smokers who did not have COPD. They observed that in the patient group the BALF recovery was lower

than either of the other 2 groups and this related to the severity of the emphysema both radiographically (measured using CT) and physiologically (TLCO) (Lofdahl et al., 2005).

Matrix metalloproteinases (MMPs) are released by macrophages and play a part of the inflammatory response in COPD, as they are able to degrade constituent of the extracellular matrix (Russell et al., 2002). MMPs are inhibited by a group of 4 proteins known as tissue inhibitors of metalloproteinases (TIMPs). Russell at al analysed macrophages from BAL from patients with COPD, and compared them to healthy subjects and smokers who did not have COPD. They demonstrated that stimulated macrophages from COPD patients released more MMP9 than those from either healthy subjects or smokers without COPD. In addition, more TIMP-1 was released by the macrophages from non-smokers when compared with either of the other 2 groups (Russell et al., 2002). BAL of smokers and ex-smokers with COPD, healthy smokers and never smokers was analysed by Babuyste and colleagues, who demonstrated that matrix metalloproteinase-12 (MMP12) positive macrophages and total number of neutrophils were higher in both of the COPD groups (Babuyste et al., 2007).

Betsuyaku and colleagues (1999) measured human neutrophil lipocalin (HNL) MMP 8 and MMP 9 in BALF from 65 individuals who were categorised by the presence or absence of emphysema on CT and by smoking status. They found that levels of HNL, MMP 8 and 9 were significantly higher in patients who smoked and had emphysema on CT imaging when compared to smokers with no evidence of emphysema despite no statistically significant difference in the total neutrophil numbers. They subsequently cultured alveolar macrophages and measured MMP 9 levels and concluded that as there

were no significant differences in MMP 9 from macrophages between any of the groups, neutrophilic inflammation was central to the development of emphysema (Betsuyaku et al., 1999). Subramanian and colleagues (2012) demonstrated an increased uptake of 18-fluorodeoxyglucose, particularly in the upper zones, on CT PET scans of patients with usual COPD when compared to patients with COPD secondary to A1ATD or to healthy controls. This increased uptake corresponded with the presence of upper zone emphysema in the COPD patient group (n=10) and the authors concluded that CT PET analysis could be utilised as a marker of neutrophilic inflammation in patients with usual COPD (Subramanian et al., 2012). These findings support the central role of the neutrophil in the pathogenesis of COPD (Stanescu et al., 1996; Pesci et al., 1998; Hoenderos et al., 2012).

1.5.3 Biopsy Biomarkers

A wealth of data has been produced in patients with COPD who have undergone endobronchial biopsy sampling during fibreoptic endoscopy. This approach is advantageous in that it provides information from within the lung itself, however multiple samples are required as there is heterogeneity to the inflammatory process. By convention, between 4 and 6 biopsies are recommended (Hattotuwa et al., 2002).

Bruno and colleagues analysed endobronchial biopsies from healthy control subjects (n=14), smokers without COPD (n=15) and smokers with COPD (n=27). They measured leptin which together with its receptor levels correlated with physiology, assessed using GOLD staging – there were significantly higher leptin positive cells with increasing GOLD stage (Bruno et al., 2005). This is of importance as the leptin receptor maybe expressed by lung tissue (Fantuzzi et al., 2000) and leptin has been shown to

have a significant role within a number of inflammatory pathways, in addition to roles within innate and adaptive immunity (Fantuzzi et al., 2000). This concurs with previous observations by Creutzberg and colleagues described above (Creutzberg et al., 2000).

In endobronchial biopsies of smokers with no evidence of COPD and patients with COPD, the nuclear transcription factor NF-κB was increased compared to healthy control subjects, and the p65 sub segment was 2 to 4 fold higher. Furthermore, the increase in NF-κB correlated inversely with FEV_1 % predicted (Di Stefano et al., 2002). NF-κB is of likely importance as it has a regulatory role in a number of cytokines and chemokines implicated in the pathophysiology in COPD, including TNFα, IL1, IL6, and IL8 (Di Stefano et al., 2002). In a further study by Di Stefano and colleagues, NK lymphocytes and macrophage inhibitory protein 1α (MIP 1 α) were also elevated in the biopsy samples of patients with COPD compared with healthy non-smokers, and in addition, there was an inverse correlation of these markers with lung function – patients with higher markers of inflammation having worse FEV_1 (Di Stefano et al., 1998).

1.5.4 Sputum Biomarkers

Daily spontaneous sputum is produced in a proportion of patients with COPD, which infers a chronic bronchitic phenotype amongst this patient subset, who have been shown to have a higher risk of respiratory tract infections and hospitalisation, (with an increased mortality rate) which contribute to a more rapid decline in FEV_1 (Vestbo et al., 1996). As an alternative to spontaneous sputum, induced sputum could be collected following the inhalation of an inducing agent, (most commonly hypertonic saline), however this has a number of disadvantages in its collection including the risk of inducing an inflammatory response and a fall in FEV_1 during the sampling procedure

and subsequent bronchospasm (Bhowmik et al., 1999). There is difficulty of collecting repeated samples as this pro-inflammatory effect may persist for some time afterwards. There is also inherent variability in the concentrations of sputum biomarkers in patients with both usual COPD and A1ATD. This can be overcome by performing repeated sampling and averaging the results, which is more problematic with sputum induction; 3 days was optimum for feasibility and reproducibility (Sapey et al., 2008 and Stone et al., 2012).

Some markers, such as sputum interleukin 8 (IL8) and neutrophil count, are elevated in the sputum of smokers with COPD, compared to asymptomatic smokers and healthy control subjects. In particular, sputum neutrophil count correlates negatively with FEV_1 (Stanescu et al., 1996). Furthermore, these measures are able to differentiate between differing stages of COPD, based on the GOLD classification using FEV_1 % predicted (Cazzola et al., 2010). Other inflammatory mediators studied in sputum in COPD include myeloperoxidase (MPO) and leukotriene B4 (LTB4). Parr et al demonstrated that the LTB4 concentration in sputum correlated with FVC decline and TLCO decline as well as the progression of emphysema, and that MPO also correlated with decline in FEV_1 (Parr et al., 2006).

Other markers studied include matrix metalloproteinases (MMPs) in induced sputum of patients with mild to moderate COPD. MMPs 8 and 9 were found to be increased in induced sputum of COPD patients when compared to healthy control subjects (Vernooy et al., 2004).

Despite this wealth of research and data, there still remains the need for robust

biomarkers that fulfil all of the parameters outlined above, in this complex, heterogeneous condition.

1.6 Proteomics

Proteomics is defined as the study of all of the proteins within an organism or genome at a point in time (Wasinger et al., 1995). It is a term which was introduced in the 1990s, although the study of proteins in relation to disease, for example using 2 dimensional electrophoresis, pre dates this term. Genes remain constant over the lifetime, whereas the translation of genes into their products (proteins) is dynamic and constantly in a state of flux, making the proteome far more complex to study than the genome. Additionally, there are more proteins than genes, (partly at least as a result of alternate splicing) and proteins can also undergo post translational modifications, including glycosylation, phosphorylation and ubiquitination (Westermeier et al., 2008). Therefore studying the end product of genes ie the proteins that are produced and influence or reflect the physiology and therefore pathophysiology in disease states, can potentially provide much more information than is gained by studying the genes in isolation.

Proteomics utilises a range of methodologies to analyse many peptides and proteins in a sample at a given time, which may provide information about the underlying pathophysiology of disease, in addition to looking for potential biomarkers. Typically, mass spectrometry is a key part of this process. A further advantage of using proteomics is the ability to analyse any bodily fluid, including plasma, serum, saliva, CSF, broncho-alveolar lavage fluid, urine and even tissue samples processed for analysis.

1.6.1 Mass Spectrometry in Proteomics

Technological advances in mass spectrometry have made this an integral part of many proteomics experiments. A mass spectrometer requires 3 parts; an ion source to generate ionisation of proteins and peptides (for example MALDI or electrospray) a mass analyser (eg time of flight (TOF), ion trap, quadrupole) which separates peptides based on their m/z ratio, and an appropriate detector. These will now be discussed in more detail.

1.6.2 Surface Enhanced Laser Desorption/Ionisation SELDI/MALDI

SELDI is a derivative of matrix assisted laser desorption/ionisation (MALDI), and these techniques use the same underlying principle for sample analysis. In a MALDI experiment, samples are prepared (of which there are many ways and optimisation of methods for this analysis and forms the basis of part of this MD thesis), co-crystallised using a matrix, and placed inside the mass spectrometer. A laser is fired at the samples, which are protected from destruction by the laser by the matrix, which also assists with the process of desorption/ionisation. Proteins and peptides generally become singly positively charged, and then are accelerated by a pulsed electromagnetic field to a detector. In a SELDI experiment, it is the surface of chip to which the proteins bind, (different chips are available, and have different binding/chromatographic properties) washing away anything in the sample which does not bind, to which matrix is then applied. SELDI has now largely been superseded by MALDI.

In MALDI experiments, samples are prepared, placed onto a metal plate and overlaid with matrix. In a MALDI-TOF instrument, samples can be analysed in 2 different

modes. In linear mode, the peptides, once ionised, travel in a straight path to a detector. This has the advantage of being able to detect peptides at higher masses, although provides MS data of lower resolution. In contrast, in reflectron mode, the peptides are accelerated, and then reaccelerated in the opposite direction to a detector. This process is shown diagrammatically in Figure 1.1. This gives data of higher resolution, but limits the mass range of detectable peptides to around 5000 Daltons. The distance to the detector is known, thus the speed and hence the mass of the peptides can be calculated. Data generated gives information expressed as the mass to charge (m/z) ratio, which in a MALDI experiment is usually a charge of +1, as peptides are usually singly positively charged.

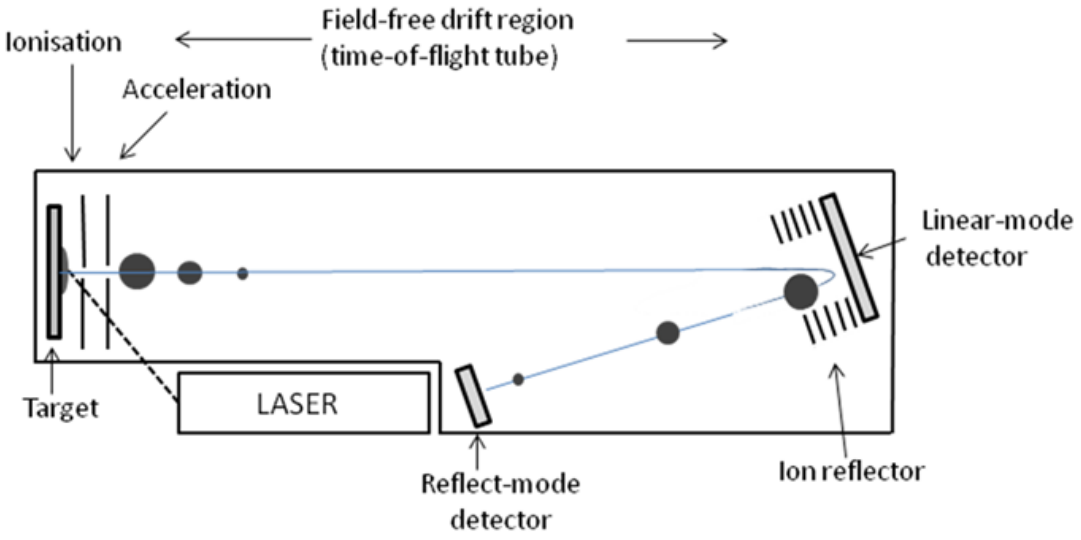

Figure 1.1 shows the inside of the Bruker Ultraflextreme MALDI mass spectrometer, depicting how the samples are accelerated in linear and reflectron modes.

Using a SELDI/MALDI approach, hundreds of samples a day may be analysed, so the throughput is high, and many individual samples can be analysed, which are usually done, at least, in duplicate. This approach is semi-quantitative in that the signal

intensities for these peaks can be compared between the groups of samples, and peaks can then be selected for identification using tandem mass spectrometry (MS/MS). In order for this to occur, the instrument needs to select ionised peptides of a known m/z and subject these ions to further fragmentation. In most mass spectrometers this is done using a technique known as collision induced dissociation (CID), however in the Bruker Ultraflextreme this is laser induced. The resulting peptide fragments are then accelerated to the detector, allowing the sequence of the peptide to be identified, as known peptides fragment in a predictable way (Westermeier et al., 2008).

1.6.3 Electrospray Ionisation (ESI)

This is an alternative approach to MALDI to generate ions. The sample containing peptides is dissolved in solvent and pumped through a narrow stainless steel capillary/needle and a high voltage is applied to create an aerosol, which is dispersed as highly charged droplets. Nitrogen is usually used to direct the sample emerging towards the detector. The solvent evaporates and the positively charged ions pass into the mass spectrometer. By using this approach, peptides may adopt multiple charges, in contrast to MALDI where they are usually singly charged. This has the advantage of extending the mass range of the analyser and is therefore of use in identifying macromolecules. ESI is often coupled with a triple quadruople or an ion trap mass analyser, interfacing with HPLC and again is useful to try to detect as many as hundreds of peptides in a sample.

1.6.4 Shotgun Proteomics

This is a term which describes a method of identifying proteins in complex mixtures, such as plasma, using a combination of high performance liquid chromatography

(HPLC) and mass spectrometry. It requires the digestion of proteins within the complex sample, to generate peptides, which are separated using HPLC. Identification of the peptides is performed using tandem mass spectrometry (MS/MS).

Plasma samples can be made less complex using an abundant protein depletion step, for which there are many commercially available products. IgY14 (Sigma Aldrich) columns are columns which contain antibodies to the 14 most abundant plasma proteins. These can be coupled with Supermix columns, which remove the next most abundant layer of proteins, working with the flow through from the IgY14 columns. Filter assisted sample preparation (FASP), using 30 kDa filters, allows the retention of proteins within filters, post abundant protein depletion, within the filters, where proteins can be reduced, alkylated and digested, an trypsin is often used in this instance. They have the advantage that larger volumes of sample can be processed, (mLs) compared to the small volumes conventionally used in standard in solution digests (typically only μL) to maximise potential peptide and subsequent protein identification (Wisniewski et al., 2009).

iTRAQ labelling (isobaric tag for relative and absolute quantitation, AB Sciex) is a labelling strategy enabling multiplex quantitation of proteins via peptide LC-MS/MS. There are currently 2 commonly used sets of labels; 4 plex and 8 plex. The label reacts with the N- termini and lysine side chains of tryptic peptides. Different samples are labelled with different isobaric tags, and samples are mixed prior to LC-MALDI. The iTRAQ labels fragment during the MS/MS stage to yield reporter groups with differing m/z ratios. The relative peak intensities of these reporter groups enable the calculation of quantitative differences between the samples. This is one method of performing

quantificative proteomics; other approaches such as tandem mass tag (TMT) and stable isotope labelling with amino acids in cell culture (SILAC) are alternatives to iTRAQ and are also widely utilised. The SILAC method is only applicable to cell culture, and would not have been possible to use in the experiments presented in this thesis. TMT is an alternative isobaric tag technique to iTRAQ labelling.

Post iTRAQ labelling, complex samples can be separated using a number of methods, to reduce their complexity, and increase the chances of protein identification. Separation in 2 dimensions, for example using a mixed mode column (eg Acclaim mixed mode WAX 1), which involves multimodal separation mechanisms, using both reverse phase and weak cation exchange properties, within a single column.

MALDI profiling can provide high throughput data on hundreds of moderately complex samples (such as plasma), and this is the approach I have utilised for this thesis. MALDI mass spectrometry is also more robust in the presence of impurities within the samples. This has also been as a result of instrument availability, and because preliminary data suggested that using a SELDI approach, it was possible to detect changes in the plasma peptidome in patients with A1ATD post treatment with pooled A1AT.

1.7 Proteomics in COPD

Some work in proteomics has been carried out previously in COPD. There are a number of samples that could potentially be analysed, including blood, sputum, tissue, exhaled breath condensate and broncho-alveolar lavage fluid (BALF). As COPD is a multi-system disease, it is possible to take samples from additional sites, such as from peripheral muscles. Barreiro and colleagues (2008) have biopsied vastus lateralis and

quadriceps muscles and used the tissue for proteomic analysis; however this review of proteomics in COPD is limited to blood and lung tissue/fluid samples. The important published work conducted to date for each of these different sample choices will be reviewed below.

1.7.1 Proteomic Analysis of Plasma/Serum

Only a small number of studies, mostly with small sample sizes, have been performed on plasma/serum in COPD. One of the best studies used protein microarray platform technology to analyse 24 markers to represent different parts of the underlying inflammatory process in COPD, and try to distinguish patients with COPD from healthy controls (Pinto-Plata et al., 2007). Forty-eight patients with COPD and a group of 48 non-smoking healthy control subjects were included in the analysis. The panel included markers of destruction and repair (eg matrix metalloproteinase 9 (MMP9)), chemo-attractants (eg (IL8)) markers of inflammation (eg TNFα). These were able to differentiate between healthy controls and COPD patients and showed a significant correlation with a number of clinical parameters including FEV_1, BODE, diffusion capacity of carbon monoxide, exacerbation rate and 6-minute walk distance, although not with BMI. The BODE index is a composite marker which aims to characterise the impact of COPD, encompassing BMI, (B), degree of airway obstruction (O), MRC dyspnoea score (D) and exercise capacity (E) measured on a 6 minute walk distance (Celli et al., 2004). This is one of the only studies published to date to correlate results from proteomics data with clinical parameters (Pinto-Plata et al., 2007).

Pinto-Plata and colleagues subsequently refined their panel of markers to include just IL6, IL6, IL16, TNFα, vascular endothelial growth factor (VEGF), MMP 9, pulmonary

and activation-related chemokine (PARC/CCL) and monocyte chemotactic protein 1 (MCP-1/CCL2). They measured these by ELISA in 253 patients with COPD and demonstrated that patients with high levels of IL6 and TNFα were more likely to have severe disease assessed by GOLD staging, and those with lower VEGF and MMP 9 had increased mortality (Pinto-Plata et al., 2012). This work demonstrates an initial set of experiments using proteomics to measure large numbers of peptides, before selecting a smaller panel to measure using ELISA – this is a common approach in proteomics, when attempting to validate potential candidate biomarkers.

Bowler et al used SELDI chips to analyse plasma from 30 patients with COPD and 30 asymptomatic smokers (Bowler et al., 2006a). There were no statistically significant differences in the peak intensities between the groups, although when they used classification and regression tree analysis, they found that 5 peaks were able to discriminate between the groups. Although the m/z ratios of these peaks were known, the peptide/proteins of origin remained unknown. The between analysis Coefficient of Variance (CVs) of this work ranged from 36% to 68%, which are values above the manufacturer's specified CV of 15-20% in SELDI spectra, and this, together with the lack of protein identification, makes it difficult to draw any meaningful or clinically useful conclusions from this work.

Rana et al (2010) analysed plasma from COPD patients who they categorised into rapid or slow decliners after analysis of their lung function decline over a 5-year follow up period (Rana et al., 2010). The rapid decliners had an average annual fall in FEV_1 of 1.52% predicted/year, whilst the slow decliners had an average annual increase of 0.73% predicted/year. They depleted the samples of abundant proteins, digested with

trypsin before using reversed phase capillary liquid chromatography (LC) with an electrospray instrument and found 55 peptides from 33 proteins to differentiate these groups. Of these, 12 were part of the complement/clotting cascade, including fibrinogen, which has previously been suggested as a possible COPD biomarker (Rana et al., 2010).

Serum amyloid alpha (SAA) was identified by Bozinoski et al (2008) in the serum of patients hospitalised with an acute exacerbation of COPD. Their work demonstrated a number of peaks in SELDI spectra that differed between stable and exacerbation states. One of these peaks had an m/z of 11 695, and a p value of 0.023. In previous work in severe acute respiratory syndrome, this peak had been identified as SAA. An immunoassay to SAA was applied and confirmed its presence in the COPD samples. The authors concluded that SAA was more sensitive than using CRP as a marker of acute exacerbations (Bozinoski et al., 2008). SAA has biological plausibility as it is a positive acute phase protein, (as is CRP) but it is also increased in other diseases, such as inflammatory bowel disease, (Murch et al., 1993) and is therefore, as with CRP, not specific to COPD.

1.7.2 Proteomic Analysis of Broncho-alveolar Lavage Fluid

In 2005 Merkel et al analysed BALF from 8 healthy subjects, 8 asymptomatic smokers and 10 smokers with COPD, using a variety of techniques including SELDI, and nano-spray chromatography with MS/MS (Merkel et al, 2005). They detected significant changes in a number of proteins between healthy controls and smokers (calgranulin A, salivary proline-rich peptide P-C, and lysozome C were up-regulated, whereas salivary proline-rich peptide P-D and Clara cell phospholipid-binding protein were down-

regulated). When comparing smokers with COPD and asymptomatic smokers, there were elevated levels of neutrophil defensins 1, 2, and calgranulins A and B. Plymoth and colleagues (2007) analysed BALF samples from 47 asymptomatic men, some never smokers, others lifelong smokers, who underwent bronchoscopy at the age of 60, using 2 dimensional electrophoresis (2DE) followed by principal component analysis. Patients underwent bronchoscopy, at which time samples were taken and stored, then were reviewed after 7 years to record outcome. During the timeframe, 7 of the smokers developed COPD, whereas none of the never smokers developed this condition. Prediction models were created and from this the authors concluded that there was a pattern of protein expression that was different between the men who developed COPD and those who did not, thus enabling them to differentiate smokers who would develop COPD from those who would not (Plymoth et al., 2007).

1.7.3 Proteomic Analysis of Lung Tissue

In 2009 Lee et al used 2 dimensional electrophoresis (2DE) followed by MALDI-TOF to look at lung tissue from patients with COPD, healthy smokers and never smokers. They found that 8 proteins were up regulated in patients with COPD compared to healthy controls. They went on to characterise 2 of these proteins, which were matrix metalloproteinase 13 (MMP 13) and thioredoxin like-2, by using western-blotting. They reported a rise of these 2 proteins in healthy smokers compared to controls, and a further rise in patients with COPD. However, this work was carried out on tissue from patients undergoing surgery for lung cancer resections, so all patients had early stage disease (Lee et al., 2009). Whether or not these findings are relevant in patients with more severe disease or in areas distant from the tumour is not known.

Ohlmeier and colleagues used 2DE on 4 patients with GOLD stage IV COPD, and found that there were differences on the gels between healthy subjects and patients with COPD. One of the proteins was identified as being surfactant protein A (SP-A). The authors then performed Western blots on samples from patients with COPD (stages II-IV) and healthy control subjects and found again that in COPD patients, SP-A was elevated, although none of the other surfactant proteins changed, suggesting it was a specific mechanism (Ohlmeier et al., 2008).

Kelsen and co-workers used 2DE on tissue from groups of patients with COPD, healthy smokers and non-smokers. They hypothesised that smoking could produce an effect in the endoplasmic reticulum of the lung known as the unfolded protein response, via the effects of reactive oxidant species. This response was believed to affect a number of gene expression functions including inflammation, protein synthesis and apoptosis. They were able to determine that 26 proteins within the lung tissue were differentially expressed (20 up regulated and 6 down regulated) in the samples from the smokers, when compared to the non-smokers, and the authors felt that this might be partially reversible with targeted therapy (Kelsen et al., 2007).

1.7.4 Proteomic Analysis of Sputum

Both induced and spontaneous sputum samples have been used for proteomics experiments however certain properties of sputum make its' analysis difficult. For example, sputum contains multiple mucins which may form crosslinks, which may impair the results of gel analyses (Pelaia et al., 2014). However, Casado et al (in 2007) used induced sputum sampling in 56 patients categorised into groups according to symptoms and CT appearances (never smokers, healthy smokers, chronic bronchitics

who had no airflow obstruction, COPD patients who had no emphysema on HRCT and COPD patients with emphysema). They used liquid chromatography ion trap quadrupole mass spectrometry and 2DE MALDI TOF approaches and found that mucin 5A was increased in all groups of smokers, compared to healthy controls (they hypothesised that this could be due to mucus gland hyper-secretion in smokers). A number of other proteins, such as Clara cell protein, β actin and proline rich 4 (PRR4) were reduced in the smoking group (Cassado et al., 2007).

Ohlmeier and colleagues (2011) analysed induced sputum from 7 patients with COPD, 7 smokers with normal spirometry and 7 healthy control subjects. They performed 2D DIGE on sputum samples and discovered 15 differentially expressed proteins between these groups. One of these was the polymeric immunoglobulin receptor (PIGR) which was subsequently measured in the plasma using an ELISA. Results from 36 non-smokers, 52 smokers and 42 patients with COPD demonstrated that PIGR was significantly elevated in the patients with COPD when compared with the group of current smokers, and both of these groups were significantly higher than the non-smokers. Furthermore, there was a correlation between plasma concentration of PIGR and airflow obstruction (Ohlmeier et al., 2011).

Gray et al obtained induced sputum from patients with CF, bronchiectasis, asthma, stable COPD patients and healthy controls and analysed the samples using SELDI-TOF. Patients with CF and bronchiectasis had the most differences from healthy subjects, thought to be a reflection of the extent of the underlying inflammatory processes. Some of these proteins, for example calgranulins A, B and C (proteins derived from neutrophils) were up-regulated in inflammatory airway disease, whilst

others such as Clara cell secretory protein were down-regulated (Gray et al., 2008).

Nicholas and colleagues analysed induced sputum from patients with COPD and healthy controls, and used 2DE followed by mass spectrometry to identify potential differences. Some of their results were validated in a larger patient group using immunoassays, and results showed that 2 potential markers, apolipoprotein A1 and lipocalcin-1 were significantly reduced in patients with COPD compared to healthy smokers (Nicholas et al., 2006), and correlated with disease severity measured using the FEV_1, FVC and FEV_1/FVC ratio.

Induced sputum samples were analysed from 6 patients with COPD, 8 patients with asthma and 5 healthy control subjects. The samples were prepared using mesoporous silica beads followed by MALDI-TOF TOF. When the spectra were analysed, there were 6 proteins which were able to distinguish these groups of patients – 3 remained unidentified and the other 3 were α defensins (human neutrophil peptides 1, 2 and 3), which were elevated in the COPD patients (Terracciano et al., 2011). From this work the authors concluded that the analysis of induced sputum was possible, that the mucins did not preclude sputum analysis and that differences could be found between patients with inflammatory lung conditions such as asthma and COPD, and healthy control subjects (Terracciano et al., 2011).

1.7.5 Proteomic Analysis of Exhaled Breath Condensate

Exhaled breath condensate (EBC) was analysed by Fumagalli and colleagues in 20 patients with emphysema secondary to A1ATD and 25 healthy control subjects. They used 2DE, HPLC and MS and found that the EBC of patients contained higher levels

of IL2, IL 15 as well as a number of cytokeratins including cytokeratins 1, 9, and 10 than that of the healthy control subjects (Fumagalli et al., 2008). A further study of EBC analysed samples from 4 groups - never smokers (n = 25), healthy smokers (n = 20), patients with COPD (n=15) and patients with A1ATD (n=23). They used LC MS/MS and found that a number of proteins including calgranulins A and B, 2 separate isoforms of SP-A, IL 1α and β, IL 2 and 12 were differentially expressed between the patient groups (Fumagalli et al., 2012). Both of these studies demonstrate that it is possible to generate proteome profiles of EBC in patients with COPD. Stolk and colleagues (2015) analysed conductivity of EBC from patients with A1ATD with evidence of emphysema and their spouses (n=7) and 18 patients with usual COPD and 6 patients with sarcoidosis Stolk et al., 2015). They were able to demonstrate that conductivity was lower in patients with A1ATD than in their healthy spouses, and that this was stable over a follow up period of 14 months. They concluded that measuring conductivity may help to overcome the dilutional variation when analysing EBC (Stolk et al., 2015).

To date, none of the potential biomarkers from these preliminary studies have been studied beyond the discovery phase and are a long way from transfer into clinical practice in COPD. This may be partly due to the complexity and heterogeneity of the condition, difficulties with each sample choice, small numbers of patients included in each analysis with little attempt to phenotype patients, cost or a lack of collaboration between clinicians, statisticians, bioinformatists and scientists from the outset of work.

1.8 Proteomics in Alpha-1-Antitrypsin Deficiency

A1ATD provides a good model for the study of proteomics in COPD. In this condition,

there is an excess of neutrophil elastase in the lung, due to a lack of its natural inhibitor, resulting in a protease/antiprotease imbalance, and proteolytic destruction of the lung parenchyma. This may result in the early onset of emphysema described above. At the point of release from the azurophil granule, where the NE is stored, the concentration of NE is 5mM, although the concentration falls exponentially with increasing distance from the point of release. This results in a concept known as the 'obligate area of damage', (Liou et al., 1996) which is greater in patients with A1ATD when compared to healthy control subjects. Even in healthy individuals, where the concentration of A1AT in the plasma is around 30μM, the concentration of NE at the point of release is several orders of magnitude greater than its inhibitor, A1AT. This means that NE remains active until its concentration has fallen (at a point a distance away from the neutrophil) to that the surrounding of A1AT, its natural plasma inhibitor. In patients with A1ATD, this is a greater problem, as the average plasma, and therefore lung interstitial concentration of A1AT is around 5μM (Liou et al., 1996), rather than the normal value of about 30μM, so the area of obligate proteolysis is exponentially greater as calculated by mathematical modelling.

As the lungs, like every other tissue and organ in the body, have a blood supply, changes within the lung parenchyma should theoretically be detectable in the blood stream due to recirculation of lung interstitial lymph. Therefore it seems likely that there will be products of the inflammation and proteolytic activity occurring in the lungs in the plasma of patients with A1ATD, and that this could be detectable by profiling the low molecular weight plasma proteome which will contain peptide fragments of degraded proteins.

Additionally, in A1ATD, there is an intervention (augmentation therapy), which can restore the serum and sputum levels of A1AT (Stockley et al., 2002). Since it is likely that augmentation is beneficial in preventing disease progression, studying samples before and during augmentation would provide data to explore potential markers of the destructive process.

After tissue sampling, which is difficult to repeat, hence has limited use as an outcome in clinical trials, blood analysis has the greatest potential to offer in the field of biomarker discovery. Blood samples are routinely taken and stored, and are minimally invasive to collect, therefore these were the samples chosen for analysis and the results are presented in this thesis.

1.9 Hypothesis

The experiments described in this thesis test the hypothesis that proteolytic degradation of lung parenchyma will be reflected by changes in the low molecular weight plasma proteome and will be useful for predicting disease progression and monitoring response to treatment with augmentation therapy. The data will therefore fulfil one or more of the roles described in section 1.5 of a clinically relevant biomarker in patients with A1ATD.

1.10 Aims of my MD

The aims of my MD thesis were to use and assess different optimised proteomic techniques, with mass spectrometry at the centre, to identify potentially useful proteins and peptides in the plasma of groups of patients with A1AT including:-

a).The analysis of plasma from blood samples from A1ATD patients that have been treated with calcium ionophore. This stimulator of neutrophils releases various inflammatory mediators including neutrophil proteinases, which have immediate proteolytic effects prior to inhibition. The data will be compared to control samples from the same patient prior to treatment. This will act as an *in vitro* model for the actions of neutrophil proteinases and help to provide possible candidate markers for this condition, which are likely to be present in the clinical samples.

b). To compare the plasma of patients with A1ATD deficiency during the stable state and during exacerbations when neutrophil activation and degranulation increases. Previous work has confirmed that during exacerbations, the inflammatory response in patients with usual COPD and those with A1ATD, is amplified returning to lower levels in the stable state (Hill et al., 1999 and Gompertz et al., 2001).

c). Analysis of samples pre and post treatment with replacement therapy as part of the EXACTLE study (a double blind, randomised controlled trial of intravenous alpha 1 antitrypsin over a two and a half year period). This will determine whether any of the peptide signals change reflecting the increase of antiprotease activity and hence a reduction in protein/tissue damage with treatment. Data will be compared to that in a group of patients receiving placebo infusions.

d). The methods will be used to compare to patients with A1ATD, usual COPD and healthy controls. This will determine whether the patterns in the A1ATD group are reflected in patients with usual COPD, or unique to A1ATD. Data will also be

compared in a second study of patients receiving A1AT augmentation as part of an interventional study assessing FDG uptake from CT PET measurement.

CHAPTER 2 METHODS

2.1 Patient Selection

The ADAPT Project (Antitrypsin Deficiency Assessment and Programme for Treatment) in Birmingham hosts the UK registry for patients with A1ATD and lung disease. Patients are referred from all over the UK from either primary or secondary care for assessment and advice. On enrolment, patients have their alpha-1 antitrypsin status reassessed for level, phenotype by isoelectric focusing and genotype by DNA sequencing in a single laboratory (Heredilab, Salt Lake City, Utah). Those who attend for review have a variety of phenotypes, although the majority are of the PiZZ genotype. Patients enrolled into interventional trials all had the PiZZ genotype, with plasma A1AT concentrations below 8μM.

The ADAPT register serves several purposes. Firstly, it acts as a centralised register for patients in the UK with this condition. Secondly, it provides data on demographics and progression of disease. Patients undergo annual review by a member of the research team, which includes accurate and detailed lung function testing, performed to the ATS/ERS and ARTP (American Thoracic Society, European Respiratory Society and the Association of Respiratory Technicians and Physiologists) guidelines, completion of quality of life questionnaires and Medical Research Council (MRC) dyspnoea score, and the collection of demographic data. Blood samples (stable state) are taken for routine biochemical and haematological testing, and aliquots of plasma and serum are stored for future biomarker and cell pellets generated for genetic studies.

From the registry, it is possible to identify suitable patients for clinical trials. Two such trials of A1AT augmentation have been the double blind EXACTLE trial, funded by

Talecris (now Grifols) (Birmingham was 1 of 3 participating centres) and the open ECLIPSE A1ATD study, which was a single centre study carried out in Birmingham. Samples from these 2 studies were used in the research presented in this thesis.

There were 77 patients enrolled into the EXACTLE trial (a randomised controlled trial of purified human A1AT therapy (Prolastin) versus placebo, consisting of 23 patients from the UK, 16 from Sweden and 38 from Denmark). Of these, there were 72 pairs of plasma samples (72 patients with samples pre and post treatment at 6 months) that were available and non-haemolysed and thus suitable for proteomic analysis. The aim of the trial was to investigate efficacy and safety of augmentation therapy and to explore the use of CT densitometry as the primary endpoint. Secondary endpoints included quality of life status pre and post treatment (measured using the St George's Respiratory Questionnaire), and the measurement of lung function parameters. The baseline and 6 month samples were used for the studies presented in this thesis.

In the ECLIPSE A1ATD trial, there were 10 patients with A1ATD, 9 healthy control subjects and 9 patients with usual COPD with plasma samples available for analysis. Patients with A1ATD had plasma samples taken at baseline and during the last of 12 weeks of weekly intravenous replacement therapy. COPD patients and healthy control subjects had plasma samples taken on the day of their screening visit alone. The aim of the ECLIPSE A1ATD trial was to compare neutrophilic inflammation in the airways, as seen on CT PET scanning, in the patients with A1ATD before and at the end of 3 months of augmentation therapy, and to compare results to patients with usual COPD and the healthy control subjects. The patients also had a urine sample taken to be analysed for cotinine concentrations, which is a metabolite of nicotine to confirm the

lack of smoking over the preceding week. The inclusion criteria for the study stipulated that the patients in the ECLIPSE A1ATD study were non- or ex-smokers, and the measurement of cotinine was to confirm this status, and thus eligibility for study enrolment. Samples analysed within this thesis from patients with A1ATD were those provided at the screening visit and prior to the final Prolastin infusion, and samples from healthy control subjects and COPD patients were those taken at the screening visit.

In both of these studies, the dose of A1ATD augmentation therapy used was 60mg/kg of body weight, and the A1AT used was Prolastin (provided by Talecris Biotherapeutics).

2.1.1 Blood Collection

All of the plasma samples were taken and processed in the same way, irrespective of the trial for which they were taken. Plasma was obtained from peripheral blood samples (using Greiner Bio-one Vacuettes (456089 + 454021) containing EDTA) and following centrifugation (Heraeus Rotina 46R) for 15 minutes at 1800 g at 21◦C samples were stored at −80°C in cryovials until analysis.

2.1.2 Urine Collections

Patients provided a mid-stream urine sample which was collected in a sterile universal container and frozen at -80^0C until subsequent analysis.

2.2 SELDI Analysis

Preliminary work was undertaken to determine the feasibility of this proteomic approach using samples from the 23 UK patients with A1ATD from the EXACTLE study pre and post 6 months' of augmentation therapy. The proteinchip arrays were loaded with Cu^{2+} as per the manufacturer's instructions: 50µL of 0.1M copper sulphate was added to each spot and incubated for 5 min at room temperature with shaking followed by washing three times with 200µL of MiliQ water.

The plasma samples were prepared by initially diluting fivefold with a solution of 8M urea in binding buffer at pH 7.0 (0.1M sodium phosphate, 0.5M NaCl and 1% by weight of CHAPS (3-[(3-Cholamidopropyl)dimethylammonio]-1) They were subsequently diluted a further 10 fold with binding buffer. One hundred µL of the diluted plasma sample was added to each spot on the chip, and left to bind for 1 hour at room temperature with shaking. After this time, the liquid was discarded and 4 washes were carried out using 200µL of buffer solution (0.1M sodium phosphate, 0.5M NaCl and 1% by weight of CHAPS (3-[(3-Cholamidopropyl) dimethylammonio]-1). Samples were placed on a plate shaker at 600 rpm for 5 minutes in between each cycle.

Two further washes were performed, using 200µL of MiliQ water, allowing 2 minutes in between each wash cycle with shaking at 600 rpm. The chips were then allowed to dry, sinapinic acid (SPA) matrix applied (1µL of a 50% saturated solution made in 50% ACN, 0.5% TFA) allowed to dry completely, before a second µL of matrix was applied and again allowed to dry completely prior to reading on the PBS IIc.

Mass spectra were acquired over the low mass range (0-20 kDa) and the high mass

range (0-150 kDa), using 600 laser shots and laser intensities of 175/225 for the low and high ranges respectively. Peaks were detected using the Ciphergen proteinchip software.

Samples were analysed in duplicate, and the peak intensities measured. Data was log transformed to achieve normality and then the mean of the 2 replicates analysed using the repeated measures test and the Huynh Feldt analysis to determine differences between the groups and between the 2 time points. A p value of <0.05 was taken as significant.

2.3 MALDI Profiling

Pooled samples from the 3 patient groups from the ECLIPSE A1ATD study were created, (using an equal volume of each individual sample) and used to optimise conditions for MALDI profiling. From these data, it was possible to assess the quality of the spectra by visual inspection, to calculate an average coefficient of variance (CV) of peak intensities and to determine how many peaks were present within the spectra. The most informative and reproducible methods were then used to analyse individual samples – initially from the ECLIPSE A1ATD study, then from the EXACTLE trial. This follows conventional proteomics experiments with the ECLIPSE A1ATD samples used for a discovery phase, whilst the EXACTLE samples provided validation of any differences found. A full description for each of the methods used is described below.

In each experiment, samples were analysed in number order of the patients' study enrolment number. For the patients with A1ATD in the ECLIPSE A1ATD and EXACTLE studies, pre and post intervention study samples were analysed

consecutively, in order to minimise intra-experiment variation for subsequent paired analyses.

2.3.1 Creation of Quality Control sample

In order to test reproducibility of the methods utilised, a quality control sample was created to process in parallel with individual samples. This consisted of a pool of plasma was made by pooling plasma from 4 different individual patients and healthy control subjects, each contributing an equal volume to the pooled sample. This allowed a Coefficient of Variance (CV) of the method to be calculated for each experiment throughout the series of experiments detailed in this thesis. The QC sample was analysed in triplicate alongside the clinical samples during each experiment to ensure reproducible results were obtained, and an inter-experiment CV was calculated for each experiment.

2.3.2 Supel Tip Profiling

Supel tips (Sigma Aldrich) are pipette tips packed with C18 reverse phase resin to allow protein/peptide binding. The tips were prepared by wetting them 3 times with 20µL of 100% acetonitrile, (ACN) before washing 3 times with 20µL of 0.1% trifluoroacetic acid (TFA). Ten µL of plasma was mixed with 40µL of 0.1% TFA in a clean tube and centrifuged at 13,000 g for 5 minutes. The proteins and peptides were then bound to the adsorbent material in the pipette tips by pipetting up and down in the diluted plasma sample 20 times with the pipette set to 20µL. The tip was then washed 5 times with 20µL of 0.1% TFA. Samples were eluted by drawing up 10µL of elution solution (50% ACN, 0.5% TFA) through the pipette tip and placing the eluant in a clean tube, prior to spotting 1.5µL of the sample on to a MALDI plate.

2.3.3 Weak Cation Exchange Beads Profiling (MB WCX)

Samples were processed according to the manufacturer's instructions. Briefly, 10µL of magnetic beads (Bruker Daltonics) were placed into a flat-bottomed 96 well plate with 10µL of binding buffer. Plasma (5µL) was added to the beads, and incubated on a plate shaker at 600 rpm at room temperature for 5 minutes.

The 96 well plate was placed on a magnetic separator for 1 minute and the liquid removed and discarded. Wash buffer (100µL) was added, and the plate left on the plate shaker for 2 minutes. The plate was then placed on a magnetic separator and the liquid removed. This wash step was repeated 3 times.

Elution buffer (5µL) and 5µL of stabilisation buffer were added to the beads. The 96 well plate was then placed on the plate shaker for 2 minutes. The beads were again held over the magnetic separator and 1.5µL of the eluant spotted on to a clean MALDI plate, and allowed to dry, prior to matrix addition.

2.3.4 MB Immobilised Metal Affinity (IMAC) Cu Bead Profiling

The manufacturer's (Bruker Daltonics) instructions were followed in detail. Briefly, 10µL of magnetic beads were placed into a flat-bottomed 96 well plate, and 10µL of binding buffer was added to activate the beads. The plate was transferred to the plate shaker at 600 rpm for 2 minutes and then held over a magnetic separator and the supernatant removed. This was repeated until 3 separate activation steps had been performed. The beads were re-suspended in 50µL of binding buffer and 10µL of plasma was added, and mixed by pipetting up and down 5 times. The 96 well plate was placed

on to the plate shaker, at 600 rpm, for 5 minutes.

The beads were then washed 3 times using 100µL of wash buffer, leaving for 2 minutes on the plate shaker after the wash buffer was added, holding the plate over a magnetic separator and the liquid discarded. The proteins/peptides were eluted from the beads using 10µL of elution solution, mixed with the beads by pipetting, and then placed over the magnetic separator for 2 minutes, to draw the beads to the bottom of each well. The eluted sample (1.5µL) was spotted onto the MALDI plate.

2.3.5 C8 and C18 Beads Profiling

The same method was used for both of these bead types. The beads (6µL) (Bruker Daltonics) were placed into the wells of a flat-bottomed 96 well plate, with 100µL of 0.1% TFA and 5µL of plasma. These were left on the plate shaker at 600 rpm at room temperature for 20 minutes to allow sufficient time for protein binding. The plate was then placed over a magnetic separator to draw the beads to the bottom and the liquid containing unbound material removed and discarded.

The beads were washed 3 times with 100µL of 0.1% TFA. Following each wash, the samples were held over the magnetic separator and liquid discarded. Proteins and peptides were eluted from the beads using 50% ACN 0.5%TFA, prior to spotting 1.5µL on to a MALDI plate.

2.3.6 SPE C8 Cartridge Profiling (Solid Phase Extraction C8 Cartridges)

Twenty µL of plasma was diluted in 500µL of 0.1%TFA, and centrifuged at 13,000 g

for 1 minute. The 100mg 1mL SPE C8 cartridges (Sigma Aldrich) were prepared by adding three aliquots of 500µL of 100% ACN, and the solvent was allowed to flow through the cartridges under gravity, and discarded. The cartridges were then washed using 3 aliquots of 500µL of 0.1% TFA. Once the TFA had passed through the cartridge, the diluted plasma sample was added to the cartridge and allowed to pass through to enable protein and peptide binding. The cartridge was again washed with 500µL of 0.1%TFA, and the peptides eluted from the cartridge using 400µL of 60% ACN 0.1% TFA. One and a half µL of eluant was spotted onto a MALDI plate.

2.3.7 Matrix Application

Once the samples had dried on the MALDI plate, they were overlaid with 1.5µL of 10mM ammonium phosphate, which was allowed to dry before application of 1.5µL of α-cyano-4-hydroxy-cinnaminic acid matrix (CHCA). The CHCA was made at a concentration of 5mg/mL in 50% ACN and water, which was vortexed for 1 minute, sonicated for 10 minutes and centrifuged for 10 minutes at 13,000 g prior to use.

2.4 MALDI Mass Spectrometry

Once the prepared samples had dried on the MALDI plate, the plate was inserted into a Bruker Ultraflextreme MALDI TOF/TOF mass spectrometer. The same instrument settings were used throughout each series of experiments. Samples were read in 2 different modes; linear and reflectron. For the linear read the settings were; detection 1000 – 20,000 m/z, detector gain 50%, 20, 000 laser shots per sample, laser offset 78% and laser power 50-55% (this was optimised for each individual experiment). For reflect mode the settings were 1000-5,600 Da, 15% detector gain, 20,000 laser shots per sample, laser offset 78%, laser power 40-45% (again this was optimised for each

experiment).

2.5 Analysis of MS Data from Profiling

Two different types of spectra were generated – linear and reflectron spectra. Linear spectra give information over a larger mass range and the higher resolution reflectron spectra provide information on accurate mass and charge state. The data were sorted into groups; for the ECLIPSE A1ATD samples this was A1AT pre and post treatment, COPD and healthy controls, and for the EXACTLE samples, placebo baseline and after 6 months of placebo infusions and active treatment at baseline and after 6 months of augmentation therapy. The spectra were loaded into ClinProTools version 2.2 (Bruker software), and peak lists and intensities compiled. The settings used in this package were peptides and proteins from 1000 to 10,000 m/z in the linear spectra with no data point reduction, following baseline subtraction and total ion current normalisation with signal to noise set to 3. The same settings were used for the reflect spectra over a more limited range of m/z 1000 to 5000. The peak picking element of the software package is designed to work on linear spectra and all linear data were used for the subsequent data analysis.

2.6 LC-MALDI Optimisation for Identification of Endogenous Plasma Peptides

The high performance liquid chromatography (HPLC) system used for this study was a Dionex HPLC UltiMate 3000, with a 15cm x 75µM C18 reverse phase column (Dionex). Two buffers were used; buffer A which was 98% HPLC grade water, 2% ACN and 0.05% TFA, and buffer B was 80% ACN 20% water and 0.04% TFA. One

hundred µL of each sample in 0.1% TFA was loaded on to the column and eluted with linear gradients of 0 – 60% buffer B. The column eluent was mixed 1:10 with matrix solution, and spotted on to a 384 spot 600µM anchorchip target plate. Three gradients were used to separate the sample over 96, 192 or 384 spots, dependent on whether throughput of samples or depth of coverage was the priority. These required different times; (a) a 96 spot gradient which runs over 65 minutes (b) a 192 spot gradient which runs over 89 minutes, which is half of a standard plate, and (c) a 384 spot gradient which runs over 105 minutes. The matrix was made of 888µL of 100% ACN, 47µL of HPLC grade water, 45µL of CHCA (saturated in 90% ACN and 10% water, vortexed for 1 minute, sonicated for 15 minutes, and centrifuged for 5 minutes at 13,00rpm) 10µL of 100mM ammonium phosphate and 10µL of 10% TFA.

MS spectra were acquired with 3500 laser shots. For calibration, a mixture of peptides and matrix was added to a pre-determined spot in between each set of 4 samples. This was made up from Pepmix calibrants (Bruker) (containing bradykinin, angiotensin, substance P, bombesin, rennin, ACTH and insulin b chain) and 300µL of HPLC matrix. Calibrant (0.2µL) was manually added to each calibrant spot once the sample was spotted out on to the plate. During the reading of the plate, the calibrant spot was read first, followed by the 4 spots around it, and this cycle continued throughout the entire plate, to calibrate each set of 4 spots accurately.

Peaks within the MS spectra with a signal to noise (S/N) of >10 were automatically selected for MS/MS and fragmented by laser induced dissociation, using 4000 laser shots, and analysed by TOF/TOF.

2.6.1 Sample Preparation for LC-MALDI

Thirty kDa and a 50 kDa molecular weight cut off filters (Sartorius Stedi, Biotech, 30kDa Vivaspin 500) were washed 5 times with 200 µL water. After the water was added, the column was centrifuged at 13,000 g and the water discarded. Plasma was mixed 1:2 with an 8M urea solution (120µL of 8M urea solution and 60µL of plasma). This was added to the filters and centrifuged at 13,000 for 60 minutes. The filtrate was acidified with 1% TFA and analysed by LC-MALDI.

2.6.2 Data Analysis LC-MALDI

The MS/MS data from the LC-MALDI runs was analysed via ProteinScape software version 2.1 (Bruker Daltonics) with MASCOT server version 2.3 (Matrix Science) and both the SwissProt Human Database and a randomised database. The search settings were as follows:- the peptide had to be first ranked, with a molecular weight search (MOWSE) score of > 40 at the protein level, > 30 for an individual peptide, and mass tolerances of the precursor ion of +/- 20ppm and of the fragment ion +/- 0.7 Da and enzyme – 'no enzyme'. The data on individual peptides and proteins was exported to Microsoft Excel 2007 for further analysis.

2.7 Urine Analyses

2.7.1 Urine Protein Content Calculation Using Bradford Assay

Each individual urine sample (20µL) was aliquoted in duplicate into a 96 well plate and 150µL of Bradford reagent (Bio Rad) were added to each sample. Bovine serum albumin (BSA) calibration standards were made using MiliQ water to concentrations of 0, 60, 120, 180, 240 and 300µg/mL, and 20µL of each was aliquoted in duplicate

into the same plate with 150μL of Bradford reagent. The absorbance was measured at 595nm. The protein content of each of the individual urine samples was calculated from the standard curve.

2.7.2 Preparation of Urine for MALDI Profiling

Urine samples were diluted to a final protein concentration of 30μg/mL and 50μL of each diluted sample was placed in a 96 well plate and acidified with10μL of 5% TFA. The samples were then Supel tipped using 20μL of 100% ACN for each 'wetting' step, 20μL of 0.1% TFA for each wash step, pipetting up and down in the samples 20 times and eluting with 10μL of 50% ACN and 0.5% TFA. Each sample (1.5μL) was spotted on to a MALDI plate in duplicate and 1.5μL of 10mM ammonium phosphate and 1.5μL of 5mg/mL CHCA added. Samples were read in both linear and reflectron modes as described in section 2.4.

2.7.3 Urine Sample Preparation for HPLC

Pooled urine samples were created, and diluted using 0.1% TFA to a final concentration of 30μg/mL, and 10μL of 5% TFA added. Samples were supel tipped as described in 2.6.2, eluted with 10μL of 50% ACN and 0.5% TFA, and 90μL of 0.1% TFA was added. Each sample was analysed in triplicate by LC-MALDI, using the 192 spot gradient described above in section 2.5.

2.8 *In Vitro* Manipulation of Samples

The purpose of this series of experiments was to activate neutrophils in whole blood

using calcium ionophore, which is a potent stimulator of neutrophils, in order to generate peptides which could act as an *in vitro* model of the actions of NE. This was done in patient with A1ATD, and in healthy control subjects, and comparisons between these groups were performed.

2.8.1 Calcium Ionophore

Freshly collected whole blood (1 mL taken in lithium heparin tubes) from 5 patients with A1ATD and 5 age matched healthy control subjects was incubated for one hour at 37^0C with 1.5µL 150µM calcium ionophore A23187, (Sigma, St Louis) dissolved in DMSO. The samples were then centrifuged at 500g for 5 minutes and the plasma harvested. For each patient and control, 1mL of blood was incubated alongside the ionophore sample and treated in the same way, but without the addition of ionophore. As soon as the samples had been centrifuged, the plasma samples were frozen at -80 ^{0}C. The time taken from the blood sample collection to being frozen was less than 90 minutes.

The calcium ionophore samples and their controls were processed using the WCX beads and the SPE C8 cartridges (as outlined above in 2.2.3 and 2.2.6) and read in linear and reflectron modes as described in 2.4. A pool was created using 20 µL of eluant from each individual post SPE C8 clean up, and analysed in triplicate using LC-MALDI (as outlined in section 2.6.3.). These experiments provided data with and without PMN activation in order to allow a comparison between the in vitro actions of proteases released from the activated neutrophils in patients with A1TAD and healthy control subjects.

2.8.1 Effects of Neutrophil Elastase (NE) on the Plasma Proteome

NE is one of the proteases released by activated neutrophils and inhibited by A1AT. Therefore the next series of experiments were performed to determine which of the peptides generated following the addition of calcium Ionophore to plasma were generated by the actions of NE. Pooled plasma from A1ATD patients at baseline and healthy control individuals from the ECLIPSE A1ATD study were used. NE (5µl of 3.4 µM NE Athens Research and Technology, made up in PBS) was added to 44µL of phosphate buffered saline (PBS) and 1µl of plasma. This was incubated at 37^0C for 1 hour. Following this time, the sample was supel tipped and then eluted with 10µL of 50% ACN 0.1% TFA. Of the eluted material, 1.5µL was spotted on to a MALDI and MS spectra generated. The remainder was analysed in triplicate by LC-MALDI using a 384 spot gradient.

2.8.2 Effects of Proteinase 3 (PR 3) on the Plasma Proteome

PR3 is another of the major serine proteases released by activated neutrophils and inhibited by A1AT. The following series of experiments was to determine which of the peptides generated following the addition of calcium Ionophore to blood were generated by the actions of PR3. Proteinase 3 was added to plasma as described above with NE. PR3 (3.4 µM Calbiochem, in PBS) was added to 44µL of PBS and 1µL of plasma and incubated for 1 hour at 37^0C. Following incubation, the samples were supel tipped and 1.5 µL of the eluted material was spotted on to a MALDI plate and spectra generated. LC-MALDI was carried out in triplicate using a 384 spot gradient.

2.9 Statistical Analysis

Peak intensity data was exported from ClinProTools (Bruker Daltonics) using the parameters outlined above. The data was entered into SPSS for Windows (Chicago Ill, version 17) and a Shapiro-Wilk test performed to determine whether or not the data was normally distributed. If the data was normally distributed, a paired or unpaired t test (as appropriate) was performed in Microsoft Excel (2007) to assess any differences in the data. If the data was not normally distributed, it was log transformed to achieve normality, and a repeat Shapiro-Wilk performed to verify a normal distribution of the data. For the log transformed ECLIPSE A1ATD data, ANOVA was performed on all of the peaks intensities, to determine if any changed significantly between the groups, and where this occurred, a post hoc analysis using a Tukey test was performed. Separate analyses were performed between A1ATD baseline and COPD and healthy controls, and between A1ATD post treatment and COPD, and healthy controls. Log transformed A1ATD baseline and post treatment samples of the ECLIPSE A1ATD study were compared by a paired t test and treatment end to baseline ratios of peak intensities were calculated.

The log transformed EXACTLE data was confirmed to be normally distributed using a Shapiro-Wilk test. A repeated measures test was performed to determine any differences between the groups and differences between the 2 time points, i.e. baseline and end of treatment samples, and the Huynh Feldt within patient factor test was used to determine the p value.

With the ionophore data, a Shapiro Wilk test confirmed that the data was not normally

distributed, and thus it was log transformed to achieve normality. A repeated measures test was again performed on the data, in order to determine differences between the groups (A1ATD patients versus controls) and between the 2 conditions – with and without the addition of calcium ionophore.

2.10 Shotgun Proteomics

Plasma samples were depleted of the most abundant proteins, digested with trypsin, labelled with isobaric tag for relative and absolute quantification (iTRAQ) and analysed by LC-MALDI as described below.

2.10.1 IgY14 Abundant Plasma Protein Depletion

Pooled samples from both ECLIPSE A1ATD and EXACTLE were used. All samples were depleted of the 14 most abundant plasma proteins (albumin, A1AT, IgM, haptoglobin, fibrinogen, 1-acid glycoprotein, HDL, LDL, IgG, IgA, transferrin, α2 macroglobulin and complement C3) using IgY14 columns (Sigma Aldrich), performed according to the manufacturer's instructions. In brief, plasma (15 µL per column) was diluted in dilution buffer (Tris-HCl 100mM with 0.15MNaCl pH 7.4), centrifuged through spin columns to remove particulates from the sample, loaded on to the IgY14 columns and incubated at room temperature for 15 minutes with mixing. The columns were centrifuged at 2000 rpm for 30 seconds and the flow through (now depleted of the 14 most abundant proteins) was collected, and used in further analysis. Bound proteins were stripped using 500 µL of, 0.1M glycine at pH 2.5 mixing for 2 minutes after each addition and centrifuging for 30 seconds at 2000 rpm. This was repeated for 4 cycles and the columns were then neutralised using 600µL of 0.1M Tris-HCl at pH 8.0 mixed and left for 5 minutes. The columns were then centrifuged for 30 seconds at 2000 rpm,

and a further 500μL of dilution buffer added. The plasma samples were either singly depleted (as above) or the flow through collected and passed back through the columns in a further cycle as described above, in order to maximise abundant protein depletion.

2.10.2 Supermix Column Protein Depletion

This was performed according to the manufacturer's instructions (Sigma Aldrich). In brief, 100μL of plasma was depleted using the IgY 14 columns, described in 2.10.1. The next layer of most abundant proteins (including complement C4, C4A, C4B, C5, factor B, C7, C8 α chain, hemopexin, fibrinogen α, β and γ chains, vitreonectin, ceruloplasmin, properdin, vitamin K dependent protein S, inter-α-trypsin inhibitors heavy chains H1 and 2, plasma protease C1 inhibitor, plasma retinol binding protein, histidine rich glycoprotein, apolipoprotein a and serum amyloid P component) was depleted from the flow through material from the IgY14 columns, using the same buffer solutions. Each sample was loaded onto Supermix LC2 column (Sigma Aldrich) and the flow through collected. The column was regenerated using 0.1M glycine at pH 2.5 to remove the bound proteins and neutralised using 0.1M Tris-HCl at pH 8.0.

The flow through material from the Supermix column was collected directly into 15mL 30,00kDa filters for filter assisted sample preparation (FASP) as described below in 2.10.3.

2.10.3 Filter Assisted Sample Preparation (FASP)

Millipore 30 kDa 50mL filters (Millipore) were washed three times with 5mL of 50mM ammonium bicarbonate (ABC) solution, centrifuged at 3500 rpm. Urea (8M) and 30mM final concentration DTT were added to the flow through material from the

supermix column. The samples were left for 1 hour at room temperature, and then loaded on to the filters and centrifuged at 3500 rpm for 10 minutes, and the flow through the filters discarded, whilst retaining the unfolded proteins within the filters.

Iodoacetemide (50mM final concentration), made up in 50mM ABC and 8M urea to a total volume of 3mL was added to each of the filters, and placed in the dark for 15 minutes. The filters were then centrifuged at 3500 for 15 minutes, and the flow through discarded, retaining the unfolded, reduced and alkylated proteins within the filters. Four filter washes with 500 µL of 50mM ABC were performed, with centrifuging after each wash at 3500 rpm. A further 2mL of 50mM ABC was then added to cover each of the filters, with 2µg trypsin and left to digest the proteins at 37^0C overnight.

Following digestion, the filters were centrifuged at 3500 rpm for 15 minutes, and the flow through, containing tryptic peptides, collected. A salt wash was performed using 3mL of 0.5M NaCl and 50mM ABC, and the flow through combined with the flow through from the previous step.

The flow through from the 30kDa filters was processed using SPE C18 cartridges, as described previously in section 2.3.6. The peptides were eluted from the cartridges using 600uL of 50% ACN made with 0.1% TFA. Following elution of peptides from the cartridges, the samples were completely dried.

2.10.4 Protein Assay Using BCA Reagent

Ten µL of BSA standards ranging from 0 to 300 µg/mL were spotted in to a 96 well plate in duplicate as described in 2.7.1. Ten µL of each sample (prior to C18 clean up)

were also spotted in duplicate into separate wells. BCA (bicinochoninic acid) reagent was made by adding a ratio of 50:1 of reagent B to reagent A (Thermo Scientific), and 150 µL were added to each of the samples and standards, and left to incubate over night at 37^0C. The plate was then read at 595nm wavelength. The absorbance data was used to create a calibration curve, and calculate the peptide concentration of each of the depleted plasma samples.

2.10.5 iTRAQ Labelling of Peptides

The samples were labelled using iTRAQ 4 plex reagents (AB Sciex) as per the manufacturer's protocol. In brief, the peptides were suspended in 40µL of dissolution buffer (0.5M triethylammonium bicarbonate (TEAB)), vortexed for 1 minute and sonicated for 10 minutes. The labelling reagents were allowed to warm to room temperature from frozen, and then 70µL of 100% ethanol were added to each vial of label. These were vortexed and sonicated, then the labelling reagents were added to the peptides, centrifuged at 13,000 rpm for 2 minutes, and left at room temperature for 1 hour.

The samples were labelled as follows:

Label	**ECLIPSE A1ATD Study**	**EXACTLE Study**
114	A1ATD Baseline	Placebo Baseline
115	A1ATD Treatment	Placebo 6 Months
116	COPD	Treatment Baseline
117	Healthy Control	Treatment Months

After 1 hour, the 4 samples were mixed for further analysis.

2.10.6 Mixed Mode Separation

The labelled samples were mixed and the peptides fragmented using a mixed mode column (Acclaim Mixed Mode WAX 1 Dionex). The iTRAQ labelled mixture was loaded on to the Mixed Mode column. A gradient of 0 - 60% buffer B, (80% ACN, 20mM ammonium formate at pH 3.0) was run over 40 minutes at 250µL per minute and 1 minute fractions collected. For the last 8 minutes, the gradient was increased from 80 to 100% buffer B. One and a half µL of each fraction was spotted on to a MALDI plate, and spectra were acquired to determine which contained peptides, and which to combine for analysis by LC-MALDI.

2.10.7 LC-MALDI

The mixed mode fractions were dried down using a speedivac and dissolved in 100µL of 0.1% TFA. These were combined to make 8 to 12 fractions to analyse by LC-MALDI as described previously.

2.10.8 Data Analysis of Shotgun Experiments

The data from each of the individual LC-MALDI runs were combined and transferred to Proteinscape software (Bruker Daltonics) as described in section 2.6.6. The settings used in the search were a MOWSE score of >30 on peptides, mass tolerance of +/- 0.7 Da on the MS/MS spectra, 30ppm on the precursor ion, enzyme = trypsin, a fixed modification of carbidomethylation and a variable modification of iTRAQ at the N terminus or lysine residues. Ratios of the intensities of the reporter group peaks were exported into Microsoft Excel 2013 for further analysis.

2.10.9 Pigment Epithelium Derived Factor (PEDF)

This was measured in individual patient's plasma using a commercially available sandwich ELISA kit (Chemicon International CYT 420), performed according to the manufacturer's protocol. This included a sample preparation step of a 1 hour incubation of the plasma samples (10µL) in 40µL of an 8M urea solution to prevent protein-protein interactions. From the standard curve produced, plasma concentrations of PEDF in the plasma samples were calculated.

2.11 Ethical Approval

The work included in this thesis focuses upon samples from 2 separate clinical trials (EXACTLE (**Ex**acerbations and **C**omputed **T**omography Scan as **L**ung **E**nd Points Trial) and ECLIPSE A1ATD Trial (**E**valuation and **C**ontrol of **L**ung **I**nflammation assessed with **P**ET **S**canning in **E**mphysema and **A**lpha 1-**A**nti**T**rypsin **D**eficiency)) and an ongoing research project (**A**nti Trypsin **D**eficiency **A**ssessment and **P**rogramme for **T**reatment (ADAPT)). Other samples utilised were from routine reviews of patients attending the ADAPT programme. The Local research Ethics Committees have supported the all of trials undertaken, with LREC numbers 2003/226 and 08/H0707/46, for the interventional studies respectively and 3396 for the overall ADAPT Project. All patients enrolled into these studies have provided written, informed consent in accordance with the Declaration of Helsinki, and were free to withdraw their consent at any time.

CHAPTER 3 SELDI PROFILING PRELIMINARY DATA

3.1 Patient Demographics

Baseline and 6 month plasma samples from the 23 patients from the UK arm of the EXACTLE study were analysed by SELDI-TOF-MS. On entry into the study, patients were randomly assigned to intravenous A1AT or placebo. The 6 months samples were taken pre infusion with either purified, human pooled A1AT (at least 75%, and containing small amounts (<5%) of other plasma proteins, including alpha$_2$-plasmin inhibitor, alpha$_1$-antichymotrypsin, C_1-esterase inhibitor, haptoglobin, antithrombin III, alpha$_1$-lipoprotein, albumin and IgA) or placebo, which was dextrose and 2% albumin. The demographic data of these patients at baseline is shown in table 3.1. Of these patients, 10 were on active drug, and 13 were receiving placebo infusions. There were no statistically significant differences in the demography of patients on the 2 arms of the study. There was a tendency for patients in the placebo group to be younger and for the placebo group to contain more female patients, although neither of these achieved the conventional statistical significance of $p<0.05$.

	Active Drug	Placebo	p Value
N	10	13	
Age	56.8 (1.6)	49.9 (3.0)	0.054
M:F	9:1	7:6	0.066
FEV_1	1.10 (0.1)	1.1 (0.3)	0.420
FEV_1 %	35.8 (4.9)	36.1 (3.0)	0.620
FVC	4.3 (0.3)	4.1 (0.3)	0.710
FVC%	109.6 (6.8)	108.6 (4.4)	0.840
Ratio	26.2 (2.8)	28.4 (2.3)	0.420
TLCO	4.3 (0.6)	5.8 (0.5)	0.072
TLCO%	47.4 (5.2)	59.8 (4.1)	0.082
KCO	0.8 (0.08)	0.90 (0.06)	0.100
KCO %	53.6 (5.2)	62.0 (4.4)	0.385

Table 3.1 Baseline characteristics of patients included in this work.
Mean age is presented in years, (SEM) Forced expiratory volume in 1 second, (FEV_1) and forced vital capacity (FVC) are mean data expressed in litres (SEM). Transfer factor of the lung to carbon monoxide (TLCO) is measured in mmol/min/kPa – the mean value is shown (SEM). KCO is measured in mmol/min/kPa/L – the mean value is shown (SEM). The FEV_1, FVC, TLCO and KCO (% predicted) are average values corrected for age height and sex with (SEM).

3.2 SELDI Profiling Results

Individual plasma samples were profiled on IMAC Proteinchip arrays as described in the methods section (section 2.2), analysed in duplicate and the peak intensities of the duplicates summed. The data were not normally distributed (using the Shapiro-Wilk test) and were therefore log transformed to achieve normality, which was confirmed by a repeat Shapiro-Wilk test. The repeated measures test was used to identify differences between the groups and between the time points, with the within factor Huynh Feldt test. A p value of <0.05 was taken as significant.

Peak intensity lists in the low mass range (1 – 20 kDa) and the high mass range (20 – 200 kDa) were combined prior to the statistical analysis. In total, there were 83 peaks within the spectra. The mean within experiment CV for this experiment was 20%, which was calculated using the peak intensities of all of the peaks from a single sample which was processed and analysed in quadruplicate during the experiment.

A typical low mass range SELDI spectrum is shown in Figure 3.1.

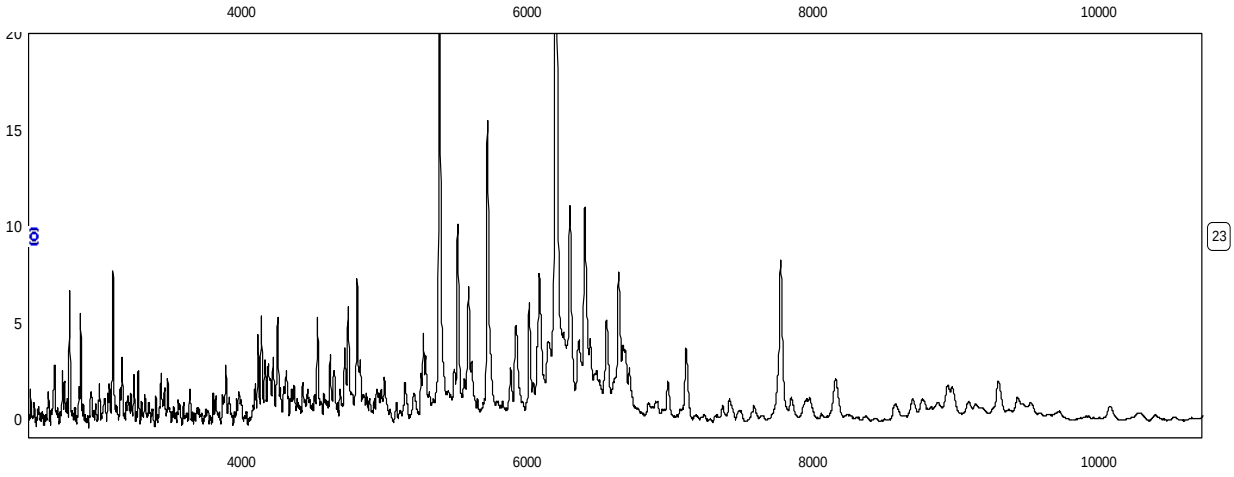

Figure 3.1 shows a typical plasma spectrum from a patient pre-treatment. The horizontal axis is the mass to charge (m/z) ratio and the vertical axis is signal intensity measured in arbitrary units.

Peaks with significantly different intensities between baseline and treatment and between the 2 groups of patients are shown below in table 3.2. There were 5 peaks within the spectra which changed in response to augmentation therapy with Prolastin, with a p value of <0.01. These were distributed throughout the mass ranges - from the smallest, which has an m/z of 3480 up to proteins with m/z ratios greater than 100,000.

p Value	m/z	Treatment Baseline	Treatment 6 Months	Fold Change	Placebo Baseline	Placebo 6 Months	Fold Change
0.001	6004	4.68	2.61	0.6 ↓	4.64	4.73	1.1 ↑
0.002	8940	1.79	2.16	1.2 ↑	1.82	1.53	0.8 ↓
<0.001	50337	0.03	0.07	2.2 ↑	0.03	0.03	1.1 ↑
0.009	101597	0.010	0.01	1.4 ↑	0.01	0.006	0.8↓
0.004	116650	0.004	0.01	2.2 ↑	0.003	0.004	1.2↑

Table 3.2 shows the statistically significant peaks which change in response to treatment. The median peak intensities in arbitrary units for each of the 4 groups is shown. The fold change is the end of treatment value divided by the baseline value for each of the groups, and the arrows demonstrate either an increase (↑) or a decrease (↓) after 6 months of treatment.

Of the peaks which change significantly, the one with the highest fold-change in intensities between the end of treatment and the start of treatment (> 2 fold and a p value of < 0.001) was at m/z of 50,337 Da, and likely corresponds to the A1AT in Prolastin. This increased in the patients receiving drug, whilst remaining unchanged in the patients receiving placebo therapy (placebo fold change 1.13). The intensities in this peak in individual patients are shown in figure 3.2, showing that the increase in the patients receiving active drug is seen all individual patients, whilst the results for those receiving placebo infusions demonstrate that the peak remains largely unchanged. Again, this lack of change is demonstrated in each individual patient.

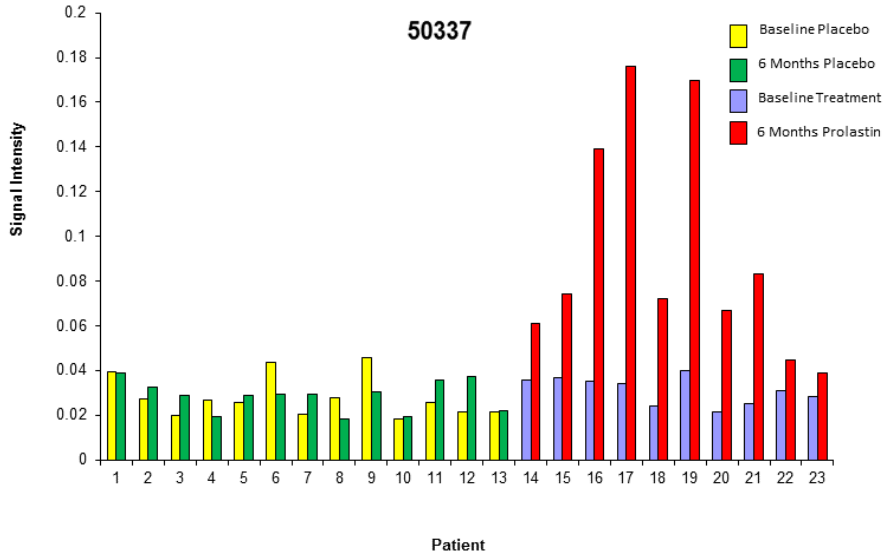

Figure 3.2 shows the individual patient values, in arbitrary units, of the patients at baseline and after 6 months, in both treatment groups, for the peak at 50, 337 Da.

Another peak which changed significantly following treatment was at m/z 6004 peak, which had a p value of <0.001 and decreased in the treated group compared to the placebo group. The ratios of peak intensities pre and post treatment were 1.02 in the placebo group, and 0.558 in the active drug group, which represents a 46% reduction in the intensity of this peak post treatment with Prolastin. The results for each of the individuals in both patient groups is represented graphically below in figure 3.3. It indicates that the change in intensities of this peak occurred, as demonstrated previously, in every treated individual, whilst again there was little change in the signal intensity in patients in the placebo group. The peak at m/z of 6004, which decreased significantly with treatment with Prolastin, is shown below in figure 3.4, which shows a pair of spectra from a single patient receiving the active drug at baseline and after 6 months of treatment.

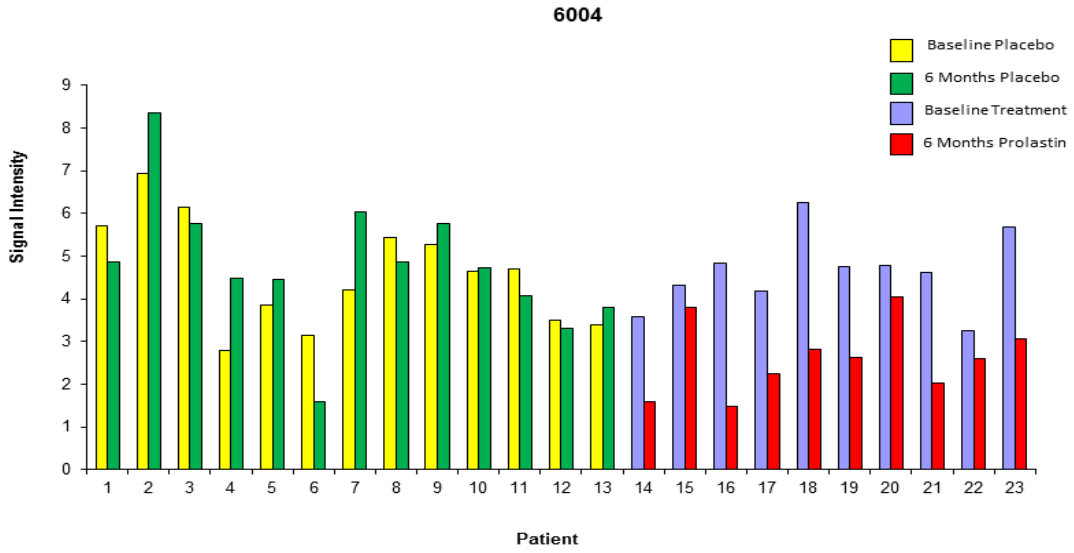

Figure 3.3 shows the individual patient values, in arbitrary units, for a peak at an m/z of 6004Da, for patients at baseline and after 6 months, in both treatment groups.

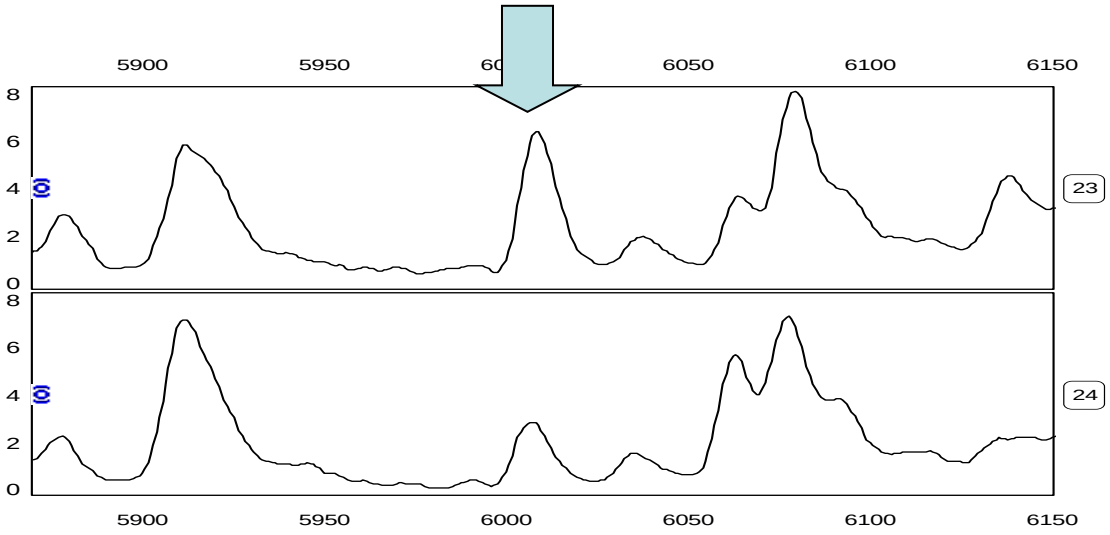

Figure 3.4 shows a pair of spectra pre (23) and post (24) treatment with Prolastin. There is a decrease in the peak intensity of the peak at 6004Da post treatment.

A further peak which demonstrated a reduction (a change in all active drug treated patients, whilst remaining relatively unchanged in the placebo treated patients) was the peak at 116554Da, which is represented graphically in figure 3.5.

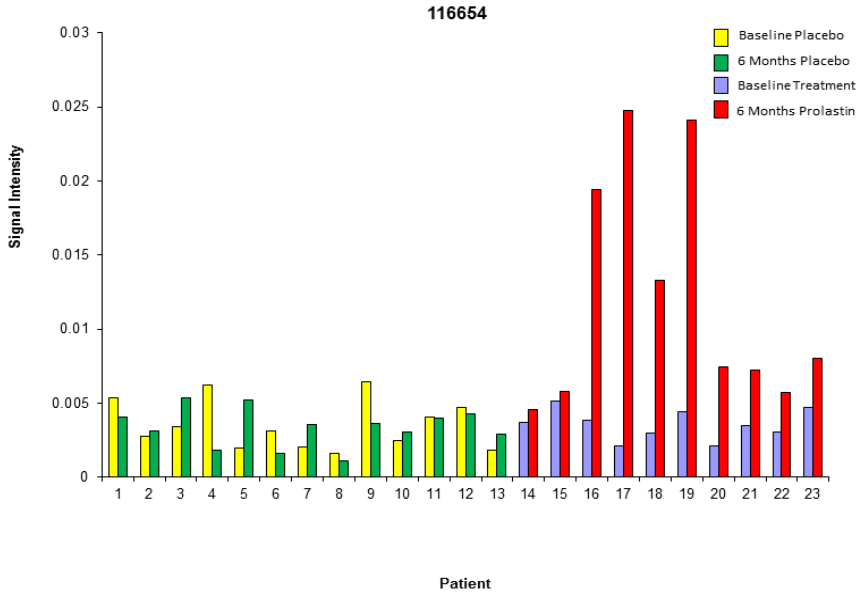

Figure 3.5 shows the individual patient values, in arbitrary units, at baseline and after 6 months, in both treatment groups, for the peak at m/z 116654 Da.

Of the other peaks which changed significantly with treatment, it is possible that the peak with an m/z of 8940Da is a fragment of complement C3a (data taken from other published work, for example work by Albrethsen in 2011). The other peaks which changed significantly with treatment remain unidentified.

3.3 Conclusions

The SELDI experiments indicated that it is possible to detect changes in the plasma proteome of patients with A1ATD when comparing pre and post augmentation therapy. From the 83 peaks present in the spectra, 5 of them changed significantly following treatment with intravenous A1AT (Prolastin).

The next step in this procedure would be to identify the proteins underlying the significant peaks, which can be very time consuming and is probably only justified for

peaks with real potential as biomarkers. The identification process requires purification of the protein followed by a digestion with trypsin, and analysis of the peptides with a mass spectrometer with tandem capability (which the PBS IIc does not have). Because this purification/digestion process is technically difficult, and the changes in peak intensities and the changes in peak intensities detected here are moderate, it made sense to perform further discovery experiments before finalising a panel of candidate biomarkers to identify.

In addition, the mass accuracy of the PBS IIc is around only 0.1. Newer instruments, with a greater mass accuracy, would be potentially more informative and provide more accurate data, therefore as the proof of principle had been established, further work was continued on a MALDI-TOF/TOF mass spectrometer, the Bruker Ultraflextreme. This instrument has a greater mass accuracy of <10 parts per million and the capability to perform tandem mass spectrometry to identify the peptides and protein fragments of interest, which change significantly in response to treatment.

In this part of the work, although the p values suggest statistically significant changes in peak intensities with Prolastin therapy, the fold changes are small. I hypothesised, therefore, that a more in depth investigation, with a more sensitive mass spectrometer with tandem capabilities should reveal more clinically useful changes in the plasma peptidome which could act as treatment (and hence pathophysiologically important) biomarkers in A1ATD.

CHAPTER 4 OPTIMISATION OF METHODS FOR MALDI PROFILING

4.1 Validation of Methods for MALDI Profiling

In SELDI experiments, there are a number of different surfaces that can be utilised to profile plasma, and they all work on the principle that proteins and peptides with different physicochemical properties bind to the surface of the chips, whilst non-binding material can be washed away. Different chip varieties have different chromatographic properties for protein and peptide binding. However, many other approaches can also be used to fractionate and de-salt plasma prior to MALDI analysis. Figure 4.1 shows the different methods assessed in this thesis to obtain MALDI spectra from the ECLIPSE A1ATD pooled plasma samples, with the number of peaks and CVs of the peak intensities for each method which was carried out in triplicate. Each is discussed in more detail below.

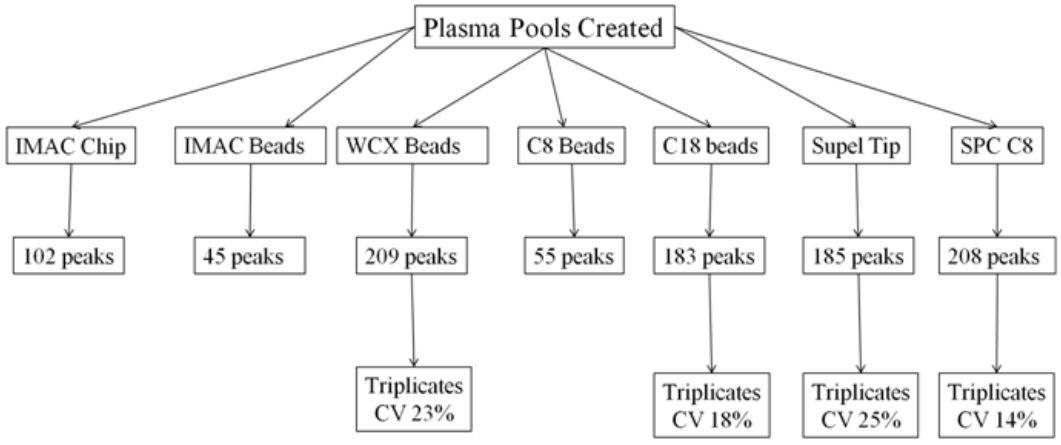

Figure 4.1 shows the profiling methods used to optimise plasma sample analysis

4.2 Matrix Optimisation

The matrix is a key component of MALDI-MS. The matrix absorbs the laser energy and assists with the desorption/ionisation process, whilst protecting the sample from destruction. A number of different matrices can be used; α-Cyano-4-hydroxy-cinnamic acid (CHCA) is widely used for tryptic digests and is well suited for the detection of peptides. Sinapinic acid (SPA) is used to analyse larger polypeptides and proteins and is also widely used in SELDI/MALDI profiling studies.

To optimise matrix addition, pooled samples from the ECLIPSE A1ATD study were spotted out on to a MALDI plate, allowed to dry and different matrices overlaid. CHCA was initially made as a saturated solution in 50%ACN/0.5%TFA, and 1.5μL was overlaid on to 1.5 μL of dried sample. For comparison, 2 x 1.5 μL of SPA was added, made as a 50% saturated solution using 50% ACN 0.5% TFA. Figure 4.2 below shows the difference in the spectra when CHCA and SPA were used in the peptide mass region (<4 kDa). There were more peaks in the CHCA spectra, with greater peak intensities. Despite its usual use in the detection of larger polypeptides, in our hands, SPA did not produce sufficiently high quality spectra of plasma peptides or proteins to be useful in profiling experiments. Therefore, CHCA was used as the matrix throughout all of the subsequent experiments.

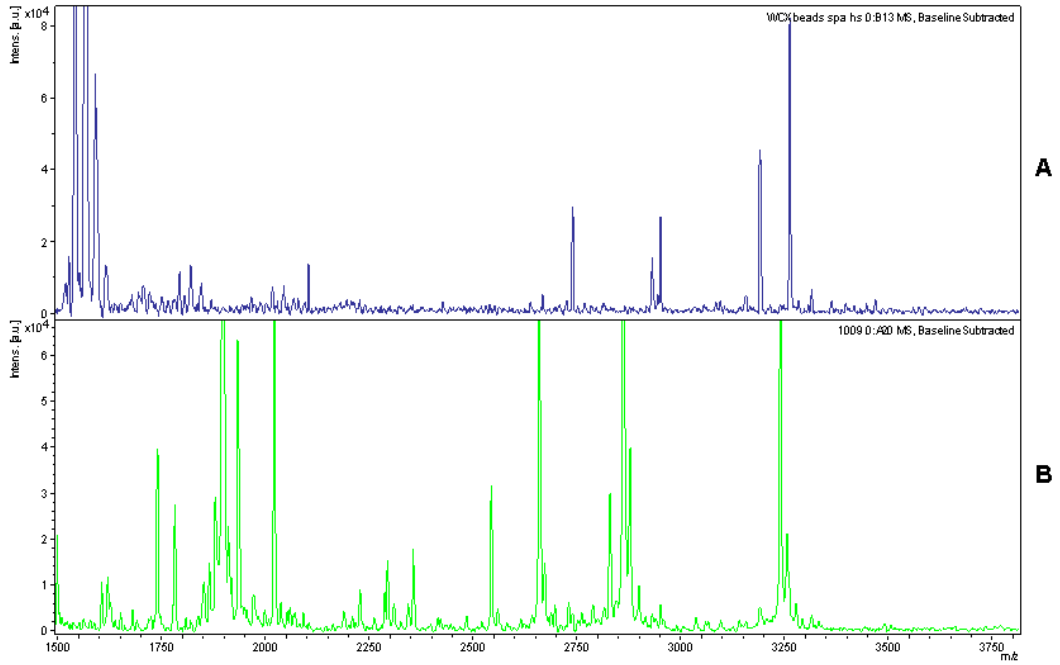

Figure 4.2 above shows the application of 2 different matrices to the same sample. A is SPA and B is CHCA. CHCA spectra contained a greater number and greater intensity of peaks, therefore this method was optimised further.

To optimise matrix addition further, we followed the method of Zhu et al., (2003) which included the addition of ammonium phosphate, which suppresses the formation of metal ion adducts. In this method, 1.5 µL of sample is allowed to air dry and then overlaid with 1.5 µL of 10mM ammonium phosphate and allowed to dry. CHCA is then made at 5mg/mL with 50% ACN and 50% H_20. Finally, 1.5 µL of 5mg/mL CHCA is added to the sample prior to MALDI analysis.

Figure 4.3 shows a single sample eluted onto the MADLI plate six times, with either 1.5µL of saturated CHCA or 1.5 µL of 10mM ammonium phosphate and 5mg/mL CHCA. The peak intensities using ammonium phosphate and 5mg/mL CHCA were much greater than using the saturated CHCA matrix. Zhu et al reported an increase using the ammonium phosphate method of around 20%, which was thought to arise as

a result of reduction in contamination of adducts and salts (Zhu X et al., 2003). The increase in peak intensities demonstrated below exceeded this expected 20%.

This improvement in peak intensities was seen using all sample preparation methods on the pooled samples, therefore this matrix method was used subsequently on all of the individual samples.

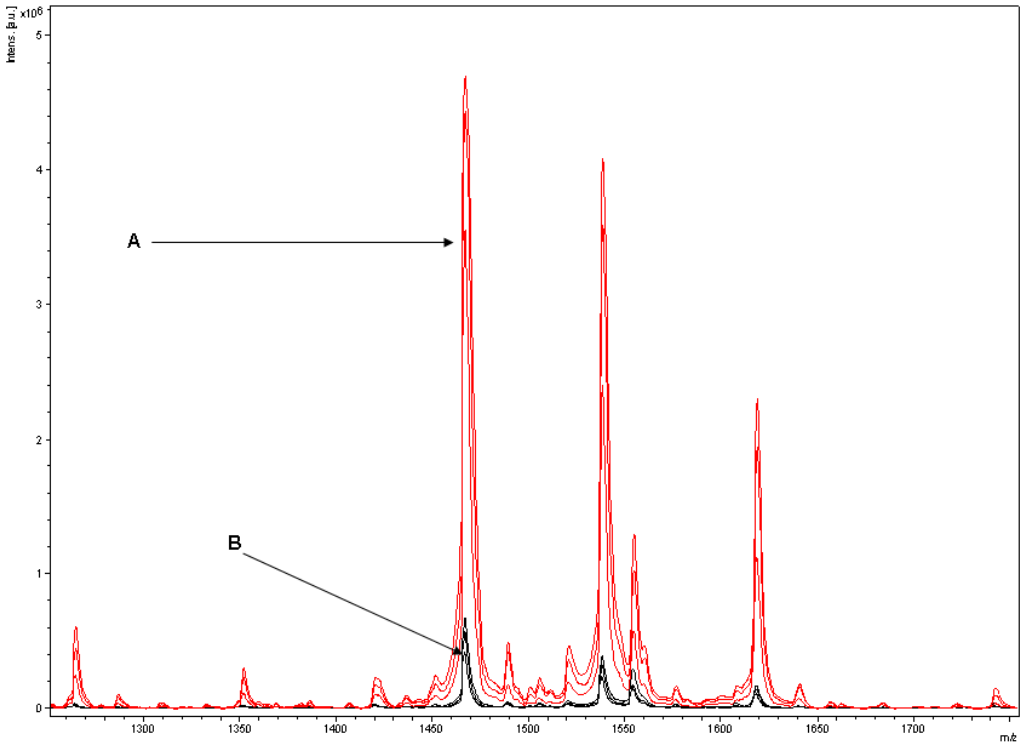

Figure 4.3 shows the difference in triplicate peak intensities between the use of CHCA 5mg/mL with 1.5µL of 10mM ammonium phosphate (A) and 1.5µL saturated CHCA (B).

4.3.1 IMAC Beads and SELDI Chips

Once the matrix had been optimised, further experiments were performed to optimise conditions for plasma profiling and MALDI TOF MS. Figure 4.1 shows that the spectra obtained with the IMAC beads and analysed using the Ultraflextreme contained the fewest peaks of any of the profiling methods. The IMAC chips, however, contained more peaks than in the SELDI experiments (102 peaks versus 83), despite the mass

range being limited to below 10kDa using the Ultraflextreme, as it is a more accurate mass spectrometer. The IMAC beads and IMAC proteinchip experiments were repeated on 2 further occasions, with similar results achieved. It was not clear why the IMAC bead spectra contained so few peaks. However, it is possible that there was something inherent in the samples which prevented peptide/protein binding, although IMAC SELDI chips (which have similar properties to IMAC beads), have been previously used successfully on serum samples. Ward et al., 2006, used SELDI chips to analyse serum from patients with colorectal cancer, and identified several peaks that were able to differentiate healthy control subjects from patients with cancer. However, in the current studies, plasma has been used and should be regarded as different from serum which is obtained after coagulation, and thus the profiles would not be directly comparable or represent the *in vivo* circulating state.

As the results were poor on 3 separate occasions with pooled samples, the IMAC beads sample preparation methodology was not performed on individual samples. Although the results of the SELDI chips read on the Ultraflextreme contained more peaks than in the preliminary work, read on the Ciphergen PBS IIc, there were other profiling methods which were better, so this technique was also abandoned for individual samples.

4.3.2 Reverse Phase Methods

The C8 and C18 beads both use a reverse phase approach, and as shown in Figure 4.1, C18 beads provided more information with a greater numbers of peaks within the spectra. Therefore, the C8 bead approach was also abandoned for individual sample analysis. Typical spectra for each of these sample preparation techniques are shown in

figure 4.4. The C18 approach was further optimised using different concentrations of ACN and TFA to elute the peptides/proteins from the beads. Concentrations used ranged from 30% to 60% ACN, and 50% ACN with 0.5% TFA was deemed to be the optimum, as it gave the greatest number of peaks, over the widest mass range, with the greatest peak intensities. This technique was therefore used on the ECLIPSE A1ATD pooled samples in triplicate, and the intra-experiment CV for all peaks using this method was 18% on average.

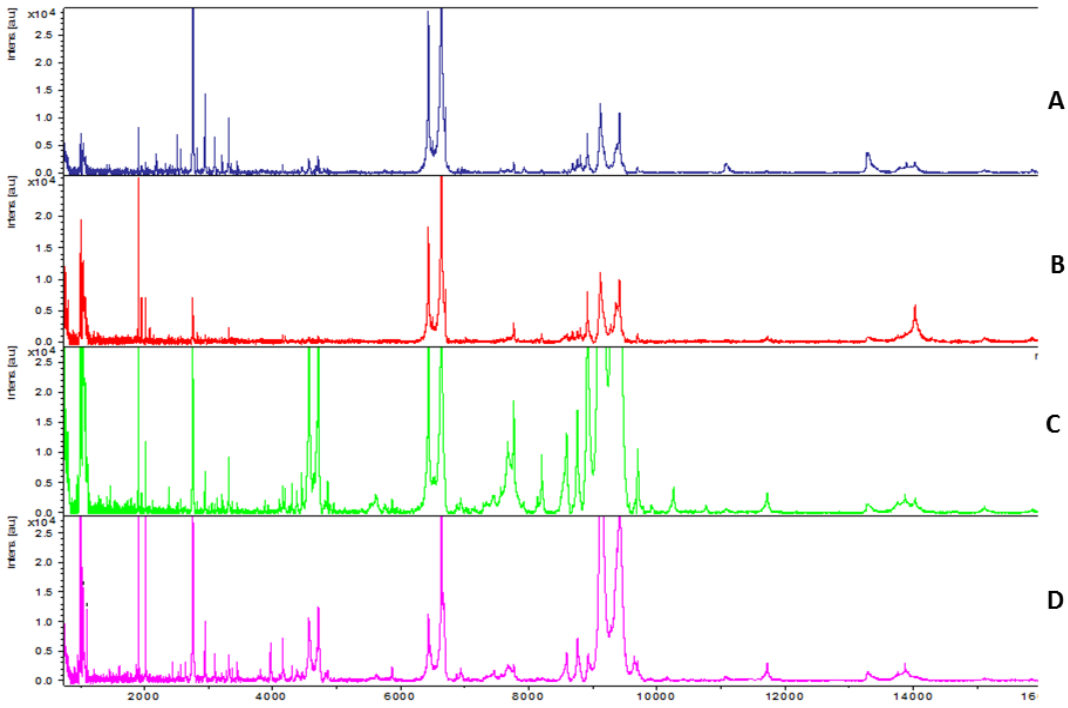

Figure 4.4 shows the MALDI spectra generated using C8 or C18 beads. A and B are replicates of spectra of plasma processed with C8 beads, and C and D are replicates of plasma processed withnC18 beads.

4.3.3 Supel Tip and SPE C8 Cartridges

Supel tipping plasma is an alternative C18 reverse phase approach to the C18 beads. This method was optimised by initially using different volumes of plasma diluted in 0.1% TFA. Volumes used were 2.5, 5 and 10µL of plasma diluted in 40µL of 0.1%

TFA. From the spectra generated, 10µL of plasma gave better spectra than 5µL or 2.5µL therefore 10 µL of plasma was used for all subsequent experiments. Typical spectra for each plasma volume are shown in figure 4.5. The supel tip spectra are particularly enriched for peaks with m/z of below 3000.

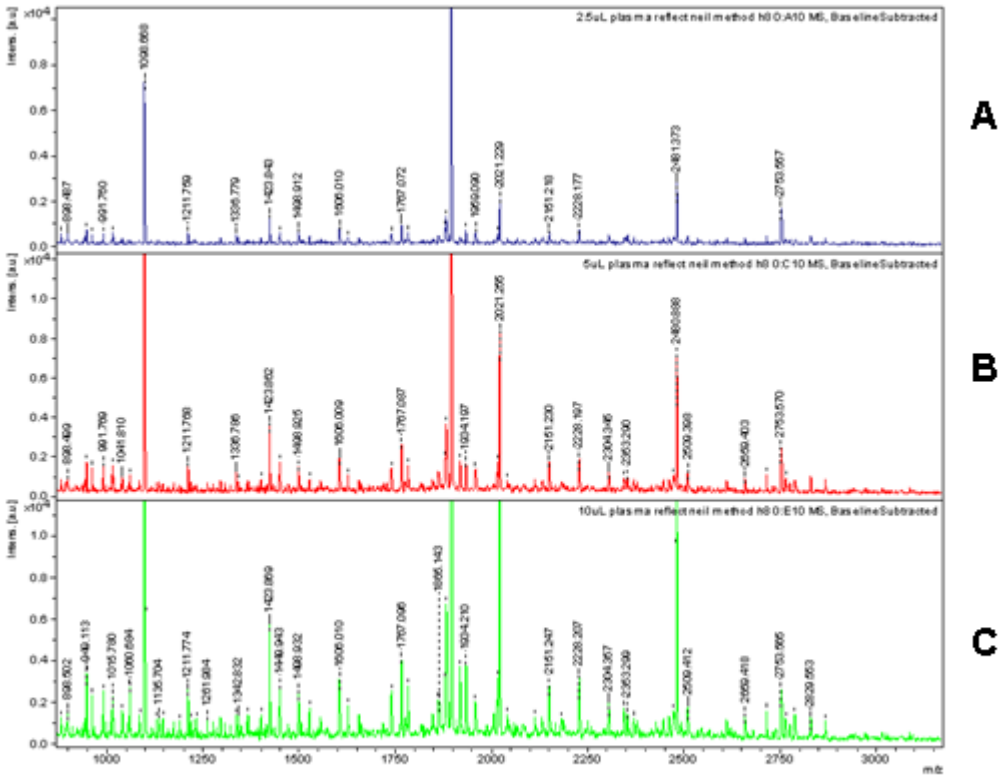

Figure 4.5 shows the results of different volumes of plasma diluted in 0.1%TFA – 2.5 µL (A), 5µL (B) and 10µL (C) and processed with supel tips.

Once the volume of plasma had been optimised, the concentration of ACN in the elution solution was assessed by eluting from the supel tips using 30% - 60% ACN with 0.5% TFA. The concentration of ACN which gave the greatest number of peaks within the spectra over the widest mass range was 50%, and therefore this was used on the subsequent samples. The optimised supel tip method was then performed in triplicate on the pooled samples from the ECLIPSE A1ATD study. The mean intra-experiment

CV of the peak intensities for each group in the pools was 25%.

C8 SPE cartridges were used as a final reverse phase approach. The data generated from the samples prepared using this technique contained a greater number of peaks with improved intra-experiment CVs when compared to supel tips. To optimise conditions for profiling, the volume of plasma was initially varied – volumes of 5, 10 and 20µL of plasma were diluted in 500µL of 0.1% TFA, centrifuged, loaded and eluted from the cartridges to obtain MALDI spectra. The volume of plasma which gave the greatest number and most intense peaks was 20µL, which was used in subsequent analyses.

The concentration of ACN used to elute the proteins/peptides from the column was optimised using different concentrations of ACN, from 40% - 60% made up with 0.1%TFA. Figure 4.6 below shows the spectra generated with each of these concentrations of ACN, and 60% was best, based on the quality of the spectra generated, and the number and intensity of the peaks present. Linear data was used to calculate the intra-experiment CV of the triplicates, which was 18%.

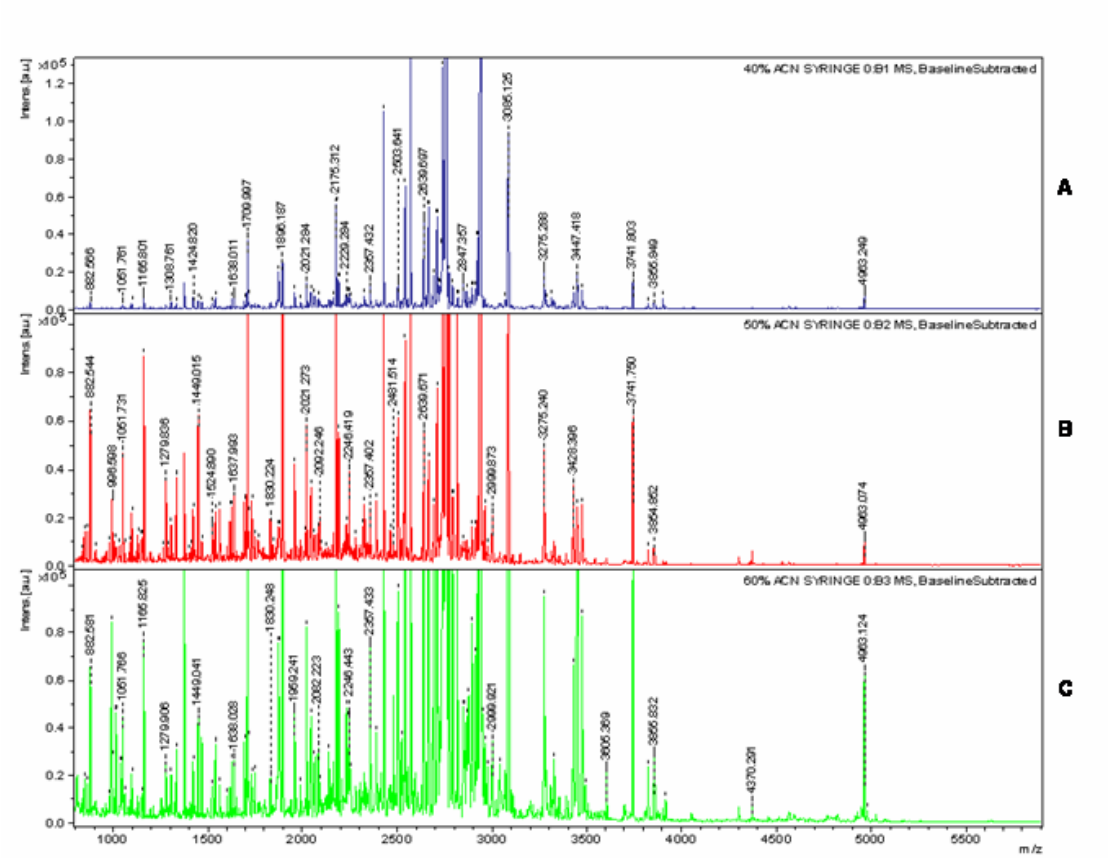

Figure 4.6 shows the results of the different concentrations of ACN used to elute from the SPE C8 cartridges – 40% (A), 50% (B) and 60% (C) ACN. The spectra with 60% ACN had more peaks, with greater peak intensities.

4.3.4 Weak Cation Exchange (WCX) Beads

The WCX bead spectra contained the greatest number of peaks of all of the methods (as shown in figure 4.1). The method was carried out in 2 ways: – according to the manufacturer's protocol, and also using half the volume of beads, solutions and plasma. The spectra generated from half of the volume contained fewer peaks than using the recommended amount, as shown in the spectra below in Figure 4.7, therefore the experiment was performed in triplicate according to the manufacturer's recommended volumes. The mean intra-experiment CV of the peak intensities in the triplicate experiment was 23%

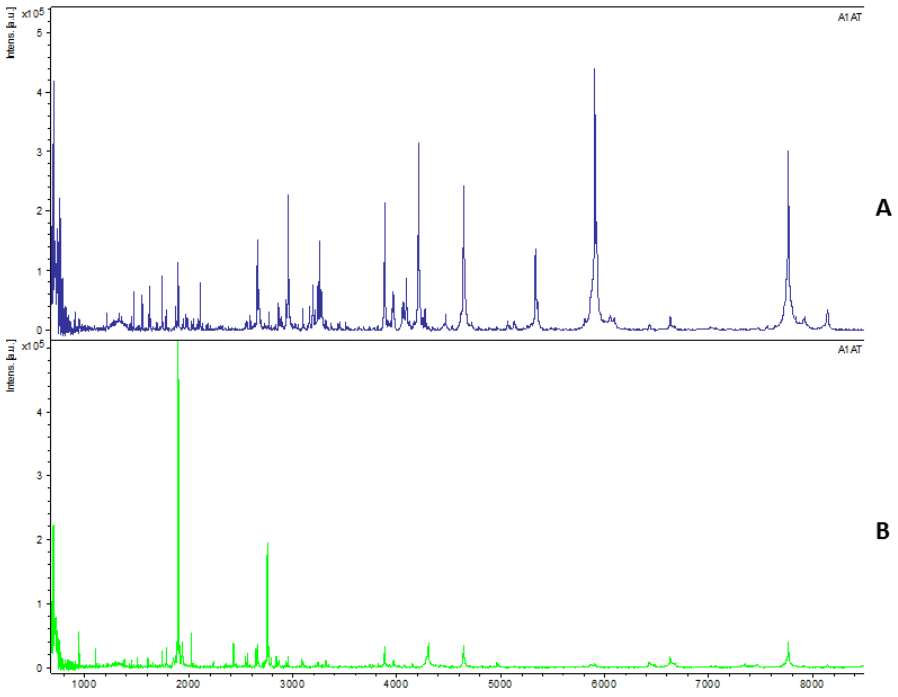

Figure 4.7 shows the difference between the use of beads and plasma according to the recommendations from the manufacturer (A) versus of half of the volume of beads and plasma (B)

4.3.5 Methods for Individual Samples

One reverse phase and one non-reverse phase method was chosen to analyse all of the individual patient samples, as the different binding properties of these approaches were likely to give complimentary information. Therefore, the methods used to analyse all of the individual samples, both from the ECLIPSE A1ATD and EXACTLE trials, and experiments on the samples following stimulation of neutrophils with a calcium ionophore, were the SPE C8 cartridges and the WCX beads, as they gave the most information (greatest number of peaks within the spectra) with the greatest peak intensities and best reproducibility which was within acceptable limits (<25%).

4.4 Plasma Peptidome Analysis by LC-MALDI

LC-MALDI was used to identify the peptides which changed significantly in the plasma

profiling experiments. For this it was necessary to enrich the peptidome and remove large proteins which take up binding capacity in the HPLC column and potentially bind irreversibly to, or precipitate in, the HPLC system, preventing it from working effectively.

4.4.1 Method Optimisation

The optimum method for preparing the samples was investigated using supel tips and 30 and 50 kDa molecular weight cut-off spin filters (Viva spin, Sartorius). Each of these methods was used and 50µL of sample (equivalent to 2µL of plasma) loaded on to the HPLC column and eluted using a 96 spot gradient. Figure 4.8 shows the initial 'survey view' of the results. Both of the filter approaches appeared to produce the greatest number of peaks present, but there was also a significant degree of sample contamination with polymer (the arrows show this as a repeating pattern of peaks in Figure 4.9). Despite further attempts using the filter methods, both 30kDa and 50kDa, including more wash steps with buffer solutions, water and 0.1% TFA, the polymer contamination problem persisted. Therefore this method was abandoned. The supel tip method appeared to be as good as the filter approaches but without the drawback of polymer contamination.

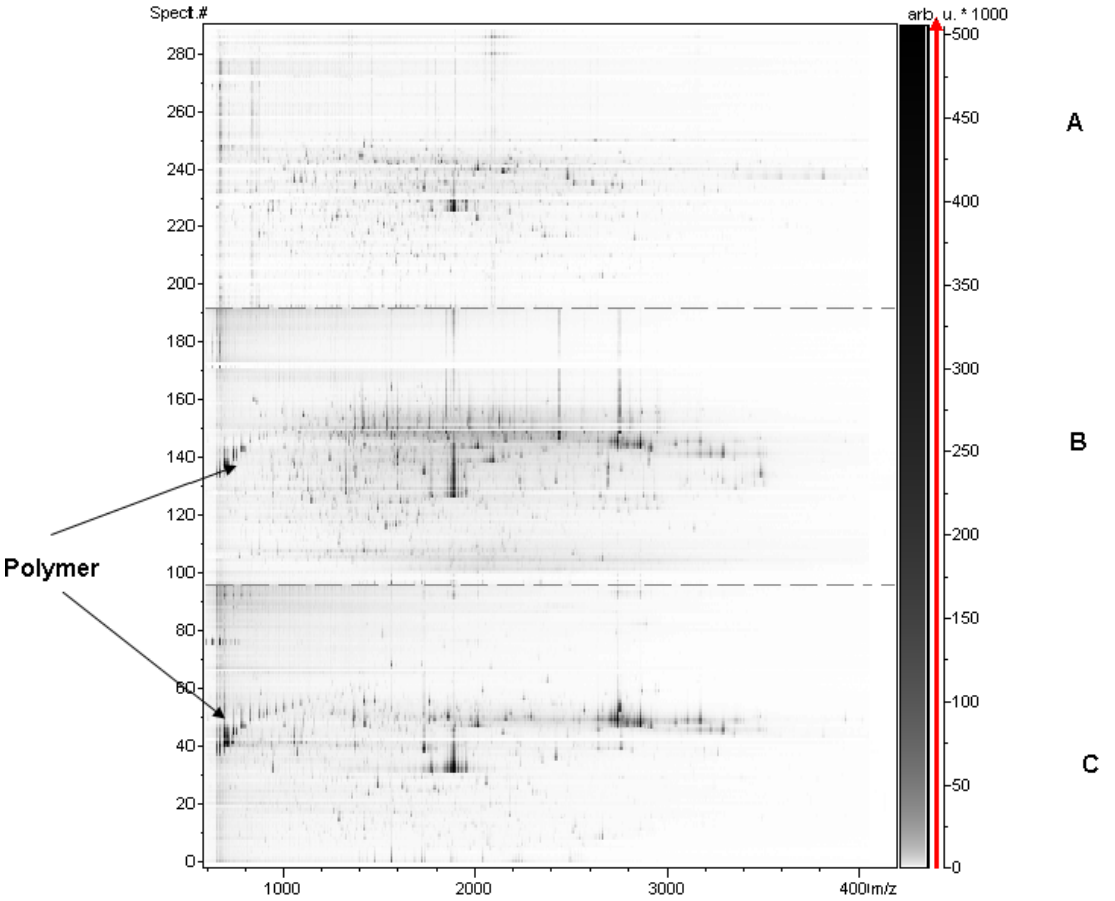

Figure 4.8 shows the survey view result of the methods used to prepare plasma prior to LC-MALDI. The horizontal axis shows the m/z ratio of peptides, the right vertical axis is signal intensity, measured in arbitrary units, and the left hand vertical axis shows the spectrum number. A was generated using the supel tip approach, B the 30kDa filter and C the 50kDa filter. The arrows show the polymer contamination seen with the 2 filter approaches.

However, as with the MALDI profiling experiments, the SPE C8 reverse phase cartridges gave more informative spectra for LC-MALDI than supel tips. Figure 4.9 shows a comparison of a supel tipped plasma sample and one prepared using the C8 SPE cartridge, with a 192 spot HPLC gradient. There was an increase in the number of peaks, and an increase in the peak intensities in the spectra when the SPE C8 approach was used rather than supel tipping, therefore the SPE C8 method was used for analysis of the ECLIPSE A1ATD and the EXACTLE pooled plasma samples.

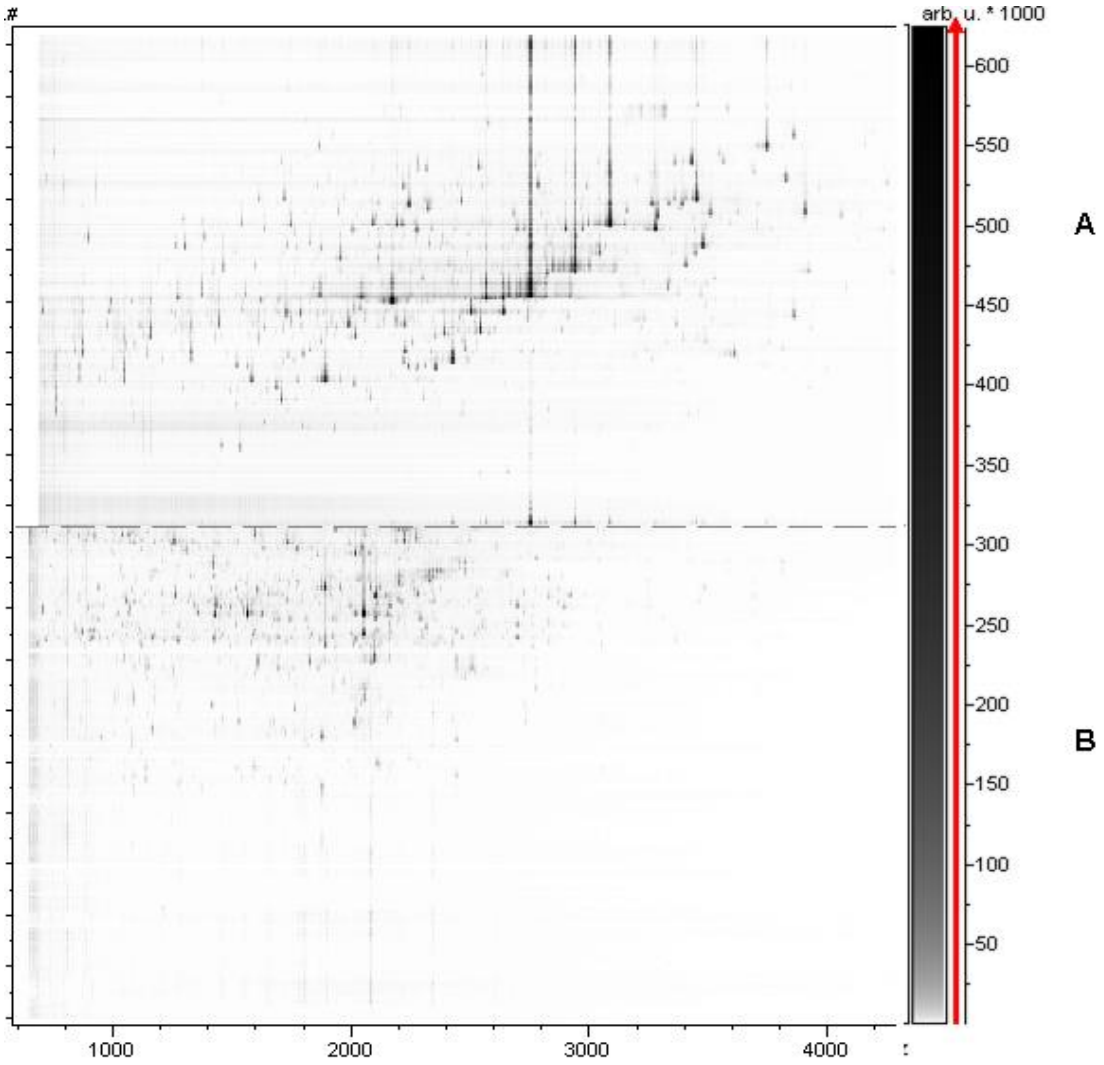

Figure 4.9 shows the survey view of 2 methods tested in preparation for LC-MALDI. A shows a sample from an SPE C8 cartridge, and B shows the same sample prepared using a supel tip. There was a greater number and intensity of peaks, across a higher mass range, when the SPE C8 cartridge was used.

4.4.2 Reproducibility

To ensure that this method was reproducible, a QC sample was processed using the cartridge approach described previously in 2.5.4. The initial plasma volume was 20µL, which was eluted using 400µL of 60% ACN with 0.1%TFA. This was completed in triplicate using a 192 fraction protocol. MS and MS/MS were performed on these samples to determine reproducibility of the technique. Table 4.1 summarises the

number of peaks contained within each spectrum and the number of MS/MS measurements performed on the samples.

Sample	Peaks in Spectra	MS/MS Measurements
QC 1	1869	398
QC 2	1782	375
QC 3	1926	509

Table 4.1 shows the number of peaks in the LC-MALDI run, and the number of MS/MS measurements performed on the QC sample when performed in triplicate

The peptides identified in each of the runs were compared. The top 10 proteins from each run were consistent between the different LC-MALDI runs, and were identified to be fragments of abundant plasma proteins including albumin, transthyretin, transferrin, complement C3, apolipoprotein CIII, A1AT and fibrinogen.

4.4.3 Optimisation of Loading Volume

Figure 4.10 shows the result of loading 4µL, 10µL, 20µL or 40µL of the 400µL of sample eluted from the SPE C8 cartridge, equivalent to 0.2µL, 0.5µL, 1µL and 2µL of plasma respectively. The number and intensities of the peaks present increased with sample loading, so 40µL was used in all subsequent work. This is important as the greater the intensity of the peaks, the greater the chance of identifying peaks of interest that reflect disease activity and or its abrogation with therapy.

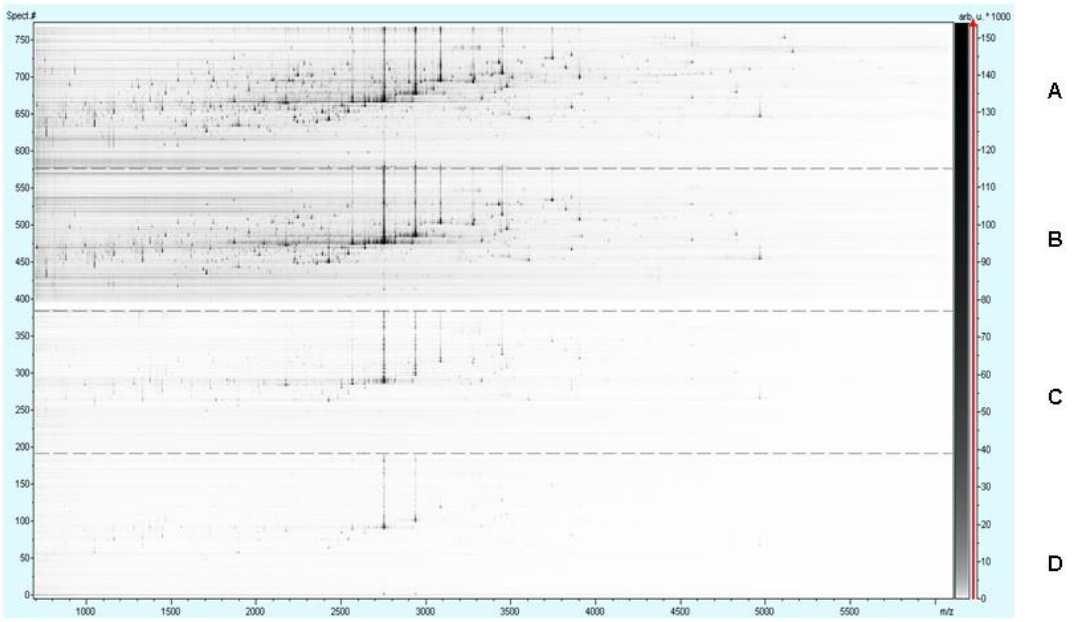

Figure 4.10 shows the results of LC-MALDI runs of the QC sample with increasing volumes of eluted sample. A is 40µL, B is 20µL, C is 10µL and D is 4µL. There are visibly more peaks of greater intensity following increasing volume loading.

4.5 Conclusions

Methods for MALDI profiling of plasma, and LC-MALDI were optimised using the different approaches described above. The 2 best methods were SPE C8 cartridges with 20µL of plasma diluted in 500 µL of 0.1% TFA and eluted with 400 µL of 50% ACN and 0.1% TFA, and the WCX beads according to the manufacturer's protocol. These methods were therefore used to profile plasma from the ECLIPSE A1ATD and EXACTLE studies, and plasma from whole blood from patients and healthy control subjects post stimulation with calcium ionophore. The results are presented in the subsequent chapters. In addition, conditions were established for the subsequent LC-MALDI MS/MS identification of endogenous plasma peptides.

CHAPTER 5 ENZYME EXPERIMENTS

Calcium ionophore is a divalent cation, highly selective for calcium and magnesium, allowing these ions to pass through cell plasma membranes into the cytosol. Through these actions, ionophore stimulates the release of proteolytic enzymes from within the neutrophils, including NE, and PR3. This chapter describes a series of experiments designed to investigate which plasma proteins are susceptible to proteolytic cleavage in A1ATD patients and the proteases responsible for the cleavages.

5.1 Patient and Healthy Control Subject Demography

Five patients with the PiZZ genotype of A1ATD attending the ADAPT project for annual follow up, and 5 healthy control subjects were included in the calcium ionophore work. Four of the healthy controls were the spouse of an A1ATD patient attending the ADAPT centre for review, evenly matching the 2 groups for age. The plasma from 3 male patients and 2 female A1ATD patients were analysed, together with the plasma from 2 male and 3 female healthy control subjects. The demographic data for the patients and healthy control subjects are shown below in table 5.1.

There were significant differences in lung function and A1AT levels between the normal subjects and the A1ATD patients; the patients had lower levels of circulating plasma A1AT and worse lung function parameters, with significantly lower FEV_1 measurements, and obstructive ratios, consistent with the diagnosis of COPD secondary to their known A1ATD. The healthy control subjects all had normal spirometry with no evidence of airflow obstruction or COPD.

	A1AT Patients	Control Subjects
Number of Subjects	5	5
M:F	3:2	2:3
Age (Years)	60.0 (4.1)	57.8 (3.8)
A1AT Level (μM)	3.1 (0.5)	30.4 (0.8) *
FEV_1 (L)	1.70 (0.3)	3.1 (0.5) *
FEV_1 % Predicted	59.4 (11.4)	104.5 (5.2) *
FVC (L)	4.3 (0.7)	3.9 (0.7)
FVC % Predicted	118.4 (13.8)	106.3 (3.2)
Ratio (FEV_1/FVC)	40.6 (8.9)	79.0 (4.7) *

Table 5.1 shows the demographic data for patients with A1ATD and healthy control subjects.

Data is presented as mean values with SEM in parentheses.

*** indicates a significant difference between the 2 groups with a p value < 0.01.**

FEV1 = forced expiratory volume in 1 second measured in litres

FVC = forced vital capacity measured in litres

A1AT level = plasma level of alpha-1-antitrypsin measured in micromoles

5.2 Plasma Profiling Post Treatment with Calcium Ionophore

The plasma samples were profiled using 2 separate approaches - WCX beads and SPE C8 cartridges as previously described (Chapter 2.2.3 and 2.3.6 respectively). Below in Figure 5.1 are spectra from plasma from an A1ATD patient plasma sample pre (A) and post (B) neutrophil stimulation with calcium ionophore and from plasma from a healthy control subject pre (C) and post (D) neutrophil stimulation with calcium ionophore. The spectra in Figure 5.1 were generated after the samples had been prepared using the WCX bead sample clean up technique. When all patients/control subjects were compared, and also when SPE C8 cartridges were used for sample preparation prior to obtaining MALDI spectra, consistent visually apparent differences were found in the spectra generated after addition of ionophore.

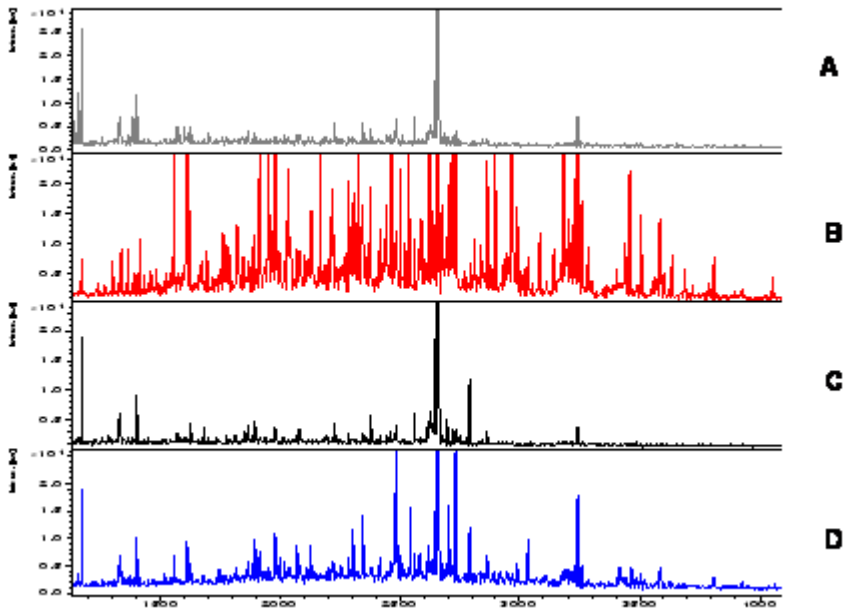

Figure 5.1 shows typical spectra of an A1ATD patient pre (A) and post (B) calcium ionophore, and a healthy control subject pre (C) and post (D) calcium ionophore.

There are greater changes in the appearance of the spectrum, consisting of many more peaks and greater peak intensities, after the addition of calcium ionophore to the plasma of A1ATD patients when compared with that of healthy controls. This is indicative of greater changes in the plasma peptidome arising from uncontrolled protease activity, following neutrophil stimulation, of the 5 A1ATD patients than is seen in that of the 5 healthy control subjects.

The peak intensity data for individual samples, following total ion current normalisation and baseline subtraction, was exported into Microsoft Excel and log transformed to achieve a normal distribution, (confirmed using the Kruskall Wallis test). The repeated measures test was performed to determine differences between the peak intensities from peptides from patient and healthy control subjects, pre and post addition of calcium ionophore. The results are presented below in Tables 5.2 and 5.3 for the 2 different profiling methodologies used.

For the SPE C8 cartridge analyses of pre and post neutrophil stimulation with ionophore in A1ATD patients and healthy control subjects, there were 212 peaks within the spectra, and of these, 24 changed significantly post neutrophil stimulation with calcium ionophore. Of these 24, 8 peptides were identified, and all were fragments of fibrinogen. The 8 fibrinogen fragments all originated from the alpha chain and each increased in intensity post neutrophil stimulation. With the exception of the peak with an m/z of 1872.6 Da, which increased more in healthy control subjects than in patients with A1ATD (fold changes 4.7 and 3.7 respectively), the intensities of these fragments of fibrinogen increased more in patients with A1ATD, with fold changes ranging from 1.1 to 11.9.

For the WCX beads experiments in A1ATD patient and healthy control samples, there were 172 peaks within the spectra, and of these, 16 changed significantly post neutrophil stimulation with calcium ionophore. Six of these 16 peptides were identified, and of these there were 3 fragments of fibrinogen (all originating from the alpha chain as was demonstrated in the SPE C8 reverse phase experiment). These increased in intensity in the A1ATD patients, whilst the intensities decreased in the healthy control subjects.

Two fragments of A1AT (with m/z ratios of 2410 and 2505 respectively) increased in all patients and control subjects post stimulation with ionophore; the peak intensities increased more for the healthy control subjects than the patients with A1ATD, with fold changes of 1.6 and 0.9 in A1ATD patients and 2.5 and 2.6 in healthy subjects. This is likely to be a result of healthy control subjects having significantly higher baseline

plasma levels of A1AT (mean 30.8μM vs 3.5 μM in patients with A1ATD p = <0.01). The detected concentration of fragments identified would be a product of the concentration of substrate and enzyme activity – therefore as the concentration of A1AT is higher in healthy subjects, more fragments are generated following the addition of calcium ionophore, by an unknown protease not completely inhibited by A1AT.

m/z	p Value	Protein	Median Patient Pre	Median Patient Post	Fold Change	Median Control Pre	Median Control Post	Fold Change
1487.7	0.004	Fibrinogen Alpha Chain	0.57	3.92	6.88 ↑	0.27	0.66	2.44 ↑
1685.3	0.001	-	0.51	6.07	11.90 ↑	0.47	1.13	2.40 ↑
1872.6	0.002	Fibrinogen Alpha Chain	1.29	4.77	3.70↑	0.41	1.93	4.71 ↑
2031.6	0.001	Fibrinogen Alpha Chain	0.60	3.63	6.05 ↑	0.37	0.93	2.51 ↑
2047.8	0.001	Fibrinogen Alpha Chain	1.98	10.57	5.34 ↑	1.27	1.71	1.35 ↑
2133.6	0.003	Fibrinogen Alpha Chain	0.80	4.06	5.08 ↑	0.37	1.03	2.78 ↑
2212.3	0.007	Fibrinogen Alpha Chain	2.08	2.12	1.02 ↑	2.05	1.05	0.51 ↓
2219.8	0.001	Fibrinogen Alpha Chain	0.83	2.91	3.51 ↑	0.72	1.15	1.60 ↑
2380.1	<0.001	-	3.55	1.48	0.42 ↓	2.63	2.37	0.90 ↓
2732.7	0.005	Fibrinogen Alpha Chain	4.45	7.54	1.69 ↑	4.19	3.18	0.76 ↓
3431.2	0.006	-	3.18	16.10	5.06 ↑	1.24	5.87	4.73 ↑
3744.7	0.004	-	7.23	43.26	5.98 ↑	13.16	34.81	2.65 ↑
3858.2	0.001	-	1.67	3.94	2.36 ↑	1.04	5.51	5.30 ↑
4148.6	0.004	-	0.48	1.75	3.65 ↑	0.54	0.47	0.87 ↓
4615.6	<0.001	-	1.17	5.12	4.38 ↑	0.52	0.99	1.90 ↑
4653.7	0.007	-	1.11	8.80	7.93 ↑	0.76	1.66	2.18 ↑

4670.5	0.005	-	0.55	2.37	4.31 ↑	0.80	0.92	1.15 ↑
4678.9	0.008	-	0.86	1.69	1.97 ↑	1.68	1.29	0.77 ↓
4891.5	0.002	-	0.35	3.60	10.29↑	0.18	0.26	1.44 ↑
4911.0	0.007	-	0.19	1.78	9.37 ↑	0.12	0.37	3.08 ↑
4929.5	0.001	-	0.25	7.72	30.88 ↑	0.32	0.80	2.50 ↑
6177.7	0.001	-	0.28	1.00	3.57 ↑	0.35	0.50	1.43 ↑
6813.0	0.001	-	0.81	2.06	2.54 ↑	1.05	0.54	0.51 ↓
6949.5	0.009	-	0.09	0.33	3.67↑	0.35	0.23	0.66 ↓

Table 5.2 shows the significant results from the profiling using SPE C8 cartridges. The fold changes compare the end of treatment to the start of treatment median value for each group and the arrows denote the direction of the change.

m/z	p Value	Protein	Median Patient Pre	Median Patient Post	Fold Change	Median Control Pre	Median Control Post	Fold Change
1349.6	0.01	Fibrinogen Alpha Chain	0.78	3.05	3.93↑	3.35	2.02	0.60 ↓
1450.6	0.01	Fibrinogen Alpha Chain	0.87	2.61	3.02↑	2.75	2.38	0.86↓
1703.1	0.004	Fibrinogen Alpha Chain	0.96	3.16	3.31 ↑	2.51	1.46	0.58↓
1734.2	0.008	-	0.84	2.08	2.48 ↑	2.62	1.99	0.760↓
2490.9	0.004	A1AT	2.13	3.43	1.61 ↑	3.58	9.10	2.54 ↑
2505.0	0.006	A1AT	1.94	1.835	0.95 ↓	1.61	4.10	2.55 ↑
2706.1	0.007	Apolipoprotein B1	2.30	2.38	1.04 ↑	2.11	3.76	1.78 ↑
4304.3	0.003	-	0.64	1.74	2.73 ↑	1.76	1.36	0.77 ↓
4487.9	0.003	-	1.62	1.21	0.75 ↓	1.88	1.41	0.75 ↓
4714.8	0.007	-	3.89	1.83	0.469 ↓	1.81	1.60	0.88 ↓
4981.9	0.003	-	5.83	7.18	1.23 ↑	4.79	28.23	5.89 ↑
5003.2	0.001	-	2.00	1.96	0.98 ↓	1.51	7.00	4.64 ↑
5019.8	<0.001	-	0.66	1.00	1.51 ↑	0.83	3.15	3.80↑
5028.4	<0.001	-	1.07	1.15	1.08 ↑	1.05	3.93	3.74 ↑
5043.4	0.001	-	0.58	0.82	1.41 ↑	1.00	2.77	2.72 ↑
9681.3	0.003	-	0.79	0.40	0.51 ↓	0.43	0.27	0.62 ↓

Table 5.3 shows the profiling results using WCX beads. The fold changes compare the end of treatment to the start of treatment median value for each group and the arrows denote the direction of the change.

A peak with an m/z of 2047 was identified from the SPE C8 experiments as a fragment of fibrinogen alpha chain, which increased in intensity in patients with A1ATD post neutrophil stimulation with ionophore. The m/z 2047 peak intensities are shown for the patients and healthy controls in Figure 5.2. There is a rise in signal intensity in all patients with A1ATD, whilst remaining largely unchanged in healthy control subjects. This rise amongst patients whilst not in healthy controls is also seen with other peaks, including the peak m/z 2219, which changed significantly only in patients with A1ATD, or with other peaks, such as those with m/z of 2031 and 2133, where the fold change was greater in patients than in healthy control subjects.

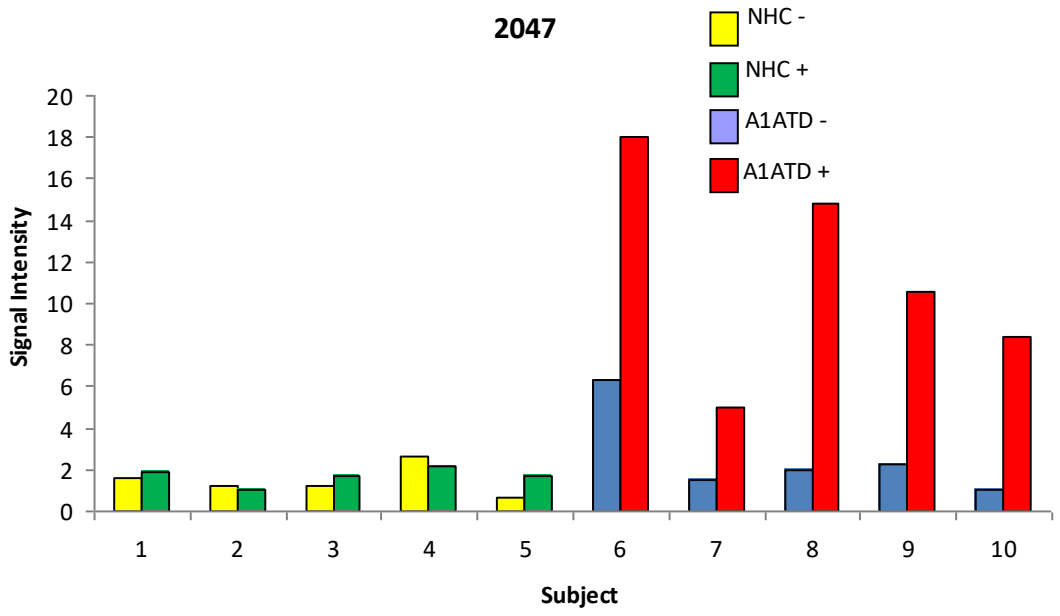

Figure 5.2 Peak intensities for individuals (measured in arbitrary units) for the fragment of fibrinogen with an m/z of 2047. NHC - = healthy controls subjects pre neutrophil stimulation with calcium ionophore, NHC + = healthy control subjects post stimulation, A1ATD - = patients with alpha-1-antitrypsin deficiency pre stimulation, and A1ATD + = patients with alpha 1 antitrypsin deficiency post neutrophil stimulation.

There were a number of peaks which were statistically significant between the patient and healthy control groups, shown in the tables above, which had an m/z above 4000Da.

This was more evident when the WCX bead approach was taken than the C8 SPE cartridges, as the WCX bead approach contained peaks within the spectra over a greater mass range (up to 10,000Da), when compared with the SPE approach in which the majority of peaks within the spectra were mainly below 4500Da. The identities of these larger peptides could not easily be obtained by MALDI-TOF-TOF MS/MS and currently remain unknown.

5.3 LC-MALDI of Ionophore Samples

Pooled samples, pre and post addition of calcium ionophore, in both the patient and control groups, were created post SPE C8 cartridge sample preparation and analysed in triplicate by LC-MALDI (as described in chapter 2.5 and 2.6.1). Figure 5.3 shows an LC-MALDI survey-view of post treatment pooled samples in A1ATD patients (A) and healthy control subjects (B).

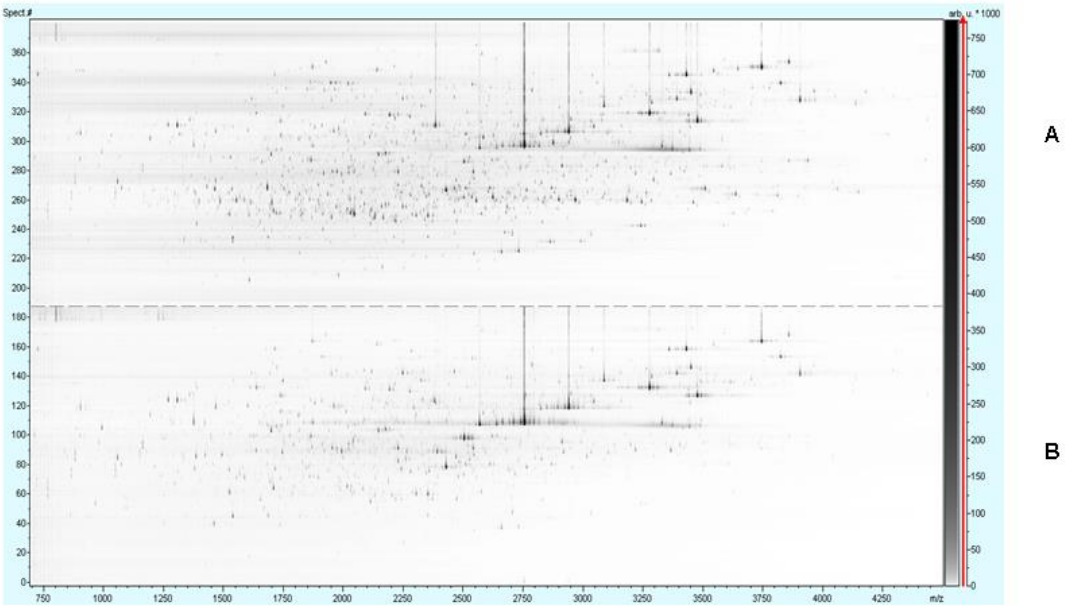

Figure 5.3 shows the survey view and demonstrates differences between post ionophore treatment of samples from (A) A1ATD patients and (B) healthy control subjects.

There are many more peaks present in the survey view, shown above, in pooled patient plasma than in pooled healthy control subject plasma, in the same way that there were a greater number, and greater intensity of peaks seen in the MALDI spectra, when results for these 2 groups were compared. This again is indicative of a greater change post addition of calcium ionophore in the plasma peptidome of patients with A1ATD when compared with that of healthy individuals.

LC-MALDI was performed in order to identify more of the peptides generated by the addition of calcium ionophore. In addition, following LC MALDI, lists of peptides identified were generated and a comparison made between those identified in healthy control subjects and patients with A1ATD. In total, there were 439 unique peptides from 49 proteins identified in A1ATD patient plasma, and 88 unique peptides from 22 proteins in the plasma of healthy control subjects. In patients with A1ATD, there were 157 unique fragments of the alpha chain of fibrinogen identified in the plasma samples post stimulation with calcium ionophore. Some of these fragments were identified, using the profiling techniques outlined previously, as signals which changed significantly in intensity between healthy control subjects and patients with A1ATD and could act as potential footprints for the effects of neutrophil proteinases in the lungs. The data generated from the ionophore work was searched using the SwissProt Human Database to identify the protein origins of the peptides, but additionally against a random database, in order to calculate a false discovery rate (FDR). There were no matches identified in the random database, indicating a very low (<1%) FDR, and increasing the validity of the results generated.

The amino acid sequence of the alpha chain of fibrinogen and the peptides identified following the addition of calcium ionophore to the blood of patients with A1ATD is shown below in Figure 5.4.

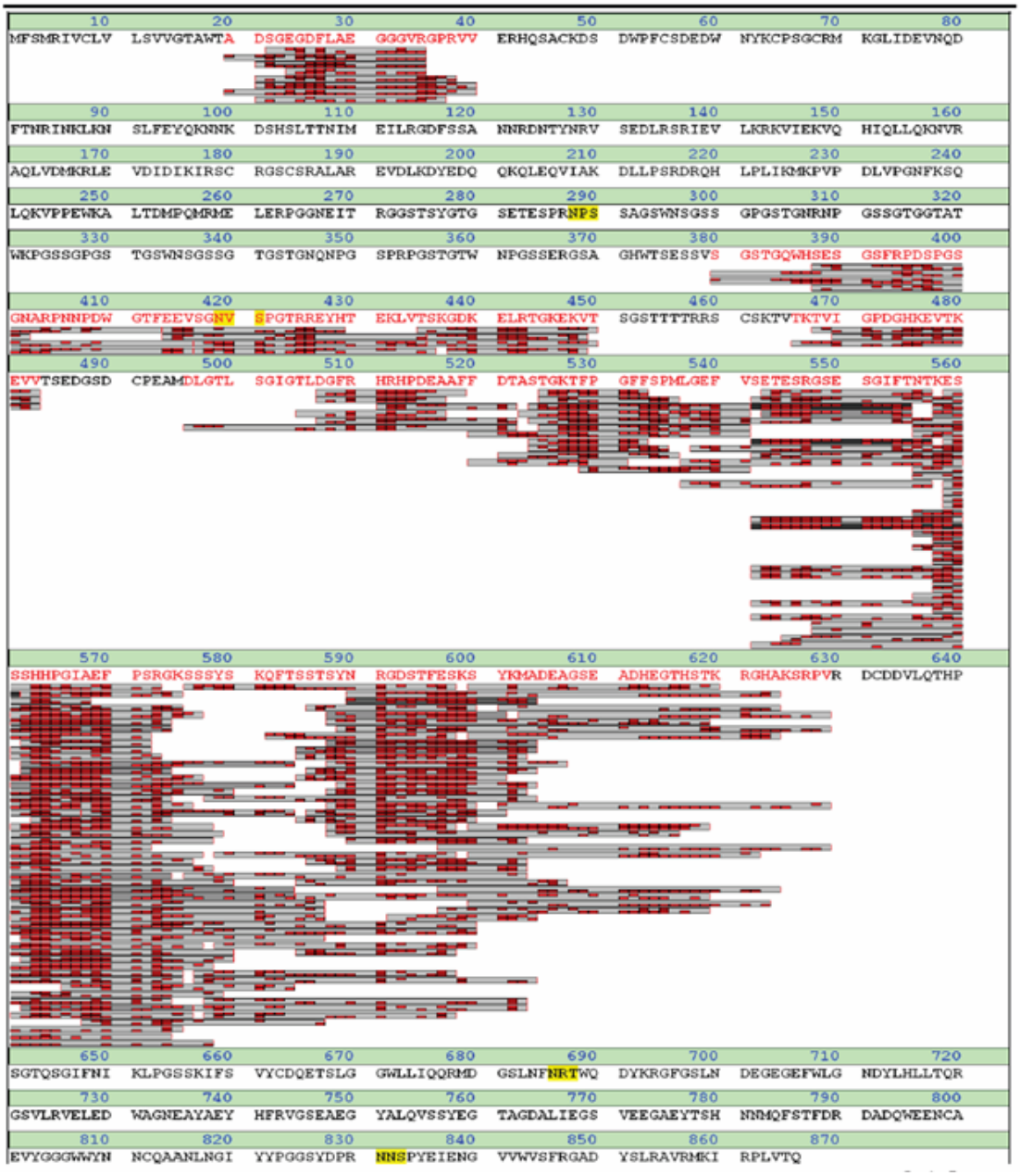

Figure 5.4 Amino acid sequence of the structure of fibrinogen. The amino acids in red are the amino acids in peptide sequences identified in patient plasma post neutrophil stimulation with calcium ionophore.

In patients with A1ATD, the largest number of fragments identified were from fibrinogen, followed by haemoglobin subunits alpha and beta. In contrast, in healthy

control subjects, far fewer peptides from fibrinogen were identified; the largest number of fragments were from haemoglobin (subunits alpha and beta), albumin and transthyretin. Pie charts summarizing this data are presented below in Figure 5.5. The charts show the top 8 proteins identified in each group, together with the proportion of peptides for each protein.

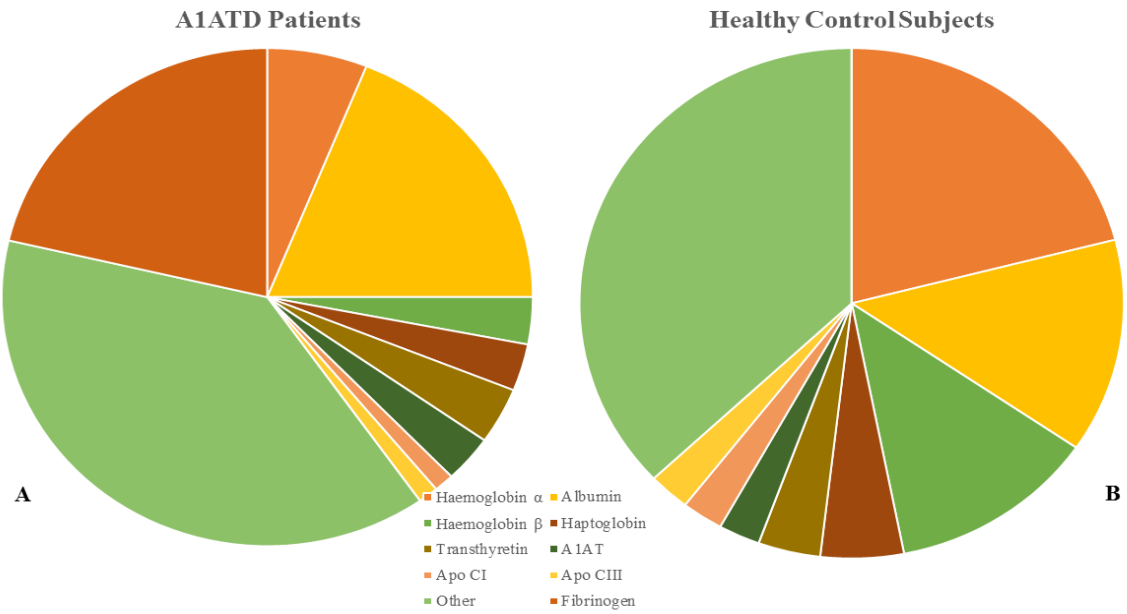

Figure 5.5 shows the origins of the most abundant peptides found in (A) plasma from patients with A1ATD and (B) healthy control subjects post addition of ionophore.

The azurophil granules of neutrophils contain multiple enzymes. Two important enzymes implicated in the underlying pathophysiology of COPD are neutrophil elastase (NE) and proteinase 3 (PR3). Ionophore stimulates the release of these proteolytic enzymes from the neutrophils. Further work therefore was undertaken to determine whether adding NE or PR3 to the plasma of patients with A1ATD could generate the fragments of fibrinogen identified in the ionophore experiments.

5.4 Neutrophil Elastase and Plasma

The following spectra were generated following the addition of NE to pooled plasma from patients with A1ATD pre augmentation and healthy control subjects. (Figure 5.6). As was seen with the addition of calcium ionophore, there were visual differences between the spectra of healthy subjects and those of patients with A1ATD, with a greater numbers of peaks with greater peak intensities in the patient plasma when compared to that of the healthy control subjects. The spectra below were generated following the SPE C8 cartridge sample preparation method; similar differences were obtained when the WCX bead method was used.

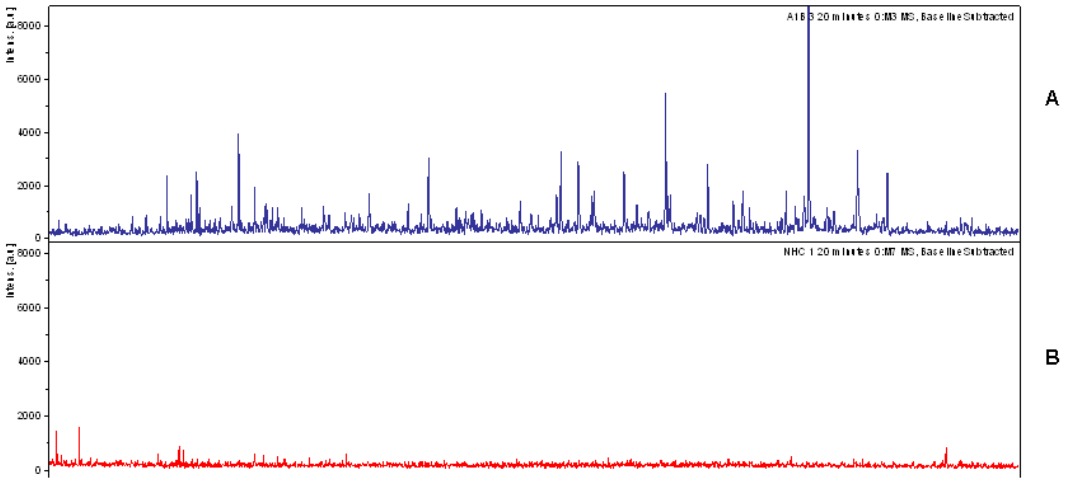

Figure 5.6 Spectra generated post addition of neutrophils elastase to pooled plasma from patients with A1ATD (A) and pooled plasma from healthy control subjects (B), using SPE C8 cartridge sample preparation method.

LC-MALDI was performed in triplicate and subsequent data analysis of the peptides generated by the addition of NE to plasma identified 632 unique peptides from 40 proteins. The single protein contributing the largest number of peptides was fibrinogen, with 134 peptides identified (21.2% of the total). Of these, the majority were fragments from the alpha chain (93) with (28) from the gamma chain and a 13 from the beta chain.

Seventy four of the peptides generated by NE were also generated by ionophore and 41 of these peptides (or 55%) were peptide fragments of fibrinogen.

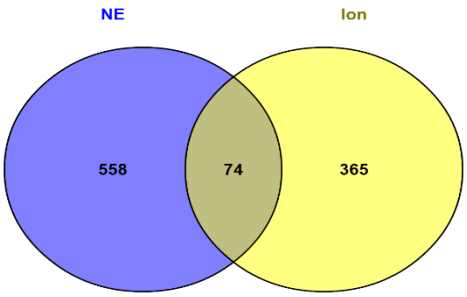

Figure 5.7 shows the total numbers and overlap between peptides generated following the addition of NE and ionophore to plasma and blood of patients with A1ATD

The venn diagram above (Figure 5.7) shows the overlap between the peptides produced from plasma from patients with A1ATD treated with ionophore and those from the addition of elastase. It also suggests that other proteases contribute to the observed ionophore effect.

5.5 Proteinase 3 and Plasma

Following the addition of PR3 to plasma from patients with A1ATD and to healthy control subjects, the following spectra were generated (Figure 5.8). As was seen with the addition of calcium ionophore and NE experiments, there were clear differences between the spectra from patients and controls, in terms of the number and intensity of the peaks present.

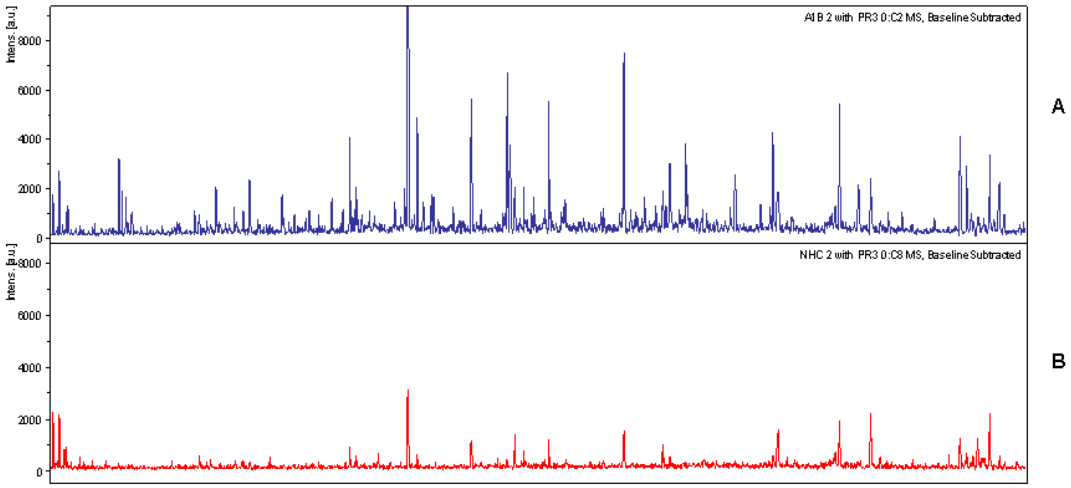

Figure 5.8 Spectra generated post addition of proteinase 3 to pooled plasma from patients with A1ATD (A) and pooled plasma from healthy control subjects (B).

LC-MALDI was performed in triplicate and subsequent data analysis identified 476 unique peptides from 37 proteins following the addition of PR3 to pooled plasma from patients with A1ATD. The single protein contributing the largest number of peptides was apolipoprotein A1 (89 peptides, 18.7%). The second protein was fibrinogen with 72 fragments (or 15.1%) identified. Of these fragments of fibrinogen, 39 were from the alpha chain, 7 were from the beta chain and 26 were from the gamma chain.

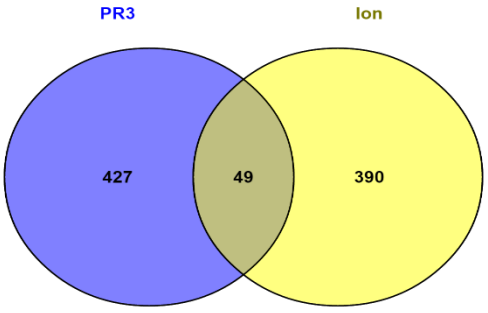

Figure 5.9 shows the total numbers and overlap between peptides generated following the addition of PR3 and ionophore to plasma and blood of patients with A1ATD

The venn diagram above (Figure 5.9) shows the number of peptides produced from blood treated with ionophore, following the addition of PR3 to plasma and the number generated by both. Of the 49 peptides produced by both ionophore and PR3, the majority (20 peptides, 40.8%) were fragments of fibrinogen.

5.6 Comparison of Ionophore, NE and PR3

The diagram below (Figure 5.10) demonstrates that 34 common peptides were generated following the addition of ionophore, NE and or PR3 to pooled plasma/whole blood from patients with A1ATD. A complete table of the m/z and peptide sequences from each of these experiments is shown in Appendix I. Of these 34 peptides, 16 (47.1%) were fragments of fibrinogen, and 10 (31.3%) were fragments of apolipoprotein.

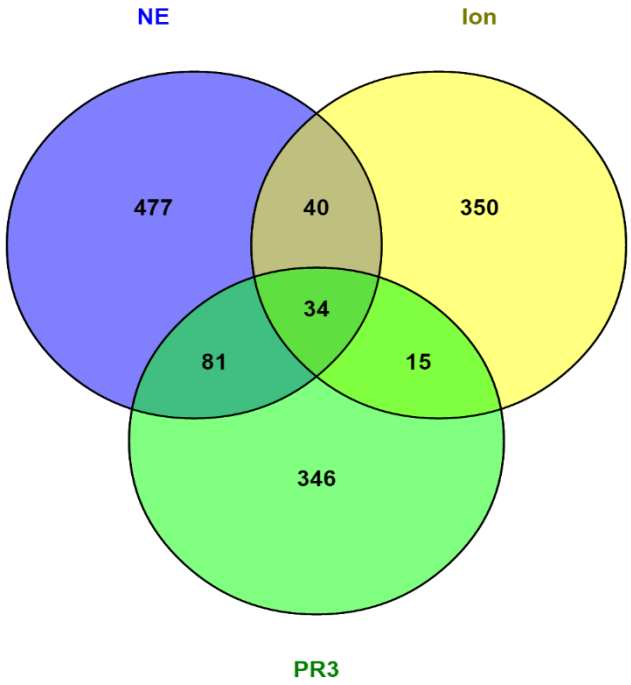

Figure 5.10 Ion is ionophore, NE is neutrophil elastase and PR3 is proteinase 3. The numbers denote the numbers of peptides generated by the addition of each enzyme to pooled plasma/blood from patients with A1ATD.

Of the 115 peptides common to both NE and PR3, the majority of peptides were from apolipoprotein (46 peptides, 45.1%). The next most abundant protein/peptides common to both of these enzymes was fibrinogen (26 peptides, 22.6%).

Table 5.4 shows the fragments of fibrinogen which were identified from the profiling experiments as changing significantly between the 2 groups studied (pre and post stimulation with ionophore), and which enzyme, identified from subsequent analyses, was responsible for generating them.

m/z	Sequence	NE	PR3	Ionophore
1349.6	D.SGEGDFLAEGGGVR.G			Yes
1450.6	R.GDSTFESKSYKMA.D			Yes
1703.1	V.SETESRGSESGIFTNT.K		Yes	Yes
1487.7	V.SETESRGSESGIFT.N	Yes	Yes	Yes
1872.6	Y.KMADEAGSEADHEGTHST.K			Yes
2031.6	T.LDGFRHRHPDEAAFFDT.A	Yes		Yes
2047.8	V.SETESRGSESGIFTNTKES.S	Yes	Yes	Yes
2133.6	V.SGNVSPGTRREYHTEKLVT.S	Yes	Yes	Yes
2212.3	T.KESSSHHPGIAEFPSRGKSSS.Y			Yes
2219.8	V.SGNVSPGTRREYHTEKLVTS.K			Yes
2732.7	G.SFRPDSPGSGNARPNNPDWGTFEEV.S	Yes		Yes

Table 5.4 shows the fibrinogen fragments which were identified as changing significantly in the profiling experiments following addition of ionophore, and which enzyme was responsible.

NE and PR3 are both serine proteases which have similar 3 dimensional structures and similar functionality (Korkmaz B 2002). During LC-MALDI, 24.2% of peptides generated by the addition of PR3 to plasma were identical to those generated by the

addition of NE to plasma. In order to determine further information about the specific cleavage sites of each enzyme, the peptide sequences were uploaded in to the web based programme 'WebLogo 3.4' to generate sequence logos of the amino acids in the peptides generated by the addition of each of the enzymes. These are shown below for each of NE, PR3 and ionophore. A sequence logo is a way of graphically displaying amino acid sequences in peptides. At each position in the amino acid, a stack is generated; the amino acids are represented by the internationally accepted single letter, and the height of each letter within the stack denotes the relative frequency of the amino acid at that site in the peptide sequence.

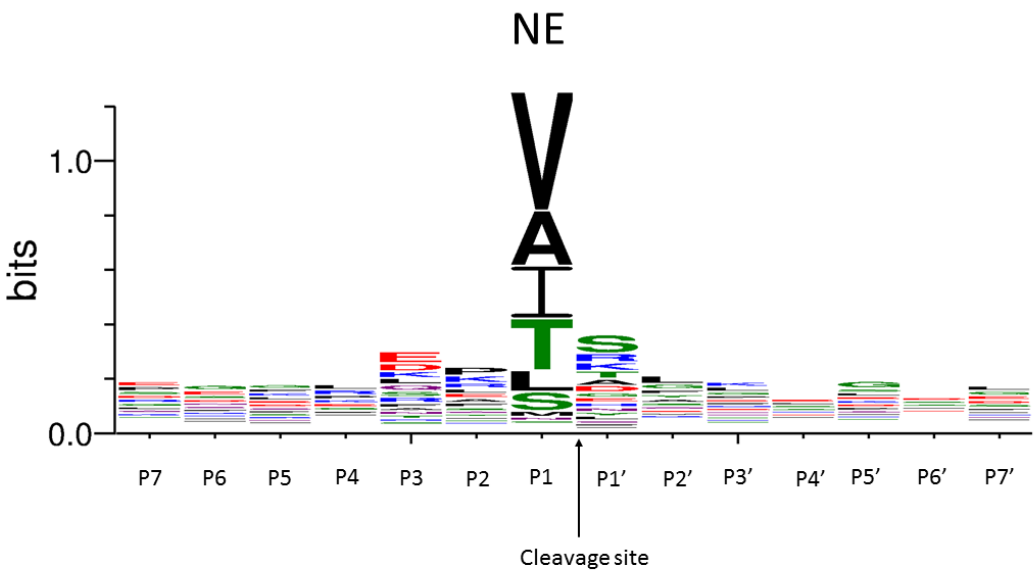

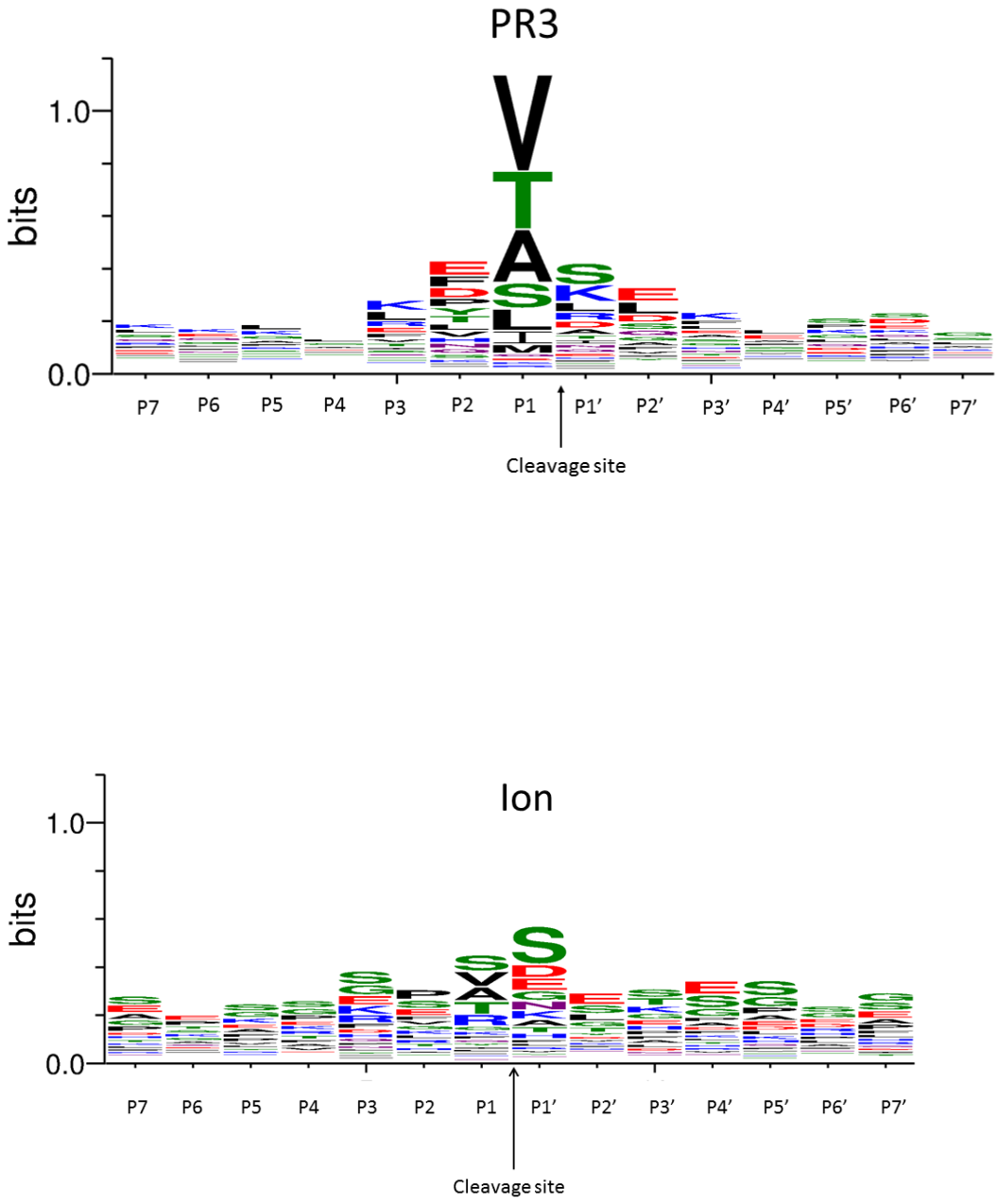

Figure 5.11 Sequence Logos for the Addition of Neutrophil Elastase (NE), Proteinase 3 (PR3) and Ionophore (Ion)

The sequence logos above demonstrate that the preferential amino acid cleavage sites for NE and PR3 are valine and alanine residues, and the top 7 preferred amino acids for each enzyme are the same. This is in agreement with published work which describe

the reportedly preferred cleavage sites for NE and PR3 as being valine and alanine residues. The ionophore logo suggests that neither NE nor PR3 are overwhelmingly responsible for the generation of peptides upon ionophore stimulation as the preferred cleavage site is at serine residues. This is likely to result from the large number of other enzymes which are found in the neutrophil azurophil granule, which include myeloperoxidase (Borregard N, 1997) in addition to NE, PR 3 and cathepsin G, and it is these other enzymes in combination which are responsible for the preferred cleavage site demonstrated in the web logo.

5.7 Discussion

This work uniquely describes the action of enzymes released from the azurophil granules of neutrophils as part of an *in vitro* model of the underlying pathophysiology of A1ATD. Calcium ionophore stimulates neutrophils, causing the release of proteolytic enzymes. Of these enzymes, NE is perceived to be one of the most crucial in the pathophysiology of disease in A1ATD. However, NE is not the only enzyme released from activated neutrophils. Upon stimulation with calcium ionophore, other enzymes such as proteinase 3 and cathepsin G are also released, and hence the rationale for undertaking further work on plasma from patients with A1ATD using PR3 and NE.

The work has highlighted the effects of proteases released by calcium ionophore in the plasma of patients with A1ATD, when compared to that of healthy control subjects. Fibrinogen is the source of the most commonly identified peptides in patients with A1ATD, whereas in healthy control subjects, the protein with the most identified peptides was haemoglobin. This suggests that A1AT inhibits some proteases released

from neutrophils but not others. The reasons for this observation are not clear; it may be due to the actions of calcium ionophore being different in the relative absence of a major protease inhibitor (namely A1AT) as is the case in patients with A1ATD, as it is possible that A1AT prevents fibrinogen degradation, or potentially due to higher baseline levels of fibrinogen in patients with A1ATD (although this was not measured directly).

The addition of calcium ionophore has identified several fragments of fibrinogen (although there were also peptides which remain unidentified due to either their size being greater than 4000 Da and their lower abundance in plasma) which could be potential markers of the actions of NE. It has also been possible to show the peptides generated following the addition of NE and PR3 to plasma, and show which fragments from the ionophore data were likely to have arisen as a result of the actions of each of these enzymes. A few peptides (3) were common to both of these enzymes.

Fibrinogen is of interest for several reasons; firstly, as is the case with A1AT, it is a positive acute phase protein. It is a precursor of fibrin and an essential component of the plasma coagulation cascade (Kamath et al., 2003). In acute inflammatory states, its concentration in plasma may rise up to three-fold when compared with the normal steady state.

Fibrinogen has previously been extensively investigated as a potential biomarker in usual COPD (Dahl et al., 2001; Groenewegen et al., 2008; Mannino et al., 2012). As is true for A1AT, it is released from the liver in response to IL6 production (Gabay et al., 1999). Fibrinogen has been shown to be elevated in COPD patients when compared to

healthy control subjects, though not related to smoking status (Dahl et al., 2001). Groenewegen et al analysed plasma fibrinogen levels in patients with COPD, and reported that higher levels of fibrinogen were measured in patients during exacerbations of their COPD, and demonstrated a subsequent fall on resolution of the exacerbation (Groenewegen et al., 2008). In small studies, this elevation of fibrinogen was more evident amongst patients with infective exacerbations, with a greater rise in plasma fibrinogen when a viral pathogen was isolated (Seemungal et al., 2001).

In the stable state, higher levels of fibrinogen were associated with a lower FEV_1 and more moderate to severe exacerbations in patients with usual COPD. These are independent factors for a more rapid decline in lung function and therefore patient performance status, symptoms and subsequent worsening disease trajectory. It has also been suggested as a marker to predict hospitalisation as a result of COPD exacerbations (Groenewegen et al., 2008).

In a 2005 meta-analysis which included 154 211 patients, Danesh et al identified during that an increased fibrinogen level was associated with an increased risk of death, from both vascular disease and COPD. In addition, Mannino et al in 2012 demonstrated that amongst 8507 patients from the Third National Health and Nutrition Examination Survey (NHANES III), overall, elevated plasma fibrinogen levels were a risk for increased all-cause mortality, including for patients with COPD. In addition, patients with COPD in GOLD stages 3 or 4 had higher levels of fibrinogen than people with normal lung function.

Furthermore, an elevated plasma fibrinogen level was demonstrated by Papaioannou et

al in a small group of patients with emphysema demonstrated on CT scan when compared to a group of patients without emphysema present on the scan (Papaioannou et al., 2010).

An integrated analysis of 5 separate studies (6376 patients were included) was performed in order to gain recognition of the use of fibrinogen as a biomarker in COPD (Mannino et al., 2015). The authors looked specifically at fibrinogen levels, and stratified patients into 2 groups – those with high fibrinogen levels (defined as concentrations greater than 350mg/dL) and those with low levels (below 350mg/dL). Those patients with higher plasma fibrinogen levels, had a higher rate of severe exacerbations, within 12 months, of their COPD requiring admission to hospital, and a greater mortality rate within the next 36 months due to all causes, supporting previous reports (Mannino et al., 2015). Both of these outcomes are clinically relevant in patients with COPD in clinical practice and when considering endpoints in clinical trials.

In summary therefore, in usual COPD, fibrinogen shows promise as a biomarker in COPD. An elevation in plasma fibrinogen levels of COPD patients is associated with a higher risk of both exacerbation and all-cause mortality. However, it is not specific for COPD, as it may be elevated in other diseases such as cardiovascular disease (Pearson et al., 2003) and the metabolic syndrome (Ford, 2003), both of which are common co-morbidities in patients with COPD, and inflammatory states. There have been no studies to date to explore this relationship in patients with A1ATD.

However, each of these studies have measured total fibrinogen concentrations, rather than peptides or fragments of fibrinogen. In patients with COPD and A1ATD related

COPD, a specific cleavage product of fibrinogen termed Aα-val 360, which is a marker of pre-inhibition activity of NE, has been studied as a potential biomarker. It has been shown, by Carter et al, to be elevated in patients with A1ATD when compared to healthy control subjects, to increase further during acute exacerbations, and to decrease following treatment with augmentation therapy. In patients in the EXACTLE study who received placebo infusions rather than active drug, there was a statistically non-significant rise in this signal at the end of the 6 months' of treatment, and a significant decrease in patients who were given Prolastin (intravenous A1AT) (Carter et al., 2011).

This is of particular interest as the enzyme experiments performed initially with calcium ionophore demonstrated a clear difference in the detected actions on the plasma peptidome of patients with A1ATD when compared to the healthy control patients; the major peptides detected in patient plasma were fragments of fibrinogen, whereas this was haemoglobin and other abundant plasma proteins in the healthy control group. Fibrinogen degradation is likely to be dysregulated in A1ATD patients due to the low level of this major serine protease inhibitor. Disappointingly, the fragment of Aα-val 360 was not detected in this series of experiments.

5.8 Conclusions

Potential markers of NE and PR3 activity in plasma have been identified using this approach, and therefore the same profiling methods were undertaken in subsequent work on clinical samples in patients with A1ATD pre and post treatment with A1AT augmentation to determine whether or not the fibrinogen peptides identified could act as biomarkers and be measured by targeted tandem mass spectrometry.

CHAPTER 6 ENDOGENOUS PLASMA PEPTIDE PROFILING

The experiments in the previous chapter identified several fragments of fibrinogen which may act as markers of NE activity in an *in vitro* environment. The following series of experiments were conducted on samples from clinical trials of augmentation therapy in patients with A1ATD to determine whether the previous experiments had identified clinically relevant markers of NE activity.

6.1 Patient Demographics ECLIPSE A1ATD

The demographic data of the patients enrolled into the ECLIPSE A1ATD study are shown in table 6.1. Patients with usual COPD and A1ATD were well matched in terms of lung function parameters, but patients with A1ATD were significantly younger (57.2 years vs 66.6 years, p= 0.03). This is consistent with the observation that patients with A1ATD typically develop symptoms at an earlier age (in their 40s) than patients with usual COPD. There was no significant age difference between healthy control subjects and patients with usual COPD. Healthy control subjects had normal lung function parameters, whereas patients with A1ATD or usual COPD had evidence of airflow obstruction, with an FEV_1/FVC ratio < 70%, consistent with the diagnosis of COPD. There was evidence of reduced gas transfer parameters, (TLCO and KCO), consistent with the presence of emphysema, which is associated with both the diagnosis of COPD and COPD secondary to A1ATD. The groups were all predominantly male. Patients with usual COPD and healthy control subjects had normal serum A1AT levels and normal A1AT genotypes, excluding a concomitant diagnosis of A1ATD, whereas those with A1ATD had low levels (below the putative protective threshold of 11µM) and the PiZZ genotype, consistent with the diagnosis of A1ATD. All patients/control subjects were ex or never smokers, which was one of the main inclusion criteria for entry into

this particular study. However, there were more ex-smokers in the A1ATD group and usual COPD group, whereas the majority of the healthy control subjects (6 out of 9 or 66.7%) had never smoked.

	A1ATD	COPD	NHC
N	10	9	9
Male: Female	9:1	8:1	7:2
Age in Years	57.2 (2.9)	66.6 (2.0) *	61.0 (2.4)
FEV_1 (L)	1.7 (0.2)	1.8 (0.3)	3.4 (0.2) ** ##
FEV_1 % Predicted	51.5 (5.7)	59.7 (6.1)	112.3 (3.3) ** ##
FVC (L)	4.7 (0.3)	4.0 (0.3)	4.5 (0.3)
FVC % Predicted	114.5 (5.2)	106.8 (2.2)	118.5 (4.3)
FEV_1/FVC	33.9 (3.4)	42.5 (4.3)	75.5 (2.3) ** ##
TLCO	5.6 (0.7)	4.6 (0.9)	9.1 (0.6) * #
TLCO % Predicted	58.8 (7.3)	54.7 (9.0)	101.1 (5.1) ** #
KCO % Predicted	60.5 (6.8)	63.8 (7.9)	105.7 (5.9) ** ##
A1AT Level (µM)	4.04 (0.5)	28.4 (2.6)	26.5 (0.9) **
Ex-smokers	9 (90%)	9 (100%)	3 (33.3%) ** ##
Never smokers	1 (10%)	0 (0%)	6 (66.7%) ** ##

Table 6.1 shows the demographic data for patients in the ECLIPSE A1ATD study.
A1ATD denotes patients with alpha-1-antitrypsin deficiency, COPD refers to patients with chronic obstructive pulmonary disease, and NHC is the normal healthy control group.
Mean age is presented (SEM). Forced expiratory volume in 1 second, (FEV_1) and forced vital capacity (FVC) are mean data expressed in litres (SEM). Transfer factor of the lung to carbon monoxide (TLCO) is measured in mmol/min/kPa – the mean value is shown (SEM). KCO is transfer of carbon monoxide corrected for alveolar volume - the mean values are shown (SEM). The FEV_1 % predicted, FVC % predicted, TLCO % Predicted and KCO (transfer of carbon monoxide corrected for alveolar volume) are the mean data for FEV_1, FVC, TLCO and KCO expressed as a percentage. A1AT is the mean level (with SEM in parentheses).

*** is a p value of < 0.05 when comparing either healthy control subjects or COPD patients with A1ATD patients, ** is a p value of < 0.01 for the same group comparisons.**
 # is a p value of < 0.05 when comparing COPD patients to healthy controls, ## is a p value of < 0.01 for the same group comparisons

6.2 Patient Demographics EXACTLE

The demographic data for the patients enrolled in to the EXACTLE trial, whose plasma samples were analysed in this work are shown in table 6.2. The patients in the Prolastin (intravenous A1AT) and placebo groups were well matched with the exception of the A1AT level at 6 months, which was elevated to above the putative protective level of 11μM in the patients who received the active drug, whilst remaining constant and well below this level in patients receiving placebo infusions. This is consistent with previous work, which has demonstrated that the trough levels, following weekly infusions, remain above this protective level (Wewers et al., 1987). There was no significant difference in the A1AT levels between the groups at baseline. The mean FEV_1 in both groups was 46.4%, which is classified as moderate disease according to the GOLD criteria for the diagnosis of COPD, and the mean FEV_1/FVC ratios were 41% in both groups, again consistent with this diagnosis. All patients had reduced gas transfer measurements, consistent with the presence of emphysema, with mean KCO % predicted values of 53.7% and 55.8% for the active drug and placebo groups respectively.

Overall, there were almost equal numbers of male and female patients recruited into the EXACTLE study (37 v 35). However, there was a trend towards more men in the group receiving Prolastin (intravenous A1AT), and more females in the placebo group, although this was due to the randomisation process and did not reach conventional statistical significance ($p = 0.055$). The smoking history in both patient groups was similar; the majority of patients had previously smoked. As was the case with the ECLIPSE A1ATD study, none of the patients were current active smokers in accordance with the study protocol.

	Prolastin Group (A1AT)	Placebo Group	Overall
UK Patients	13	10	23
Swedish Patients	8	8	16
Danish Patients	15	18	33
Age in years	55.6 (1.3)	55.1 (1.6)	55.3 (1.7)
Male : Female	22 : 12	15 : 23	37 : 35
FEV_1 (L)	1.4 (0.1)	1.3 (0.1)	1.4 (0.1)
FEV_1 % Predicted	46.4 (3.2)	46.4 (3.4)	46.4 (2.4)
FVC (L)	3.7 (0.2)	3.5 (0.1)	3.6 (0.1)
FVC % Predicted	95.6 (3.7)	97.1 (3.9)	96.4 (2.7)
FEV_1/FVC Ratio	41.0 (2.9)	41.0 (2.8)	41.0 (2.0)
TLCO (mmol/min/kPa)	4.5 (0.4)	4.7 (0.3)	4.6 (0.2)
TLCO % Predicted	49.3 (3.3)	52.2 (2.5)	50.9 (2.0)
KCO % Predicted	53.7 (3.5)	55.8 (2.5)	54.8 (2.1)
Baseline A1AT Level (µM)	7.47 (0.6)	6.87 (0.4)	7.2 (0.4)
A1AT Level at 6 Months (µM)	15.2 (0.9) **	8.31 (0.8)	NA
Never smokers	3 (9%)	2 (6%)	5 (8%)
Ex-smokers	33 (91 %)	34 (94%)	67 (92%)

Table 6.2 shows the demographic data of the patients in the EXACTLE trial.

Age is expressed in years (SEM in parentheses). Forced expiratory volume in 1 second, (FEV_1) and forced vital capacity (FVC) mean data expressed in litres, (SEM in parentheses). Transfer factor of the lung to carbon monoxide (TLCO) mean data are shown (SEM in parentheses). KCO is transfer of carbon monoxide corrected for alveolar volume mean data is shown (SEM in parentheses). FEV_1 % predicted, FVC % predicted, TLCO % predicted and KCO% predicted are the mean data for FEV_1, FVC, TLCO and KCO expressed as a percentage. Mean A1AT levels (SEM in parentheses) are presented

**** denotes significant difference between Prolastin group and placebo groups with a p value < 0.01**

A comparison of demographic data between the ECLIPSE A1ATD group of patients and all of the patients in the EXACTLE study is shown in table 6.3. There were no significant differences between patients enrolled in to either study in terms of age or

lung function. There was a higher proportion of male patients in the ECLIPSE A1ATD study, (9 patients (90%) versus 36 (50%) respectively), and the ECLIPSE A1ATD patients had lower levels of A1AT at baseline). However, this may be due to differences in the assay used to measure the A1AT levels. The EXACTLE study patients had their A1AT levels measures in mg/dL, and these values were subsequently converted to μM, whereas patients in the ECLIPSE A1ATD study has levels measured in μM. However, all patients had the most severe deficiency of A1ATD (the PiZZ genotype), and had A1AT levels below the putative protective threshold of 11μM (mean 4.02 and 6.2 μM respectively for the ECLIPSE A1ATD and EXACTLE patients). The post treatment values were measured in the EXACTLE study but not in the ECLIPSE A1ATD due to differences in the study protocols (post treatment A1AT levels were not a requirement of the ECLIPSE A1ATD study). However, previous work has clearly demonstrated that a weekly infusion at the dose given to both of these patient groups, leaves a trough level above 11 μM, thus making the measurement of A1AT unnecessary after 3 months of treatment in the ECLIPSE A1ATD study (Wewers et al., 1987).

	ECLIPSE A1ATD	EXACTLE
Age	57.2 (2.9)	55.3 (1.7)
FEV_1 (L)	1.7 (0.2)	1.4 (0.1)
FEV_1 % Predicted	51.5 (5.7)	46.4 (2.4)
FVC (L)	4.7 (0.3)	3.6 (0.1) **
FVC % Predicted	114.5 (5.2)	96.4 (2.7) *
FEV_1/FVC	33.9 (3.4)	41.0 (2.0)
TLCO	5.6 (0.7)	4.6 (0.2)
TLCO % Predicted	58.8 (7.3)	50.9 (2.0)
KCO % Predicted	60.5 (6.8)	54.8 (2.1)
Male	9 (90%)	36 (50%) **
Never smokers	1 (10%)	5 (8%)
Ex-smokers	9 (90%)	67 (92%)
A1AT Baseline Level (µM)	4.0 (0.4)	6.2 (0.4) *

Table 6.3 shows the comparison between the demographics of the patients in the ECLIPSE A1ATD study and the EXACTLE study.

Mean age is presented, (SEM in parentheses). Forced expiratory volume in 1 second, (FEV_1) and forced vital capacity (FVC) mean data expressed in litres, (SEM in parentheses). Transfer factor (TLCO) mean values for the groups are shown (SEM in parentheses). KCO mean values for the groups are shown (SEM parentheses). The FEV_1 % predicted, FVC % predicted, TLCO % predicted and KCO% predicted are the mean data for FEV_1, FVC, TLCO and KCO expressed as a percentage. A1AT levels were measured in µM, and the mean values shown (with SEM in parentheses).

*** denotes a significant difference between the groups with a p value < 0.05**

****denotes a significant difference between the groups with a p value <0.01**

6.3 ECLIPSE A1ATD Plasma Sample Inclusion

During the initial MALDI profiling of the ECLIPSE A1ATD plasma samples, it was evident that 2 of the A1ATD patients had baseline samples which were different from the remainder of the samples; the spectra generated using these samples contained a dominant peak with an m/z ratio of 5900kDa. This peak (from previous published data

from Ward et al., 2010) was likely to be a fragment of fibrinogen, which is commonly seen as an intense peak in serum samples, whilst being virtually absent from plasma. It was likely that the presence of this peak represented a degree of haemolysis and clotting within the samples at the time of the sample collection. These samples (both pre and post augmentation) were therefore removed from further analysis, leaving total numbers of patients in each group of 8 patients with A1ATD pre and post augmentation therapy, 9 COPD patients and 9 healthy control subjects. The haemolysed samples were also not included in the pooled sample analysis during the more in depth shotgun work (chapter 7).

6.4 ECLIPSE A1ATD Urine Collection

Urine samples were collected in sterile sample pots from the patients and control subjects recruited to the ECLIPSE A1ATD trial. For healthy control subjects and patients with usual COPD, the samples were taken at the screening visit. For patients with A1ATD, samples were collected at the screening visit and at immediately before the final infusion of Prolastin.

6.4.1 Urinary Protein Concentration Determination

The urinary protein content of the ELCIPSE A1ATD samples was measured as per the method described in chapter 2.7.1. There was a wide variation in the urine protein concentration of the samples from 30 to 80 µg/mL. This did not vary according to the treatment group to which the individual patients belonged. The protein concentration therefore was standardised to 30 µg/mL prior to sample preparation, by dilution with de-ionised water. All of the patients and healthy control subjects had both normal renal function parameters and plasma albumin levels, and did not have any other medical

history of conditions affecting the renal tract or evidence of significant proteinuria, which could potentially influence the results of this experiment.

6.4.2 Urine Supel Tip Results

The diluted urine samples were prepared in duplicate using the supel tip method described in chapter 2.7.2. Data from duplicate experiments were analysed independently, following log transformation to normalise the distribution of the data, then the mean value for each of the peak intensities for each study subject was calculated and the data re-analysed. There were 171 peaks in the MALDI spectra, and the intra-experiment CV for the QC sample was 14%. Using ANOVA, there were only 8 peaks which differed between the 3 patient groups (A1AT, COPD and healthy control subjects) with a p value of < 0.05. Using paired analysis, there was only 1 peak which differed between A1ATD samples at baseline and at the end of 3 months of treatment, (m/z ratio 5555.8 Da and a p value of 0.004). The m/z of this peptide was >4000 Da, and therefore not possible to identify the protein origin of the peptide using MS/MS with the Ultraflextreme. The remainder of the results are shown below in tables 6.4 and 6.5.

m/z	p Value	Baseline v COPD	Baseline v NHC	COPD v NHC
1520.8	0.0034	0.071	0.0053	0.953
3842.1	0.0016	0.0012	0.268	0.376

Table 6.4 shows the results of the ECLIPSE A1ATD ANOVA analysis of urine, between A1ATD at baseline, COPD and normal healthy control subjects (NHC)

m/z	p Value	Post Treatment v COPD	Post Treatment v NHC
3842.1	0.001	0.001	0.531
4026.6	0.013	0.01	0.19
4930.9	0.005	< 0.001	0.852
5530.4	0.006	0.004	0.135
5555.8	0.002	0.002	0.625
6655.8	0.008	0.006	0.118
8241.9	0.002	0.001	0.097

Table 6.5 shows the results of the ECLIPSE A1ATD ANOVA analysis of urine data, between A1ATD post 3 months of treatment and COPD and normal healthy control subjects (NHC)

There were few differences in the urinary peptidome between these groups of patients, and of those peaks which were significantly different, the majority (7) were above 4000Da, making them above the threshold to identify using MS/MS with this mass spectrometer. There were more changes post treatment (7 v 2), and these were differences between patients with A1ATD and COPD patients.

Following LC-MALDI of the pooled urine samples, it was also possible to use comparative analysis software (Profile Analysis Software (Bruker Daltronics)) to analyse the peak intensities from the LC-MALDI data, and this did not reveal any further additional differences to those listed above. It was therefore felt that there were too few changes present between patients pre and post augmentation therapy, and between patients with A1AT pre-treatment compared to COPD or healthy control subjects, to warrant further in depth urine investigation in these patient groups. In addition, there were no urine samples collected during the EXACTLE study, as this was not part of the study protocol, to use as a validation of potential findings from the ECLIPSE A1ATD samples. Therefore, we concluded that the MALDI analyses of the urinary peptidome did not reveal any disease associated changes worthy of further investigation.

6.5 Plasma Reverse Phase SPE C8 Cartridge Data

Plasma from both the ECLIPSE A1ATD study and EXACTLE study were profiled using SPE C8 cartridges and the data for each series of experiments is presented below.

6.5.1 ECLIPSE A1ATD Results

Typical spectra from the ECLIPSE A1ATD study processed and analysed using SPE C8 cartridges are shown in Figure 6.1. Individual ECLPISE A1ATD samples were processed singly using the SPE C8 cartridges, but spotted on to the MALDI plate in triplicate and the mean peak intensities used. The data presented below is the average of the linear MALDI TOF MS data.

There were a total of 247 peaks within the spectra. A QC sample was analysed and the intra-experiment CV of the QC sample was 15%. The data was analysed in 2 ways after log transformation to achieve normal distribution of data; firstly a paired analysis was performed on the pre-treatment and post treatment samples (Table 6.6), followed by ANOVA between the A1ATD baseline samples with COPD data and healthy control sample data (Table 6.7), and ANOVA between the post treatment data compared to healthy controls and COPD samples (Table 6.8).

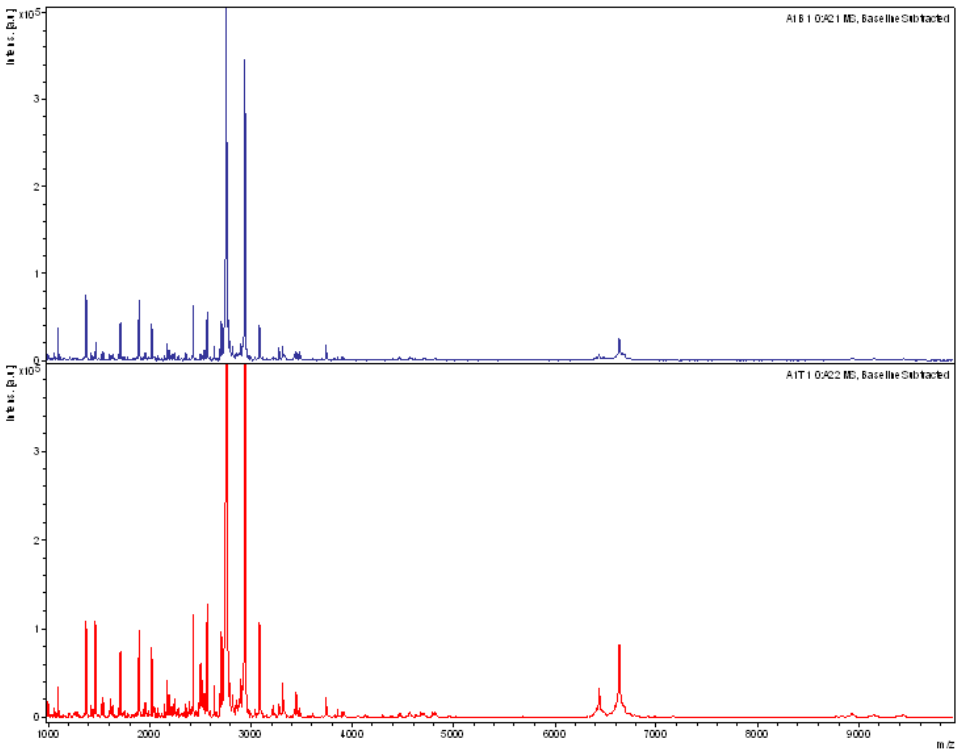

Figure 6.1 Spectra from a patient with A1ATD pre (A) and post treatment (B) from the ECLIPSE A1ATD study post sample preparation with SPE C8 cartridges.

m/z	p Value	Protein	Sequence	Median Base	Median End	Fold Change
1099.4	0.0033	Complement C3	I.HWESASLLR.S	10.60	6.37	0.60 ↓
1564.4	0.0019	Albumin	R.DAHKSEVAHRFKDL.G	0.79	0.62	0.79 ↓
1607.4	0.0028			1.73	1.2	0.69 ↓
1738.2	0.0094	Complement C4	R.NGFKSHALQLNNRQI.R	1.46	1.17	0.80 ↓
1935.9	0.00040	Complement C3	S.SKITHRIHWESASLLR.S	2.86	1.81	0.63 ↓
2022.9	0.0069	Complement C3	R.SSKITHRIHWESASLLR.S	30.29	23.94	0.79 ↓
2038.6	0.0048	Transthyretin	A.ALLSPYSYSTTAVVTNPKE.-	1.45	1.19	0.82 ↓
2392.2	0.0016	A1AT	L.MIEQNTKSPLFMGKVVNPTQK.-	0.81	2.27	2.27 ↑
2491.1	0.0023			0.52	1.72	3.34 ↑
2505.6	0.00040	A1AT	F.LMIEQNTKSPLFMGKVVNPTQK.-	1.51	6.68	4.42 ↑
2521.5	0.00079			1.27	4.60	3.63 ↑
2537.3	0.0024	Complement C3	G.SPMYSIITPNILRLESEETMVL.E	1.07	1.56	1.45 ↑
4679.7	0.00039			0.85	1.56	1.85 ↑
4781.3	0.00096			0.40	0.68	1.69 ↑
4791.9	0.00034			0.56	1.18	2.11 ↑
4812.7	0.0083			1.00	1.29	1.30 ↑

Table 6.6. Significant changes pre and post augmentation therapy in patients with A1ATD in the ECLIPSE A1ATD study.

m/z is the mass to charge ratio of peaks which change significantly with treatment. Sequence is the amino acid sequence of the peptide, and protein is the protein from which the peptide originated. The fold change is the end of treatment peak intensity, measured in arbitrary units, divided by the baseline value, and the arrows denote the direction of change.

m/z	p Value	Baseline v COPD	Baseline v Healthy Control	COPD v Healthy Control	Protein	Sequence
2392.2	0.05	0.004	0.008	0.359	A1AT	L.MIEQNTKSPLFMGKVVNPTQK.-
2483.8	0.005	0.004	0.205	0.156		
2505.6	<0.001	<0.001	<0.001	0.534	A1AT	F.LMIEQNTKSPLFMGKVVNPTQK.-
2521.5	<0.001	<0.001	<0.001	0.74		
4679.7	0.005	0.017	0.007	0.927		
4781.3	<0.001	<0.001	0.003	0.494		
4791.9	<0.001	<0.001	<0.001	0.196		
4812.7	0.002	0.001	0.219	0.061		
6487.3	0.006	0.007	0.029	0.807		
6767.7	0.007	0.006	0.046	0.629		
6784.4	0.01	0.014	0.027	0.958		

Table 6.7 shows the results of ANOVA analysis between A1ATD patients at baseline, and COPD and healthy control subjects. m/z is the mass to charge ratio. Sequence is the amino acid sequence of the peptide.

m/z	p Value	Treated v COPD	Treated v Healthy Control	Protein ID	Sequence
2392.2	0.386	0.628	0.913	A1AT	L.MIEQNTKSPLFMGKVVNPTQK.-
2483.8	0.151	0.25	0.988		
2505.6	0.42	0.409	0.914	A1AT	F.LMIEQNTKSPLFMGKVVNPTQK.-
2521.5	0.8	0.924	0.961		
4679.7	0.819	0.809	0.973		
4781.3	0.316	0.351	0.979		
4791.9	0.269	0.727	0.676		
4812.7	0.079	0.425	0.563		
6487.3	0.057	0.054	0.173		
6767.7	0.098	0.083	0.362		
6784.4	0.131	0.144	0.23		

Table 6.8. Results of the ANOVA analysis of the SPE C8 cartridge data between patients with A1ATD after 3 months of treatment and COPD patients and healthy control subjects.

There were 16 peaks in the MALDI spectra which changed significantly pre and post treatment with intravenous A1AT. Of these peaks, the one with the most significant fold change (4.42 increase) is a fragment of A1AT, with an m/z of 2505. This is elevated in the post treatment samples when compared to the baseline. The values for individuals are presented in Figure 6.2, and shows that this effect is seen in each individual patient. Other peaks which also behave in this way are the peaks with m/z ratios of 1607, which decreased in all patients receiving treatment, (a fragment of an unidentified protein) and 2392 which increased in all patients (a further fragment of A1AT); these are also shown in the histograms below.

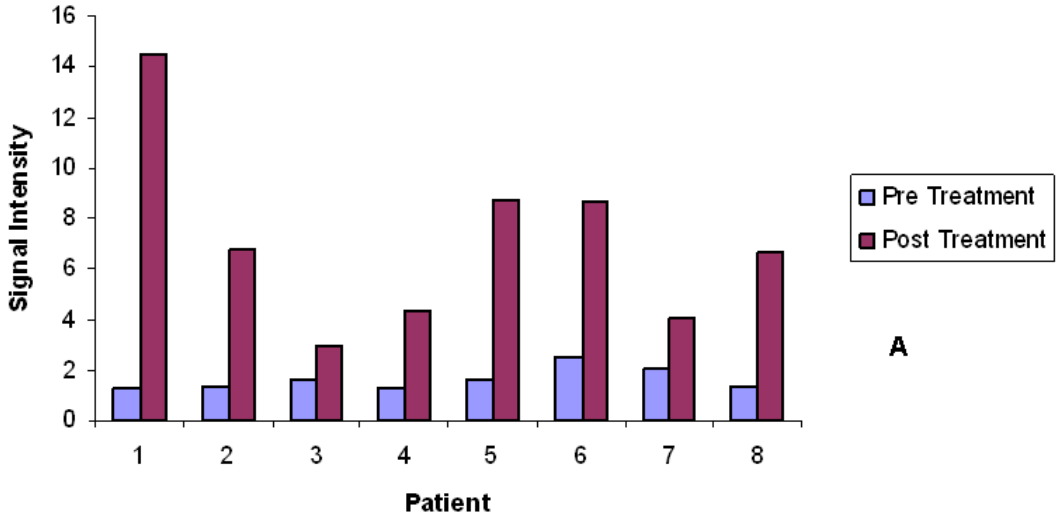

A

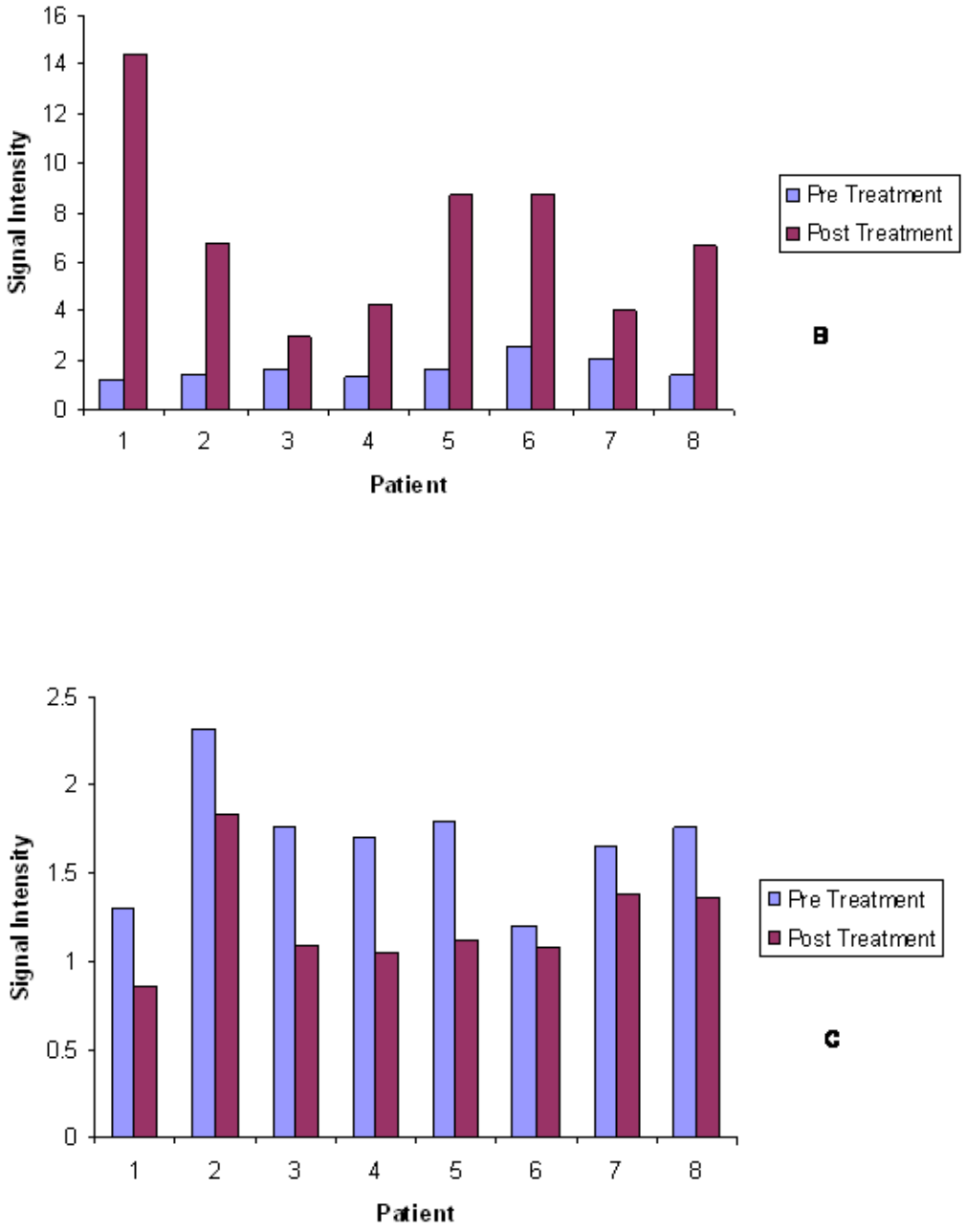

Figure 6.2 Signal intensities for individual patients in the ECLIPSE A1ATD study pre and post treatment with Prolastin for the peaks with the most significant p values and greatest fold change. (A) is a fragment of A1ATD with an m/z of 2392 Da, and (B) is a fragment of A1AT with an m/z of 2505 Da and (C) is a fragment with an m/z of 1607 Da. In A and B, in every patient post treatment, there is an increase in signal intensity post treatment. In C, there is a reduction in signal intensity in each patient post treatment.

In total there were 2 fragments of the A1AT protein identified as changing significantly in response to treatment with intravenous A1AT. The ANOVA data shows that the peak intensities were lower in patients than in all other groups pre-treatment but normalizes with treatment. The results for each individual demonstrating this relationship are shown in figure 6.3.

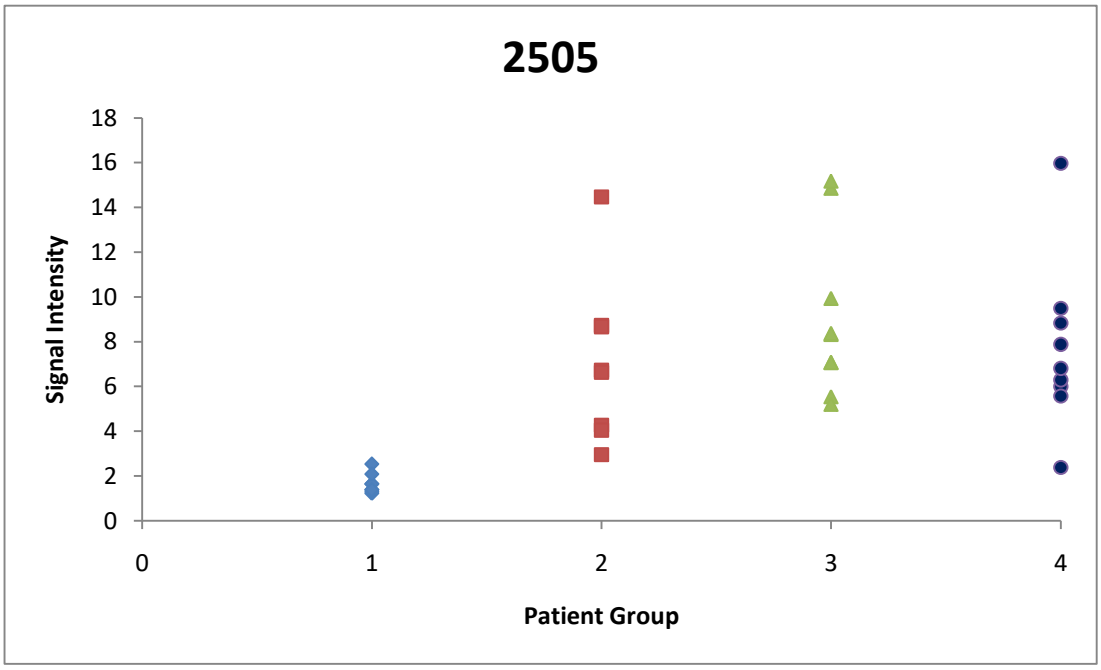

Figure 6.3. Individual peak intensities (in arbitrary units) for the fragment of A1AT with an m/z of 2505. Group 1 are the patients with A1ATD at baseline, group 2 are the patients with A1ATD following 3 months of augmentation therapy, group 3 are the patients with usual COPD, and group 4 are the healthy control subjects.

In total, there were 11 peaks in the MALDI spectra which were significantly different between the 3 groups (patients with A1ATD at baseline, and patients with COPD and healthy control subjects). Post treatment, there are no significant differences between these groups, and there were no new differences identified.

6.5.2 EXACTLE Plasma Peptide Profiling

The EXACTLE samples were prepared and analysed using the same methodology as the ECLIPSE A1ATD samples. There were 215 peaks within the spectra of these

samples, and the intra-experiment CV calculated, on the QC sample was 17%. The samples were spotted onto the MALDI plate and analysed in triplicate, the data log transformed, and the mean of the duplicates calculated and used in further data analyses.

The peaks which changed significantly following treatment with Prolastin are presented below in table 6.9. In total, there were 7 peaks which changed significantly, and in each if these cases, there was an increase in the intensity of the peak post treatment with Prolastin, whilst there was no change post treatment amongst the patients receiving placebo infusions.

The peak intensities for individual patients for the peak with an m/z of 2505, which is one of the peaks with the most significant p value (<0.001) and is a fragment of A1AT, are shown below in figure 6.3. This demonstrates a rise in the intensity of this fragment in patients who receive Prolastin, and remains unchanged in patients in the placebo arm of the trial. The same relationship was seen in the ECLIPSE A1ATD samples, and the fold changes were 4.42 in the ECLIPSE A1ATD samples and 2.20 in the EXACTLE samples.

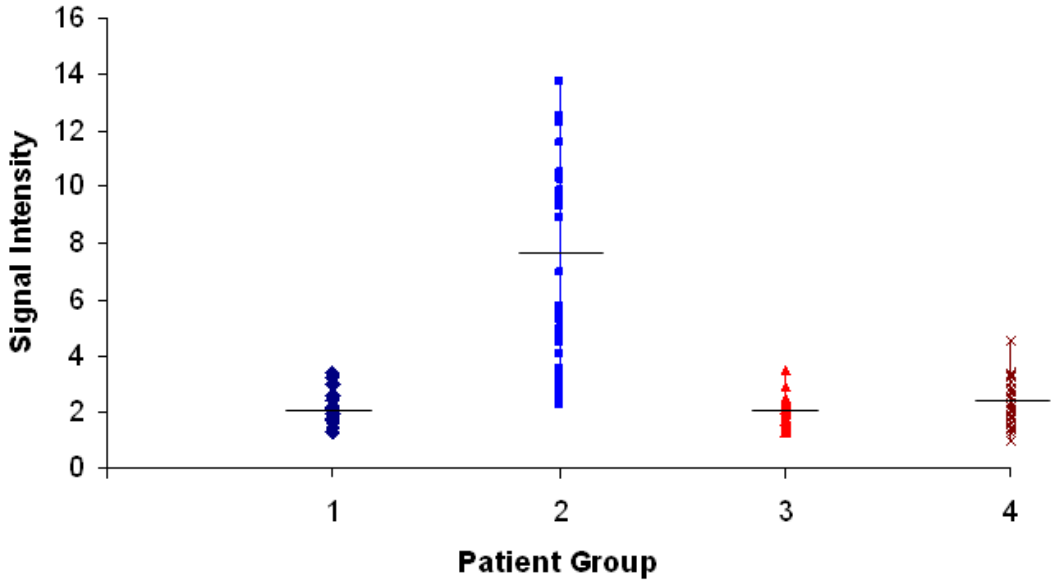

Figure 6.4 shows the individual 2505 peak intensities for all of the patients in the EXACTLE study. Group 1 is patients in the Prolastin at baseline, group 2 is patients on Prolastin after 6 month's treatment, group 3 is patients who received placebo at baseline and group 4 is patients receiving placebo after 6 months of treatment. The median value for each group is shown by the horizontal line. There was a significant difference between the groups between the baseline and 6 month samples (p <0.001).

p Value	m/z	Protein	Median Baseline Placebo	Median End Placebo	Fold Change	Median Baseline Drug	Median End Drug	Fold Change
0.001	2392.2	A1AT	0.92	0.98	1.06 ↔	0.90	1.87	2.10 ↑
<0.001	2505.6	A1AT	1.14	1.20	1.05 ↔	1.17	3.16	2.70 ↑
0.001	2521.5		1.16	1.190	1.03 ↔	1.10	2.41	2.20 ↑
<0.001	2537.3	Complement C3	1.07	1.15	0.93 ↔	1.09	1.85	1.69 ↑
0.001	4679.7		0.82	0.89	1.08 ↔	1.00	1.21	1.21 ↑
0.001	4791.9		0.59	0.61	1.03 ↔	0.64	0.96	1.50 ↑
0.005	4812.7		0.84	0.80	1.03 ↔	0.77	0.99	1.29 ↑

Table 6.9 shows the significant peaks from the EXACTLE trial samples following 6 months of treatment with either Prolastin or placebo. The median values of peak intensities for each group, measured in arbitrary units, are displayed, together with the fold change of the end of treatment to baseline values. The arrows demonstrate the direction of change.

Each of the peaks with a p value < 0.01 which change demonstrates a fold change of 1.21 to 2.70 in the patients receiving active drug, whilst in the placebo group, the fold changes of range from 0.96 to 1.08, indicating little change in the peptidome in the placebo group, as would be anticipated.

6.5.3 Comparison of Results from ECLIPSE A1ATD and EXACTLE

Table 6.10 shows a comparison of results using the same sample preparation technique from both independent sets of samples (ECLIPSE A1ATD and EXACTLE). There were 7 peaks which were significantly different pre and post treatment with augmentation therapy that were present in both experiments. There were 3 fragments of A1ATD that increased in both sets of patient samples post augmentation therapy, whilst remaining unchanged in patients receiving placebo (demonstrated in the EXACTLE samples only as there was no placebo arm in ECLIPSE A1ATD). Of the remaining peaks, the fold changes were in agreement across the 2 experiments; increasing in both sets of samples. There were more peaks which changed significantly following augmentation therapy in the ECLIPSE A1ATD samples, although this may reflect false positive results due to smaller patient numbers included in the analysis (8 samples pre and post compared to 72 pairs of samples in EXACTLE). As previously described, there were a number of peaks with m/z ratios above 4000Da which were significantly different between the baseline and post treatment samples, which remained unidentified.

m/z	Protein	p Value ECLIPSE	Fold Change ECLIPSE A1ATD	p Value EXACTLE	Fold Change EXACTLE
2392.2	A1AT	0.0023	3.34 ↑	0.001	2.10 ↑
2505.6	A1AT	0.00040	4.42 ↑	<0.001	2.70 ↑
2521.5		0.00079	3.63 ↑	0.001	2.20 ↑
2537.3	Complement C3	0.0024	1.45 ↑	<0.001	1.69 ↑
4679.7		0.00039	1.85 ↑	0.001	1.21 ↑
4791.9		0.00034	2.11 ↑	0.001	1.50 ↑
4812.7		0.0083	1.30 ↑	0.005	1.29 ↑

Table 6.10. Comparison of the significant peaks, p values and fold changes between patients in the ECLIPSE A1ATD Study and the active drug group of the EXACTLE Study.

6.6 WCX Bead Data Plasma Analysis

The results for the WCX bead analyses, performed as per the methodology in chapter 2.3.3, for both the ECLIPSE A1ATD and EXACTLE studies are presented in the tables and figures below.

6.6.1 ECLIPSE A1ATD Results

There were 197 peaks within the WCX bead spectra when samples from the ECLIPSE A1ATD study were analysed. The intra-experiment CV calculated from the QC sample was 16%. Typical spectra generated using WCX beads as the preparation method and linear MS are shown below in Figure 6.5

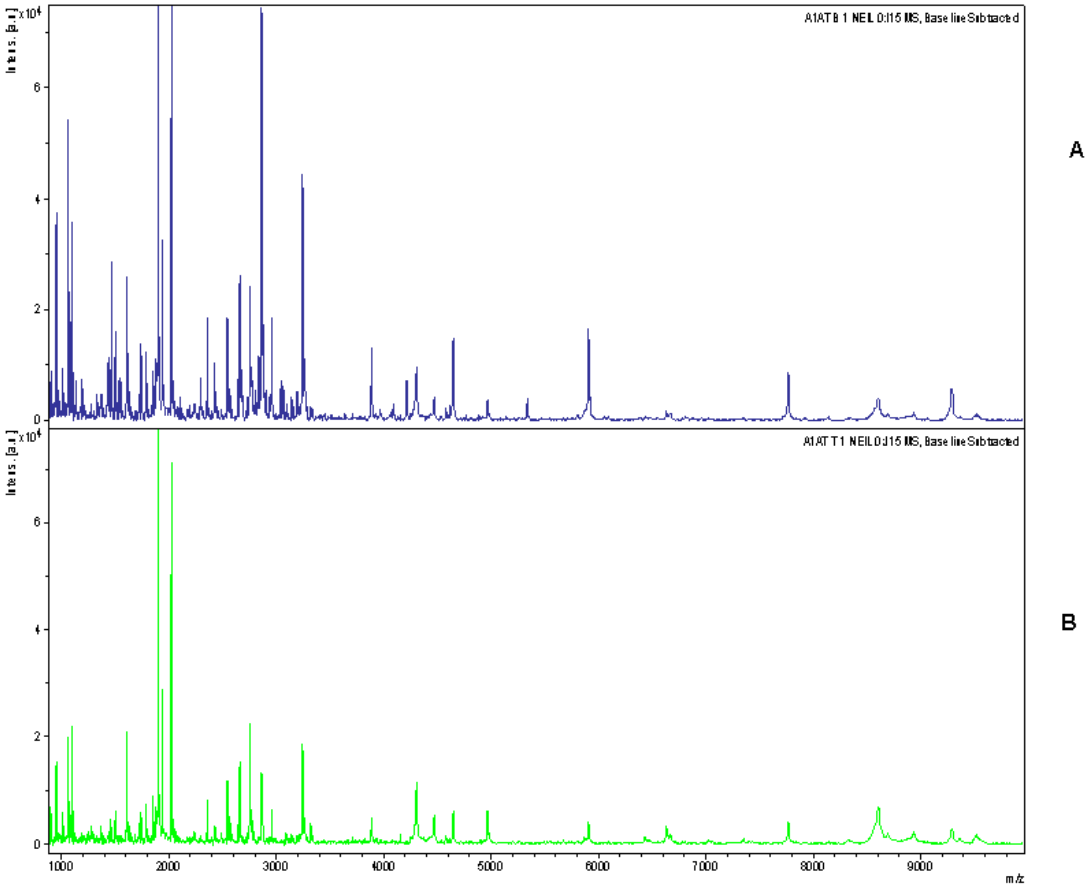

Figure 6.5 Typical spectra from patients with A1ATD pre (A) and post treatment (B) with augmentation therapy as part of the ECLIPSE A1ATD study.

The samples were processed in triplicate and spotted on to the MALDI plate in triplicate. The data was log transformed and a mean calculated and used for further analysis. The peaks which changed significantly between baseline and post 3 months of treatment with intravenous A1AT are shown in table 6.11. There were only 6 peaks which differed between the start and end of 3 months of treatment, and of these, there were only 2 which were in the mass range where it was possible to identify them using LC-MALDI MS/MS. It was only possible to identify 1 of these and this was a fragment of albumin which increased following 3 months of treatment with intravenous A1AT, with a fold change of 1.73.

m/z	p value	Protein	Sequence	Median Baseline	Median 3 Months	Fold Change
2660.9	0.004			14.76	17.87	1.21 ↑
2741.01	0.009	Albumin	R.DAHKSEVAHRFKDLGEENFKALVL.I	2.85	4.95	1.73 ↑
5068.01	0.009			0.51	0.40	0.78 ↓
6879.8	0.005			0.44	0.26	0.59 ↓
8872.1	0.003			1.01	0.81	0.81 ↓
9290.6	0.021			3.21	3.98	1.24 ↑

Table 6.11 Significant changes pre and post augmentation therapy in patients with A1ATD in the ECLIPSE A1ATD study

m/z is the mass to charge ratio of peaks which change significantly with treatment. Sequence is the amino acid sequence of the peptide and protein is the protein from which the peptide originated. The fold change is the end of treatment peak intensity, measured in arbitrary units, divided by the baseline value and the arrow denotes the direction of change.

The results from the ANOVA analysis, initially between A1ATD patients at baseline and COPD and healthy control subjects are presented in table 6.12. The ANOVA results for the analysis between A1ATD patients after augmentation therapy and COPD and healthy control subjects are shown in table 6.13. There were 18 changes identified between the A1ATD patients at baseline and the usual COPD patients and healthy control subjects. Of these, 4 were identified, and 3 were fragments of albumin and 1 was a fragment of IgG2. The majority of these were significant differences between patients with A1ATD and healthy control subjects.

Post treatment there were 18 changes between the patient groups when ANOVA was performed, again the majority of these were between A1AT patients and the healthy control subjects. However, it was not possible to identify most of these changes using LC-MALDI MS/MS, therefore limiting the utility of the data generated.

m/z	p Value	Baseline v COPD	Baseline v Healthy Control	COPD v Healthy Control	Protein	Sequence
1296.8	0.01	0.011	0.039	0.839	Ig G2	D.PEVQFNWYVD.G
1607.0	0.01	0.766	0.012	0.048		
1720.2	0.008	0.228	0.006	0.18		
2429.0	0.009	0.009	0.049	0.714	Albumin	R.DAHKSEVAHRFKDLGEENFKA.L
2741.1	0.005	0.031	0.005	0.677	Albumin	R.DAHKSEVAHRFKDLGEENFKALVL.I
2754.4	0.007	0.021	0.01	0.94	Albumin	R.DAHKSEVAHRFKDLGEENFKALVLA.I
2790.1	0.004	0.038	0.003	0.536		
3883.9	0.01	0.11	0.008	0.427		
3903.9	0.004	0.053	0.003	0.405		
3911.2	0.001	0.017	0.001	0.348		
3919.9	0.001	0.035	0.001	0.165		
3955.6	0.005	0.42	0.004	0.064		
4715.7	0.001	0.204	0.001	0.048		
5133.7	0.001	0.104	0.001	0.067		
6882.2	0.006	0.009	0.018	0.957		
7349.9	0.007	0.462	0.006	0.078		
7567.3	0.001	0.052	0.001	0.043		
9292.4	0.009	0.1	0.007	0.435		

Table 6.12. Results of the ANOVA analysis between patients with A1ATD at baseline with usual COPD and healthy control subjects

m/z	p Value	Treated v COPD	Treated v NHC	Protein	Sequence
1296.8	0.004	0.006	0.017	Ig G2	D.PEVQFNWYVD.G
1607.0	0.022	0.926	0.031		
1720.2	0.053	0.576	0.045		
2229.5	0.008	0.008	0.042		
2429.0	0.138	0.119	0.416		
2741.1	0.009	0.05	0.008	Albumin	R.DAHKSEVAHRFKDLGEENFKALVL.L
2754.4	0.097	0.194	0.105	Albumin	R.DAHKSEVAHRFKDLGEENFKALVLA.I
2790.1	0.015	0.145	0.012		
3883.9	0.054	0.313	0.043		
3903.0	0.016	0.189	0.012		
3911.2	0.003	0.079	0.002		
3919.9	0.003	0.136	0.002		
3955.5	0.095	0.99	0.173		
4072.0	0.004	0.389	0.003		
4715.7	0.002	0.319	0.001		
5133.7	0.008	0.403	0.006		
6882.2	0.487	0.473	0.669		
7349.9	0.031	1	0.059		
7567.3	0.004	0.376	0.003		
7641.1	0.006	0.521	0.006		
8144.1	0.006	0.313	0.005		
9292.4	0.064	0.353	0.051		

Table 6.13 Results of the ANOVA analysis between patients with A1ATD after 3 months of treatment, and patients with usual COPD and healthy control subjects.

6.6.2 EXACTLE WCX Bead Results

The sample preparation was carried out in triplicate, and spotted on to the MALDI plate in triplicate. Post log transformation, a mean was calculated and used in further analyses. The spectra from the WCX bead preparation of the EXACTLE samples contained 185 peaks. The intra-experiment CV for this experiment was 19%.

The significant peaks between the active drug (Prolastin) and the placebo groups between the baseline and post 6 months of treatment are demonstrated below in table

6.14. There were 8 peaks with a p value of < 0.01. The protein identification of these peptides are demonstrated within the table. Of the 3 possible identifications, there was a fragment of albumin which increased in the group of patients in the placebo arm of the trial, whilst remaining unchanged in the group on active treatment, and a fragment of complement C3 which decreased in patients receiving active drug whilst remaining unchanged in the placebo group.

p Value	m/z	Protein	Median Baseline Placebo	Median 6 Months Placebo	Fold Change	Median Baseline Drug	Median 6 Months Drug	Fold Change
0.002	1136.9	Complement C3	1.53	1.69	1.105 ↔	1.545	1.175	0.76 ↓
0.001	2429.1	Albumin	1.165	1.565	1.343 ↑	1.26	1.265	1.00 ↔
<0.001	2741.1	Albumin	1.475	1.54	1.044 ↔	1.355	3.115	2.29 ↑
0.0065	2862.3		7.9	7.13	0.903 ↔	9.445	20.705	2.19 ↑
0.01	3818.1		0.465	0.655	1.409 ↑	0.525	0.5	0.952 ↔
0.001	4614.9		1.07	1.405	1.313 ↑	1.23	0.955	0.77 ↓
6.82317E-06	5000.3		0.42	0.79	1.881 ↑	0.34	0.915	2.69 ↑
0.004	6882.2		0.32	0.395	1.234 ↑	0.3	0.24	0.80 ↓

Table 6.14. Significant peaks post WCX sample preparation of the EXACTLE samples. The median values for each group are shown, measured in arbitrary units. The fold changes are presented and the arrows denote the direction of change.

6.6.3 Comparison of ECLIPSE A1ATD and EXACTLE WCX Bead Data

There was much less agreement between the data generated from the WCX bead analyses between the ECLIPSE A1ATD and EXCATLE analyses than was seen with the SPE C8 data for the same analyses. Pre and post treatment there was only 1 peak in the MALDI spectra which was significant in both WCX bead datasets – this was a peak with an m/z of 2741.1 and was identified as a fragment of albumin. This increased in both experiments – with a fold change of 1.73 in the ECLIPSE A1ATD samples and 2.29 in the EXACTLE samples. None of the other peaks behaved consistently across the 2 separate sets of experiments.

The spectra generated from the WCX beads was across a greater mass range than was seen using the SPE C8 cartridges, where the majority of the peptides were in the mass range below 4000Da. Sixty-one percent of the peaks in the WCX bead spectra were above 4000Da, compared to 49% in the SPE C8 cartridge experiments. However, as demonstrated previously, it was not possible to identify these peptides and therefore proteins. In order to prepare samples for LC-MALDI to increase peptide identification, the SPE C8 cartridge methodology was used. This was to ensure that none of the WCX beads caused damage to the HPLC column. This may, in part at least, explain the lack of identifications following profiling with WCX beads.

6.7 Responder Analysis

CT scans were performed at baseline and at 12 and 24 months on patients in the EXACTLE Study. CT densitometry was measured and overall there was a trend towards a reduction in progression of emphysema (as reflected in a reduced loss of lung

density) in the patients who received active drug compared to patients who had received placebo. However, the number of patients in each arm of the study was small (38 on active drug 39 receiving placebo). Responder analysis based on individual data has yet to be validated as it has an inherent patient variability even on placebo and with data from the larger, more recent RAPID Study (Chapman et al, 2015) which included 93 patients in the active treatment arm and 87 in the placebo arm. Responder analysis using CT densitometry is being assessed as part of a phase 4 study of 400 patients requested by the FDA. Individual patient data from the EXACTLE study is owned by Grifols, and has not been released using the "end-point" CT densitometry analysis and hence was not possible with the current limited dataset even though mean data has been published. To partially address the question of a responder analysis, this was achieved biochemically as an alternative using the Aα-val^{360} assay data which is both reproducible and reflects proteinase control by treatment.

Aα-Val^{360} is an NE specific cleavage of fibrinogen that has been measured in patients with A1ATD, healthy control subjects and patients with usual COPD who were recruited into the ECLIPSE A1ATD trial. Carter et al demonstrated that this was elevated in patients with A1ATD compared to healthy control subjects, it related to severity of lung disease measured using CT densitometry and lung physiology, and, importantly, levels decreased following treatment with A1AT replacement intravenously (Carter et al., 2011; Carter et al., 2013).

Aα-Val^{360} was measured in the baseline and 6 month samples of the EXACTLE study by Carter et al, according to their published methodology (Carter et al., 2011). A median value for Aα-Val^{360} for each of the following 4 groups (placebo baseline and post 6

months' treatment and Prolastin baseline and post 6 months' treatment) was calculated for the patients included in this study, together with a median reduction between the start and end of treatment in the active drug and placebo groups. The data from the WCX bead and SPE C8 MALDI profiling analyses in the EXACTLE study from this series of experiments were re-analysed using patients in the active treatment group who had a reduction in this signal which was greater than the median for the group. The data are presented below in tables 6.15 and 6.16. This subgroup analysis was only performed on the EXACTLE dataset, even though Aα-Val^{360} had been measured in the ECLIPSE A1ATD study. In addition there were only 8 patients with samples analysed in the A1ATD group in the ELCIPSE A1ATD study, and reducing this number further would have made interpretation of further statistical analysis less valid.

The SPE C8 cartridge data did not show any further peaks that emerged to become significant when this sub-group data analysis was undertaken; the fold changes for 6 of the 7 significantly different peaks were higher in this sub-group data analysis. The signals with the most significant change were the fragments of A1AT, which increased post treatment suggesting it reflected the overall plasma replenishment with A1AT alone and hence (potentially) better NE control in vivo.

From the WCX bead data, it is possible to see that there are 4 further peaks which demonstrate a significant difference, in addition to the 9 previously highlighted. The majority of these are in the higher mass range, (> 4000Da) and, as previously noted, it was not possible to identify the proteins from which the peptides originated. Therefore, this re-analysis of data did not identify any further markers to indicate a response to treatment in patients with A1ATD who receive intravenous replacement therapy.

m/z	p Value	Median Placebo Base	Median Placebo End	Fold Change	Median Prolastin Baseline	Median Prolastin End	Fold Change
2392.2	< 0.001	0.945	1.005	1.06 ↔	0.715	1.61	2.25 ↑
2505.6	< 0.001	1.24	1.295	1.04 ↔	1.27	3.095	2.44 ↑
2521.5	< 0.001	1.185	1.22	1.03 ↔	1.185	2.655	2.24 ↑
2537.3	< 0.001	1.09	1.07	0.98 ↔	1.07	1.905	1.78 ↑
4679.7	0.008	0.9	0.85	0.94 ↔	0.865	1.17	1.35 ↑
4792.0	< 0.001	0.57	0.545	0.96 ↔	0.535	0.985	1.84 ↑
4812.7	0.006	0.805	0.708	0.88 ↓	0.685	1.01	1.47 ↑

Table 6.15 The SPE C8 cartridge data re-analysed using the data from those patients on active drug with a greater than mean reduction in $^{A\alpha\ val}$ 360.

The fold change is the end of treatment value divided by the baseline value, and the arrow denotes the direction of change.

m/z	p Value	Median Placebo Baseline	Median Placebo End	Fold Change	Median Prolastin Baseline	Median Prolastin End	Fold Change
1136.9	0.001	1.53	1.69	1.10 ↑	1.59	0.965	0.61 ↓
1378.0	0.005	1.985	2.01	1.01 ↔	2.125	1.33	0.63 ↓
1466.6	< 0.001	2.47	2.605	1.05 ↔	2.685	1.47	0.55 ↓
1552.6	0.002	1.515	1.715	1.13 ↑	2.15	0.79	0.37 ↓
2429.0	0.005	1.165	1.565	1.34 ↑	1.285	1.275	0.99 ↔
2741.1	< 0.001	1.355	1.54	1.14 ↑	1.4	3.625	2.59 ↑
2862.3	0.008	9.445	7.13	0.75 ↓	7.175	21.96	3.06 ↑
3086.1	0.004	0.785	0.76	0.97 ↔	0.865	0.57	0.66 ↓
3968.9	0.01	0.52	0.625	1.20 ↑	0.58	0.475	0.82 ↓
4614.9	0.003	1.07	1.405	1.31 ↑	1.145	0.935	0.82 ↓
6551.5	0.008	0.5	0.47	0.94 ↔	0.52	0.375	0.72 ↓
6882.2	0.004	0.3	0.395	1.32 ↑	0.355	0.24	0.68 ↓
9521.9	0.009	0.27	0.29	1.07 ↔	0.32	0.17	0.53 ↓

Table 6.16 shows the results of the WCX bead data including only those with a greater than the mean fall in Aα val ^{360} levels. The median value, measured in arbitrary units, is shown for each group. The fold change is the ratio of the end of treatment value to the start of treatment value for each group and the arrow denotes the direction of change.

6.8 Discussion

The SPE C8 cartridge data and WCX bead approaches allowed reproducible profiling to be performed in plasma and urine of patients with A1ATD. The 2 separate approaches allowed differential properties to be utilized to complement one another. On the whole, they identified few changes in the plasma and urinary peptidomes in response to treatment with intravenous A1AT in patients with A1ATD. The average intra-experiment CV for each of these experiments was below 20%, which was the previously quoted value using other sample preparation techniques (such as SELDI profiling), indicating that this approach is at least as good as the other technique in terms of reproducibility, whilst providing more potentially clinically useful information.

6.8.1 Urine Data Analysis

Urine is analysed in a number of different diseases, both of the renal and urinary tracts, and of non-related diseases. Small peptides and proteins may be filtered by the kidney. Therefore, it was hypothesised that small, proteolytic fragments, originating during proteolysis in the lungs, would be cleared from the plasma by the kidney, and thus amenable to detection following the analysis of urine samples.

Previous published work has been carried following analysis of urine samples in patients with usual COPD. For example, hydroxydeoxyguanosine, which is a marker of oxidative stress, was compared in the urine of 19 COPD patients and compared to that of 13 healthy control subjects; levels were significantly elevated in the COPD patients when compared with the healthy control group, from which the authors concluded that this was indicative of increased oxidative stress in the COPD group

(Igishi, 2003). Other possible markers have included the analysis of urinary desmosine as a marker of elastin and collagen breakdown. Results from studies of desmosine differ; some have reported that this is increased where lung function decline is rapid; (Stone et al., 1995) whilst others have reported that there is no association between urinary desmosine and FEV_1. In addition, it has been suggested that desmosine may be affected by other variables including diet (Stone et al., 1994) and renal function, (Davies et al., 1983) and elastin degradation outside the lung which limit its widespread use.

Huang et al measured desmosine in the plasma and urine of patients with COPD, both in the stable state and during exacerbations, in patients with asthma and in healthy control subjects - both smokers and non-smokers. Using mass spectrometry they demonstrated that during COPD exacerbations, the urinary concentrations of desmosine were elevated and that in plasma, there was an association between patients with elevated levels of desmosine and a low transfer factor (Huang et al., 2012). Despite this positive observation, desmosine has still not been validated sufficiently for routine use in clinical practice.

Urine has a lower total protein concentration than that of plasma, and is thus theoretically easier to analyse using mass spectrometry. It is routinely collected and relatively operator independent in its collection, and also minimally invasive to collect which means repeated collections, such as pre and post an intervention, are possible. This means, therefore, that collection and analysis of urine has many potential advantages over other biological and tissue samples, such as blood, lung tissue/BALF.

Patients enrolled in to the ECLIPSE A1ATD study had urine samples collected pre and post treatment. This was primarily to test for urinary cotinine to ensure that none of the patients recruited into the study were current smokers, as this was an exclusion criterion from the study protocol. Unfortunately, there were only 9 differences detected between the 4 groups when the data was analysed using ANOVA, and only 1 difference between the baseline and post treatment samples. In addition, the protocol for the EXACTLE study did not include urine sample collection, and therefore there was not a larger dataset for comparison/validation of the results. Therefore, LC-MS/MS was not performed on these samples, as any data generated would be limited to a small number of individuals, and would not be able to replicate on a larger dataset to test any hypotheses that were generated.

6.9.2 Clinical Significance of A1AT Fragments

This work has demonstrated an increase, post treatment, of fragments of A1AT in patients who received active drug, but remained unchanged in patients receiving placebo infusions. This occurred irrespective of the duration of treatment (in ECLIPSE A1ATD study, the samples were taken at 3 months post treatment initiation, in the EXACTLE study the second time point was 6 months). These same fragments were also detected in the plasma of healthy control subjects, and patients with usual COPD, and post augmentation there were no statistically significant differences between patients with A1ATD and either of the other 2 groups. The fragments are all from the C terminus of the A1AT protein.

It has been well demonstrated that patients on intravenous A1AT therapy have a rise in

the total plasma concentration of A1AT, and therefore it is biologically plausible that fragments of this protein are detectable in the plasma of patients with A1ATD after they have received treatment with augmentation therapy as such fragments are likely to be present in purified A1AT from healthy subjects.

Previous work by Niemann et al (1997) investigated a 44 residue peptide of the C terminus of the A1AT protein (termed SPAAT – short peptide of A1AT) and found that this fragment of the A1AT protein, which was first isolated from human placental cells, was an inhibitor of a number of serine proteases, including NE, pancreatic elastase and chymotrypsin. Unlike the complete A1AT protein, it binds reversibly to the enzymes. They concluded that, *in vivo*, SPAAT may have a role in the protection of extracellular proteins from the proteolytic actions of proteases, as a further protective mechanism (Niemann et al., 1997).

The amino acid sequence of the SPAAT peptide, published by Niemann and colleagues, is as follows:-

MFLEAIPMSIPPEVKFNKPFVFLMIEQNTKSPLMGKVVNPTQK (Niemann et al., 1997)

Two of the fragments of A1AT which were significantly different pre and post treatment with intravenous A1AT from the profiling experiments were sections of this previously described C-terminal peptide. Of these, LMIEQNTKSPLFMGKVVNPTQK and MIEQNTKSPLFMGKVVNPTQK (2506 and 2392 respectively) are the same fragment but with 1 less amino acid in the peak at 2392. The underlined section of SPAAT demonstrates the fragments identified in the profiling work.

Figure 6.6 shows the 3-dimensional structure of A1AT determined by x-ray crystallography. The blue area denotes the fragment that Niemann and colleagues named SPAAT. The red sections demonstrate the terminal sequence identified in the profiling experiments which was a segment of the C terminus of SPAAT.

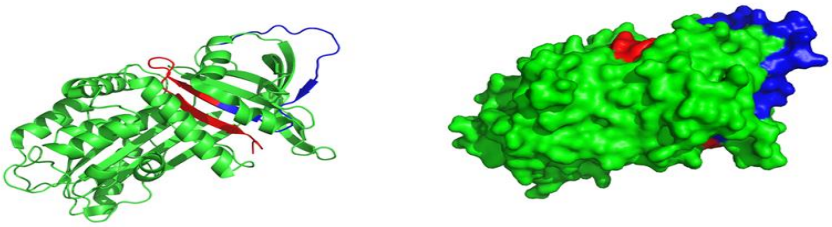

Figure 6.6 shows the 3 dimensional structure of A1AT

6.9.4 Complement C3

Complement C3 is a further abundant plasma protein (9th most abundant; Tirumalai et al (2003), and an integral part of the classical complement pathway (Marc et al., 2004). Type II pneumoncytes in the lungs are able to make C3 and C3 fragments, and animal models have suggested that some of these, including C3a and C5a (which are generated following proteolysis is C3 and C5 respectively) may produce some of the features seen in COPD, including contraction of smooth muscle (Marc et al., 2004). The SPE C8 cartridge analyses demonstrated an increase signal intensity in a peptide of complement C3 in both the ECLIPSE A1ATD samples and those from the EXACTLE study following treatment with intravenous A1AT. Marc et al, however, demonstrated that

levels of C3a were increased in induced sputum samples in patients with COPD when compared to healthy controls. The WCX bead data demonstrated that a separate fragment of complement C3 (m/z 1136.9) decreased in intensity post treatment with augmentation therapy in the patients in the EXACTLE study, whilst remaining unchanged in patients who were receiving placebo infusions (fold changes of 0.76 and 1.1 respectively). This may be related to the observation by Marc and colleague, however, the fold changes demonstrated are small.

6.9.5 WCX Bead Analyses

The WCX bead data provided fewer peptide identifications than the SPE C8 approach. This was in part due to the size of the peptides – there were a greater proportion of peptides which had m/z ratios above 4000Da with the WCX bead approach. Of the proteins which were shown to change significantly with treatment, 3 of the proteins identified as changing significantly in patients receiving placebo infusions were fragments of albumin. The data generated from the WCX bead analyses from these clinical samples was less consistent than that produced when the samples were prepared using the SPE C8 cartridges. The data only identified 1 peptide which changed in the same way in both independent datasets – and this was a fragment of albumin and therefore of limited clinical value, as previously panels of markers together have been required to detect differences between patient groups in COPD (Rana et al., 2010) and in malignant diseases (Useland et al., 2011). When the WCX beads were used to analyse the ionophore samples, there were easily identifiable differences. The intra-experiment CVs for both the EXACTLE and ECLIPSE A1ATD studies were below 20% and therefore the lack of consistent findings across the 2 separate experiments was

not due to the way the experiments were conducted. At the method optimization stage, it was the number of peaks and the peak intensities which were used to determine the best techniques for profiling, rather than through identification of peptides using LC-MALDI MS/MS.

As would have been anticipated, the remainder of the low molecular weight plasma proteome remained unchanged post augmentation therapy, and this was a finding across both of the profiling techniques utilized in this work. All of the proteins which were identified as changing significantly in response to augmentation therapy were in the group of high abundance plasma proteins. This approach did not identify a new candidate protein worthy of further study in the attempt to find biomarkers to predict a response to treatment in patients with A1ATD. It did correctly identify a change in fragments of A1AT, however, total A1AT levels are easily measurable and therefore this alone did not generate new clinically relevant information.

6.9.6 Comparison of *in vitro* and Clinical Sample Results

Following neutrophil stimulation with calcium ionophore, differences were seen in the plasma profiles of patients with A1ATD compared to healthy control subjects; the majority of these differences were fragments of fibrinogen, particularly the fragments of fibrinogen α chain. These could represent potential candidate markers of the actions of NE. During the profiling experiments, there were no peaks within the MALDI spectra to correspond to the fragments of fibrinogen identified as potential markers during the ionophore experiments. This does not imply that the fragments were not present – the signals may have been masked by the presence of more highly abundant

peptides.

Furthermore, when LC-MALDI was performed in order to maximize peptide identification, only 2 of the 11 fibrinogen fragments from the ionophore data were identified in the clinical samples from ECLIPSE A1ATD and EXACTLE studies (namely W.YSMRKMSMKIRPFFPQ.Q and D.SGEGDFLAEGGGVR.G). This again does not mean that the potential candidate biomarkers were not present in the clinical samples or that they do not change significantly in response to treatment. These signals may have been present but the mass spectrometer was not able to overcome the diverse concentration range (fibrinogen typically has a concentration of 1.5 to 4.5g/L in human plasma in contrast to albumin, which has a concentration of 60-80g/L) in the presence of more abundant proteins, in particular albumin.

6.9.7 Complexity of the Plasma Proteome

Plasma is one of the most difficult clinical samples to analyse using mass spectrometry, yet one of the most potentially informative, as every tissue and organ in the body requires a blood supply. It is, therefore, theoretically possible to detect changes within any tissue or organ by analysing plasma or serum. Plasma and serum have the advantages that such samples are routinely collected, and minimally invasive in doing so, and research samples may be taken alongside samples taken for routine clinical care. In addition, samples may be easily taken for analysis pre and post an intervention.

However, the utility of plasma is limited by the dynamic range of the concentrations of proteins present within it. The total protein content of plasma is around 70mg/ml

(Tirumalai et al., 2003). The most abundant plasma protein is albumin, which accounts for almost half of this, and the top 22 proteins make up 99% of the total plasma protein content (Tirumalai et al., 2003). It is therefore, the remaining 1% of plasma proteins which are of particular interest when attempting to characterise the plasma proteome, certainly in the application of proteomics in other branches of medicine such as in cancer studies, and to detect differences or changes within this which have the potential to act as a marker of disease. This dynamic range of plasma protein concentrations means therefore that the plasma proteome is the most complex proteome, and thus the most difficult to interrogate for biomarker discovery.

Plasma does however give the opportunity for repeated sampling, for example, if a marker was detected and used as an endpoint in a clinical trial, samples could easily be taken pre and post intervention, as was the case with both of the studies in this thesis whereby samples pre and post treatment with intravenous A1AT were analysed. Using other modalities, such as tissue from biopsy specimens or BALF are not so easily suited to this purpose, especially not on a large scale, without subjecting patients to invasive procedures.

Many proteomics experiments to date have been carried out in patients with malignant diseases. In this scenario, a tumour may be small (in the order of cms), and plasma has been analysed to identify changes which may be related to the presence of this small tumour. The surface area of the alveoli is several orders of magnitude higher than that of a small tumour, in order to promote efficient gas exchange, and the volume of blood in contact with this significantly higher, theoretically than would be expected in the presence of a small neoplasm. Hence, in theory at least, the rationale for the application

of proteomic technology to the plasma in patients with A1ATD, where there is an imbalance between neutrophil elastase in the lung and its natural inhibitor A1AT, and therefore, in theory at least, fragments of proteolytic destruction in the lung could be detectable in plasma.

MALDI profiling has allowed the measurement of fragments of the most abundant plasma proteins in these patient cohorts. There were some differences identified, namely fragments of A1AT and other abundant proteins, such as albumin, which changed significantly in patients receiving augmentation therapy. However, no robust biomarker has been identified from this work so far. By performing profiling experiments, only the surface of the plasma peptidome has been analysed, thus it is not surprising that the proteins which changed significantly arise from the most abundant plasma proteins. Other markers of inflammation which have been implicated in COPD, such as interleukins and matrix metalloproteinases are cytokines and chemokines and these are of much lower concentrations in the plasma than the proteins and peptides detected in the profiling experiments. Furthermore, the concentrations of these cytokines are several orders of magnitude lower in concentration than that of the abundant plasma proteins identified in these experiments – the concentrations of plasma proteins spans more than 10 orders of magnitude (Tirumalai et al) from albumin at 60-80g/L to interleukin 6 at picograms per mL, and currently there is no mass spectrometer which has the ability to detect proteins across this complete and diverse concentration range.

The results generated in the profiling work were unlikely to have been due to inter-current disease states. Each of the individuals that were enrolled into the ECLIPSE

A1ATD were rigorously screened for the presence of comorbid conditions. Furthermore, each patient or control subject had undergone a CT PET scan to exclude underlying inflammatory and neoplastic conditions. One healthy control subject was excluded from further participation in the study when a possible renal abnormality was detected on his scan, although this was subsequently determined to be a false positive result. This is essential in proteomics experiments to ensure that patients are adequately phenotyped at the outset to ensure that any observed differences between patient groups reflects underlying pathophysiology of disease to be studied.

6.10 Conclusions

The profiling experiments identified fragments of A1AT which increase in intensity in the MALDI spectra following treatment with augmentation therapy. These 2 fragments are of a previously identified short segment of A1AT known as SPAAT. This is biologically plausible and proves the validity of the data generated by these experiments. However, this does not add any new information in the search for biomarkers in response to treatment with intravenous A1AT. The complexity of plasma and the presence of abundant plasma proteins may mask lower intensity signals within the spectra, thus making them difficult to detect, and therefore a more in depth approach using shotgun proteomics with abundant plasma protein depletion was may be needed to unmask clinically useful biomarkers.

CHAPTER 7 SHOTGUN PROTEOMICS

Shotgun proteomics is a term given to the process of identifying proteins in complex mixtures, such as plasma, using a combination of high performance liquid chromatography (HPLC) and mass spectrometry. It requires the digestion of proteins within the complex sample, to generate peptides, which are separated using HPLC. Identification of the peptides generated is performed using tandem mass spectrometry (MS/MS). Plasma is the most complex clinical sample to analyse due to the wide range of protein concentrations that are contained within it, and separating and simplifying this with abundant protein depletion is central this process.

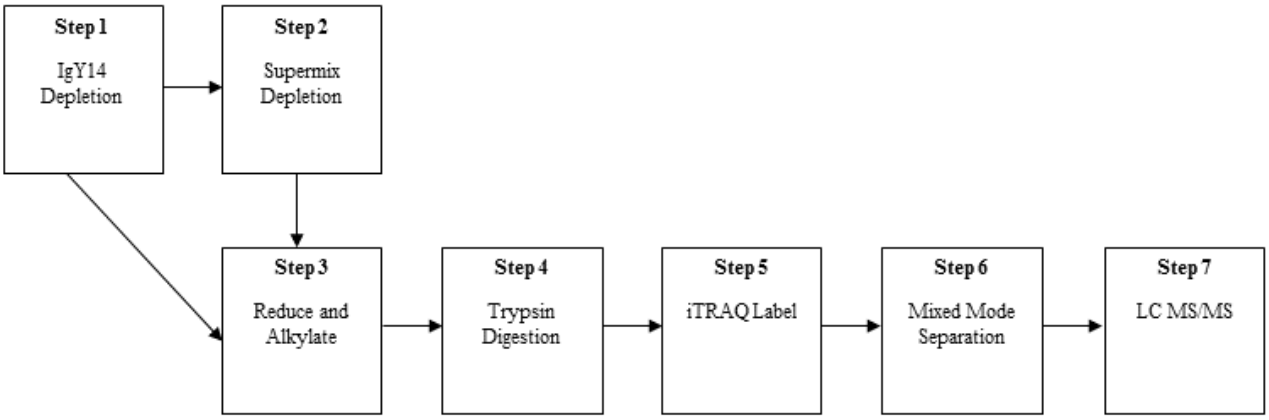

Figure 7.1 Steps involved in the workflow of the shotgun experiments. Step 2 was not performed in all experiments. iTRAQ allows quantification of peptides identified with LC-MS/MS

The workflow used for these experiments is demonstrated in Figure 7.1. Labelling the N terminus of peptides with iTRAQ allowed relative quantification of peptides in the samples. This experimental workflow was conducted initially on pooled samples from the ECLIPSE A1ATD study, with and without step 2 (the Supermix depletion step) followed by the EXACTLE pools, performed with step 2, and the results from individual experiments are presented below.

7.1 ECLIPSE A1ATD Post IgY14 Depletion

This experiment was firstly performed on 40µL of pooled plasma from the ECLIPSE A1ATD study, processed without step 2, as shown in figure 7.1. Following iTRAQ labelling, the peptides were separated using mixed mode separation, which separated the peptides into 48 fractions based on hydrophobic properties and charge states. Mixed mode separation is a multimodal separation technique, based on reverse phase and anion exchange within a single column. Figure 7.2 shows that this was an effective separation technique. A similar effective separation was seen in both of the subsequent shotgun experiments (data not shown). The majority of the peptides were distributed amongst the middle of the gradient, and these peptide containing fractions were combined and analysed by LC-MALDI.

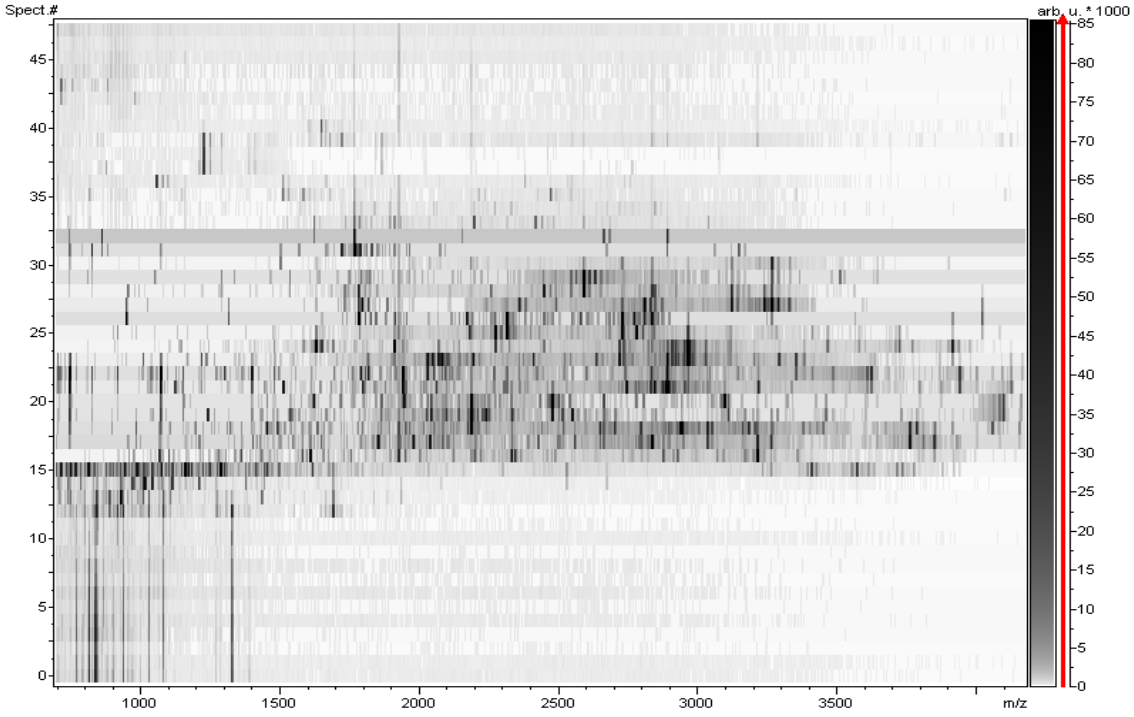

Figure 7.2. Survey view of the mixed mode fractions post abundant protein depletion.
m/z is along the horizontal axis, with the spectrum number and signal intensity, measured in arbitrary units on the vertical axes. The majority of the peptides are distributed across the middle of the gradients (fractions 10-40)

In total there were 144 proteins identified and quantified. Peptides which were not labelled with iTRAQ markers, and therefore not quantifiable, were removed from further analysis. In addition, there were 2 peptides of keratin identified within the samples; these are usually contaminants within proteomics experiments and were therefore also removed from further data analysis. This was the case in all of the shotgun data analyses.

In the ECLIPSE A1ATD samples, multiple comparisons between the relative iTRAQ reporter ion peak intensities were performed as previously described in chapter 6; between A1ATD at baseline compared to A1ATD post treatment, COPD and healthy control subjects, and between COPD and healthy control subjects. However – the most clinically relevant analyses to determine a response to treatment with intravenous A1AT were those between patients with A1ATD pre and post treatment and compared to healthy control subjects, and these will be presented in the remainder of this series of results.

The most abundant proteins were albumin (135 peptides), transferrin (84 peptides), A1AT (53 peptides) and fibrinogen (21 peptides). Post treatment with augmentation therapy, the iTRAQ data show that levels of A1AT increase, with a median ratio of baseline to the end of 3 months of treatment of 2.7, proving the validity of subsequent results generated as it has been well documented that total A1AT levels rise with treatment with intravenous A1AT (Wewers et al., 1987).

However, as the abundant protein depletion step was not complete, as shown by the presence, identification and quantification of abundant plasma proteins such as

albumin, A1AT and fibrinogen, the proteome coverage of this series of experiments was limited. The experiment was repeated with the extra level of abundant protein depletion using a Supermix column as demonstrated by step 2 in Figure 7.1, and this was then replicated with the EXACTLE pooled samples.

7.2 ECLIPSE A1ATD Post Supermix Depletion

The experiment was performed using 100µL of plasma which was depleted using the IgY14 method described in chapter 2.10.1, followed by the second level of depletion using the Supermix column (step 2, 2.10.2), to increase abundant protein depletion.

In total, there were 362 peptides from 77 unique proteins identified and quantified, and these are presented in Appendix II. Peptides which were not labelled with iTRAQ reagent (2) were removed from further analysis. Of the labelled and identified peptides, there were 120 peptides from albumin, 58 peptides from transferrin and 28 from alpha-2 macroglobulin. These are again abundant plasma proteins, which should theoretically have been removed during the IgY14 depletion step; the depletion is only up to 95% efficient, according to the manufacturer's specifications – and hence some peptides from these highly abundant proteins may still be present. The same patient group comparisons were made as described in 7.1. These are demonstrated in the waterfall plots below (Figures 7.3-7.5)

Post treatment with augmentation therapy, A1AT increases, and the ratio of pre to post treatment is 2.38↑. When comparisons are made between healthy control subjects and patients with A1ATD, A1AT levels are 2.1 times higher in the healthy controls. Following treatment with intravenous A1AT, this difference between patients with

A1ATD is removed and the ratios between the groups is 0.87 (levels higher in healthy control subjects).

Two further potentially interesting proteins changed with augmentation therapy; these were pigment epithelial derived factor (PEDF) and corticosteroid binding globulin (CBG). PEDF was elevated in the A1ATD baseline samples compared to healthy control subjects (9.29), and reduced but remained elevated post treatment (3.38), and in patients post treatment with intravenous A1AT, decreased (2.74). CBG was elevated in patients with A1ATD at the start of treatment compared to healthy control subjects (5.54 ↑), and reduced following treatment with augmentation therapy when compared to baseline in patients with A1ATD (2.43↓).

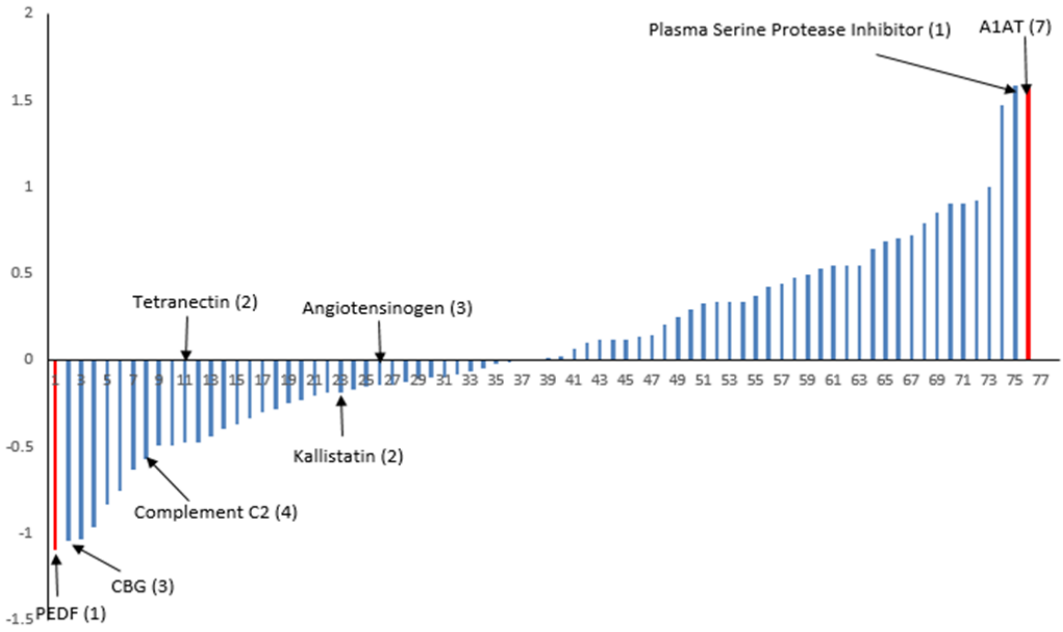

Figure 7.3. Waterfall plot demonstrating the pre-treatment compared to the post treatment ratios of identified peptides from the ECLIPSE A1ATD study
The number in brackets denotes the number of peptides identified and quantified from each protein. The labelled proteins are proteins which changed significantly either in

this or in the subsequent analyses. The ratios of peak intensities were log transformed to base 2; an increase of 1 indicates a doubling of the intensity, and -1 denoted a halving.

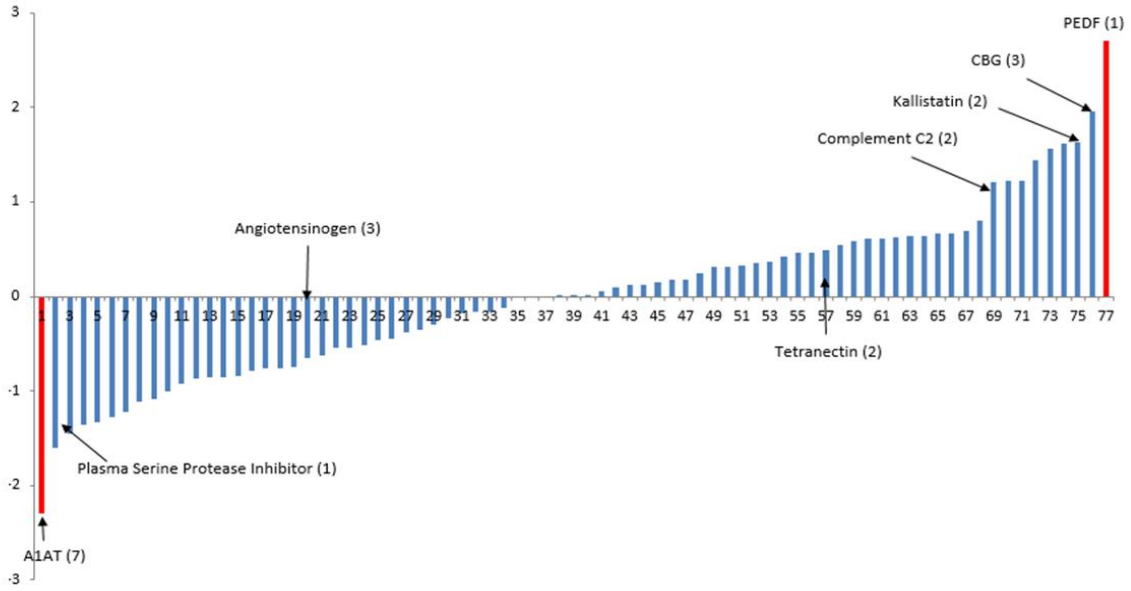

Figure 7.4. Waterfall plot demonstrating the median ratios between the ECLIPSE A1ATD patients pre-treatment and healthy control subjects

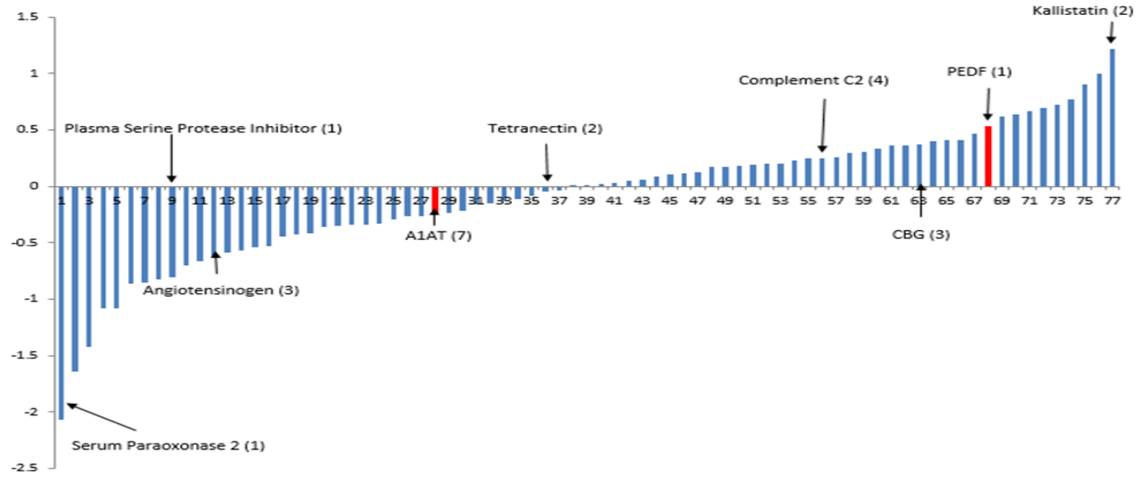

Figure 7.5 Waterfall plot demonstrating the median ratios between the ECLIPSE A1ATD patients post treatment and healthy control subjects.

7.3 EXACTLE Post Supermix Depletion

There were 161 peptides from 57 proteins identified and quantified in this experiment and these are presented in Appendix II. As there were still abundant plasma proteins, including A1AT and albumin, in the ECLIPSE A1ATD following a single IgY14 depletion strategy, the plasma from the EXACTLE study were doubly depleted using the IgY14 columns prior to the second depletion step using the Supermix column.

There were 2 analyses performed on the data generated; a comparison of pre and post treatment in the active drug treated group of patients, and pre and post in the placebo treated patient group. The results are presented in the 2 waterfall plots below, in Figures 7.6 and 7.7.

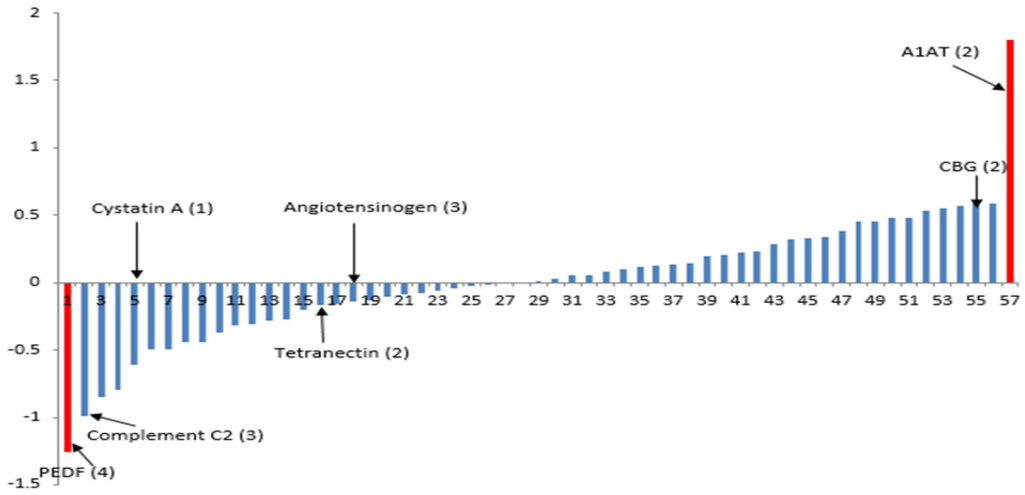

Figure 7.6 Waterfall plot demonstrating the ratios of post to pre-treatment in the EXACTLE pooled plasma samples in the group of patients on Prolastin (Intravenous A1AT).

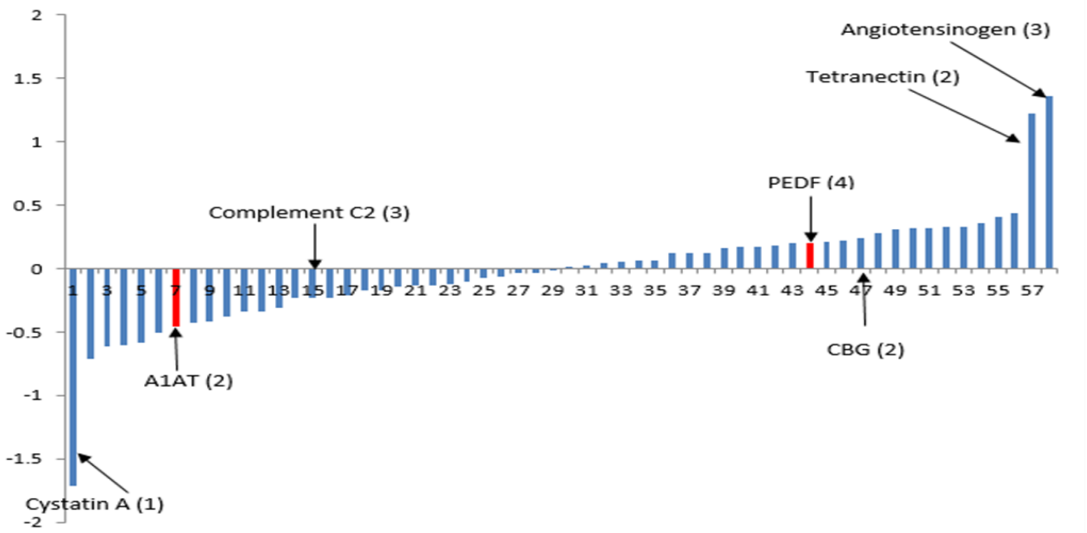

Figure 7.7 Waterfall plot demonstrating the ratios of post to pre-treatment in the EXACTLE pooled plasma samples in the group of patients on placebo infusions.

A1AT again demonstrates a rise post treatment with Prolastin, with a ratio of post treatment to pre-treatment of 3.5. There were 2 peptides of A1AT identified and quantified and these should in theory have been removed by the preceding depletion steps. However, these demonstrated a rise in the patients who received active drug and again confirmed the validity of the results generated. There was no significant change in A1AT in the patients who received placebo infusions, as demonstrated in Figure 7.7 above. There was little change in the plasma proteome post augmentation therapy as was demonstrated with the profiling experiments– most of the proteins on the waterfall plots fall within a narrow range implying no significant change with treatment.

CBG behaved differently in the EXACTLE experiments to those from the ECLIPSE A1ATD; instead of a reduction post augmentation therapy as was demonstrated in the ECLIPSE A1ATD experiments, it increased in the EXACTLE samples, with a fold change of 1.5. In the EXACTLE group of patients who received placebo infusions,

there was no significant change when the baseline and 6 month analyses were performed (fold change 0.91).

PEDF, however, demonstrated the same effect in the EXACTLE samples, as in the ECLIPSE A1ATD - decreasing with treatment when the baseline and either 3 or 6 month samples were analysed, whist remaining unchanged in the patients who received placebo infusions (fold changes 2.45 in the active drug group versus 0.89 in the placebo treated group). Therefore, as 2 independent experiments on independently collected pools of samples indicated the same change in this protein, PEDF was studied in greater detail as a possible marker of response to treatment in patients with A1ATD, and measured using a sandwich ELISA (Chemicon International CYT 420) on individual plasma samples from both studies (see below).

Other potential candidates included angiotensinogen and tetranectin (both increased in EXACTLE samples in patients receiving placebo, whilst remaining unchanged in patients on intravenous A1AT), cystatin A (which decreased in patients receiving placebo infusions in the EXACTLE samples, whilst not changing significantly in patients on intravenous A1AT but was not detected at all in the ECLIPSE A1ATD samples) and complement C2 (in the EXCATLE samples patients in the placebo group did not demonstrate any significant change after 6 months of treatment, whilst in patients receiving intravenous A1AT the levels were higher).

7.4 Pigment Epithelium Derived Factor (PEDF)

The MS/MS spectrum for the PEDF peptide identified in the ECLIPSE A1ATD pooled samples is shown below in Figure 7.8. It shows both the peptide fragmentation and the

iTRAQ reporter ions indicating that PEDF was higher in patients with A1ATD pre-treatment and decreased with treatment.

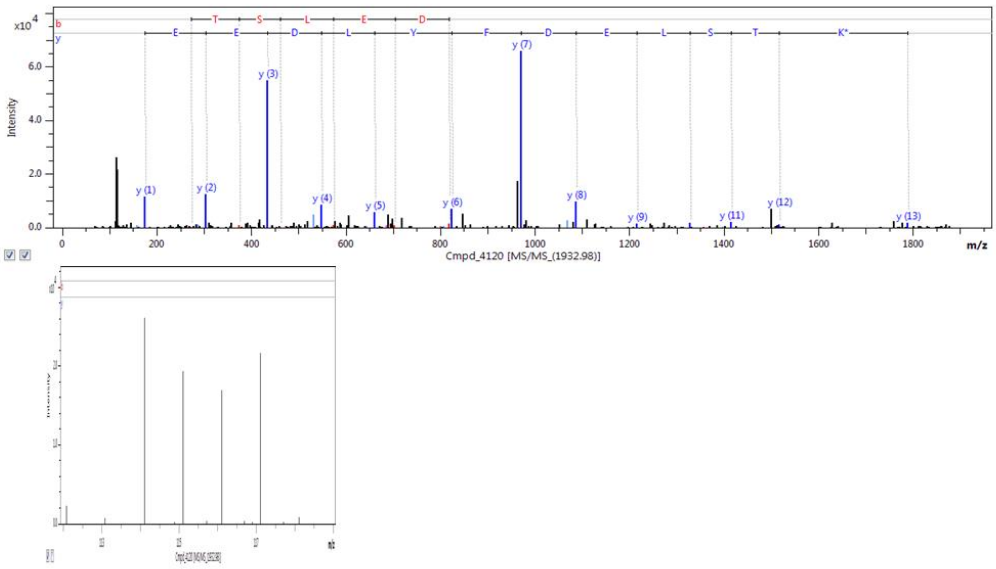

Figure 7.8 PEDF fragment m/z 1932 from the pooled ECLIPSE A1ATD samples.
114 = A1ATD patients at baseline
115 = A1ATD patients after 3 months of treatment
116 = COPD
117 =Normal healthy control subjects

The reduction in PEDF post treatment looked promising as a biomarker and this was confirmed by the EXACTLE samples. Therefore PEDF concentrations were measured in the UK samples from the EXACTLE study and all of the patients in the ECLIPSE A1ATD study as described in chapter 2.10.9. The results are shown in Tables 7.1 and 7.2 for the ECLIPSE A1ATD and EXACTLE samples respectively. There was no significant difference between PEDF in healthy control subjects compared to patients with A1ATD, and there was no significant reduction post treatment, in either the samples from the ECLIPSE A1ATD study or the EXACTLE study, as was suggested by the data from the shotgun experiments. In addition, there was no significant

difference in the values measured from the patients with A1ATD from the 2 separate clinical trials.

ECLIPSE A1TATD	Median	IQR	
A1AT Baseline	14.6	9.6	18.6
A1AT 3 months	15.1	12.8	18.0
COPD	15.9	13.7	16.9
NHC	14.4	11.7	15.7

Table 7.1 Median values and interquartile ranges for PEDF concentrations, measured in micrograms per mL, for patient groups in the ECLIPSE A1ATD study. A1AT Baseline is the median value for A1ATD patients pre-treatment, A1AT 3 months is the median value for A1ATD patients after 3 months of augmentation therapy, COPD is the median value for the group of patients with COPD and NHC is the median value for healthy control subjects.

EXACTLE	Median	IQR	
Placebo Baseline	12.7	9.5	15.4
Placebo 6 months	14.4	11.0	17.5
Treatment Baseline	12.3	10.8	19.0
Treatment 6 months	15.5	11.1	20.6

Table 7.2 Median values and interquartile ranges for PEDF concentrations, measured in micrograms per mL, for patients in the EXACTLE study. Placebo baseline and end of treatment are the median values for the placebo treated patients at baseline and after 6 months of placebo infusions. Treatment base and end are the median values for the patients receiving active drug at baseline and after 6 months of treatment.

7.5 Discussion

The shotgun proteomic experiments were intended to provide an in depth analysis of the plasma proteome to be undertaken in order to determine whether there were any significant effects with intravenous replacement therapy in patients with A1ATD. As was demonstrated during the profiling series of experiments, the majority of the detectable plasma proteins remained unchanged following treatment with augmentation therapy. However, despite abundant protein depletion strategies, it was not possible to interrogate deeper into the plasma proteome.

7.5.1 Use of Pooled Samples

Shotgun proteomics investigates further into the plasma proteome, and analyses the digested peptides (in this instance tryptic digests) rather than endogenous plasma peptides. Such experiments require several steps, and are very time consuming and therefore it becomes difficult to perform these on individual plasma samples (72 pairs of samples were utilised from the EXACTLE study). Pools were therefore used for further analysis. In this series of experiments, 2 separate groups of pools were created – samples from the ECLIPSE A1ATD study and in addition pools from the EXACTLE study. Equivalent volumes of individual samples were added to create the pools. The aim of the shotgun experiments was to uncover potential candidate biomarkers which change in response to a treatment or intervention (in this instance to intravenous A1AT), which could then be validated using an alternative method, carried out on individual samples, such as by ELISA.

The use of pooled samples for in depth analysis is not universally accepted. Some groups feel that pooled samples should be avoided entirely, and that only individual samples should be analysed. This allows full characterisation of the studied proteome and allows biological and methodological differences to be studied. (Westermeier et al., 2008). Conversely, others, such as Diz et al (2009), have studied the effects of undertaking proteomics experiments on pooled samples, and they concluded that this is a valid approach to take (Diz AP et al., 2009). With the complexity of the shotgun experiments, and the amount of time taken to doubly deplete plasma, the quantity of plasma required and the instrument time needed to perform LC MALI MS/MS, it was not feasible to perform this on each individual sample. If single samples from each group had been randomly selected for analysis, they may not have been representative

of the group to which they belonged, and thus comparisons may have been inaccurate and the results invalid. Therefore, pooling samples was the approach taken. Furthermore, Diz and colleagues proved during their analyses that this approach could make differences and similarities between groups easier to detect as the effects of biological variation will be removed (Diz et al., 2009).

In this series of experiments, using 2 separate pools of samples – ECLIPSE A1ATD and EXACTLE, allowed confirmation of changes identified on an independent set of samples, adding further evidence to any changes discovered. Examples of this from this work include the decrease in PEDF with augmentation therapy, which was elevated in patients in the ECLIPSE A1ATD study with A1ATD at baseline when compared to healthy control subjects, and deceased with treatment. The duration of treatment did not affect the results of the experiments as a decrease was also seen in patients in the EXACTLE study who received active drug, whereas no change was seen in patients who received placebo.

Despite its many advantages, the use of pooled samples, however, has disadvantages, and one such example is the problem that one individual may be an outlier, and subsequently affect the results from the entire pooled sample. This may have been the reason for the conflicting results found with CBG, which decreased with augmentation therapy in the ECLIPSE A1ATD study, but behaved in the opposite way and increased in the EXACTLE study. It is not clear why this protein behaved differently in these separate pools of samples, however, one patient who was enrolled in to the ECLIPSE A1ATD study died 18 months after the end of the study of a malignancy, which was either a neoplasm of the head of the pancreas or bile duct, and this was complicated by

an episode of decompensated liver failure. As this pool was made of only a small number of patients (n=8), the data in the pooled sample created could have been skewed by anomalous results in this individual. This individual had undergone 2 separate CT PET scans according to the study protocol (at baseline and following 3 months' of treatment) which had not identified any abnormality, and his liver function tests during the study had been within the normal range. To answer this question specifically, further work could be undertaken to measure the levels of CBG in this individual at screening and after treatment to determine whether or not this individual was responsible for the effect seen. An alternative explanation could be that the results demonstrated may have been false positive results and that CBG remains unchanged following augmentation therapy.

7.5.2 PEDF

PEDF is a member of the serpin supergene family, although unlike other members of this family of proteins, such as A1AT, it does not have protease inhibitory activity (Filleur et al., 2009). It has a number of properties including being anti-angiogenic, anti-tumourogenic and is neurotrophic. It was first discovered in foetal retinal pigment cells, but has since been identified in a number of other different tissue varieties including liver, skeletal muscle, heart, ovary and lung (Li et al., 2015).

In the field of respiratory disease, PEDF has been implicated in the pathogenesis of a number of conditions including idiopathic pulmonary fibrosis (IPF), non-small cell lung cancer and more recently in COPD. Cosgrove et al in 2004 discovered PEDF concentrations to be elevated in the fibroblastic foci of patients with idiopathic pulmonary fibrosis when measured using a microarray, and in BALF fluid of IPF

patients when compared to control subjects when this was measured using an ELISA (Cosgrove et al., 2004). This was felt to be due to the antiangiogenic actions of PEDF.

In tumours, the antiangiogenic properties demonstrated by PEDF may have a protective effect. Furthermore, in cancers where PEDF expression is reduced, there is a greater propensity to tumour progression to metastatic disease and therefore a worse prognosis, making treatments targeting PEDF an exciting avenue of research. In non-small cell lung cancer (NSCLC), where PEDF levels were reduced, this was of prognostic importance, and patients had an increased rate of mortality (Zhang et al., 2006). These authors studied the levels of PEDF and PEDF mRNA in 91 patients with non-small cell lung cancer who had undergone surgical resections of their tumours. They found lower total levels of PEDF in 57% of patients, and PCR analysis of mRNA showed a significantly lower concentration in cancer tissue when compared to healthy tissue taken at the same time as the surgical resection. Furthermore, there was a significantly lower survival in the patients with lower levels of PEDF (Zhang et al., 2006).

In 2009, Chen et al used 77 NSCLC tissue samples to measure PEDF using quantitative PCR. They compared results from the cancer tissue to those obtained from biopsy samples collected at the same time from normal sections of lung. They demonstrated that there was a significant reduction in PEDF in patients who had evidence of lymph node involvement ($p = 0.007$) and that there was a significantly reduced survival in the group with lower PEDF levels ($p = 0.0459$) (Chen et al., 2009). The authors concluded that this observation was due to the ability of PEDF to perform an antiangiogenic role, and this is lacking when levels of PEDF are low, thus promoting tumour growth and subsequent spread.

In COPD, Li et al (2015) explored the relationship between PEDF and rat pulmonary epithelial cells exposed to cigarette smoke, and found that there was a significant rise in the levels of PEDF in the cells compared to those of control samples which had not been exposed to cigarette smoke. The authors subsequently measured PEDF levels in the plasma of 80 subjects – 10 smokers with normal spirometry, 50 stable state patients with COPD and 20 healthy control subjects. This was performed using a multiplex enzyme-linked immunosorbent assay, which also included measurements of CRP, IL6, IL8 and TNF alpha. They demonstrated that PEDF levels were increased in the plasma of patients with COPD compared to healthy control subjects and healthy non-smokers (551 +/-23.6 ng/mL in the COPD patients, versus 378 +/- 27.9 ng/mL in the non-smokers and 439ng/mL in the healthy smokers). PEDF levels correlated with CRP, Il6, IL8 and TNF although not with disease severity (Li et al., 2015). This was felt to merit further investigation as to the potential role of PEDF in the pathophysiology of COPD. To date, however, there has been no published data looking specifically at PEDF in patients with COPD secondary to A1ATD.

It was hypothesised from the shotgun data that in patients with A1ATD, the deficiency in a member of the serpin gene superfamily results in a compensatory rise in other members of this supergene family, namely PEDF. Therefore, PEDF was measured in individual samples from ECLIPSE A1ATD and in the UK arm of the EXACTLE trial using an ELISA which failed to confirm the findings from the shotgun proteomics experiments; there were no significant differences pre and post treatment (14.6 (IQR 9.6 -18.6) vs 15.1 (IQR 12.8-18.0 µg/mL) and there were no significant differences between patients with A1ATD and healthy control subjects (14.4 vs 14.6 µg/mL). There

are a number of potential reasons for this observation. Firstly, the results could have been false positive results, although as the protein was elevated in both the ECLIPSE A1ATD and EXACTLE samples at baseline, and decreased with treatment, this would be less likely. It could be due to fact that the peptides from PEDF from the mass spectrometry were only fragments of the entire protein, and therefore the peptides which changed significantly in the shotgun data were surrogate markers for the entire protein. The ELISA kit used (Chemicon International CYT 420) contains mouse monoclonal antibody and measures the levels of the entire protein within a sample. In the shotgun experiments, there was only 1 peptide from PEDF that was detected in the ECLIPSE A1ATD samples and there were 4 from the EXACTLE samples – these were found towards the C terminus of the PEDF protein. The amino acid sequence of the PEDF protein and the fragments identified form the EXACTLE samples is shown below in Figure 7.9.

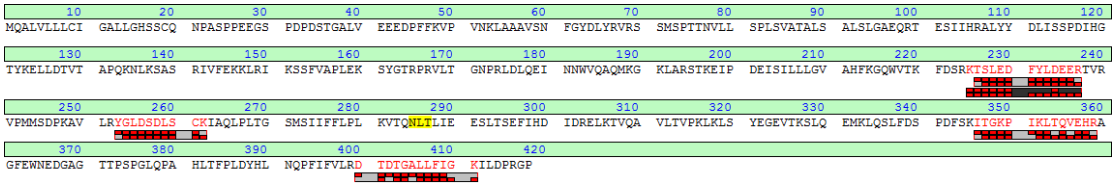

Figure 7.9. Amino acid sequence of PEDF. The sequences in red were identified in the EXACTLE pooled samples.

The single peptide identified from the ECLIPSE A1ATD samples was not one of the 4 peptides detected in the EXACTLE experiments. The protein scores were 106.2 for the ECLIPSE A1ATD and 197.0 for the EXACTLE pooled samples, which are both well above the pre-determined cut off score, hence the rationale for performing the ELISA. However, the data was normalised to generate the waterfall plots above, and within the EXACTLE samples, this may have enhanced the reduction post treatment, and be a reason that the ELISA results did not support the results from the shotgun data.

7.5.3 Corticosteroid Binding Globulin

Corticosteroid binding globulin is a further member of the serine protease inhibitor family (serpin) although unlike A1AT, it does not have protease inhibitory effects, but has important functions with regards to the transport of glucocorticoids (van Gent et al., 2003). From the shotgun experiments it looked like a promising candidate for further work in patients with A1ATD. However, in the 2 sets of samples analysed, it behaved in the opposite way – there was a fall in the ratio measured in the ECLIPSE A1ATD study and a rise in the EXACTLE study samples. There were 3 peptides from CBG in the ECLIPSE A1ATD study and 2 peptides from CBG from the EXACLTE study – the peptides were identified were not the same from both series of experiments. It was hypothesised after the ECLIPSE A1ATD samples were analysed that there could be a compensatory rise in this member of the serpin gene super family in patients with A1ATD, and that this was normalised when patients received augmentation therapy. However, this was not supported by the EXACTLE samples, and the hypothesis was limited due to the lack of protease inhibition actions of CBG.

7.5.4 Other Potential Candidate Proteins

There were a number of other proteins that could have been analysed in further detail and these include cystatin A, angiotensinogen, tetranectin, and complement C2. As these proteins were not detected in 2 independent experiments, they were not prioritised for further study within my research project. However, of these, angiotensinogen, which is also a further member of the serpin gene family, and complement c2, are described below.

Angiotensinogen is produced almost entirely by the liver, and like PEDF, it has no protease inhibiting activity (Shrikrishna et al., 2012). However, it is an integral part of the renin angiotensin system. Once it is cleaved by renin, angiotensinogen produces angiotensin I which is converted to angiotensin II by angiotensin converting enzyme (Shrikrishna et al., 2012). During this process, other products such as kinins are generated which may have localised effects within the lungs as well as within skeletal muscle, and these may produce some of the extra-thoracic manifestations of COPD such as skeletal muscle dysfunction. In the ECLIPSE A1ATD samples, angiotensinogen was lower in patients both pre and post treatment when compared to healthy control subjects, and did not change significantly when patients were compared pre and post treatment. Within the EXACTLE samples, angiotensinogen remained unchanged in the patients who received the active drug, whilst increased at the end of the placebo infusions. Due to these inconsistencies, and due to time and sample availability, angiotensinogen was not studied in any further detail, although could represent a possible target for future analysis.

The complement system is a complex system which is an integral part of the immune system. Complement C2 forms part of the classical and lectin pathways, and may be made by type II pneumocytes within the lungs (Pandaya et al., 2014). A number of inflammatory cytokines, including IL6 and TNF α may initiate complement factor synthesis within the lung micro-environment. However, unlike other parts of the complement system, including C3, C3a and C5, there have been no studies demonstrating the role of complement C2 in the pathogenesis of COPD (Pandaya et al., 2014). In the shotgun experiments, complement C2 was lower in patients with A1ATD at baseline compared to post treatment levels, and was higher in healthy control subjects

compared to A1ATD patients. In the EXACTLE samples, patients in the placebo group did not demonstrate any significant change after 6 months of treatment, whilst in patients receiving intravenous A1AT the levels were higher.

7.5.5 Protein Depletion

In the first shotgun experiment performed on the ECLIPSE A1ATD, 40µL of plasma in each pool were depleted of the 14 most abundant proteins using the IgY14 columns, and there was no further depletion using the supermix column. The LC-MALDI results revealed that the depletion step was not adequate as there were fragments of the 14 highly abundant proteins detected despite attempts at its removal.

The shotgun experiment was repeated on 100µL of plasma from the ECLIPSE A1ATD samples with the extra depletion step using the supermix column. Again, the most fragments detected were from common plasma proteins, namely albumin, A1AT, haptoglobin and fibrinogen.

In the EXACTLE shotgun experiment, the 100µL of pooled plasma was doubly depleted (same methodology used twice on the samples to ensure abundant depletion) using the IgY14 method, as recommended by the manufacturer. In this instance, the protein depletion was effective, but the amount of protein remaining after the supermix step was low at 18µg, which is lower than reported by Quian et al (2008) who used the IgY12 columns rather than IgY14, and recovered 55 µg of plasma from 225µL (Quian et al., 2008). This could mean that valuable information was lost through more depletion of proteins bound to the abundant proteins, and this may account for the lower number of labelled peptides and proteins studied in the EXACTLE samples compared

to the ECLIPSE A1ATD samples. This resulted in too little material left for the sensitivity of the mass spectrometer to identify sufficient numbers of peptides to uncover clinically significant differences.

Plasma protein concentration ranges from 60-80g/L. Albumin is the most abundant plasma protein at a concentration of 35-50g/L, and the lowest concentrations include cytokines and chemokines whose concentrations are up to 10 orders of magnitude lower than this. Therefore, it is difficult for any mass spectrometer to analyse these proteins, which are at much lower concentrations in the plasma, in the presence of more abundant plasma proteins. This is the rationale for using commercially available products in order to facilitate abundant protein depletion – ranging from simple resins which bind only to albumin, to more complex columns with polyclonal antibodies to some of the abundant plasma proteins (such as the IgY14 columns used here). Whilst these methods have good results, there is always the theoretical risk that because albumin acts as a co-transporter of other, smaller proteins, valuable information may potentially be lost from the sample. With each additional step in a complex experiment, such as here with a dual depletion strategy, there is a risk of non-specific protein binding and subsequent loss of information or of contamination. Ideally, a sample preparation with the fewest possible steps involved whilst still providing effective abundant protein depletion would constitute the best possible scenario. In addition, there is no series of experiments that can provide information and coverage of an entire proteome – in COPD that could involve tissue – from lung or skeletal muscle, in addition to plasma, sputum, exhaled breath condensate and urine proteomes.

Overall, in this series of experiments, peptides from 23 proteins were identified and quantified in both the ECLIPSE A1ATD and EXACTLE pooled samples, and overall,

the abundant plasma protein depletion was effective and allowed identification and quantification of proteins that were not identified during the profiling experiments due to their signal potentially being masked by abundant plasma proteins. The pie charts in Figure 7.10 demonstrate that most of the proteins originate from the extracellular compartment and that the nuclear and cytoplasmic proteins which are of more interest as potential markers of tissue leakage only make up a small proportion of this. This implies that very few peptides from tissue leakage were identified during these experiments.

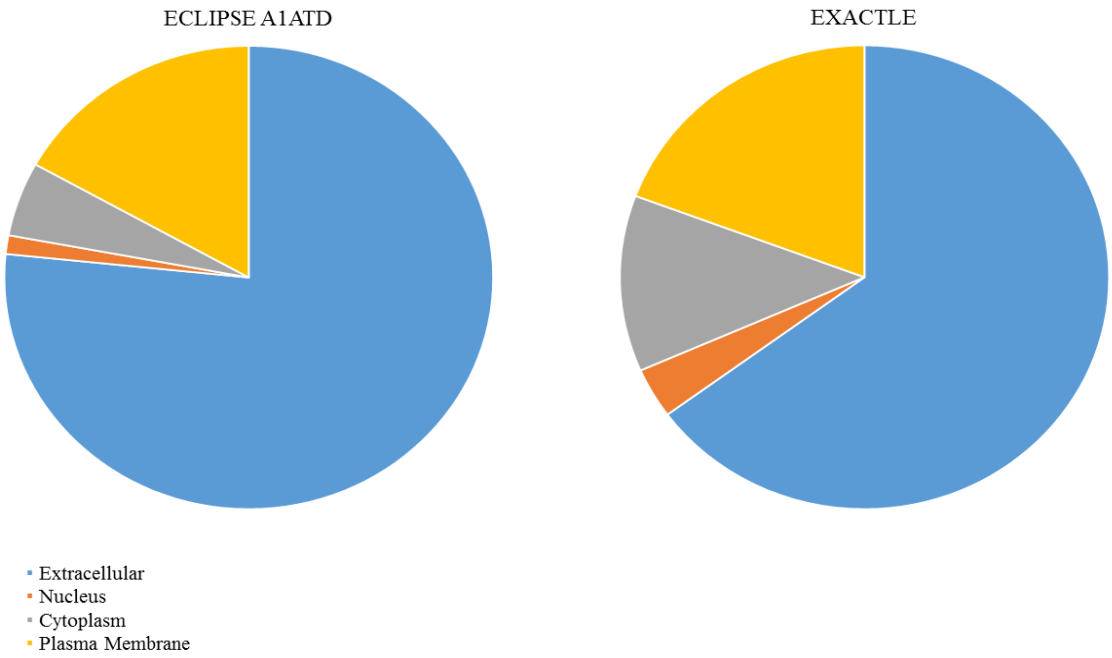

Figure 7.10 Pie charts showing the proportions of peptides and their cellular compartmentalisation.

7.6 Conclusions

The shotgun experiments were undertaken in order to analyse the plasma proteome in greater detail than was possible during the profiling work. Experiments of this sort, with multiple complex steps, would take months to optimise further, due to the increased

level of complexity and number of stages involved, and would require further analyses that were beyond the time frame of this thesis. An experiment of this length could take months to optimise each step, and additionally have a resource implication in terms of plasma and instrument time. This series of experiments did, however, in agreement with the profiling work, demonstrate that the majority of the most abundant layer of the plasma proteome remained unchanged following treatment with intravenous A1AT in patients with A1ATD. Whilst PEDF initially looked promising as a potential candidate worthy of further investigation, this was not confirmed by the ELISA analysis. Overall, no clinically relevant marker of response to treatment was identified during the shotgun experiments. It has previously been demonstrated that despite abundant protein depletion, it is not possible to identify and quantify other markers – such as cytokines, which have previously been studied in the pathophysiology of COPD.

CHAPTER 8 DISCUSSION

The ADAPT project in Birmingham holds the UK registry and is the UK national centre for patients with A1ATD and respiratory disease. Patients with liver related complications of their A1ATD are not routinely referred to and followed up at this centre. The ADAPT project however allows the collection and analysis of unique data into the respiratory complications of this genetic condition, and allows patients to be enrolled in clinical trials of therapy. Such studies have included the ECLIPSE A1ATD and EXACTLE commercially funded clinical trials, in addition to smaller independent studies and research, such as the *in vitro* ionophore and protease work presented within this thesis.

The patients who attend this centre for annual review are very well characterised in terms of demographic data, health status (measured using the SGRQ, CAT and SF36) and lung physiology, which is crucial when undertaking biomarker research, and when aiming to determine and interpret meaningful outcomes. This is because COPD secondary to A1ATD, like that seen in usual COPD, is a heterogeneous condition, with different rates of decline and different phenotypes, despite having a common underlying genetic basis (Dawkins et al., 2009).

Proteomic technologies have evolved and been widely utilised over the last few decades, since the term proteomics was first introduced in the 1990s, despite the study of proteins pre dating the introduction of this term. This widespread use is clearly demonstrated through the rapid increase throughout the last 2 decades in the number of publications accessible through Pubmed and other on line search engines using this

technology. These approaches have been used in a vast range of different disease processes including COPD, although their greatest use has been in the field of oncology in the hunt for biomarkers of disease which could be used clinically to monitor and treat the disease.

A1ATD introduced the protease/antiprotease hypothesis in to the pathogenesis of COPD. In this condition, individuals with the PiZZ genotype have a genetically determined low plasma levels of an important protease inhibitor, A1AT, which can predispose to the unopposed action of proteases, including NE, in the lung, leading to the early onset of emphysema. The rationale and hypotheses therefore for the series of experiments conducted within this thesis were to try to detect the effects of this putative protease/antiprotease imbalance by analysing plasma from patients with A1ATD pre and post treatment with the aim to detect fragments of proteins by plasma profiling.

8.1 Plasma Profiling

The 2 clinical trials of augmentation therapy presented in this thesis were the ECLIPSE A1ATD study and the EXACTLE study. Patients in the ECLIPSE A1ATD study received infusions for a total of 12 weeks, whereas in the EXACTLE study, patient samples were obtained from a 2 year study of therapy with A1AT or placebo, using samples taken at an interim point of 6 months. In a previous short-term study, only 6 weeks of therapy was required to show a reduction in sputum inflammatory signals, such as IL8 and LTB4 concentrations (Stockley et al., 2002). Both the EXACTLE and ECLIPSE A1ATD samples were taken after a longer treatment time period than this short study. Analysing the 2 sets of independent samples allowed a discovery phase to be undertaken, followed by a validation phase, in independent experiments, to gain

further confidence in the subsequent data generated. It was also the rationale behind analysing the 6 month samples from the EXACTLE study, as this was the nearest time point at which samples were available to the 3 month duration of the ECLIPSE A1ATD study.

It was possible to optimise plasma profiling techniques to study the samples from these clinical trials, and to obtain reproducible sample preparation and analysis methods with low intra-experimental CVs. The plasma and urinary peptidomes of patients with A1ATD pre and post augmentation therapy have been analysed and studied in this work. Mass spectra were generated using MALDI profiling techniques, following on from preliminary work undertaken using SELDI profiling. Significant differences were identified using LC-MALDI. However, the majority of the differences identified were fragments of the most abundant plasma proteins, namely A1AT, albumin and the complement system, and further work was required in order to attempt to reveal potential biomarkers of neutrophil elastase activity in the tissues.

An acceptable CV for any proteomics experiment is ~20%, (Bowler et al., 2006b) and each of the techniques I have used has had a similar CV when the QC sample has been analysed, during each separate experiment. This figure is also the accepted CV quoted by most manufacturers of SELDI proteinchips. Some of the published work carried out so far in COPD, for example by Bowler et al (2006 a) who used SELDI proteinchips on the plasma of 30 patients with COPD and 30 healthy control subjects, obtained CVs of almost 70% (Bowler et al., 2006 a). This highlights the difficulty to perform such experiments reproducibly, and optimisation of methods at the outset, to ensure reproducibility, is a crucial initial step. This is necessary as these techniques are

extremely sensitive to very small intra experimental changes, which would make interpretation of results difficult with high variability.

Furthermore, attention to detail at every step in the process is crucial – from sample collection, to sample processing and storage, to the number of freeze thaw cycles the samples have been exposed to. Mitchell et al (2005) undertook a study to determine the effects of repeated freeze after thaw cycles had on the quality of data subsequently generated using plasma samples. Following ACN precipitation of peptides, they were able to demonstrate that following 2 or more freeze thaw cycles, there was a trend towards a difference in peak intensities in the MALDI spectra generated, with samples that had more than 2 freeze thaw cycles having lower peak intensities in the spectra, whereas the duration of time spent with the samples stored below -70^0C had little effect on the subsequent analysis. It was felt that the repeated freezing and thawing of samples led to degradation of proteins and peptides contained within them, and hence the differences in terms of lower peak intensities they identified in the subsequent MALDI spectra (Mitchell et al., 2005). The samples utilised in this thesis analysis had been taken and stored in the same way, and stored in cryovials at -80^0C, and the number of freeze thaw samples minimised to maintain the quality of the samples. During the method optimisation phase, pooled samples were created and these used to perform experiments, to maintain the integrity and quality of the peptides and proteins in the remaining individual clinical samples. In addition, the number of freeze thaw cycles each sample underwent was minimised and no clinical sample was subjected to this on more than 2 occasions.

Two methods were selected to profile individual patient samples – WCX beads and SPE C8 cartridges, as they gave the most information and were the most reproducible. The supel tip, SPE C8 cartridges, C8 and C18 bead methods utilise the same underlying principle – namely reverse phase. The SPE C8 cartridges were the optimum reverse phase approach to use, as the spectra contained the most peaks and the lowest CVs of the reverse phase techniques.

The WCX beads gave more information above 4,000 Da, whereas information using the reverse phase approach with the C8 cartridges was limited to a lower mass range, so the approaches were complementary, although there was also a significant degree of overlap with the data produced. However, differences at higher mass ranges are more difficult to identify using MS/MS, as the proteins/peptides are too large to generate interpretable fragment patterns and therefore identify using this approach. The LC-MALDI data generated from these samples, unfortunately, did not give any identifications above 4000Da.

This has demonstrated the difficulties of undertaking work on biomarker discovery on plasma samples. Plasma is the most complex proteome to study, despite being potentially the most informative. An alternative approach would be to undertake proteomic analysis of lung tissue. This could be undertaken from samples obtained when patients undergo lung transplantation (proteomic analyses to date have largely been done on patients with concurrent malignancy with tissue samples taken from areas away from the tumour) as this would provide information at the site of lung tissue damage and potential biomarkers would not be hidden by abundant plasma proteins. This is potentially more applicable to patients with A1ATD rather than those with usual

COPD as patients with A1ATD tend to be younger when they develop symptoms, which may result in patients having end stage disease at an earlier age and thus more likely to be considered for lung transplantation. Any changes detected at this time using tissue analysis could potentially be transformed into serological tests for future study.

8.2 SELDI Compared to MALDI Profiling

SELDI analysis techniques differ from MALDI techniques in that SELDI uses Proteinchips and samples are incubated directly on to the surface of the chromatographic chip before matrix addition and generation of mass spectra. In MALDI experiments, the samples are prepared prior to being transferred to a plate where they are overlaid with matrix prior to analysis. The initial SELDI sample analyses presented in this thesis generated data across a wide mass range – from 1000 to 120000 Da. It was possible to detect peaks within the SELDI spectra with m/z ratios greater than 100,000Da. Within the MALDI spectra, the data generated was more limited; the majority of the peaks within these spectra were concentrated below 5000Da, therefore limiting the search to the endogenous plasma peptidome, rather than the entire proteome. Although it would have been difficult to identify larger proteins, which would have required a purification followed by digestion step, there were few peaks in the MALDI spectra detectable above 10,000 Da. This was despite the use of different matrices; SPA in particular has previously been used in the detection of larger proteins, and was the matrix of choice for the proteinchips used in the previous SELDI experiments. This was therefore the matrix used with the proteinchips, both in the preliminary work and following the move to a more sensitive mass spectrometer during this series of experiments. In changing mass spectrometer, conducting the same

experiment on proteinchips yielded a similar number of peaks within the spectra as with the Ciphergen PBS IIc mass spectrometer, however the mass range became more limited with few peaks observed above 10,000Da. This was also the case when other sample preparation techniques besides proteinchips were utilised with SPA as the matrix. The change to the Bruker Ultraflextreme from the Ciphergen PBS IIc was thought to be important because of improved mass resolution, however the more sophisticated analyser did not seem to work as well at the higher mass range. At that point it was not possible to change back to the previous mass spectrometer as it had been decommissioned. This resulted in information from the higher mass range being lost, but the sample preparation techniques used allowed more data to be generated in the mass range where subsequent identifications were possible.

8.3 Proteomics in Malignancy

Using plasma profiling in the search for biomarkers in some malignant conditions has led to the transfer of investigations from the research arena to routine clinical practice. Initially, there was anticipation and high expectation that proteomics would offer great success in the field of biomarker discovery. However, despite this, there have been few clinically useful biomarkers identified this way. This is in part due to the volume of data produced during experiments and need for the development of bioinformatics platforms to interpret the data, in order to determine which of the hundreds of proteins and peptides measured are of clinical relevance.

An example of the translation of clinical experimentation into clinical practice this is the use of the OVA 1 test in ovarian cancer. This is a combination of 5 proteins, namely CA 125 II, transthyretin, β_2-microglobulin, apolipoprotein A1 and transferrin, which

have formed the basis of a serological test which can be used in patients with a suspected ovarian malignancy. Measurements of these 5 proteins are analysed using an algorithm to determine the likelihood of the patient having a malignancy (Useland et al., 2011). This test has been approved by the FDA for use in clinical practice, and is superior to the measurement of CA 125 alone, with an increase in sensitivity 60% to 89% and an increase in negative predictive value from 90 to 94% (Abraham, 2010).

Within the field of respiratory medicine, Veristrat is a serological test developed to be used in patients with non-small cell lung cancer. Taguchi et al used MALDI technology to generate algorithm based on 8 specific peaks in MALDI spectra, which may predict the outcome of treatment with epidermal growth factor (EGFR) tyrosine kinase inhibitors (TKIs) (Taguchi et al., 2007). They analysed serum and plasma taken pre-treatment with either erlotinib or gefitinib in 2 separate patient cohorts and classified these patients into 2 groups: – those who demonstrated a good response to treatment (median survival 306/207days respectively) or a poor response to treatment (median survival 107/92 days respectively) with hazard ratios of 0.5 and 0.41 (CI 0.24 to 0.78 and 0.17 to 0.63). This is of clinical benefit pre-treatment when determining optimal second line treatment strategies – i.e. whether or not to give conventional chemotherapy or to give one of the newer EGFR targeted therapies such as erlotinib and gefitinib, based on the likelihood of responding to treatment.

Other work, such as that by Ward et al in 2006, used SELDI proteinchips and plasma from patients with and without colorectal cancer and discovered a number of peaks within the spectra, corresponding to transferrin, A1AT, compliment C3a des-arg and apolipoprotein A1, which when used in combination were able to distinguish between

patients with colorectal cancer and those without (Ward et al., 2006). The specificity and sensitivity of this combination of markers was 91% and 95% respectively, compared to that of CEA alone which has a sensitivity of between 30 and 40% for early stage disease.

The work from the OVA I, Veristrat and the study of colorectal cancer have demonstrated that the search for a single biomarker is likely to be unrealistic, as in these examples only panels of markers have been shown to be informative. COPD is a complex heterogeneous disease, even amongst patients with COPD secondary to A1ATD, and panels of markers together in well phenotyped groups of patients, may be more clinically relevant.

To date, the majority of published work using plasma proteomics in the analysis of clinical samples has been studying patients with cancer. In malignant disease, without treatment, there is inevitably disease progression. This is also a heterogeneous process and may occur at different rates between different individuals, and affect different distal sites away from the primary source, (Sallam, 2015) however progression and subsequently death are usually the expected outcomes. COPD, however, is a far more heterogeneous condition; there are many different phenotypes, the pathophysiology is not clearly understood and the disease trajectory differs from patient to patient. The ECLIPSE investigators measured FEV_1 in 2163 patients with COPD on 8 occasions over a 3 year period (Vestbo et al., 2011). They described a wide range in decline in FEV_1 between groups they characterized into those with emphysema on CT, those with chronic bronchitis, presence of bronchodilator reversibility and patients with cardiovascular disease, proving the highly variable nature of this condition.

Additionally, it is not a disease confined to a single organ i.e. the lung – it is a multi-system disease with well described comorbidities outside the lungs, including cardiovascular disease (Sin et al., 2003), osteoporosis (Agusti 2005), depression (Wagena et al., 2001) and an increased lifetime risk of lung cancer (Noruma et al., 1991). This is further complicated by transient worsening in symptoms with recovery which may not return to the previous baseline when patients experience exacerbations of their COPD. Therefore the search for biomarkers in COPD is inherently more complex than in the case of malignancy, and may, at least in part, explain the lack of transfer of any of the potential candidates identified to date using proteomic techniques to routine clinical practice in COPD.

This is complicated further by many of the observations that the proteomes of people who smoke but do not have COPD, may differ from those who have never smoked and those who do have COPD. Even in A1ATD, there is heterogeneity of the clinical presentation of symptoms amongst patients with the same genotype (PiZZ), highlighted by differences amongst siblings (Dawkins et al., 2009). Hence there is a critical need to phenotype patients accurately prior to embarking on proteomics experiments, and even that may not result in the discovery of useful biomarkers as in the current study.

8.3 Ionophore and Protease Work

The ionophore series of experiments demonstrated clear differences in the actions of calcium ionophore between healthy control subjects and patients with A1ATD, in particular the generation of peptides from fibrinogen in patients with A1ATD. Further work could be undertaken to determine whether or not the plasma peptide profile

following neutrophil stimulation with ionophore of patients with A1ATD is normalized when patients receive augmentation therapy. In the UK, this is not currently possible outside a research project, as augmentation therapy is not licensed for routine clinical use, apart from certain exceptional circumstances (for example panniculitis with ulceration of lesions). To be replicated, this experiment has to be carried out on fresh, whole blood samples, where neutrophils are present and still viable, hence to replicate this work, would require samples from a cohort of patients who were about to commence augmentation therapy. This would allow the pre and post treatment analyses within the same individuals in order to specifically answer this question, to discover whether or not fibrinogen fragments (for instance) is the predominant peptides which are detected post stimulation with ionophore, and remains an area for possible future study.

The ionophore series of experiments was performed on whole blood. Whole blood contains leucocytes other than neutrophils, including lymphocytes and eosinophils, although neutrophils make up the largest proportion at > 60% of the total (Palmer et al., 2006). Future work could be undertaken on neutrophils (though less physiological) isolated using techniques described by Sapey et al (Mikami et al., 1998) to confirm that the results of the ionophore experiments are specifically due to release of proteases from neutrophils and not from other cell types.

8.5 Exacerbation Samples

Exacerbations of COPD are defined as ‘a worsening of a patient’s symptoms beyond the normal day to day variation’ (NICE 2010) and may manifest as an increase in cough, sputum production, change in colour or viscosity of sputum, or worsening dyspnea.

COPD exacerbations are a significant cause of morbidity and mortality amongst this patient group, and a wealth of evidence supports the finding that measures of inflammation increase during exacerbations of COPD and in COPD secondary to A1ATD (Gompertz et al., 2001 and Hill et al., 1999). I originally aimed to profile plasma from patients taken at baseline and during exacerbations of their airways disease. The samples I used were collected as part of a study published in 1999, which included sputum and serum samples from 11 patients with the PiZZ genotype of A1ATD who were experiencing well characterized exacerbations of their airways disease. This included assessment of sputum purulence in addition to measurement of markers of inflammation such as IL8 and LTB4, and serum markers including CRP and A1AT.

However, the samples had been collected in the late 1990s, and had undergone multiple freeze thaw cycles for previous analyses of inflammatory markers, including those published in the paper (Hill et al., 1999), and the quality of the samples was therefore likely to be inappropriate for plasma peptide profiling. The total number of samples was limited (11 baseline and 10 on day 1 of exacerbation) due to the nature of the study, and the spectra generated contained very few peaks (65 compared to >170 for the ECLIPSE A1ATD and EXACTLE samples) which were of low signal intensity, despite the same sample preparation techniques used throughout the remainder of this thesis. Furthermore, the sample intra-experiment CV was 18% when performed on the QC sample which was analysed throughout all of the series of experiments, implying that it was the exacerbation samples themselves rather than technical error of the experiments which was responsible for the poor results generated. It was likely due to the reduction in quality of the samples secondary to repeated freeze thaw cycles that

the samples had been subjected to, as previously described in 8.1. The data was not of sufficient quality therefore to analyse and generate clinically useful results, and there was insufficient time to gain further ethical approval to conduct a new clinical trial and hence collect new exacerbation samples to profile. Therefore this section of work was not completed as planned in the aims section of this thesis, but remains a potential future series of experiments to perform. However, the same difficulties experienced in profiling plasma would still be present and therefore unless there were changes in the abundant plasma proteome, clinically relevant changes may not be generated.

8.6 Shotgun Experiments

The identification of a rise in fragments of A1AT in the plasma of patients who had received A1AT replacement therapy whilst remaining unchanged in patients receiving placebo demonstrates the ability of the experiments to produce some positive results, and acted as an extra level of validation. However, it also demonstrates the difficulties in profiling plasma whereby potential biomarkers or lung tissue fragments are not detectable or identifiable in the vast excess and abundance of plasma proteins. The shotgun series of experiments was performed to analyse the plasma proteome in greater depth than in the profiling work, in order to use a complementary approach to the high throughput profiling work. The work demonstrated some success of the abundant protein depletion strategy used – the proteins which were subsequently identified and quantified were from lower abundance proteins including vitamin D binding protein, tetraspanin, vascular cell adhesion protein and thyroxine binding globulin. A full list of proteins is presented in Appendix II. The majority of proteins were from the extracellular space highlighting the difficulty of detecting peptides from tissue damage within the plasma amongst other more abundant proteins. There were a number of

proteins which changed post treatment with intravenous A1AT but it was not possible to analyse them all in more detail – these include, cystatin A and tetranectin. However as they were not identified in both sets of samples, PEDF (which was identified in both datasets), was prioritized to measure on individual samples.

The shotgun experiments also demonstrated the potential difficulties when depleting samples of abundant proteins – namely that of loss of valuable material and hence potential future biomarkers. However, despite this, it was not possible to identify and quantify other markers, such as cytokines and chemokines, which have been investigated in the pathophysiology of COPD, as these are difficult to quantify due to their low plasma concentrations.

8.7 Electrospray-Peptidome Analyses

ESI ionization differs from MALDI in that the analysates are sprayed into the mass spectrometer which allows direct interfacing with separation technologies such as HPLC or capillary electrophoresis. ESI has been utilized successfully in plasma and serum and data published in the literature. For example, in lung cancer, Ueda and colleagues performed size exclusion chromatography and were able to detect 3537 peptides in the serum of patients and with lung adenocarcinoma and compare these to healthy control subjects (Ueda et al., 2011). They found that of these, 118 were statistically significant between the cancer patients and the control group, and went on to perform MS/MS on the samples and discovered that fragments of apolipoprotein A4, fibrinogen alpha chain and limbin were differentially expressed in patients with lung cancer and therefore could be investigated further in biomarker discovery (Ueda et al., 2011).

Thus, ESI MS may allow more in depth peptidome analysis than MALDI profiling. ESI analysis of the pooled samples was attempted during the experimental phase of this thesis using a Bruker Maxis post ACN precipitation of peptides from plasma. Ten µL of plasma was diluted in 90 µL of ACN and centrifuged at 500g for 5 minutes. The supernatant was transferred to a clean tube, placed into the speedivac until dry, and peptides re-suspended in 10 µL of 0.1% formic acid for ESI analysis. One of the major advantages of this approach is the ability to use automation to analyse samples. This technique was not successful with the current set of samples (data not shown) as repeatedly the experiments stopped mid-processing due to problems with the HPLC column blocking with excess peptide and particulate material.

Others have used ESI successfully coupled with tandem mass spectrometry to measure drug levels within plasma. Bazoti and colleagues used liquid chromatography with ESI to optimise conditions to measure the levels of the antibiotic daptomycin in human plasma. This was subsequently proven to be a sensitive enough test to perform on patient plasma (Bazoti et al., 2011). This approach remains a possible area for future work in the attempt at biomarker discovery in A1ATD. However, measurement of small molecules is easier than measuring peptides and proteins. Geyer and colleagues published a methodology that analysed 1µL of plasma, and using a combination of steps starting with a reduction, alkylation and digestion of proteins (performed within an hour), followed by analysis of LC MS/MS and by optimizing the HPLC gradient were able to identify almost 1000 proteins. This methodology has taken many years to optimize to this workflow, but demonstrates that label free identification and quantification of plasma peptides is possible (Geyer et al., 2016).

8.8 Future Work

The observation that SPAAT increased on augmentation was unique and hence unexpected. The role of these A1AT peptides is currently unknown and may reflect peptides that remain inhibitors of NE are retain other biological properties of A1AT. To investigate SPAAT further a specific assay for the SPAAT peptide could be created using multiple reaction monitoring (MRM). MRM is a targeted mass spectrometry approach where the SPAAT peptide would be pre-selected for isolation and fragmentation using a triple quadrupole mass analyser and coupled with a heavy isotope labelled version of SPAAT to allow absolute quantitation of SPAAT in clinical samples.

An alternative approach would be to undertake mass spectrometry analysis of Prolastin directly. This would allow confident exclusion of the rise in the SPAAT signal following treatment being merely due to the presence of the SPAAT peptide in the replacement therapy. This should also be done by profiling plasma before and immediately after direct addition of Prolastin in case analytical sensitivity for SPAAT is strongly influenced by matrix effects.

A final approach might be to develop a specific immune-assay for the SPAAT peptide/s which could be used not only to track its' presence but also as a means to immune purify the peptide/s and enable in vitro studies of the properties.

Further experiments could include the use of the approach described above by Geyer et al., and perform the same comparative analyses presented in the current thesis. The

authors of this methodology paper are able to identify up to 1000 proteins from 1µL of plasma, which may reveal potential candidate markers of response to augmentation therapy in A1ATD. This approach combined with the latest generation of mass spectrometers with higher mass accuracy, faster data acquisition and increased sensitivity would allow a deeper analysis of the plasma proteome/peptidome. Additionally the increasing availability of highly multiplexed immunoassay platforms (e.g. olink proteomics) may circumvent the difficulty of detecting very low abundance species by mass spectrometry.

8.9 Conclusions

Using these proteomic techniques in the search for potential biomarkers in patients with the PiZZ genotype of A1ATD has revealed that post augmentation therapy, the majority of the plasma peptidome remains unchanged. The main differences post augmentation therapy were increases in signal intensity of fragments of A1AT previously described and termed SPAAT.

On further, more in depth analysis of pooled samples, again the majority of the detectable plasma peptidome remained unchanged post augmentation therapy. There were no peptides or proteins identified using any of the approaches in the work in this thesis that could act as biomarkers in the use of augmentation therapy in patients with A1ATD. This lack of a clear signal could be a result of either there being no actual changes in the plasma proteome following treatment with augmentation therapy, changes present but too small to detect, or changes present but the peptides at low concentrations below the limit of detection of the techniques and mass spectrometers utilized. Aα-Val 360 has been demonstrated to decrease with augmentation therapy in

the patient samples analysed within this thesis, which clearly negates the first option suggesting any signal is too small to detect without more specific or sensitive methodologies. At the start of this thesis the use and sensitivity of proteomics was largely unknown and hence this became an exploratory study. Power calculations depend upon knowing the reproducibility of the method both within sample and between samples.

There are other proteomic techniques that could be utilized, including ESI techniques, and these, in addition to the continual improvement in the technology of mass spectrometers, mean that plasma proteomics in COPD whilst challenging at present, may still offer potential biomarker discovery in the future. Clearly, however, careful validation will be an essential part of the development to enable sensible power calculations to be made before embarking on patient studies including any influence of patient phenotype.

CHAPTER 9 REFERENCES

Abraham J. (2010) OVAI test for preoperative assessment of ovarian cancer *Community Oncology* 7, 249-51.

Albrethsen J. (2011) The first decade of MALDI protein profiling: A lesson in translational biomarker research *Journal of Proteomics* 74, 765-773.

Agusti AG. (2005) Systemic effects of chronic obstructive pulmonary disease *Proceedings of the American Thoracic Society* 2, 367-370.

Agusti AG, Edwards LD, Celli B, MacNee W, Calverley PM, Mullerova H, Lomas DA, Wouters E, Bakke P, Rennard S, Crim C, Miller BE, Coxson HO, Yates JC, Tal-Singer R, Vestbo J, ECLIPSE Investigators. 2013. Characteristics, stability and outcomes of the 2011 GOLD COPD groups in the ECLIPSE cohort, *European Respiratory Journal*, 42(3), 636-646.

Agusti AG, Edwards LD, Rennard SI, MacNee W, Tal-Singer R, Miller BE, Vestbo J, Lomas DA, Calverley PMA, Wouters E, Crim C, Yates JC, Silverman EK, Coxson HO, Kakke P, Mayer RJ, Celli B for the ECLIPSE investigators (2012) Persistent systemic inflammation is associated with poor clinical outcomes in COPD: a novel phenotype *PLoSOne*. 7(5), 1-10.

Babustye A, Stravinskaite K, Jeroch J, Lotvall J, Sakalauskas R, Sitkauskienne B. (2007) Patterns of airway inflammation and MMP-12 expression in smokers and ex-smokers with COPD. *Respiratory Research*, 8, 81-89.

Barreiro E, Rabinovich R, Marin-Corral J, Barbera J A `, Gea J, Roca J. (2008). Chronic endurance exercise induces quadriceps nitrosative stress in patients with severe COPD *Thorax* 64, 13-19.

Bazoti FN, Gikas E, Skoutelis A, Tsarbopoulos A. (2011). Development and validation of an ultra-performance liquid chromatography- tandem mass spectrometry method for the quantification of daptomycin in human plasma. *Journal of Pharmaceutical and Biomedical Analysis*, 56(1), 78-85.

Betsuyaku T, Nishimura M, Takeyabu K, Tanino M, Venge P, Xu S, Kawakami Y. (1999). Neutrophil granule proteins in bronchoalveolar lavage fluid from subjects with subclinical emphysema. *American Journal of Respiratory and Critical Care Medicine*, 159, 1985-1991.

Bhowmik A, Seemungal TA, Sapsford RJ. Devalia JL, Wedzica JA. (1998). Comparison of spontaneous and induced sputum for investigation of airway inflammation in chronic obstructive pulmonary disease. *Thorax* 53(11), 953-956.

Borregaard N, Cowland JB. (1997) Granules of the human ploymorphonuclear leukocyte. *Blood*, 89 (10), 3503-3521.

Bowler RP, Caneham ME and Ellison MC. (2006a). Surface enhanced laser desorption/ionisation (SELDI) time of flight mass spectrometry to identify patients with chronic obstructive pulmonary disease. *Journal of COPD,* 3, 41-50.

Bowler RP, Ellison MC and Reisdorph N. (2006b). Proteomics in pulmonary medicine. *Chest,* 130,567-574.

Bozinovski S, Hutchinson A, Thompson M, MacGregor L, Black J, Giannakis E, Karlsson A, Silvestrini R, Smallwood D, Vlahos R, Irving LB and Anderson GP. (2008). Serum amyloid A is a marker of acute exacerbations of chronic obstructive pulmonary disease. *American Journal of Respiratory and Critical Care Medicine,* 177, 269-278.

Brantly M. (2002). α1 antitrypsin: not just a protease. *American Journal of Respiratory Cell and Molecular Biology,* 27, 652-654.

Broeckaert F, Bernard A. (2000). Clara cell secretory protein (CC16): characteristics and perspectives as lung peripheral biomarker. *Clinical and Experimental Allergy,* 30, 469–475.

Bruce N, Perez-Padilla R, and Abalak R. (2000). Indoor air pollution in developing countries: a major environmental and public health challenge. Bull WHO 78.

Bruno A, Chiappara G, Siena L, Giammanco S, Gjomarkav M, Bonsignore G, Bousquet J, Vignola AM. (2005). Does leptin play a cytokine-like role within the airways of COPD patients? *European Respiratory Journal,* 26(3), 398-405.

Cassado B, Iadarola P, Pannell LK, Liusetti M, Corsico A, Ansaldo E, Reffarotti I, Boschett P and Baranuik J. (2007). Protein expression in sputum of smokers and chronic obstructive pulmonary disease patients: a pilot study by CapLC-ESI-Q-TOF *Journal of Proteome Research,* 6, 4615-4623.

Carter RI, Mumford RA, Treonze KM, Finke PE, Davies P, Si Q, Humes JL, Dirksen A, Piitulainen E, Ahmad A and Stockley RA. (2011). The fibrinogen cleavage product Aα-Val^{360}, a specific marker of neutrophil elastase activity *in vivo. Thorax,* 66,686-691.

Carter RI, Ungurs MJ, Pillai A, Mumford RA, Stockley RA. The relationship of the fibrinogen cleavage biomarker Aα-Val 360with disease severity and activity in α-1 antitrypsin deficiency. (2013). *Chest,* 148(2), 382-388.

Cazzola M and Novelli G. (2010). Biomarkers in COPD. *Pulmonary Pharmacology and Therapeutics,* 23(6), 493-500.

Celli BR and MacNee W. (2004). Standards for the diagnosis and treatment of COPD. *European Respiratory Journal,* 23, 932-946.

Celli B, Cote G, Marin JM, Casanova C, Montes de Oca M, Mendez RA, Pinto Plata V, and Cabral HJ. (2004). The body-mass index, airflow obstruction, dyspnoea and

exercise capacity index in chronic obstructive pulmonary disease. *New England Journal of Medicine,* 350, 1005-1012.

Chapman KR, Burdon JGW, Piitulainen E, Sandhaus RA, Seersholm N, Stocks JM, Stoel BC, Huang L, Yao Z, Edelman JL, McElvaney NG. On behalf of the RAPID Trial Study Group. Intravenous augmentation treatment and lung density in severe α1 antitrypsin deficiency (RAPID): a randomised, double-blind, placebo-controlled trial. (2015). *Lancet*, 386, 360-368.

Chen J, Ye L, Zhang L and Jiang WG (2009). The molecular impact of pigment epithelium derived factor on lung cancer cells and the clinical significance. *International Journal of Oncology*, 35, 159-166.

Cosgrove GP, Brown KK, Schiemann WP, Serls AE, Parr JE, Geraci MW, Schwarz MI, Cool CD and Worthen GS (2004). Pigment-epithelium derived factor in idiopathic pulmonary fibrosis: a role in aberrant angiogenesis. *American Journal of Respiratory and Critical Care Medicine*, 170, 242-251.

Creutzberg EC, Wouters EF, Vanderhoven-Augustin IM, Denetner MA, Schols AM. (2000). Disturbances in leptin metabolism and related to energy imbalance during acute exacerbations of chronic obstructive pulmonary disease. *American Journal of Respiratory and Critical Care Medicine,* 162, 1239-1245.

Dahl M, Tybjaerg-Hansen A, Vestbo J. (2001). Elevated plasma fibrinogen associated with reduced pulmonary function and increased risk of chronic obstructive pulmonary disease. *American Journal of Respiratory and Critical Care Medicine,* 164, 1008-1011.

Danesh J, Lewington S, Thompson SG, Lowe GDO, Collins R, Kostis JB, Wilson AC, Folsom AR, Wu K, Benderley M. (2005). Plasma fibrinogen level and the risk of major cardiovascular diseases and nonvascular mortality: an individual participant meta-analysis. *Journal of the American Medical Association***,** 294, 1799–1809.

Davies SF, Offord KP, Brown MG, Campe H and Niewoehner D. (1983). Urine desmosine is unrelated to cigarette smoking or to spirometric function. *American Reviews of Respiratory Disease,* 128, 473-475.

Dawkins PA, Dawkins CL, Wood AM, Nightingale PG, Stockley JA and Stockley (2009). Rate of progression of lung function impairment in alpha-1-antitrypin deficiency. *European Respiratory Journal*, 33, 1338-1344.

De Torres, Pinto-Plata V, Casanova C, Mullerova H, Cordoba-Lanus E, Muros de Fuentes M, Aguirre Jamie A and Celli B. (2008). C-reactive protein levels and survival in patients with moderate to very severe COPD. *Chest,* 133, 1336-1343.

Dirksen A, Dijkman JH, Madsen F, Stoel B, Hutchison DCS, Ulrik CS, Skovgaard LT, Kok-Jensen A, Rudolphus A, Seersholm N, Vrooman HA, Reiber JHC, Hansen NC, Heckscher T, Viskum K and Stolk J. (1999). A randomised clinical trial of α1-antitrypsin augmentation therapy. *American Journal of Respiratory and Critical Care Medicine,* 160, 1468-1472.

Dirksen A, Piitulainen E, Parr DG, Deng C, Wencker M, Shaker SB and Stockley RA. (2009). Exploring the role of CT densitometry: a randomised study of augmentation therapy in α1-antitrypsin deficiency. *European Respiratory Journal,* 33, 1345-1353.

Di Stefano A, Capelli A, Lusuardi M, Balbo P, Vecchio C, Maestrelli P, Mapp CE, Fabbri L, Donner CF, Saetta M. (1998). Severity of airflow limitation is associated with severity of airway inflammation in smokers. *American Journal of Respiratory and Critical Care Medicine,* 158, 1277-1285.

Di Stefano A, Caramori G, Oates T, Capelli A, Lusuardi M, Gnemmi I, Ioli F, Chung KF, Donner CF, Barnes PJ, Adcock IM. 2002. Increased expression of nuclear factor-κB in bronchial biopsies from smokers and patients with COPD. *European Respiratory Journal,* 20, 556-563.

Diz AP, Truebano M and Skibinski DO (2009). The consequences of sample pooling in proteomics: an empirical study. *Electrophoresis,* 30(17**),** 2967-2975.

Doll R, Peto R, Wheatley K, Gray R and Sutherland I. (1994). Mortality in relation to smoking: 40 years' observations on male British doctors. *British Medical Journal,* 309, 901 – 911.

Fantuzzi G, Faggioni R. (2000). Leptin in the regulation of immunity, inflammation and hematopoesis. *Journal of Leukocyte Biology,* 68, 437-446.

Filleur S, Nelius T, de Riese W and Kennedy RC (2009). Characterization of PEDF: a multi-functional serpin family protein. *Journal of Cellular Biochemistry,* 106, 769–775.

Ford ES. (2003).The metabolic syndrome and C-reactive protein, fibrinogen, and leukocyte count: findings from the Third National Health and Nutrition Examination Survey. *Atherosclerosis,* 168, 351–358.

Fregonese L and Stolk J. (2007). Hereditary alpha-1-antitrypsin deficiency and its clinical consequences. *Orphanet Journal of Rare Diseases,* 3, 16-25.

Fregonese L, Ferrari F, Fumagalli M, Luisetti M, Stolk J, Iadrola P. (2011). Long-term variability of desmosine/isodesmosine as biomarker in alpha-1-antitrypsin deficiency-related COPD. *Journal of Chronic Obstructive Pulmonary Disease,* 8, 329-333.

Fukada Y, Masuda Y, Ishizaki M, Masugi Y, and Ferrans VJ. (1989). Morphogenesis of abnormal elastic fibres in lungs of patients with panacinar and centriacinar emphysema. *Human Pathology,* 20, 652-659.

Fumagalli M, Dolcini L, Sala A, Stolk J, Fregonese L, Ferrari F, Viglio S, Luisetti M, Iadarola P. (2008). Proteomic analysis of exhaled breath condensate from single patients with pulmonary emphysema associated to α1-antitrypsin deficiency. *Journal of Proteomics,* 71, 211-221.

Fumagalli M, Ferrari F, Luisetti M, Stolk J, Hiemstra PS, Capuano D, Viglio S, Fregonese L, Cerveri I, Corana F, Tinelli C, Iadarola P. (2012). Profiling the proteome of exhaled breath condensate in healthy smokers and COPD patients by LC-MS/MS. *International Journal of Molecular Sciences,* 13, 13894-13910.

Gabay C, Kushner I. (1999). Acute-phase proteins and other systemic responses to inflammation. *New England Journal of Medicine,* 340, 448–54.

Gadek JE, Klein HG, Holland PV and Crystal RG. (1981). Replacement therapy of alpha-1-antitrypsin deficiency. Reversal of protease-anti-protease imbalance within the alveolar structures of PiZ subjects. *Journal of Clinical Investigation,* 68, 1158-1165.

Geyer PE, Kulak NA, Pichler G, Holdt LM, Teupser D, Mann M. (2016). Plasma proteome profiling to assess human health and disease. *Cell Systems,* 2, 185-195.

Gompertz S, O'Brien C, Bayley DL, Hill SL and Stockley RA. (2001). Changes in bronchial inflammation during exacerbations of chronic bronchitis. *European Respiratory Journal,* 17(6), 1112-1119.

Gotfredsen NS, Lam TH, Hansel TT, Leon ME, Gray N, Dresler C, Burns DM, Prescott E, Vestbo J. (2008). COPD-related morbidity and mortality after smoking cessation: status of the evidence. *European Respiratory Journal,* 32, 844-853.

Gottlieb DJ, Luisetti M, Stone PJ, Allegra L, Cantey-Kiser JM, Grassi C, Snier GL. (2000). Short-term supplementation therapy does not affect elastin degradation in severe alpha-1-anti-trypsin deficiency. The American Italian AATD Study Group. *American Journal of Respiratory and Critical Care Medicine,* 162(6), 2069-2072.

Gotzsche PC and Johansen HK. (2010). Intravenous alpha-1-antitrypsin augmentation therapy for treating patients with alpha-1-antitrypsin deficiency and lung disease. Cochrane Database of Systematic Reviews, Issue 7. Art. No. CD007851. DOI10.1002/14651858.CD007851.pub2.

Gray RD, MacGregor G, Noble D, Imrie M, Dewar M, Boyd CA, Innes JA, Porteous DJ and Greening AP. (2008). Sputum proteomics in inflammatory and suppurative respiratory diseases. *American Journal of Respiratory and Critical Care Medicine,* 178, 444-452.

Greenbaum D, Colangelo C, Williams K and Gerstein M. (2003). Comparing protein abundance and mRNA expression levels on a genome level. *Genome Biology,* 4(9), 117.1-117.8.

Grimstein C, Choi Y, Wasserfall C, Satoh M, Atkinson M, Brantly M, Campbell-Thompson M and Song S. (2011). Alpha-1-antitrypsin protein and gene therapies decrease autoimmunity and delay arthritis development in mouse model. *Journal of Translational Medicine,* 9, 21-31.

Groenewegen KH, Postma DS, Hop WCJ, Wielders PLML, Schlosser NJJ and Wouters EFM. (2008). Increased systemic inflammation is a risk factor for COPD exacerbations *Chest,* 133, 350-357.

Hattotuwa K, Gamble EA, O'Shaughnessy T, Jeffery PK, Barnes NC. (2002). Safety of bronchoscopy, biopsy, and BAL in research patients with COPD. *Chest,* 122, 1909-1912.

Hill AT, Campbell EJ, Bayley DL, Hill SL and Stockley RA. (1999). Evidence for excessive bronchial inflammation during an acute exacerbation of chronic obstructive pulmonary disease in patients with α1-antitrypsin deficiency (PiZ). *American Journal of Respiratory and Critical Care Medicine,* 160, 1968-1975.

Hoenderos K, Condliffe A. (2012). The neutrophil in chronic obstructive pulmonary disease too little, too late or too much, too soon? *American Journal of Respiratory Cellular and Molecular Biology,* 48(5), 531-539.

Huang J T-J, Chaudhuri R, Albarbarawi O, Barton A, Grierson C, Rauchaus P, Weir CJ, Messow M, Stevens N, McSharry C, Feuerstein G, Mukhopadhyay S, Brady J, Palmer C NA, Miller D, Thomson NC. (2012). Clinical validity of plasma and urinary desmosine as biomarkers for chronic obstructive pulmonary disease. *Thorax,* 67, 502-508.

Hubbard RC, Sellers S, Czerski D, Stephens L and Crystal RD. (1988). Biochemical efficacy and safety of monthly augmentation therapy for alpha-1-antitrypsin deficiency. *Journal of the American Medical Association,* 260, 1259-1264.

Hubbard RC, Brantly ML, Sellers SE, Mitchell ME and Crystal RG. (1989). Anti-neutrophil elastase defences of the lower respiratory tract in alpha-1-antitrypsin deficiency directly augmented with an aerosol of alpha-1-antitrypsin. *Annals of Internal Medicine,* 111, 206-212.

Igishi T, Hitsuda Y, Kato K, Sako T, Burioka N, Yusada K. (2003). Elevated 8-hydroxydeoxyguanosine, a biomarker of oxidative stress and lack of association with antioxidant vitamins in chronic obstructive pulmonary disease. *Respirology,* 8(4), 455-460.

Janciauskiene SM, Nita IM and Stevens T. (2007). α1-antitrypsin, old dog, new tricks. α1-antitrypsin exerts in vitro anti-inflammatory activity in human monocytes by elevating cAMP. *The Journal of Biological Chemistry,* 282, 8573-8582.

Kammath S, Lip GYH (2003) Fibrinogen: biochemistry, epidemiology and determinants. *Quarterly Journal of Medicine,* 96, 711-29.

Kardag F, Karul AB, Cildag, Yilmaz M and Ozcan H. (2008). Biomarkers of systemic inflammation in stable and exacerbation phases of COPD. *Lung,* 186, 403-409.

Kelsen S, Duan X, Ji R, Perez O, Liu C and Merali S. (2007). Cigarette smoke induces an unfolded protein response in the human lung a proteomics response. *American Journal of Respiratory Cell and Molecular Biology,* 38, 541-550.

Larson RK, Barman RL, Kueppers F, Fudenberg HH. 1970. Genetic and environmental determinants of chronic obstructive pulmonary disease. *Annals of Internal Medicine,* 72, 627-632.

Lee EJ, In KH, Lee SY, Shin C, Shim JJ, Kang KH, Yoo SH, Kim CH, Kim HK, Lee SH and Uhm CS. (2009). Proteomic analysis in lung tissue of smokers and COPD patients. *Chest,* 135, 344-352.

Li X, Wang T, Yang T, Shen Y, Liu L, Dong J, Guo L, Li D, Zhang X, Chen L, Xu D, Wen F. (2015). Elevated levels of pigment epithelium-derived factor correlated with inflammation and lung function in COPD patients. *International Journal of COPD,* 10, 587-594.

Liou TG, and Campbell EJ. (1996). Quantum proteolysis resulting from release of single granules by human neutrophils: a novel, nonoxidative mechanism of extracellular proteolytic activity. *Journal of Immunology,* 157, 2624-2631.

Lofdahl JM, Cederlund K, Nathell L, Eklund A, Skold CM. (2005). Bronchoalveolar lavage in COPD: fluid recovery correlates with the degree of emphysema. *European Respiratory Journal,* 25, 275-281.

Lomas DA. (2000). Loop-sheet polymerisation: the mechanism of alpha-1-antitrypsin deficiency. *Respiratory Medicine,* 94, (supplement C) S3-S6.

Lomas DA and Parfrey H. (2004). α-1-antitrypsin deficiency 4: molecular pathophysiology. *Thorax,* 59, 529-535.

Lomas DA, Silverman EK, Edwards LD, Miller BE, Coxson HO, Tal-Singer R, on behalf of the ECLIPSE investigators. (2008). Evaluation of serum CC-16 as a biomarker for COPD in the ECLIPSE cohort. *Thorax,* 63, 1058-1063.

Lomas DA, Silverman EK, Edwards LD, Locantore NW, Miller BE, Horstman DH, Tal-Singer R on behalf of the Evaluation of COPD Longitudinally to Identify Predictive Surrogate Endpoints study investigators. (2009) Serum surfactant protein D is steroid sensitive and associated with exacerbations of COPD. *European Respiratory Journal,* 34, 95-102.

Lopez AD and Murray CC. (1998). The global burden of disease 1990 – 2020. *Nature Medicine,* 4(11), 1241 – 1243.

Lopez SD, Shibuya K, Rao C, Mathers CD, Hansell AL, Held LS, Schmid V, Buist S. (2006). Chronic obstructive pulmonary disease: current burden and future projections. *European Respiratory Journal,* 27, 397-412.

Lozano R, Naghavi M, Foreman K, Lim S, Shibuya K, Aboyans V, Abraham J, Adair T, Aggarwal R, Y Ahn S, AlMazroa MA, Alvarado M, Anderson LM, Andrews KG,

Atkinson C, Baddour LM, Barker-Collo S, Bartels DH, Bell ML, Murray C. (2012). Global and regional mortality from 235 causes of death for 20 age groups in 1990 and 2010: a systematic analysis for the Global Burden of Disease Study 2010. *Lancet,* 380, 2095-2128.

Luisetti M and Sneersholm H (2004). α1-antitrypsin deficiency 1: the epidemiology of α1-antitrypsin deficiency. *Thorax,* 59, 164-169.

Ma S, Lin YY, He J, Rouhani FM, Brantly M, Turino GM. (2013). Alpha-1-antitrypsin augmentation therapy and biomarkers of elastin degradation. *COPD*, 10(4), 473-481.

Ma S, Lin YY, Cantor JO, Chapman KR, Sandhaus RA, Fries M, Edelman JM, McElvaney GN, Turino GM. (2017).The effect of alpha 1 proteinase inhibitor of biomarkers of elastin degradation in alpha-1-antitrypsin deficiency: an analysis of the RAPID/RAPID extension trials. *Journal of the COPD Foundation*, 4(1), 34-44.

Man SF, Connett JE, Anthonisen NR, Wise RA, Tashkin DP and Sin DD. (2006). C-reactive protein in mild to moderate chronic obstructive pulmonary disease. *Thorax,* 61, 849-853.

Mannino D, Valvi D, Mullerova H, Tal-Singer R. (2012) Fibrinogen, COPD and mortality in a nationally representative US cohort. *COPD*, 9 (4), 359-366.

Mannino D, Tal-Singer R, Lomas D, Vestbo J,Barr RG, Tetzlaff K, Lowings M, Rennard SI, Snyder J, Goldman M, Martin UJ, Merrill D, Martin AL, Simeone JC, Fahrbach K, Murphy B, Leidy N, Miller B. (2015). Plasma fibrinogen as a biomarker for mortality and hospitalised exacerbations in patients with COPD. *Chronic Obstructive Pulmonary Disease,* 2(1), 23-34.

Marc MM, Korosec P, Kosnik M, Kern I, Flezar M, Suskovis S, Sorli J. (2004). Compliment factors C3a, C4a and C5a in chronic obstructive pulmonary disease and asthma. *American Journal of Respiratory Cell and Molecular Biology,* 31, 216-219.

Marciniak SJ and Lomas DA. (2008). What can naturally occurring mutations tell us about the pathogenesis of COPD? *Thorax,* 64, 359-364.

Mast AE, Enghild JJ, Pizzo SV, Salvesen G. (1991). Analysis of the plasma elimination kinetics and conformational stabilities of native, proteinase-complexed and reactive site cleaved serpins: comparison of .alpha.1-proteinase inhibitor, alpha.1-antichymotrypsin, antithrombin III, .alpha.2-antiplasmin, angiotensinogen, and ovalbumin. *Biochemistry*, 30, 1723-1730.

Merkel D, Rist W, Seither P, Weith A and Lenter MC. (2005). Proteomic study of human bronchoalveolar lavage fluids from smokers with chronic obstructive pulmonary disease by combining surface enhanced laser desorption/ionisation-mass spectrometry profiling with mass spectrometric protein identification. *Proteomics*, 5(11), 2972-2980.

Mikami M, Llewellyn-Jones CG, Bayley D, Hill SL, Stockley RA. (1998). The chemotactic activity of sputum from patients with bronchiectasis. *American Journal of Respiratory and Critical Care Medicine,* 157(3), 723–728.

Miniatai M, Monti S, Basta G, Cocci F, Fornai E, Bottai M. (2011). Soluble receptor for advanced glycation end products in COPD: relationship with emphysema and chronic cor pulmonale: a case-control study. *Respiratory Research,* 12, 37.

Mitchell BL, Yasui Y, Li CI, Fitzpatrick AL, Lampe PD. (2005). Impact of freeze thaw cycles and storage time on plasma samples used in mass spectrometry based biomarker discovery projects. *Cancer Informatics,* 1, 98-104.

Mogues T, Edzerodt M, Hall C, Engelich G, Graversen JH and Hartshorn KL. (2004).Tetranectin binds to the kringle 1-4 form of angiostatin and modifies its functional activity. *Journal of Biomedicine and Biotechnology,* 2, 73-78.

Mulgrew AT, Taggart CC and McElvaney NG. (2007). Alpha-1-antitrypsin deficiency: current concepts. *Lung,* 185, 191-201.

Murch SH, Braegger CP, Walker-Smith JA and MacDonald TT. (1993). Location of tumour necrosis factor alpha by immunohistochemistry in chronic inflammatory bowel disease. *Gut,* 34, 1705-1709.

National Clinical Guideline Centre. (2010). Chronic obstructive pulmonary disease: management of chronic obstructive pulmonary disease in adults in primary and secondary care. London: National Clinical Guideline Centre. Available from: http://guidance.nice.org.uk/CG101/Guidance/pdf/English

Needham M and Stockley RA (2004). α1-antitrypsin deficiency 4: clinical manifestations and natural history. *Thorax,* 59 (5), 441-445.

Nicholas B, Skipp P, Mould R, Tennard S, Davies D, O'Connor CD and Djukanovic R. (2006). Shotgun proteomics analysis of human-induced sputum. *Proteomics,* 6, 4390-4401.

Nieman MA, Baggott JE, Miller EJ. (1997) Inhibition of human serine proteases by SPAAT, the C-terminal 44-residue peptide from α1-antitrypsin. *Biochemica et Byophysica Acta,* 1340, 123-130.

Nocturnal Oxygen Therapy Trial Group (1980). Continuous or nocturnal oxygen therapy in hypoxaemic chronic obstructive lung disease: a clinical trial. *Annals of Internal Medicine,* 93, 391-398.

Nomura A, Stemmermann GN, Chyou PH, Marcus EB, Buist AS. (1991). Prospective study of pulmonary function and lung cancer. *American Reviews of Respiratory Disease,* 144, 307-311.

Ohlmeier S, Vuolanto M, Toljamo T, Vuopala K, Salmenkivi K, Myllarniemi M and Kinnula V. (2008). Proteomics of human lung tissue identifies surfactant protein A as

a marker of chronic obstructive pulmonary disease. *Journal of Proteome Research,* 7, 5125-5132.

Ohlmeier S, Mazur W, Linja-aho A, Louhelainen N, Ronty M, Toljamo T, Bergmann U, Kinnula VL. (2011). Sputum proteomics identifies elevated PIGR levels in smokers and mild-to-moderate COPD. *Journal of Proteome Research,* 11, 599-608.

O' Riordan K, Blei A, Rao MS, Abecassis M. (1997). Alpha-1-antitrypsin deficiency associated panniculitis: resolution with intravenous alpha-1-antitrypsin administration and liver transplantation. *Transplantation,* 63, 480-482.

Pandya PH, Wilkes DS. (2014). Complement system in lung disease. *American Journal of Respiratory Cell and Molecular Biology,* 51(4), 467-473.

Palmer C, Diehn M, Alizadeh AA, O Brown P. (2006). Cell type specific gene expression profiles of leukocytes in peripheral blood. *Biomed Central Genomics,* 7, 115-150.

Papaioannou AI, Mazioti A, Kiropoulos T, Tsiliono I, Koutsokera A, Tanou K, Nikoulis DJ, Georgoulias P, Zakynthinos E, Gourgoulianis KI, and Kostikas K. (2010). Systemic and airway inflammation and the presence of emphysema in patients with COPD. *Respiratory Medicine,* 104, 275–282.

Park HY, Churg A, Wright JL, Li Y, Tam S, Man SF, Tashkin D, Wise RA, Connett JE, Sin DD. (2013). Club cell protein 16 and disease progression in chronic obstructive pulmonary disease. *American Journal of Respiratory and Critical Care Medicine,* 188(12), 1414-1419.

Parr DG, White AJ, Bayley DL, Guest PJ, Stockley RA. (2006). Inflammation in sputum relates to progression of disease in subjects with COPD: a prospective, descriptive study. *Respiratory Research,* 7(1), 136-148.

Pearson TA, Mensah GA, Alexander RW, Anderson JL, Cannon RO, Criqui M, Fadl YY, Fortmann SP, Hong Y, Myers GL, Rifai N, Smith SC, Taubert K, Tracy RP and Vinicor F. (2003). Markers of inflammation and cardiovascular disease: application to clinical and public health practice: A statement for healthcare professionals from the Centers for Disease Control and Prevention and the American Heart Association. *Circulation,* 107, 499–511.

Pelaia G, Terracciano R, Vatrella A, Gallelli L, Busceti MT, Calabrese C, Stellato C, Savino R, Maselli R. (2014). Application of proteomics and peptidomics to COPD. *Biomedical Research International,* vol. 2014, Article ID 764581, 8 pages.

Pesci A, Majori M, Cuomo A, Borciani N, Bertacco S, Cacciani G, Gabrielli M. (1998). Neutrophils infiltrating bronchial epithelium in chronic obstructive pulmonary disease. *Respiratory Medicine,* 92, 863–870.

Pillai SG, Ge D, Zhu G, Kong X, Shianna KV, Need AC, Feng S, Bakke P, Ruppert A, Lodrup KC, Roses A, Andersen W, ICGN Investigators, Rennard SI, Lomas DA, Silverman EK, Goldstein DB. (2009). A genome-wide association study in chronic

obstructive pulmonary disease (COPD): identification of 2 major susceptibility loci *PLoS Genetics,* 5(3), 1-8.

Pinto-Plata V, Toso T, Lee K, Park D, Bilello J, Mullerova H, De Souza MM, Vessey R, and Celli B. (2006). Profiling serum biomarkers in patients with COPD: associations with clinical parameters. *Thorax,* 62 (7), 595-601.

Pinto-Plata V, Casanova C, Mullerova H, de Torres JP, Corado H, Varo N, Cordoba E, Zeineldine S, Paz H, Baz R, Divo M, Cortopassi F, Celli BR. (2012). Inflammatory and repair serum biomarker pattern. Association to clinical outcomes in COPD. *Respiratory Research,* 13, 71-79.

Plymoth A, Lofdahl C, Ekberg-Jansson A, Dahlback M, Broberg P, Foster M, Fehniger TE and Marko-Varga G. (2007). Protein expression patterns associated with progression of chronic obstructive pulmonary disease in bronchoalveolar lavage of smokers. *Clinical Chemistry,* 54(4), 636-644.

Quian W, Kaletta DT, Petritis BO, Jiang H, Liu T, Zhang X, Mottaz HM, Varnum SM, Camp DG, Huang L, Fang X, Zhang W, Smith RD. (2008). Enhanced detection of low abundance human plasma proteins using a tandem IgY12 Supermix immunoaffinity separation strategy. *Molecular and Cellular Proteomics,* 7, 1963-1973.

Rabinovich RA, Miller BE, Wrobel K, Ranjit K, Williams MC, Drost E, Edwards LD, Lomas DA, Rennard SI, Agusti A, Tal-Singer R, Vestbo J, Wouters EF, John M, van Beek EJ, Murchison JT, Bolton CE, MacNee W, Huang JT. Evaluation of COPD Longitudinally to Identify Predictive Surrogate Endpoints (ECLIPSE) Investigators. (2016). Circulating desmosine levels do not predict emphysema progression but are associated with cardiovascular risk and mortality in COPD. *European Respiratory Journal*, 47(5), 1365-1373.

Rana GSJB, York TB, Edmiston JS, Zedler BK, Poungs JG, Adkins JN, Smith RD, Liu Z, Li Guoya, Webb BT, Murelle EL and Flora JW. (2010). Proteomic biomarkers in plasma that differentiate rapid and slow decline in lung function in adult smokers with chronic obstructive pulmonary disease. *Analytical and Bioanalytical Chemistry,* 397, 809-819.

Rennard SI, Calverley PA, Goethring UM and Martinez FJ. (2011) Reduction of exacerbations by the PDE4 inhibitor roflumilast - the importance of defining different subsets of patients with COPD. *Respiratory Research,* 12, 1112-1118.

Russell REK, Culpitt SV, DeMatos C, Donnelly L, Smith M, Wiggins J, Barnes PJ. (2002). Release and activity of matrix metalloproteinase-9 and tissue inhibitor of metalloproteinase-1 by alveolar macrophages from patients with chronic obstructive pulmonary disease. *American Journal of Cellular and Molecular Biology,* 26, 602-609.

Sallam RM (2015). Proteomics in cancer biomarker discovery: challenges and applications. *Disease Markers,* 15, 1-12.

Sandford AJ and Silverman EK. (2002). Chronic obstructive pulmonary disease 1: Susceptibility factors for COPD the genotype–environment interaction. *Thorax,* 57, 736-741.

Sapey E, Bayley D, Ahmad A, Newbold P, Snell N, Stockley RA. (2008). Inter-relationships between inflammatory markers in stable COPD patients with bronchitis: the intra and inter patient variability. *Thorax,* 63, 493-499.

Seemungal T, Harper-Owen R, Bhowmik A, Moric I, Sanderson G, Message S, Maccallum P, Meade TW, Jeffries DJ, Johnston SL and Wedzicha JA . (2001). Respiratory viruses, symptoms, and inflammatory markers in acute exacerbations and stable chronic obstructive pulmonary disease. *American Journal of Respiratory and Critical Care Medicine,* 164, 1618–1623.

Shrikrishna D, Astin R, Kemp PR and Hopkinson N. (2012). Renin-angiotensin system blockade: a novel therapeutic approach in chronic obstructive pulmonary disease. *Clinical Science,* 123, 487-498.

Sin DD and Man SFP. (2003).Why are patients with chronic obstructive pulmonary disease at increased risk of cardiovascular diseases? The potential role of systemic inflammation in chronic obstructive pulmonary disease. *Circulation,* 107, 1514-1519.

Sin DD, Leung R, Gan WQ and Man SFP. (2007). Circulating surfactant protein D as a potential lung-specific biomarker of health outcomes in COPD: a pilot study. *BCM Pulmonary Medicine,* 7, 13-19.

Sin DD, Pahlavan PS, Paul Man SF. (2008).Surfactant protein D: a lung specific biomarker in COPD? *Therapeutic Advances in Respiratory Disease,* 2(2), 65-74.

Smith DJ, Yerkovich ST, Towers MA, Carroll ML, Thomas R, Upham JW. 2011. Reduced soluble receptor for advanced glycation end-products in COPD. *European Respiratory Journal,* 37, 516-522.

Stanescu D, Sanna A, Veriter C, Kostianev S, Calcagni PG, Fabbri LM, Masetrelli P. (1996). Airways obstruction, chronic expectoration and rapid decline in FEV_1 in smokers are associated with increased levels of sputum neutrophils. *Thorax,* 51, 267-271.

Stockley RA, Bayley DL, Unsal I and Dowson LJ. (2002). The effect of augmentation therapy on bronchial inflammation in α1-antitrypsin deficiency. *American Journal of Respiratory and Critical Care Medicine,* 165, 1494-1498.

Stockley RA. (2007). Biomarkers in COPD: time for a deep breath. *Thorax,* 62, 657-660.

Stockley RA, Parr DG, Piitulainen E, Stolk J, Stoel B and Dirksen A. (2010). Therapeutic efficacy of alpha-1-antitrypsin augmentation therapy on the loss of lung tissue: an integrated analysis of 2 randomised clinical trials using computed tomography densitometry. *Respiratory Research,* 11, 136-143.

Stockley RA. (2013). large chronic obstructive pulmonary disease cohorts: advantages and caution in biomarker discovery/validation. *American Journal of Respiratory and Critical Care Medicine,* 188, 1387-1388.

Stolk J, Fumagalli M, Viglio S, Iadarola P. 2015. Conductivity in exhaled breath condensate from subjects with emphysema and type ZZ alpha-1-antitrypsin deficiency. *Journal of Chronic Obstructive Pulmonary Disease*, 12 (S1), 32-35.

Stone H, McNab G, Wood AM, Stockley RA, Sapey E. (2012). Variability of sputum inflammatory mediators in COPD and α1-antitrypsin deficiency. *European Respiratory Journal,* 40, 561-599.

Stone PJ, Lucey EC, Snider GL and Franzblau C. (1994). Effect of diet on urinary excretion of desmosine and hydroxylysyl pyridinoline *American Journal of Respiratory and Critical Care Medicine,* 149, 174-177.

Stone PJ, Gottlieb DJ, O' Connor GT, Ciccolella DE, Breuer R, Bryan Rhadfi. (1995). Elastin and collagen degradation products in urine of smokers with and without chronic obstructive pulmonary disease. *American Journal of Respiratory and Critical Care Medicine,* 151(4), 952-959.

Stuart-Harris C, Bishop JM, Clark TJH, Dornhorst AC, Cotes JE, Flenley DC, Howard P, Oldham PD. (1981). Long term domiciliary oxygen therapy in chronic hypoxic cor pulmonale complicating chronic bronchitis and emphysema. Report of the Medical Research Council Working Party. *Lancet,* 317, 681-686.

Subramanian DR, Jenkins L, Edgar R, Quraishi N, Stockley RA, Parr DG. (2002). Assessment of pulmonary neutrophilic inflammation in emphysema by quantitative positron emission tomography. *Thorax,* 186(11), 1125-1132.

Takabatake N, Nakamura H, Abe S Inoue S, Hino T, Saito H, Yuki H, Kato S and Tomoike H. (2000). The relationship between chronic hypoxaemia and activation of the tumour necrosis factor alpha system in patients with chronic obstructive pulmonary disease. *American Journal of Respiratory and Critical Care Medicine,* 161, 1179-1184.

Taguchi F, Solomon B, Gregorc V , Roder H, Gray R, Kasahara K, Nishio M, Brahmer J, Spreafico A, Ludovini V, Massion PP, Dziadziuszko R, Schiller J, Grigorieva ,J Tsypin M, Hunsucker SW, Caprioli R, Duncan MW, Hirsch FR, Bunn PA, Carbone DP. (2007). Mass spectrometry to classify non – small-cell lung cancer patients for clinical outcome after treatment with epidermal growth factor receptor tyrosine kinase inhibitors: a multi-cohort cross-institutional study. *Journal of the National Cancer Institute,* 99(11), 838-846.

Tashkin DP, Clark VA, Coulson AH, Simmons M, Bourque LB, Reems C, Detels R, Sayre JW and Rokaw SN. (1984). The ULCA population studies of chronic obstructive respiratory disease. Viii. Effects of smoking cessation on lung function; a prospective study of a free-living population. *American Reviews of Respiratory Disease,* 130, 707 – 715.

Terracciano R, Preiano M, Palladino GP, Carpagnano GE, Foschino Barbaro MP, Pelaia G, Savino R, Maselli R. (2011). Peptidome profiling of induced sputum by mesoporous silica beads and MALDI TOF MS for non-invasive biomarker discovery of chronic inflammatory lung diseases. *Proteomics*, 11, 3402-3414.

Thomsen M, Ingebrigsten TS, Morott JL, Dahl M, Lange P, Vestbo J, Nordestgaard BG. (2013). Inflammatory biomarkers and exacerbations in chronic obstructive pulmonary disease. *Journal of the American Medical Association*, 309, 2353-2361.

Tirado-Conde G, Lara B and Miravitlles M. (2008). Augmentation therapy for emphysema due to alpha-1-antitrypsin deficiency. *Therapeutic Advances in Respiratory Disease*, 2(1), 13-21.

Tirumalai RS, Chan KC, Prieto DA, Issaq HJ, Conrads TP and Veenstra TD. (2003). Characterisation of the low molecular weight serum proteome. *Molecular and Cellular Proteomics*, 2, 1096-1103.

Ueda K, Saichi N, Takami S, Kang D, Toyama A, Diago Y, Ishikawa N, Kohno N, Tamura K, Shuin T, Nakayama N, Sato TA, Nakamura Y, Nakagawa H. (2011). A comprehensive peptidome profiling technology for the identification of early detection biomarkers for lung adenocarcinoma. *PLoS One*, 6(4), 1-12.

Useland FR, Desimone CP, Seamon LG, Miller RA, Goodrich S, Podzielinski I, Sokoll L, Smith A, Van Nagell JR and Zhang Z. (2011). Effectiveness of a multivariate index assay in the preoperative assessment of ovarian tumours. *Obstetrics and Gynaecology*, 117(6), 1289-97.

Van Gent D, Sharp P, Morgan K, Kalsheker N. (2003). Serpins: structure, function and molecular evolution. *International Journal of Biochemistry and Cellular Biology*, 35(11), 1536-1547.

Vernooy, JHJ, Lindeman JHN, Jacobs JA,Hanemaaijer R, Wouters EFM. (2004). Increased activity of matrix metalloproteinase-8 and matrix metalloproteinase-9 in induced sputum from patients with COPD. *Chest*, 126(6), 1802-1810.

Vestbo J, Prescott E, Lange B. (1996). Association of chronic mucus hypersecretion with FEV1 decline and chronic obstructive pulmonary disease morbidity. Copenhagen Heart Study Group. *American Journal of Respiratory and Critical Care Medicine*, 153, 1530-1535.

Vestbo J, Edwards LD, Scanlon PD, Yates JC, Agusti A, Bakke P, Calverley PMA, Celli B, Coxson HO, Crim C, Lomas DA, MacNee W, Miller BE, Silverman EK, Tal-Singer R, Wouters E, Rennard SI. On behalf of the ECLIPSE investigators. (2011). Changes in forced expiratory volume in 1 second over time in COPD. *New England Journal of Medicine*, 365, 1184-1192.

Viglio S, Zanaboni G, Luisetti M, Trisolini R, Grimm R, Cetta G, Iadarola P. (1998). Micellar electrokinetic chromatography for the determination of urinary desmosine and

isodesmosine in patients affected by chronic obstructive pulmonary disease. *Journal of Chromatography B: Biomedical Sciences and Applications,* 714, 87–98.

Viglio S, Annovazzi L, Luisetti M, Stolk J, Casado B, Iadarola P. (2007). Progress in the methodological strategies for the detection in real samples of desmosine and isodesmosine, two biological markers of elastin degradation. *Journal of Separation Science,* 30, 202–213.

Von Haehling S, Hopkinson NS, Polkey MI, Niethammer M, Anker SD and Genth-Zots S. (2009). Elevated TNF alpha production in whole blood in patients with severe COPD: the potential link to disease severity. *The Central European Journal of Medicine,* 121, 303-308.

Wagena EJ, Huibers MJH and van Schayck CP (2001). Antidepressants in the treatment of patients with COPD: possible associations between smoking cigarettes, COPD and depression. *Thorax,* 56, 587-588.

Ward DG, Suggett N, Cheng Y, Wei W, Johnson H, Billingham LJ, Ismail T, Wakelam MJ, Johnson PJ, and Martin A (2006). Identification of serum biomarkers for colon cancer by proteomic analysis. *British Journal of Cancer,* 94(12), 1898-1905.

Ward DG, Wei W, Buckels J, Taha AM, Hegab B, Tariciotti L, Salih R, Qi YQ, Martin A, Johnson PJ (2010). Detection of pancreatic adenocarcinoma using circulating fragments of fibrinogen. *European Journal of Gastroenterology and Hepatology,* 22(11), 1358-1363.

Wasinger VC, Cordwell SJ, Cerpa-Polijak A, Yan JX, Gooley AA, Wilkins MR, Duncan MW, Harris R, Williams KL, Humphrey-Smith I. (1995). Progress with the gene-product mapping of the Mollicutes: Mycoplasma genitalium. *Electrophoresis,* 16, 1090-1094.

Westermeier, R, Naven T and Hopker H. (2008). Proteomics in practice. A guide to successful experimental design. Second Edition, Wiley-VCH

Wewers MD, Casolaro MA, Sellers SE, Swayze SC, McPhaul KM, Wittes JT and Crystal RG. (1987). Replacement therapy for alpha-1-antitrypsin deficiency associated with emphysema. *New England Journal of Medicine,* 316, 155-62.

Wisniewski JR, Zougman A, Nagaraj N, Mann M. (2009). Universal sample preparation methods for proteome analysis. *Nature Methods,* 6(5), 359-62.

Wood AM, Harrison RM, Semple S, Ayres JG and Stockley RA. (2009). Outdoor air pollution is associated with disease severity in alpha-1-antitrypsin deficiency. *European Respiratory Journal,* 34(2), 346-353.

Yende S, Waterer GW, Tolley EA, Newman AB, Bauer DC, Taaffe DR, Jensen R, Crapo R, Rubin S, Nevitt M, Simonsick EM, Satterfield S, Harris T, Kritchevsky SB. (2006). Inflammatory markers are associated with ventilatory limitation and muscle dysfunction in obstructive lung disease in well-functioning elderly subjects. *Thorax,*

61, 10-16.

Yoon HI, Li Y, Man SFP, Tashkin D, Wise RA, Connett JE, Anthonisen NA, Churg A, Wright JL , Sin DD. (2012). The complex relationship of serum adiponectin to COPD outcomes. *Chest,* 142, 983-999.

Zhang L, Chen J, Ke Y, Mansel RE and Jiang W (2006). Expression of pigment derived epithelial factor is reduced in non-small cell lung cancer and is linked to clinical outcome. *International Journal of Molecular Medicine,* 17, 937-944.

Zhu X and Papayannopoulos I. (2003). Improvement in the Detection of Low Protein Digests on a MALDI TOF/TOF Workstation by Reducing α-Cyano-4 - hydroxycinnamic Acid Adduct Ions. *Journal of Biomolecular Techniques,* 14(4), 298-307.

List of Abstracts Resulting from this Thesis

Presence of a 6kDa Protein as a Potential Marker in Alpha-1-Antitrypsin Deficiency
Poster Discussion
H. Stone, D.G. Ward and R.A. Stockley
ATS Conference 2010.

Identification of a 6kDa Protein as a Potential Biomarker in Alpha-1-Antitrypsin Deficiency
Poster Presentation
H. Stone, D.G. Ward and R.A. Stockley
COPD 7, 2010.

Plasma Peptide Profiling in Alpha-1-Antitrypsin Deficiency
Poster Presentation
H. Stone, R.A. Stockley and D.G. Ward
East Midlands Proteomics Society, 2010.

Plasma Profiling in Alpha-1-Antitrypsin Deficiency
Poster Presentation
H. Stone**,** R.A. Stockley and D.G. Ward
British Society for Proteome Research Meeting, 2011.

Plasma Peptide Analysis in Alpha-1-Antitrypsin Deficiency
Poster Discussion
H. Stone, D.G. Ward and R.A. Stockley
ERS Conference 2011.

APPENDIX I

Peptide/Protein Identifications from Neutrophil Elastase Experiments

m/z	Scores	Sequence	Protein	m/z	Scores	Sequence	Protein
2530.15	188	C.HPNSPLDEENLTQENQDRGTHV.D	Alpha-1-antichymotrypsin	907.37	60.1	T.SHNGMQFS.T	Fibrinogen gamma chain
2296.04	140.8	P.NSPLDEENLTQENQDRGTHV.D	Alpha-1-antichymotrypsin	1363.65	58.5	I.QYKEGFGHLSPT.G	Fibrinogen gamma chain
2430.03	129.8	A.EDPQGDAAQKTDTSHHDQDHPT.F	Alpha-1-antitrypsin	1982.92	51.7	L.RVELEDWNGRTSTADYA.M	Fibrinogen gamma chain
2932.32	69.9	A.EDPQGDAAQKTDTSHHDQDHPTFNKI.T	Alpha-1-antitrypsin	1659.85	84.1	L.TIGEGQQHHLGGAKQV.R	Fibrinogen gamma chain
1948.08	72.4	A.KKQINDYVEKGTQGKIV.D	Alpha-1-antitrypsin	1606.78	101.3	S.KASTPNGYDNGIIWA.T	Fibrinogen gamma chain
1569.82	42.4	I.FFKGKWERPFEV.K	Alpha-1-antitrypsin	1394.69	79.5	T.GTTEFWLGNEKI.H	Fibrinogen gamma chain
2030.00	84.4	I.FFLPDEGKLQHLENELT.H	Alpha-1-antitrypsin	1445.72	64.6	I.GEGQQHHLGGAKQV.R	Fibrinogen gamma chain
2508.27	127.6	I.FFLPDEGKLQHLENELTHDII.T	Alpha-1-antitrypsin	1736.78	57.4	I.QLTYNPDESSKPNMI.D	Fibrinogen gamma chain
1465.75	46.1	I.TKFLENEDRRSA.S	Alpha-1-antitrypsin	2285.90	68.3	G.DAGDAFDGFDFGDDPSDKFFT.S	Fibrinogen gamma chain
1761.99	61.3	M.SIPPEVKFNKPFVFL.M	Alpha-1-antitrypsin	1407.66	86	A.STPNGYDNGIIWA.T	Fibrinogen gamma chain
4133.30	84.6	M.SIPPEVKFNKPFVFLMIEQNTKSPLFMGKVVNPTQK.-	Alpha-1-antitrypsin	2829.53	143.1	A.TWKTRWYSMKKTTMKIIPFNRL.T	Fibrinogen gamma chain
1504.82	70	S.EGLKLVDKFLEDV.K	Alpha-1-antitrypsin	3043.65	47.5	A.TWKTRWYSMKKTTMKIIPFNRLTI.G	Fibrinogen gamma chain
1752.87	49.7	T.EIPEAQIHEGFQELL.R	Alpha-1-antitrypsin	2781.09	185.2	A.YFAGGDAGDAFDGFDFGDDPSDKFFT.S	Fibrinogen gamma chain
2010.03	121.2	T.EIPEAQIHEGFQELLRT.L	Alpha-1-antitrypsin	1553.81	40.8	A.MFKVGPEADKYRL.T	Fibrinogen gamma chain
1447.81	54.5	T.TGNGLFLSEGLKLV.D	Alpha-1-antitrypsin	1654.86	49.1	A.MFKVGPEADKYRLT.Y	Fibrinogen gamma chain
1847.92	47.4	V.FSNGADLSGVTEEAPLKL.S	Alpha-1-antitrypsin	2399.95	144.5	A.GGDAGDAFDGFDFGDDPSDKFFT.S	Fibrinogen gamma chain
1322.71	93.4	V.KKLYHSEAFTV.N	Alpha-1-antitrypsin	2068.02	72.8	V.KAHYGGFTVQNEANKYQI.S	Fibrinogen beta chain
2811.41	134.1	V.NFGDTEEAKKQINDYVEKGTQGKIV.D	Alpha-1-antitrypsin	2247.10	89.3	T.RMGPTELLIEMEDWKGDKV.K	Fibrinogen beta chain
1959.99	75.1	V.NYIFFKGKWERPFEV.K	Alpha-1-antitrypsin	2446.24	60.4	T.RMGPTELLIEMEDWKGDKVKA.H	Fibrinogen beta chain
2242.09	102.3	I.LSDETLPAPEFSPEPESGRAL.R	Alpha-1B-glycoprotein	1833.02	64.3	S.LRPAPPPISGGGYRARPA.K	Fibrinogen beta chain
1625.82	75.3	M.HHGESSQVLHPGNKV.T	Alpha-1B-glycoprotein	1378.72	42.7	M.SMKIRPFFPQQ.-	Fibrinogen beta chain
1850.06	83.8	S.KLLELTGPKSLPAPWLS.M	Alpha-1B-glycoprotein	1160.65	43	M.KIRPFFPQQ.-	Fibrinogen beta chain
2699.46	52.5	V.DFQLRRGEKELLVPRSSTSPDRI.F	Alpha-1B-glycoprotein	2753.42	159.5	I.IRKGGETSEMYLIQPDSSVKPYRV.Y	Fibrinogen beta chain
2049.06	43.9	V.DLKPPFGGSAPSERLELHV.D	Alpha-1B-glycoprotein	2970.43	53.5	I.QNRQDGSVDFGRKWDPYKQGFGNVAT.N	Fibrinogen beta chain
2597.30	95.3	V.ELILSDETLPAPEFSPEPESGRAL.R	Alpha-1B-glycoprotein	2640.34	92	I.RKGGETSEMYLIQPDSSVKPYRV.Y	Fibrinogen beta chain
2866.48	94.6	V.ELILSDETLPAPEFSPEPESGRALRL.R	Alpha-1B-glycoprotein	1572.78	76.3	I.RNSVDELNNNVEAV.S	Fibrinogen beta chain
3273.61	87	V.TFLLRREGDHEFLEVPEAQEDVEATFPV.H	Alpha-1B-glycoprotein	1675.93	51.4	V.TSKGDKELRTGKEKV.T	Fibrinogen alpha chain
3489.83	105.4	L.KGFPRGDKLFGPDLKLVPPMEEDYPQFGSPK.-	Alpha-2-antiplasmin	1776.98	41.7	V.TSKGDKELRTGKEKVT.S	Fibrinogen alpha chain
1162.64	47.5	A.AGPVVPPCPGRI.R	Alpha-2-HS-glycoprotein	2149.92	61	A.ANPNGRYYWGGQYTWDMA.K	Fibrinogen beta chain
1083.59	83	A.APPGHQLHRA.H	Alpha-2-HS-glycoprotein	1868.88	73.6	A.HYGGFTVQNEANKYQI.S	Fibrinogen beta chain
941.46	41.7	A.HYDLRHT.F	Alpha-2-HS-glycoprotein	3589.98	65.7	A.RGHRPLDKKREEAPSLRPAPPPISGGGYRARPA.K	Fibrinogen beta chain
1474.72	71.1	A.HYDLRHTFMGVV.S	Alpha-2-HS-glycoprotein	1937.06	92.2	V.TKTVIGPDGHKEVTKEVV.T	Fibrinogen alpha chain
1861.91	60.5	I.DYINQNLPWGYKHTL.N	Alpha-2-HS-glycoprotein	2759.22	80.6	V.SGSTGQWHSESGSFRPDSPGSGNARPN.N	Fibrinogen alpha chain
2560.24	91.3	I.DYINQNLPWGYKHTLNQIDEV.K	Alpha-2-HS-glycoprotein	2873.26	70.3	V.SGSTGQWHSESGSFRPDSPGSGNARPNN.P	Fibrinogen alpha chain
1357.65	61.3	I.NQNLPWGYKHT.L	Alpha-2-HS-glycoprotein	3933.75	65.1	V.SGSTGQWHSESGSFRPDSPGSGNARPNNPDWGTFEEV.S	Fibrinogen alpha chain
2169.07	97.8	I.NQNLPWGYKHTLNQIDEV.K	Alpha-2-HS-glycoprotein	2320.99	73	V.SGSTGQWHSESGSFRPDSPGSGN.A	Fibrinogen alpha chain
1527.84	75.7	I.SRAQLVPLPPSTYV.E	Alpha-2-HS-glycoprotein	3687.03	82.6	V.SGNVSPGTRREYHTEKLVTSKGDKELRTGKEKV.T	Fibrinogen alpha chain
1666.66	40.4	I.YRQPNCDDPETEEA.A	Alpha-2-HS-glycoprotein	3788.05	44.3	V.SGNVSPGTRREYHTEKLVTSKGDKELRTGKEKVT.S	Fibrinogen alpha chain
1154.63	75.6	L.AAPPGHQLHRA.H	Alpha-2-HS-glycoprotein	2131.09	71.8	V.SGNVSPGTRREYHTEKLVT.S	Fibrinogen alpha chain
893.50	44.1	L.KLDGKFSV.V	Alpha-2-HS-glycoprotein	2030.05	61.6	V.SGNVSPGTRREYHTEKLV.T	Fibrinogen alpha chain
992.57	69.6	L.KLDGKFSVV.Y	Alpha-2-HS-glycoprotein	3807.85	138.9	V.SETESRGSESGIFTNTKESSSHHPGIAEFPSRGKSS.S	Fibrinogen alpha chain
1267.70	74	L.LAAPPGHQLHRA.H	Alpha-2-HS-glycoprotein	3720.80	123.5	V.SETESRGSESGIFTNTKESSSHHPGIAEFPSRGKS.S	Fibrinogen alpha chain
761.42	40.2	S.APHGPGLI.Y	Alpha-2-HS-glycoprotein	3292.54	68.6	V.SETESRGSESGIFTNTKESSSHHPGIAEFPS.R	Fibrinogen alpha chain
2744.37	103	V.AIDYINQNLPWGYKHTLNQIDEV.K	Alpha-2-HS-glycoprotein	3505.63	56.7	V.SETESRGSESGIFTNTKESSSHHPGIAEFPSRG.K	Fibrinogen alpha chain
1657.85	74.3	V.KVWPQQPSGELFEI.E	Alpha-2-HS-glycoprotein	2045.95	53.4	V.SETESRGSESGIFTNTKES.S	Fibrinogen alpha chain
2459.22	139	V.KVWPQQPSGELFEIEIDTLET.T	Alpha-2-HS-glycoprotein	1486.65	47.7	V.SETESRGSESGIFT.N	Fibrinogen alpha chain
2560.25	131.9	V.KVWPQQPSGELFEIEIDTLETT.C	Alpha-2-HS-glycoprotein	1507.82	83.7	V.IGPDGHKEVTKEVV.T	Fibrinogen alpha chain

1380.79	92.4	V.LLAAPPGHQLHRA.H	Alpha-2-HS-glycoprotein
2000.99	66.5	V.RQLKEHAVEGDCDFQLL.K	Alpha-2-HS-glycoprotein
1309.65	51	V.SLGSPSGEVSHPR.K	Alpha-2-HS-glycoprotein
1538.80	101.5	V.SLGSPSGEVSHPRKT.R	Alpha-2-HS-glycoprotein
1637.87	71.5	V.VSLGSPSGEVSHPRKT.R	Alpha-2-HS-glycoprotein
864.47	42.6	M.HGPEGLRV.G	Alpha-2-macroglobulin
1210.65	61.1	S.DVMGRGHARLV.H	Alpha-2-macroglobulin
1425.61	98.3	V.GFYESDVMGRGHA.R	Alpha-2-macroglobulin
1793.87	83.4	V.GFYESDVMGRGHARLV.H	Alpha-2-macroglobulin
2144.18	64.8	V.KKDNSVHWERPQKPKAPV.G	Alpha-2-macroglobulin
1171.65	41.5	A.ELQEGARQKL.H	Apolipoprotein A-I
2049.10	83.4	A.ELQEGARQKLHELQEKL.S	Apolipoprotein A-I
2792.44	96	A.ELQEGARQKLHELQEKLSPLGEEM.R	Apolipoprotein A-I
3290.69	153	A.ELQEGARQKLHELQEKLSPLGEEMRDRA.R	Apolipoprotein A-I
3517.84	71.3	A.ELQEGARQKLHELQEKLSPLGEEMRDRARA.H	Apolipoprotein A-I
3754.00	114.1	A.ELQEGARQKLHELQEKLSPLGEEMRDRARAHV.D	Apolipoprotein A-I
1198.60	52.6	A.EYHAKATEHL.S	Apolipoprotein A-I
1285.63	72.6	A.EYHAKATEHLS.T	Apolipoprotein A-I
1386.66	76.8	A.EYHAKATEHLST.L	Apolipoprotein A-I
2211.14	154.8	A.EYHAKATEHLSTLSEKAKPA.L	Apolipoprotein A-I
3022.58	47.2	A.EYHAKATEHLSTLSEKAKPALEDLRQG.L	Apolipoprotein A-I
3444.86	231.1	A.EYHAKATEHLSTLSEKAKPALEDLRQGLLPV.L	Apolipoprotein A-I
2944.64	105.6	A.KATEHLSTLSEKAKPALEDLRQGLLPV.L	Apolipoprotein A-I
1548.92	40.5	A.KPALEDLRQGLLPV.L	Apolipoprotein A-I
3128.59	48.6	A.KVQPYLDDFQKKWQEEMELYRQKV.E	Apolipoprotein A-I
3467.79	87.8	A.KVQPYLDDFQKKWQEEMELYRQKVEPL.R	Apolipoprotein A-I
1252.72	51.7	A.LEDLRQGLLPV.L	Apolipoprotein A-I
1497.84	87.1	A.RLEALKENGGARLA.E	Apolipoprotein A-I
2165.13	97.1	A.RQKLHELQEKLSPLGEEM.R	Apolipoprotein A-I
2663.40	120.1	A.RQKLHELQEKLSPLGEEMRDRA.R	Apolipoprotein A-I
2890.54	55.5	A.RQKLHELQEKLSPLGEEMRDRARA.H	Apolipoprotein A-I
3126.67	83.8	A.RQKLHELQEKLSPLGEEMRDRARAHV.D	Apolipoprotein A-I
2745.51	78.6	A.TEHLSTLSEKAKPALEDLRQGLLPV.L	Apolipoprotein A-I
1728.87	57	A.TVYVDVLKDSGRDYV.S	Apolipoprotein A-I
1639.91	78.6	L.AARLEALKENGGARLA.E	Apolipoprotein A-I
1426.70	42	L.GEEMRDRARAHV.D	Apolipoprotein A-I
2601.32	87.7	L.HELQEKLSPLGEEMRDRARAHV.D	Apolipoprotein A-I
1089.56	76.5	L.KLLDNWDSV.T	Apolipoprotein A-I
1316.68	90.3	L.NLKLLDNWDSV.T	Apolipoprotein A-I
1964.11	101.6	L.SEKAKPALEDLRQGLLPV.L	Apolipoprotein A-I
1723.87	67.7	L.SPLGEEMRDRARAHV.D	Apolipoprotein A-I
2265.29	148.6	L.STLSEKAKPALEDLRQGLLPV.L	Apolipoprotein A-I
1325.61	48.4	Q.DEPPQSPWDRV.K	Apolipoprotein A-I
1752.85	51.4	Q.DEPPQSPWDRVKDLA.T	Apolipoprotein A-I
1853.89	60.7	Q.DEPPQSPWDRVKDLAT.V	Apolipoprotein A-I
2215.10	46.8	Q.DEPPQSPWDRVKDLATVYV.D	Apolipoprotein A-I
1927.05	141.6	S.ALGKQLNLKLLDNWDSV.T	Apolipoprotein A-I
2028.10	145.9	S.ALGKQLNLKLLDNWDSVT.S	Apolipoprotein A-I
2216.16	54.1	S.ALGKQLNLKLLDNWDSVTST.F	Apolipoprotein A-I
1039.62	67.4	S.KLREQLGPV.T	Apolipoprotein A-I
2117.91	71.8	T.WNPGSSERGSAGHWTSESSV.S	Fibrinogen alpha chain
1878.88	67.1	V.DLKDYEDQQKQLEQV.I	Fibrinogen alpha chain
4043.83	61.8	T.SYNRGDSTFESKSYKMADEAGSEADHEGTHSTKRGHA.K	Fibrinogen alpha chain
3169.34	43.2	T.SYNRGDSTFESKSYKMADEAGSEADHEGT.H	Fibrinogen alpha chain
1568.69	96	T.SYGTGSETESPRNPS.S	Fibrinogen alpha chain
1477.66	75.4	T.SYNRGDSTFESKS.Y	Fibrinogen alpha chain
1899.86	109.5	T.SYNRGDSTFESKSYKM.A	Fibrinogen alpha chain
1970.89	113.7	T.SYNRGDSTFESKSYKMA.D	Fibrinogen alpha chain
2246.01	81.1	T.SSTSYNRGDSTFESKSYKMA.D	Fibrinogen alpha chain
2174.97	61.6	T.SSTSYNRGDSTFESKSYKM.A	Fibrinogen alpha chain
1675.94	50.8	T.SKGDKELRTGKEKVT.S	Fibrinogen alpha chain
1574.89	70.5	T.SKGDKELRTGKEKV.T	Fibrinogen alpha chain
2026.92	129.6	T.RGGSTSYGTGSETESPRNPS.S	Fibrinogen alpha chain
2340.14	126.3	T.NTKESSSHHPGIAEFPSRGKSS.S	Fibrinogen alpha chain
3181.52	150	T.NTKESSSHHPGIAEFPSRGKSSSYSKQFT.S	Fibrinogen alpha chain
3456.64	106.5	T.NTKESSSHHPGIAEFPSRGKSSSYSKQFTSST.S	Fibrinogen alpha chain
1824.86	75.6	T.NTKESSSHHPGIAEFPS.R	Fibrinogen alpha chain
2253.11	127.6	T.NTKESSSHHPGIAEFPSRGKS.S	Fibrinogen alpha chain
1279.70	59.8	T.KTVIGPDGHKEV.T	Fibrinogen alpha chain
2966.46	78.8	T.KESSSHHPGIAEFPSRGKSSSYSKQFT.S	Fibrinogen alpha chain
1215.58	78.7	T.GKTFPGFFSPM.L	Fibrinogen alpha chain
1760.86	88.5	T.GKTFPGFFSPMLGEFV.S	Fibrinogen alpha chain
2275.98	86.5	T.GTWNPGSSERGSAGHWTSESSV.S	Fibrinogen alpha chain
2125.05	49.8	T.KESSSHHPGIAEFPSRGKSS.S	Fibrinogen alpha chain
3702.63	41.6	S.TGQWHSESGSFRPDSPGSGNARPNNPDWGTFEEV.S	Fibrinogen alpha chain
2045.01	116.7	T.ADSGEGDFLAEGGGVRGPRVV.E	Fibrinogen alpha chain
1474.71	41.1	T.ASTGKTFPGFFSPM.L	Fibrinogen alpha chain
2019.99	100.1	T.ASTGKTFPGFFSPMLGEFV.S	Fibrinogen alpha chain
2897.35	50.8	S.SSHHPGIAEFPSRGKSSSYSKQFTSST.S	Fibrinogen alpha chain
2622.27	62.8	S.SSHHPGIAEFPSRGKSSSYSKQFT.S	Fibrinogen alpha chain
1265.58	44	S.SSHHPGIAEFPS.R	Fibrinogen alpha chain
1780.89	72.1	S.SSHHPGIAEFPSRGKSS.S	Fibrinogen alpha chain
2535.24	92.1	S.SHHPGIAEFPSRGKSSSYSKQFT.S	Fibrinogen alpha chain
2810.33	75.4	S.SHHPGIAEFPSRGKSSSYSKQFTSST.S	Fibrinogen alpha chain
3367.61	66.9	S.KSYKMADEAGSEADHEGTHSTKRGHAKSRPV.R	Fibrinogen alpha chain
1375.69	74.4	S.RGKSSSYSKQFT.S	Fibrinogen alpha chain
1650.82	57.2	S.RGKSSSYSKQFTSST.S	Fibrinogen alpha chain
1779.76	77	S.SAGSWNSGSSGPGSTGNRN.P	Fibrinogen alpha chain
1933.85	46.6	S.SAGSWNSGSSGPGSTGNRNPG.S	Fibrinogen alpha chain
2265.98	106.1	S.SAGSWNSGSSGPGSTGNRNPGSSGT.G	Fibrinogen alpha chain
2552.11	102.3	S.SAGSWNSGSSGPGSTGNRNPGSSGTGGTA.T	Fibrinogen alpha chain
2653.14	101.6	S.SAGSWNSGSSGPGSTGNRNPGSSGTGGTAT.W	Fibrinogen alpha chain
3121.38	43.9	S.SAGSWNSGSSGPGSTGNRNPGSSGTGGTATWKPG.S	Fibrinogen alpha chain
1178.56	43.7	S.SHHPGIAEFPS.R	Fibrinogen alpha chain
1606.82	81	S.SHHPGIAEFPSRGKS.S	Fibrinogen alpha chain
3599.80	42.9	S.GIFTNTKESSSHHPGIAEFPSRGKSSSYSKQFT.S	Fibrinogen alpha chain
1777.88	50.5	S.GIGTLDGFRHRHPDEA.A	Fibrinogen alpha chain
1848.89	41.1	S.GIGTLDGFRHRHPDEAA.F	Fibrinogen alpha chain
2430.18	43.9	S.GIGTLDGFRHRHPDEAAFFDTA.S	Fibrinogen alpha chain
3222.51	42	M.ELERPGGNEITRGGSTSYGTGSETESPRNPS.S	Fibrinogen alpha chain

2178.24	121.6	S.TLSEKAKPALEDLRQGLLPV.L	Apolipoprotein A-I	2011.97	56.8	N.SLFEYQKNNKDSHSLTT.N	Fibrinogen alpha chain
2644.47	183.3	T.EHLSTLSEKAKPALEDLRQGLLPV.L	Apolipoprotein A-I	2364.16	93.6	M.DLGTLSGIGTLDGFRHRHPDEA.A	Fibrinogen alpha chain
1273.73	61.4	T.FSKLREQLGPV.T	Apolipoprotein A-I	2435.21	60.7	M.DLGTLSGIGTLDGFRHRHPDEAA.F	Fibrinogen alpha chain
1597.84	61.4	T.HLAPYSDELRQRL.A	Apolipoprotein A-I	1864.90	52.8	L.SGIGTLDGFRHRHPDEA.A	Fibrinogen alpha chain
1739.92	70.4	T.HLAPYSDELRQRLAA.R	Apolipoprotein A-I	1935.93	48	L.SGIGTLDGFRHRHPDEAA.F	Fibrinogen alpha chain
2077.21	117.6	T.LSEKAKPALEDLRQGLLPV.L	Apolipoprotein A-I	2260.05	50.2	I.GTLDGFRHRHPDEAAFFDTA.S	Fibrinogen alpha chain
1461.80	80	T.STFSKLREQLGPV.T	Apolipoprotein A-I	2127.96	157.8	I.TRGGSTSYGTGSETESPRNPS.S	Fibrinogen alpha chain
1627.83	93.2	T.VYVDVLKDSGRDYV.S	Apolipoprotein A-I	1336.62	50.8	L.DGFRHRHPDEA.A	Fibrinogen alpha chain
2263.09	59.8	T.VYVDVLKDSGRDYVSQFEGS.A	Apolipoprotein A-I	1407.66	40.2	L.DGFRHRHPDEAA.F	Fibrinogen alpha chain
2296.20	84.3	V.DALRTHLAPYSDELRQRLAA.R	Apolipoprotein A-I	1607.77	45.8	I.GTLDGFRHRHPDEA.A	Fibrinogen alpha chain
1266.63	49.5	V.DVLKDSGRDYV.S	Apolipoprotein A-I	1678.80	52.1	I.GTLDGFRHRHPDEAA.F	Fibrinogen alpha chain
3327.73	145.7	V.KAKVQPYLDDFQKKWQEEMELYRQKV.E	Apolipoprotein A-I	1858.93	78.8	D.SGEGDFLAEGGGVRGPRVV.E	Fibrinogen alpha chain
3666.92	145.4	V.KAKVQPYLDDFQKKWQEEMELYRQKVEPL.R	Apolipoprotein A-I	1173.56	64.3	G.FFSPMLGEFV.S	Fibrinogen alpha chain
1862.94	134.3	V.LESFKVSFLSALEEYT.K	Apolipoprotein A-I	2733.21	70.2	G.SFRPDSPGSGNARPNNPDWGTFEEV.S	Fibrinogen alpha chain
2575.35	108.9	V.LESFKVSFLSALEEYTKKLNTQ.-	Apolipoprotein A-I	2464.09	67.7	G.STGTWNPGSSERGSAGHWTSESSV.S	Fibrinogen alpha chain
3240.61	48.7	V.QPYLDDFQKKWQEEMELYRQKVEPL.R	Apolipoprotein A-I	1849.87	41.2	A.STGKTFPGFFSPMLGEF.V	Fibrinogen alpha chain
1159.55	77.2	V.SFLSALEEYT.K	Apolipoprotein A-I	1948.93	107.5	A.STGKTFPGFFSPMLGEFV.S	Fibrinogen alpha chain
1743.91	96.8	V.SFLSALEEYTKKLNT.Q	Apolipoprotein A-I	1403.66	84.6	A.STGKTFPGFFSPM.L	Fibrinogen alpha chain
1871.97	124.4	V.SFLSALEEYTKKLNTQ.-	Apolipoprotein A-I	1375.63	67.7	A.FFDTASTGKTFPG.F	Fibrinogen alpha chain
1264.65	68.2	V.SQFEGSALGKQL.N	Apolipoprotein A-I	1984.90	124.5	A.FFDTASTGKTFPGFFSPM.L	Fibrinogen alpha chain
1491.77	90.2	V.SQFEGSALGKQLNL.K	Apolipoprotein A-I	1973.95	132.1	A.DSGEGDFLAEGGGVRGPRVV.E	Fibrinogen alpha chain
2562.29	155.3	V.SQFEGSALGKQLNLKLLDNWDSV.T	Apolipoprotein A-I	2049.99	95	I.EGVDAEDGHGPGEQQKRKI.V	Complement factor B
2663.35	56.2	V.SQFEGSALGKQLNLKLLDNWDSVT.S	Apolipoprotein A-I	1694.87	56.6	I.GTRKVGSQYRLEDSV.T	Complement factor B
3085.53	49.4	V.SQFEGSALGKQLNLKLLDNWDSVTSTFS.K	Apolipoprotein A-I	1583.76	74.7	I.ILMTDGLHNMGGDPI.T	Complement factor B
1539.70	62.4	V.TQEFWDNLEKET.E	Apolipoprotein A-I	2146.13	67.3	I.NYEDHKLKSGTNTKKALQA.V	Complement factor B
1838.86	62.3	V.TQEFWDNLEKETEGL.R	Apolipoprotein A-I	2245.18	158.5	I.NYEDHKLKSGTNTKKALQAV.Y	Complement factor B
2383.07	139	V.TQEFWDNLEKETEGLRQEM.S	Apolipoprotein A-I	2478.30	63.6	I.RDLLYIGKDRKNPREDYLDV.Y	Complement factor B
2470.13	86.4	V.TQEFWDNLEKETEGLRQEMS.K	Apolipoprotein A-I	2445.20	76.9	S.KKDNEQHVFKVKDMENLEDV.F	Complement factor B
3183.47	144	V.TQEFWDNLEKETEGLRQEMSKDLEEV.K	Apolipoprotein A-I	2694.33	164.5	S.SLTETIEGVDAEDGHGPGEQQKRKI.V	Complement factor B
1562.86	83.1	V.TSTFSKLREQLGPV.T	Apolipoprotein A-I	1309.72	57.7	V.ASYGVKPRYGLV.T	Complement factor B
1528.77	86	V.YVDVLKDSGRDYV.S	Apolipoprotein A-I	1764.86	110	V.DAEDGHGPGEQQKRKI.V	Complement factor B
2164.00	78.6	V.YVDVLKDSGRDYVSQFEGS.A	Apolipoprotein A-I	1863.94	68.4	V.DAEDGHGPGEQQKRKIV.L	Complement factor B
1897.98	70.6	A.EAKSYFEKSKEQLTPL.I	Apolipoprotein A-II	2234.07	71.2	V.KVSEADSSNADWVTKQLNEI.N	Complement factor B
2837.56	87.2	A.EAKSYFEKSKEQLTPLIKKAGTELV.N	Apolipoprotein A-II	2055.09	110.4	V.NINALASKKDNEQHVFKV.K	Complement factor B
1697.90	73.9	A.KSYFEKSKEQLTPL.I	Apolipoprotein A-II	1241.65	55.9	V.TYATYPKIWV.K	Complement factor B
2637.46	165.2	A.KSYFEKSKEQLTPLIKKAGTELV.N	Apolipoprotein A-II	1291.70	73.2	V.YVFGVGPLVNQV.N	Complement factor B
958.59	46.6	L.IKKAGTELV.N	Apolipoprotein A-II	1823.78	83	V.SSAMEPDREYHFGQAV.R	Complement factor H
2048.05	125.6	V.LKPEEEAPAPEVGASKPEGI.D	Vitronectin	1446.70	68.6	A.AFFDTASTGKTFPG.F	Fibrinogen alpha chain
1107.54	67.2	S.SLSAVFEHFA.M	Vitronectin	2055.94	127.1	A.AFFDTASTGKTFPGFFSPM.L	Fibrinogen alpha chain
1698.82	97.4	T.SDLQAQSKGNPEQTPV.L	Vitronectin	1582.77	124.6	T.HYSSSGSLGGLYELI.Y	Complement component C9
1476.90	84.4	T.EYKKKLAERLKA.K	Vitamin D-binding protein	1155.66	43.7	V.KGEIHLGRFV.M	Complement component C9
1646.81	94.6	I.RDVWGIEGPIDAAFT.R	Vitronectin	1335.68	44.8	L.MLHYEFLQRV.K	Complement component C8 beta chain
1394.69	55.6	V.RVVAEGFDFANGI.N	Serum paraoxonase/arylesterase 1	2442.29	127.3	V.TLSSTGRNGFKSHALQLNNRQI.R	Complement C4-A
1653.95	46.6	V.LRIQNILTEEPKVT.Q	Serum paraoxonase/arylesterase 1	1156.58	50.7	V.YELNPLDHR.G	Complement C4-A
1639.85	78.5	V.ELFKFQEEEKSLL.H	Serum paraoxonase/arylesterase 1	1953.03	53.1	T.GRNGFKSHALQLNNRQI.R	Complement C4-A
2232.22	121.2	V.ELFKFQEEEKSLLHLKTI.R	Serum paraoxonase/arylesterase 1	1739.93	84.4	R.NGFKSHALQLNNRQI.R	Complement C4-A
1294.75	46.1	T.RLNALREVQPV.E	Serum paraoxonase/arylesterase 1	1896.04	57.4	R.NGFKSHALQLNNRQIR.G	Complement C4-A
2004.06	79.3	S.SGLKYPGIKSFNPNSPGKI.L	Serum paraoxonase/arylesterase 1	2314.04	125.3	V.QKEDIPPADLSDQVPDTESET.R	Complement C3
2091.11	95.6	I.SSGLKYPGIKSFNPNSPGKI.L	Serum paraoxonase/arylesterase 1	2583.24	142	V.QKEDIPPADLSDQVPDTESETRI.L	Complement C3

1271.68	68	I.QNILTEEPKVT.Q	Serum paraoxonase/arylesterase 1	2809.42	104	V.QKEDIPPADLSDQVPDTESETRILL.Q	Complement C3
1431.84	73.1	I.RHKLLPNLNDIV.A	Serum paraoxonase/arylesterase 1	4062.10	40.6	V.RTLDPERLGREGVQKEDIPPADLSDQVPDTESETRI.L	Complement C3
1601.94	75.5	I.RHKLLPNLNDIVAV.G	Serum paraoxonase/arylesterase 1	1246.67	114.7	V.TAEGKGQGTLSVV.T	Complement C3
1466.68	40.3	I.SNHQNSNRYLYA.R	Serum amyloid A-4 protein	1705.94	96.4	I.RGLEEELQFSLGSKI.N	Complement C4-A
1745.86	72.4	A.RGNYDAAQRGPGGVWAA.K	Serum amyloid A-4 protein	3016.38	97.2	L.DHRGRTLEIPGNSDPNMIPDGDFNSYV.R	Complement C4-A
1520.81	46.9	V.ARLSQRFPKAEFA.E	Serum albumin	2340.25	137	V.KWLILEKQKPDGVFQEDAPV.I	Complement C3
1504.84	61.3	V.RYTKKVPQVSTPT.L	Serum albumin	1939.98	51	V.AQMTEDAVDAERLKHLI.V	Complement C3
1945.11	62.1	V.RYTKKVPQVSTPTLVEV.S	Serum albumin	2039.05	46.1	V.AQMTEDAVDAERLKHLIV.T	Complement C3
2100.14	79.9	V.AHRFKDLGEENFKALVLI.A	Serum albumin	2932.49	114	V.HYLDETEQWEKFGLEKRQGALELI.K	Complement C3
1661.83	97	V.AHRFKDLGEENFKA.L	Serum albumin	996.62	51.4	T.RILLQGTPV.A	Complement C3
1774.92	111.3	V.AHRFKDLGEENFKAL.V	Serum albumin	1766.98	44.2	T.VAVRTLDPERLGREGV.Q	Complement C3
1873.98	119.8	V.AHRFKDLGEENFKALV.L	Serum albumin	2362.18	67	T.AKDKNRWEDPGKQLYNVEAT.S	Complement C3
2203.04	91.6	S.ALEVDETYVPKEFNAETFT.F	Serum albumin	1651.89	70.2	I.KKGYTQQLAFRQPS.S	Complement C3
2937.53	65.7	R.DAHKSEVAHRFKDLGEENFKALVLIA.F	Serum albumin	1136.56	46.1	I.THRIHWESA.S	Complement C3
2157.06	57.4	A.KLHDRNTYEKYLGEEYV.K	Serotransferrin	2868.37	65	R.EGVQKEDIPPADLSDQVPDTESETRI.L	Complement C3
1703.88	62.4	A.HRFKDLGEENFKAL.V	Serum albumin	1241.68	63.1	L.NLDVSLQLPSR.S	Complement C3
1802.95	72.1	A.HRFKDLGEENFKALV.L	Serum albumin	3102.58	43.9	I.AVHYLDETEQWEKFGLEKRQGALELI.K	Complement C3
1677.89	43.9	A.RLSQRFPKAEFAEV.S	Serum albumin	1471.68	49.4	A.QYQKDAPDHQEL.N	Complement C3
1381.76	59.2	A.SLQKFGERAFKA.W	Serum albumin	1912.91	72.8	A.QYQKDAPDHQELNLDV.S	Complement C3
1801.94	119.1	A.SAQAKALSKHQDFNSAV.Q	Prothrombin	1838.91	124.8	A.SLLRSEETKENEGFTV.T	Complement C3
1191.67	95	A.SLLQAGYKGRV.T	Prothrombin	1629.91	91.6	A.LLQLKDFDFVPPVV.R	Complement C3
2045.97	109.3	I.DGRIVEGSDAEIGMSPWQV.M	Prothrombin	1388.67	60	A.NYMNLQRSYTV.A	Complement C3
2475.21	54.4	I.YIHPRYNWRENLDRDIALM.K	Prothrombin	2024.01	107.9	I.LQDTKALHQVFEHMLDV.S	Complement C2
2357.23	63.6	L.FEKKSLEDKTERELLESYI.D	Prothrombin	1619.76	46.7	V.IFKSDFSNEERFT.G	Complement C1s subcomponent
1581.97	54.1	T.HVFRLKKWIQKV.I	Prothrombin	1506.68	44.9	I.FKSDFSNEERFT.G	Complement C1s subcomponent
1220.68	45.1	T.RYERNIEKI.S	Prothrombin	1174.69	40.5	I.RLEKGFQVVV.T	Complement C1s subcomponent
1048.50	41.8	V.AFSDYIHPV.C	Prothrombin	2241.96	52.2	V.SVHPDYRQDESYNFEGDIA.L	Complement C1r subcomponent
1345.84	40.3	V.FRLKKWIQKV.I	Prothrombin	1985.95	117	V.DLLFFTDESGDSRGWKL.R	Complement C1r subcomponent
1036.62	52.4	V.NLPIVERPV.C	Prothrombin	2094.06	127.6	T.LHLKFLEPFDIDDHQQV.H	Complement C1r subcomponent
1292.62	61	V.TGWGNLKETWT.A	Prothrombin	2234.09	64.6	V.AGEHNIEETEHTEQKRNVI.R	Coagulation factor IX
2131.05	129.5	V.TGWGNLKETWTANVGKGQPS.V	Prothrombin	2289.14	47.4	S.IPPWEAPKEHKYKAEEHTV.V	Coagulation factor XII
1176.66	62.6	V.ISKMLFVEPI.L	Plasma protease C1 inhibitor	1980.98	91	L.HLKFLEPFDIDDHQQV.H	Complement C1r subcomponent
1517.85	91.9	V.ISKMLFVEPILEV.S	Plasma protease C1 inhibitor	1336.71	62.5	V.SRKNPKFMETV.A	Clusterin
1885.86	65.4	V.RGEEDFSWFGYSLHGV.T	Phosphatidylinositol-glycan-specific phospholipase D	1783.98	65.4	V.NKEIQNAVNGVKQIKT.L	Clusterin
1908.12	59.9	V.KDLLGIYEKLYGRKVI.T	Phosphatidylinositol-glycan-specific phospholipase D	991.45	42.8	V.MQDHFSRA.S	Clusterin
1444.72	42	A.RHDVREGKEYGV.V	N-acetylmuramoyl-L-alanine amidase	934.48	64.8	V.KLFDSDPI.T	Clusterin
1409.71	47.8	V.GAHTLGHNSRGFGV.A	N-acetylmuramoyl-L-alanine amidase	1915.02	65.9	V.AEKALQEYRKKHREE.-	Clusterin
1337.65	64	V.QRIFENGYDPV.N	Neutrophil elastase	1862.91	53	T.REPQDTYHYLPFSLP.H	Clusterin
2244.19	87.6	V.SAAFKGLKSLEYLDLSFNQI.A	Lumican	1586.72	89.8	T.HMLDVMQDHFSRA.S	Clusterin
2315.21	119.3	V.SAAFKGLKSLEYLDLSFNQIA.R	Lumican	1673.76	74.8	T.HMLDVMQDHFSRAS.S	Clusterin
1713.86	50.4	I.SNIPDEYFKRFNAL.Q	Lumican	1360.76	45.3	T.LIEKTNEERKT.L	Clusterin
2069.01	73.8	V.DAALKKYNSQNQSNNQFV.L	Kininogen-1	1270.60	58.5	T.QGEDQYYLRV.T	Clusterin
1882.97	113.8	V.TQNNFRLLFKGSEMVV.A	Inter-alpha-trypsin inhibitor heavy chain H4	1630.81	73.6	S.SIIDELFQDRFFT.R	Clusterin
1900.91	85.5	V.QLLDSSNQEERLPEGSV.S	Inter-alpha-trypsin inhibitor heavy chain H4	1280.63	66	R.SLMPFSPYEPL.N	Clusterin
1783.92	53.7	V.TQNNFRLLFKGSEMV.V	Inter-alpha-trypsin inhibitor heavy chain H4	2157.03	61.9	I.IDELFQDRFFTREPQDT.Y	Clusterin
1605.76	51.2	V.HSGSTFFKYYLQGA.K	Inter-alpha-trypsin inhibitor heavy chain H4	1624.77	75.7	L.NFHAMFQPFLEMI.H	Clusterin
1704.84	102.7	V.HYFAPEGLTTMPKNV.V	Inter-alpha-trypsin inhibitor heavy chain H4	1318.63	61.8	I.DSLLENDRQQT.H	Clusterin
1053.57	41.1	T.QWRPSLVPA.S	Inter-alpha-trypsin inhibitor heavy chain H4	1791.85	94.5	I.HFHSPAFQHPPTEFI.R	Clusterin
1440.77	88.9	V.AGKLQDRGPDVLTA.T	Inter-alpha-trypsin inhibitor heavy chain H4	1430.69	62	I.IDELFQDRFFT.R	Clusterin
1640.90	61.1	V.AGKLQDRGPDVLTATV.S	Inter-alpha-trypsin inhibitor heavy chain H4	1717.83	82.2	A.SSIIDELFQDRFFT.R	Clusterin

1655.84	78.9	S.SRQLGLPGPPDVPDHA.A	Inter-alpha-trypsin inhibitor heavy chain H4	2272.00	109.1	G.DQTVSDNELQEMSNQGSKYV.N	Clusterin
1568.82	62.9	S.RQLGLPGPPDVPDHA.A	Inter-alpha-trypsin inhibitor heavy chain H4	1978.04	113.9	V.HLKNLASRPYTFHSHGI.T	Ceruloplasmin
2526.30	66	M.NFRPGVLSSRQLGLPGPPDVPDHA.A	Inter-alpha-trypsin inhibitor heavy chain H4	1343.64	87.6	V.KWYLFGMGNEV.D	Ceruloplasmin
1742.88	42.5	L.SSRQLGLPGPPDVPDHA.A	Inter-alpha-trypsin inhibitor heavy chain H4	1836.86	95.4	V.KWYLFGMGNEVDVHAA.F	Ceruloplasmin
1897.98	89.8	I.ILLTDGDPTVGETNPRSI.Q	Inter-alpha-trypsin inhibitor heavy chain H4	1919.88	92.2	V.NKDDEEFIESNKMHAI.N	Ceruloplasmin
2808.43	86.8	I.ILLTDGDPTVGETNPRSIQNNVREAV.S	Inter-alpha-trypsin inhibitor heavy chain H4	1115.55	40.8	A.FQHPPTEFI.R	Clusterin
1786.97	80	I.KILDDLSPRDQFNLI.V	Inter-alpha-trypsin inhibitor heavy chain H4	1485.84	40.7	A.KLRRELDESLQV.A	Clusterin
1545.78	51.1	I.LDDLSPRDQFNLI.V	Inter-alpha-trypsin inhibitor heavy chain H4	1736.86	62.3	V.HFHGHSFQYKHRGV.Y	Ceruloplasmin
2160.11	88.9	I.RFKPTLSQQQKSPEQQET.V	Inter-alpha-trypsin inhibitor heavy chain H4	1976.83	86.4	V.DKDNEDFQESNRMYSV.N	Ceruloplasmin
2419.10	45.2	I.TFQTESSVAEQEAEFQSPKYI.F	Inter-alpha-trypsin inhibitor heavy chain H4	2176.08	92.4	I.GIIETTWDYASDHGEKKLI.S	Ceruloplasmin
1155.66	43	L.ALDNGGLARRI.H	Inter-alpha-trypsin inhibitor heavy chain H4	1440.76	52.8	I.IFKNMATRPYSI.H	Ceruloplasmin
3160.52	51	L.ALDNGGLARRIHEDSDSALQLQDFYQEV.A	Inter-alpha-trypsin inhibitor heavy chain H4	2057.99	62.6	I.SVDTEHSNIYLQNGPDRI.G	Ceruloplasmin
2105.12	91.9	I.DKSGSMSGRKIQQTREALI.K	Inter-alpha-trypsin inhibitor heavy chain H4	2092.00	56.2	I.YFSGNTYLWRGERRDTA.N	Ceruloplasmin
1319.68	47.5	I.GLLFWDGRGEGL.R	Inter-alpha-trypsin inhibitor heavy chain H4	1892.05	57.1	I.YLQNGPDRIGRLYKKA.L	Ceruloplasmin
2023.88	133.6	I.HEDSDSALQLQDFYQEV.A	Inter-alpha-trypsin inhibitor heavy chain H4	1635.86	44.1	T.RIYHSHIDAPKDIA.S	Ceruloplasmin
1955.03	78.4	G.VLSSRQLGLPGPPDVPDHA.A	Inter-alpha-trypsin inhibitor heavy chain H4	2912.23	109.2	T.YCSEPEKVDKDNEDFQESNRMYSV.N	Ceruloplasmin
1534.79	56.4	A.SAENVNKARSFAAGI.Q	Inter-alpha-trypsin inhibitor heavy chain H4	1549.75	65.5	A.LYLQYTDETFRT.T	Ceruloplasmin
2092.04	66.5	V.KSMEDKGMTNINDGLLRGI.S	Inter-alpha-trypsin inhibitor heavy chain H3	2203.04	69.7	V.TWPDESKAGGSWDLAVQERA.A	Carboxypeptidase N subunit 2
1766.83	51.5	V.AGRLVDEDMNSFKADV.K	Inter-alpha-trypsin inhibitor heavy chain H3	1430.76	63.7	I.LYEPPAEKEQKV.L	CD5 antigen-like
1649.90	63.6	V.HFFAPQGLPVVPKNV.A	Inter-alpha-trypsin inhibitor heavy chain H3	2038.02	51.8	A.FFHGQALTNKNYRIDTI.N	Ceruloplasmin
2446.14	47.8	A.RRIYEDSDADLQLQGFYEEV.A	Inter-alpha-trypsin inhibitor heavy chain H3	2059.09	42.3	A.NLQSVPHASASRPRVTEPI.S	Apolipoprotein L1
1831.89	49.5	I.MLTDGDANVGESRPEKI.Q	Inter-alpha-trypsin inhibitor heavy chain H3	1675.86	85.3	I.LNNNYKILQADQEL.-	Apolipoprotein L1
1333.75	42.6	V.VFDVQIPKGAFI.S	Inter-alpha-trypsin inhibitor heavy chain H2	1709.05	43.7	T.RGIGKDIRALRRARA.N	Apolipoprotein L1
1726.77	108.3	V.TQNNFHNYFGGSEIV.V	Inter-alpha-trypsin inhibitor heavy chain H2	2413.23	80.6	V.YESKHLHEGAKSETAEELKKV.A	Apolipoprotein L1
1825.84	109.9	V.TQNNFHNYFGGSEIVV.A	Inter-alpha-trypsin inhibitor heavy chain H2	2788.45	60.8	V.YLVYESKHLHEGAKSETAEELKKV.A	Apolipoprotein L1
2893.33	122.2	V.LETLAQMDDLQDFLSKDKHADPDFT.R	Inter-alpha-trypsin inhibitor heavy chain H2	1648.84	44.2	V.YQAGAREGAERGLSAI.R	Apolipoprotein E
1193.55	56.9	V.QFNYPHTSVT.D	Inter-alpha-trypsin inhibitor heavy chain H2	1834.85	84.1	S.WFEPLVEDMQRQWA.G	Apolipoprotein E
1407.66	108	V.QFNYPHTSVTDV.T	Inter-alpha-trypsin inhibitor heavy chain H2	1226.65	53.9	V.GSLAGQPLQERA.Q	Apolipoprotein E
2127.03	83.1	V.KENIQDNISLFSLGMGFDV.D	Inter-alpha-trypsin inhibitor heavy chain H2	1313.73	70.7	V.RAKLEEQAQQI.R	Apolipoprotein E
2097.10	44	V.HFFAPDNLDPIPKNILFV.I	Inter-alpha-trypsin inhibitor heavy chain H2	1508.86	50.1	I.RERLGPLVEQGRV.R	Apolipoprotein E
1737.91	106.9	V.HFFAPDNLDPIPKNI.L	Inter-alpha-trypsin inhibitor heavy chain H2	1807.05	66	I.RERLGPLVEQGRVRAA.T	Apolipoprotein E
1518.83	53.9	V.ADAKRYIEKIQPS.G	Inter-alpha-trypsin inhibitor heavy chain H2	1033.53	54.2	I.RLQAEAFQA.R	Apolipoprotein E
1341.75	71.1	S.GGTNINEALLRAI.F	Inter-alpha-trypsin inhibitor heavy chain H2	1426.76	86	A.TVGSLAGQPLQERA.Q	Apolipoprotein E
1940.86	115.9	T.DVTQNNFHNYFGGSEIV.V	Inter-alpha-trypsin inhibitor heavy chain H2	1086.57	41.7	A.QAWGERLRA.R	Apolipoprotein E
1642.85	83.4	T.ILDDLRAEDHFSVI.D	Inter-alpha-trypsin inhibitor heavy chain H2	2109.02	100.5	V.KDKFSEFWDLDPEVRPT.S	Apolipoprotein C-III
1312.72	61.4	I.NQLLAERSLAPT.A	Inter-alpha-trypsin inhibitor heavy chain H2	1759.86	129.7	T.AKDALSSVQESQVAQQA.R	Apolipoprotein C-III
2019.97	110	I.YGNQDTSSQLKKFYNQV.S	Inter-alpha-trypsin inhibitor heavy chain H2	1504.69	98.2	T.DGFSSLKDYWSTV.K	Apolipoprotein C-III
2437.09	70.7	L.AQMDDLQDFLSKDKHADPDFT.R	Inter-alpha-trypsin inhibitor heavy chain H2	1199.53	41.1	L.SFMQGYMKHA.T	Apolipoprotein C-III
1675.81	79	L.GMGFDVDYDFLKRL.S	Inter-alpha-trypsin inhibitor heavy chain H2	1300.58	54.1	L.SFMQGYMKHAT.K	Apolipoprotein C-III
2427.13	82.1	L.GMGFDVDYDFLKRLSNENHGI.A	Inter-alpha-trypsin inhibitor heavy chain H2	1529.71	63.8	L.SFMQGYMKHATKT.A	Apolipoprotein C-III
1804.91	79.9	I.DFNQNIRTWRNDLI.S	Inter-alpha-trypsin inhibitor heavy chain H2	1842.91	94.2	A.SLLSFMQGYMKHATKT.A	Apolipoprotein C-III
1884.05	133.3	I.ILVSDGDPTVGELKLSKI.Q	Inter-alpha-trypsin inhibitor heavy chain H2	1613.77	87.2	A.SLLSFMQGYMKHAT.K	Apolipoprotein C-III
2840.35	44.8	I.RGMADQDGLKPTIDKPSEDSPPLEML.G	Inter-alpha-trypsin inhibitor heavy chain H1	1512.72	87.6	A.SLLSFMQGYMKHA.T	Apolipoprotein C-III
1746.92	44.4	I.RGRFPLYNLGFGHNV.D	Inter-alpha-trypsin inhibitor heavy chain H1	2116.05	48.1	S.ELSAKMREWFSETFQKV.K	Apolipoprotein C-I
2384.22	80.7	T.IDKPSEDSPPLEMLGPRRTFV.L	Inter-alpha-trypsin inhibitor heavy chain H1	2390.30	126.2	S.SALDKLKEFGNTLEDKARELI.S	Apolipoprotein C-I
2890.43	166.4	V.AGRIADNKQSSFKADVQAHGEGQEFSI.T	Inter-alpha-trypsin inhibitor heavy chain H1	2889.52	225.9	G.TPDVSSALDKLKEFGNTLEDKARELI.S	Apolipoprotein C-I
2229.11	124.1	V.LALTQNHHKQYYEGSEIVV.A	Inter-alpha-trypsin inhibitor heavy chain H1	2815.44	76.9	I.SRIKQSELSAKMREWFSETFQKV.K	Apolipoprotein C-I
1577.87	58.4	V.LFGTRVQSWKGSLV.Q	Inter-alpha-trypsin inhibitor heavy chain H1	2691.42	181.2	P.DVSSALDKLKEFGNTLEDKARELI.S	Apolipoprotein C-I
1151.63	45.2	V.TAWKQYRKA.A	Inter-alpha-trypsin inhibitor heavy chain H1	1989.94	47.9	S.SYWESAKTAAQNLYEKT.Y	Apolipoprotein C-II
1335.74	43.9	V.TAWKQYRKAAI.S	Inter-alpha-trypsin inhibitor heavy chain H1	1634.84	58.1	T.GIFTDQVLSVLKGEE.-	Apolipoprotein C-II

2989.47	87	V.VAGRIADNKQSSFKADVQAHGEGQEFSI.T	Inter-alpha-trypsin inhibitor heavy chain H1	1998.05	53.4	T.YLPAVDEKLRDLYSKST.A	Apolipoprotein C-II
1447.80	46.8	A.DAKRYIEKIQPS.G	Inter-alpha-trypsin inhibitor heavy chain H2	2069.09	75.3	T.YLPAVDEKLRDLYSKSTA.A	Apolipoprotein C-II
1944.06	44.5	L.GGPSVFLFPPKPKDTLMI.S	Ig gamma-4 chain C region	2140.10	61.4	T.YLPAVDEKLRDLYSKSTAA.M	Apolipoprotein C-II
2409.04	118.9	V.TNDWIPEGEEDDDYLDLEKI.F	Heparin cofactor 2	2114.94	104.4	A.SEAEDASLLSFMQGYMKHA.T	Apolipoprotein C-III
2177.00	72.8	I.FKYSHYNERDEIPHNDI.A	Hyaluronan-binding protein 2	1024.49	44.1	A.RGWVTDGFS.S	Apolipoprotein C-III
2304.15	43.9	V.VLGDQDLKKEEFHEQSFRV.E	Hyaluronan-binding protein 2	2104.01	157.8	A.RGWVTDGFSSLKDYWSTV.K	Apolipoprotein C-III
1497.79	47.6	V.WKSHKWDRELI.S	Hemopexin	2146.12	125.6	V.SQFTLPKSVSDGIAALDLNAV.A	Apolipoprotein B-100
1574.80	71.6	V.DAAFRQGHNSVFLI.K	Hemopexin	1814.96	63.3	V.SSKLRRNLQNNAEWV.Y	Apolipoprotein B-100
1346.68	52.2	I.SERWKNFPSPV.D	Hemopexin	2285.21	49.3	V.STTKTEVIPPLIENRQSWSV.C	Apolipoprotein B-100
2040.10	78.4	I.RHYEGSTVPEKKTPKSPV.G	Haptoglobin	1186.60	59	V.YDKSLWDFL.K	Apolipoprotein B-100
2449.19	74.7	A.LYSGNDVTDISDDRFPKPPEIA.N	Haptoglobin-related protein	1213.56	51.4	A.KMREWFSET.F	Apolipoprotein C-I
1303.75	64.9	I.SLLLWGRQLFA.L	Haptoglobin-related protein	1715.85	81.7	A.KMREWFSETFQKV.K	Apolipoprotein C-I
927.43	53.7	A.HGYVEHSV.R	Haptoglobin	2260.10	102.6	V.RIHSGSFQSQVELSNDQEKA.H	Apolipoprotein B-100
2249.14	98.9	A.ATASRGASQAGAPQGRVPEARPN.S	Gelsolin	1797.05	73.4	V.RVPSYTLILPSLELPV.L	Apolipoprotein B-100
1443.78	104.3	A.HLMSLFGGKPMII.Y	Gelsolin	1114.51	49	V.NKYHWEHT.G	Apolipoprotein B-100
1511.73	60.4	A.YLWVGTGASEAEKT.G	Gelsolin	2706.39	52.9	V.QFLEYELNVLGTHKIEDGTLASKT.K	Apolipoprotein B-100
2378.22	80.2	A.YLWVGTGASEAEKTGAQELLRV.L	Gelsolin	1964.84	104.3	V.DHFGYTKDDKHEQDMV.N	Apolipoprotein B-100
2904.42	120.2	C.SNKIGRFVIEEVPGELMQEDLATDDV.M	Gelsolin	2248.98	113.1	V.DHFGYTKDDKHEQDMVNGI.M	Apolipoprotein B-100
1188.60	53.5	I.ANVERVPFDAA.T	Gelsolin	1514.77	44.9	V.GFHLPSREFQVPT.F	Apolipoprotein B-100
1862.99	40	I.FVWKGKQANTEERKAA.L	Gelsolin	3346.43	54.6	V.GMDMDEDDDFSKWNFYYSPQSSPDKKLT.I	Apolipoprotein B-100
2462.16	113.6	I.GRFVIEEVPGELMQEDLATDDV.M	Gelsolin	2461.14	129.4	V.LVDHFGYTKDDKHEQDMVNGI.M	Apolipoprotein B-100
1674.87	52.6	I.LYNYRHGGRQGQII.Y	Gelsolin	1963.27	44.5	V.ALKAGKLKFIIPSPKRPV.K	Apolipoprotein B-100
1338.67	49.6	I.TKMDYPKQTQV.S	Gelsolin	2416.29	66.9	T.SSFALNLPTLPEVKFPEVDVLT.K	Apolipoprotein B-100
1434.76	113	I.TVVKQGFEPPSFV.G	Gelsolin	2937.51	67.4	T.LNLNDFQVPDLHIPEFQLPHISHTI.E	Apolipoprotein B-100
1567.83	42.3	I.WRIEGSNKVPVDPA.T	Gelsolin	1812.90	103.1	T.KYSQPEDSLIPFFEI.T	Apolipoprotein B-100
1585.87	47.9	I.WRVEKFDLVPVPT.N	Gelsolin	1098.60	56	S.AFGYVFPKAV.S	Apolipoprotein B-100
1667.81	48	I.YKGGTSREGGQTAPAST.R	Gelsolin	1390.62	80.8	S.SFHDFPDLGQEV.A	Apolipoprotein B-100
1062.60	65.9	M.SLFGGKPMII.Y	Gelsolin	1903.95	63.3	T.AFVYTKNPNGYSFSIPV.K	Apolipoprotein B-100
2520.31	48.2	S.AAYLWVGTGASEAEKTGAQELLRV.L	Gelsolin	1806.00	52.7	T.ALTKKYRITENDIQI.A	Apolipoprotein B-100
1438.73	71.3	S.HIANVERVPFDAA.T	Gelsolin	1613.92	48.4	T.DLHLRYQKDKKGI.S	Apolipoprotein B-100
1525.78	79.5	S.SHIANVERVPFDAA.T	Gelsolin	1386.70	54	T.FHVPFTDLQVPS.C	Apolipoprotein B-100
2259.19	51.7	T.SAKRYIETDPANRDRRTPI.T	Gelsolin	1185.62	61.8	M.SAFGYVFPKAV.S	Apolipoprotein B-100
2096.01	134.6	V.FVWVGKDSQEEEKTEALT.S	Gelsolin	1445.71	89.4	I.EMSAFGYVFPKAV.S	Apolipoprotein B-100
2313.02	57.8	V.GWFLGWDDDYWSVDPLDRA.M	Gelsolin	3193.67	126.3	I.KFDKYKAEKSHDELPRTFQIPGYTVPV.V	Apolipoprotein B-100
2534.33	139.6	V.LGPKPALPAGTEDTAKEDAANRKLA.K	Gelsolin	1049.65	52.4	I.QIYKKLRT.S	Apolipoprotein B-100
3165.76	50.2	V.LGPKPALPAGTEDTAKEDAANRKLAKLYKV.S	Gelsolin	1603.85	57.3	I.RQIDDIDVRFQKA.A	Apolipoprotein B-100
1198.66	45.5	V.QSRVVQGKEPA.H	Gelsolin	1871.03	51.8	I.TLPDFRLPEIAIPEFI.I	Apolipoprotein B-100
1947.91	42.4	V.QVAEGSEPDGFWEALGGKA.A	Gelsolin	2182.21	78.1	I.TLPDFRLPEIAIPEFIIPT.L	Apolipoprotein B-100
2699.43	42.1	V.RANSAGATRAVEVLPKAGALNSNDAFV.L	Gelsolin	1662.86	58.4	I.TTPPLKDFSLWEKT.G	Apolipoprotein B-100
1700.92	68.2	V.SKGIRDNERSGRARV.H	Gelsolin	1541.77	58.4	L.FGKQGFFPDSVNKA.L	Apolipoprotein B-100
2038.06	46.7	V.SVLPEGGETPLFKQFFKN.W	Gelsolin	1911.04	92.7	L.NLPTLPEVKFPEVDVLT.K	Apolipoprotein B-100
2936.47	57.4	V.SVLPEGGETPLFKQFFKNWRDPDQT.D	Gelsolin	2591.30	47.2	A.ALGKLPQQANDYLNSFNWERQV.S	Apolipoprotein B-100
1616.86	65.2	V.WKGKQANTEERKAA.L	Gelsolin	2033.13	94.2	A.HLDIAGSLEGHLRFLKNI.I	Apolipoprotein B-100
1137.53	77	V.YYQGGTYSKA.S	Fibrinogen gamma chain	2871.51	48.3	V.SQKIGDNLRELQQRLEPYADQLRT.Q	Apolipoprotein A-IV
1536.70	56.4	V.YYQGGTYSKASTPN.G	Fibrinogen gamma chain	3098.63	52.5	V.SQKIGDNLRELQQRLEPYADQLRTQV.N	Apolipoprotein A-IV
2155.95	109.7	V.YYQGGTYSKASTPNGYDNGI.I	Fibrinogen gamma chain	2588.34	87.5	V.NTQAEQLRRQLTPYAQRMERV.L	Apolipoprotein A-IV
2269.03	88	V.YYQGGTYSKASTPNGYDNGII.W	Fibrinogen gamma chain	1529.80	48.4	V.RGNLRGNTEGLQKS.L	Apolipoprotein A-IV
2526.20	150.2	V.YYQGGTYSKASTPNGYDNGIIWA.T	Fibrinogen gamma chain	1713.94	84.3	V.RGNLRGNTEGLQKSLA.E	Apolipoprotein A-IV
2627.17	43.8	V.YYQGGTYSKASTPNGYDNGIIWAT.W	Fibrinogen gamma chain	1902.86	91.9	V.MWDYFSQLSNNAKEAV.E	Apolipoprotein A-IV
2016.93	84.6	T.TGQSYNQYSQRYHQRT.N	Fibronectin	1922.91	86.8	V.NSFFSTFKEKESQDKT.L	Apolipoprotein A-IV

2232.05	54.5	T.TGQSYNQYSQRYHQRTNT.N	Fibronectin
2445.14	42.9	T.TGQSYNQYSQRYHQRTNTNV.N	Fibronectin
1782.74	76.6	V.SHYAVGDEWERMSES.G	Fibronectin
2036.07	71.6	V.TLPHPNLHGPEILDVPSTV.Q	Fibronectin
1661.86	68.6	A.TFRLLGEVDHYQLA.L	Ficolin-3
1712.88	51.5	I.DWASGRGVGHPYRRV.R	Ficolin-3
2696.25	72.6	S.SYRAGFGNQESEFWLGNENLHQL.T	Ficolin-3
2276.00	102.5	V.RPEHPAETEYDSLYPEDDL.-	Fibrinogen gamma chain
1727.76	74.4	V.ELEDWNGRTSTADYA.M	Fibrinogen gamma chain
1232.72	46.5	T.TMKIIPFNRL.T	Fibrinogen gamma chain
1446.85	48.3	T.TMKIIPFNRLTI.G	Fibrinogen gamma chain
3015.20	194.8	T.YAYFAGGDAGDAFDGFDFGDDPSDKFFT.S	Fibrinogen gamma chain
2527.40	91.4	T.RWYSMKKTTMKIIPFNRLTI.G	Fibrinogen gamma chain
1262.71	41.2	S.FLEKDLRDKV.N	Apolipoprotein A-IV
3092.65	95.8	T.ELHERLAKDSEKLKEEIGKELEELRA.R	Apolipoprotein A-IV
1700.89	122.3	L.RQKLGPHAGDVEGHLS.F	Apolipoprotein A-IV
2944.59	145.7	L.RQKLGPHAGDVEGHLSFLEKDLRDKV.N	Apolipoprotein A-IV
1807.00	88.7	L.TFQMKKNAEELKARI.S	Apolipoprotein A-IV
2419.25	119.5	L.GPHAGDVEGHLSFLEKDLRDKV.N	Apolipoprotein A-IV
2651.38	182.1	V.KSPELQAEAKSYFEKSKEQLTPL.I	Apolipoprotein A-II
3091.72	188	V.KSPELQAEAKSYFEKSKEQLTPLIKKA.G	Apolipoprotein A-II
3249.79	110.7	V.KSPELQAEAKSYFEKSKEQLTPLIKKAGT.E	Apolipoprotein A-II
3590.98	253.8	V.KSPELQAEAKSYFEKSKEQLTPLIKKAGTELV.N	Apolipoprotein A-II
889.46	52.9	V.NFLSYFV.E	Apolipoprotein A-II
1298.63	82.8	V.TDYGKDLMEKV.K	Apolipoprotein A-II
2592.38	100.1	A.KIDQNVEELKGRLTPYADEFKV.K	Apolipoprotein A-IV
2351.20	108.2	I.DQNVEELKGRLTPYADEFKV.K	Apolipoprotein A-IV
1955.03	109.8	I.SASAEELRQRLAPLAEDV.R	Apolipoprotein A-IV

Peptide/Protein Identifications from Proteinase 3 Experiments

m/z	Score	Sequence	Protein	m/z	Score	Sequence	Protein
3775.71	113.9	A.EDPQGDAAQKTDTSHHDQDHPTFNKITPNLAEFA.F	Alpha-1-antitrypsin	1749.84	111.5	R.SLMPFSPYEPLNFHA.M	Clusterin
2172.16	47.3	A.LVNYIFFKGKWERPFEV.K	Alpha-1-antitrypsin	1543.78	64.7	S.IIDELFQDRFFT.R	Clusterin
1007.62	41.9	A.SLHLPKLSI.T	Alpha-1-antitrypsin	1711.84	92.8	S.LLENDRQQTHMLDV.M	Clusterin
1569.81	53.9	I.FFKGKWERPFEV.K	Alpha-1-antitrypsin	1662.80	70.7	S.LMPFSPYEPLNFHA.M	Clusterin
1578.79	49.6	I.ITKFLENEDRRSA.S	Alpha-1-antitrypsin	1630.82	78.2	S.SIIDELFQDRFFT.R	Clusterin
2127.13	118.9	I.TGTYDLKSVLGQLGITKVFS.N	Alpha-1-antitrypsin	2097.12	94.3	T.NNPSQAKLRRELDESLQV.A	Clusterin
1194.62	49.6	K.KLYHSEAFTV.N	Alpha-1-antitrypsin	1371.66	78.5	T.QGEDQYYLRVT.T	Clusterin
2390.24	114.2	L.MIEQNTKSPLFMGKVVNPTQK.-	Alpha-1-antitrypsin	1472.71	51.9	T.QGEDQYYLRVTT.V	Clusterin
1591.86	103.1	L.SEGLKLVDKFLEDV.K	Alpha-1-antitrypsin	1967.95	116.6	T.QGEDQYYLRVTTVASHT.S	Clusterin
2259.21	108.5	M.IEQNTKSPLFMGKVVNPTQK.-	Alpha-1-antitrypsin	3667.98	47.4	T.REPQDTYHYLPFSLPHRRPHFFFPKSRIV.R	Clusterin
1501.83	80.7	M.SIPPEVKFNKPFV.F	Alpha-1-antitrypsin	2014.07	63.7	T.VAEKALQEYRKKHREE.-	Clusterin
1761.98	53.9	M.SIPPEVKFNKPFVFL.M	Alpha-1-antitrypsin	1915.02	71	V.AEKALQEYRKKHREE.-	Clusterin
4133.31	121.4	M.SIPPEVKFNKPFVFLMIEQNTKSPLFMGKVVNPTQK.-	Alpha-1-antitrypsin	1758.94	119.2	V.KLFDSDPITVTVPVEV.S	Clusterin
2579.31	96.4	T.AIFFLPDEGKLQHLENELTHDI.I	Alpha-1-antitrypsin	3076.65	80.8	V.KLFDSDPITVTVPVEVSRKNPKFMETV.A	Clusterin
1545.83	54.6	T.KSPLFMGKVVNPTQ.K	Alpha-1-antitrypsin	2690.29	94.6	V.MQDHFSRASSIIDELFQDRFFT.R	Clusterin
1673.94	110.9	T.KSPLFMGKVVNPTQK.-	Alpha-1-antitrypsin	1336.71	50.1	V.SRKNPKFMETV.A	Clusterin
2169.10	40.7	V.DKFLEDVKKLYHSEAFTV.N	Alpha-1-antitrypsin	3232.71	89.6	V.SRKNPKFMETVAEKALQEYRKKHREE.-	Clusterin
1322.71	88.8	V.KKLYHSEAFTV.N	Alpha-1-antitrypsin	1961.03	50.7	V.TVPVEVSRKNPKFMETV.A	Clusterin
3142.74	56.6	V.LGQLGITKVFSNGADLSGVTEEAPLKLSKAV.H	Alpha-1-antitrypsin	3274.80	42.8	V.VVKLFDSDPITVTVPVEVSRKNPKFMETV.A	Clusterin
1960.02	86.6	V.NYIFFKGKWERPFEV.K	Alpha-1-antitrypsin	1327.75	64.4	G.SIPIPQKLFGEV.T	Complement C1r subcomponent
2049.08	42.1	V.DLKPPFGGSAPSERLELHV.D	Alpha-1B-glycoprotein	2022.06	93.4	R.IIGGQKAKMGNFPWQVFT.N	Complement C1r subcomponent
1964.97	77.7	I.KEDFLEQSEQLFGAKPV.S	Alpha-2-antiplasmin	1240.72	82.6	S.IPIPQKLFGEV.T	Complement C1r subcomponent
1961.97	84.7	L.KLVPPMEEDYPQFGSPK.-	Alpha-2-antiplasmin	1669.81	60.2	T.DESGDSRGWKLRYT.T	Complement C1r subcomponent
2216.13	93.1	A.ALVAIDYINQNLPWGYKHT.L	Alpha-2-HS-glycoprotein	1906.03	54.3	T.NIHGRGGGALLGDRWILT.A	Complement C1r subcomponent
1861.92	93.6	A.IDYINQNLPWGYKHT.L	Alpha-2-HS-glycoprotein	2460.32	67.3	V.FLGHTNVEELMKLGNHPIRRV.S	Complement C1r subcomponent
2673.33	80.9	A.IDYINQNLPWGYKHTLNQIDEV.K	Alpha-2-HS-glycoprotein	1487.76	40.6	V.MEEKIAHDLRFV.R	Complement C1r subcomponent
1115.57	42.3	Q.NLPWGYKHT.L	Alpha-2-HS-glycoprotein	1934.98	57.6	V.SGFGVMEEKIAHDLRFV.R	Complement C1r subcomponent
1451.77	54	S.LGSPSGEVSHPRKT.R	Alpha-2-HS-glycoprotein	3139.47	83.4	V.SVHPDYRQDESYNFEGDIALLELENSV.T	Complement C1r subcomponent
1842.91	66.9	T.FMGVVSLGSPSGEVSHPR.K	Alpha-2-HS-glycoprotein	1174.70	61.8	I.RLEKGFQVVV.T	Complement C1s subcomponent
2072.06	142.4	T.FMGVVSLGSPSGEVSHPRKT.R	Alpha-2-HS-glycoprotein	1619.77	77.4	V.IFKSDFSNEERFT.G	Complement C1s subcomponent
1932.96	105.2	V.AIDYINQNLPWGYKHT.L	Alpha-2-HS-glycoprotein	1894.89	60	V.IFKSDFSNEERFTGFA.A	Complement C1s subcomponent
1909.00	78.9	V.LLAAPPGHQLHRAHYDL.R	Alpha-2-HS-glycoprotein	2612.29	62.5	A.KDKNRWEDPGKQLYNVEATSYA.L	Complement C3
2303.24	83	V.LLAAPPGHQLHRAHYDLRHT.F	Alpha-2-HS-glycoprotein	1388.66	55.1	A.NYMNLQRSYTV.A	Complement C3
1309.65	51.8	V.SLGSPSGEVSHPR.K	Alpha-2-HS-glycoprotein	2559.41	75.4	A.VDKGVFVLNKKNKLTQSKIWDV.V	Complement C3
1538.80	98.6	V.SLGSPSGEVSHPRKT.R	Alpha-2-HS-glycoprotein	1098.58	70.7	I.HWESASLLR.S	Complement C3
1408.72	77.7	V.VSLGSPSGEVSHPR.K	Alpha-2-HS-glycoprotein	1751.77	58.7	L.NEQRYYGGGYGSTQAT.F	Complement C3
1637.86	97.1	V.VSLGSPSGEVSHPRKT.R	Alpha-2-HS-glycoprotein	2168.06	63.7	Q.ALAQYQKDAPDHQELNLDV.S	Complement C3
864.46	49	M.HGPEGLRV.G	Alpha-2-macroglobulin	1493.72	64.5	Q.KDAPDHQELNLDV.S	Complement C3
1447.72	67	M.HGPEGLRVGFYES.D	Alpha-2-macroglobulin	3576.84	93	R.EGVQKEDIPPADLSDQVPDTESETRILLQGTPV.A	Complement C3
1661.80	83.9	M.HGPEGLRVGFYESDV.M	Alpha-2-macroglobulin	1551.81	50.8	R.SSKITHRIHWESA.S	Complement C3
2639.38	74.7	M.HGPEGLRVGFYESDVMGRGHARLV.H	Alpha-2-macroglobulin	1208.65	65.6	T.KLMNIFLKDS.I	Complement C3
1210.66	56.5	S.DVMGRGHARLV.H	Alpha-2-macroglobulin	1860.09	50.6	T.YLIMNKGRLLKAGRQV.R	Complement C3
1793.84	89.8	V.GFYESDVMGRGHARLV.H	Alpha-2-macroglobulin	3879.07	52.6	V.HYLDETEQWEKFGLEKRQGALELIKKGYTQQL.A	Complement C3
1568.88	50.9	A.ARLEALKENGGARLA.E	Apolipoprotein A-I	2334.15	102.1	V.IVEPTEKFYYIYNEKGLEV.T	Complement C3

1550.82	79.8	A.ELQEGARQKLHEL.Q	Apolipoprotein A-I	3147.57	111.1	V.KSGQSEDRQPVPGQQMTLKIEGDHGARVV.L	Complement C3
2792.38	131.8	A.ELQEGARQKLHELQEKLSPLGEEM.R	Apolipoprotein A-I	1472.71	71.4	V.NFLLRMDRAHEA.K	Complement C3
1285.62	65.3	A.EYHAKATEHLS.T	Apolipoprotein A-I	1737.95	85.7	V.REPGQDLVVLPLSITT.D	Complement C3
2211.15	161	A.EYHAKATEHLSTLSEKAKPA.L	Apolipoprotein A-I	2333.26	86.2	V.SLQLPSRSSKITHRIHWESA.S	Complement C3
2681.33	176.6	A.EYHAKATEHLSTLSEKAKPALEDL.R	Apolipoprotein A-I	2829.42	46.1	A.SRYLDKTEQWSTLPPETKDHAVDL.I	Complement C4-A
3444.86	215.6	A.EYHAKATEHLSTLSEKAKPALEDLRQGLLPV.L	Apolipoprotein A-I	1896.03	95.5	R.NGFKSHALQLNNRQIR.G	Complement C4-A
1710.92	108.7	A.KATEHLSTLSEKAKPA.L	Apolipoprotein A-I	3185.67	55.3	R.NGFKSHALQLNNRQIRGLEEELQFSLGS.K	Complement C4-A
2944.66	182.5	A.KATEHLSTLSEKAKPALEDLRQGLLPV.L	Apolipoprotein A-I	2751.31	145.3	R.TLEIPGNSDPNMIPDGDFNSYVRVT.A	Complement C4-A
1252.70	54.6	A.LEDLRQGLLPV.L	Apolipoprotein A-I	2388.42	60.9	S.KINVKVGGNSKGTLKVLRTYNV.L	Complement C4-A
1581.86	61.1	A.LEDLRQGLLPVLES.F	Apolipoprotein A-I	1934.09	78.4	V.KVGGNSKGTLKVLRTYNV.L	Complement C4-A
1956.11	75.7	A.LEDLRQGLLPVLESFKV.S	Apolipoprotein A-I	2932.51	73.4	V.SYKHKGALHNYKMTDKNFLGRPVEV.L	Complement C5
2043.15	60.6	A.LEDLRQGLLPVLESFKVS.F	Apolipoprotein A-I	2467.33	44.3	A.SSINDAPVLISQKLSPIYNLVPV.K	Complement component C9
1366.71	73.5	A.LEEYTKKLNTQ.-	Apolipoprotein A-I	1155.65	56.3	V.KGEIHLGRFV.M	Complement component C9
3220.69	55.1	A.LKENGGARLAEYHAKATEHLSTLSEKAKPA.L	Apolipoprotein A-I	1756.96	57.8	V.QELQKRLDRLEETV.Q	Coronin-1A
2736.30	46.4	A.RHFWQQDEPPQSPWDRVKDLAT.V	Apolipoprotein A-I	1465.65	57.7	A.DSGEGDFLAEGGGVR.G	Fibrinogen alpha chain
1625.81	51.6	A.RLAEYHAKATEHLS.T	Apolipoprotein A-I	1973.94	56.1	A.DSGEGDFLAEGGGVRGPRVV.E	Fibrinogen alpha chain
2551.34	124.5	A.RLAEYHAKATEHLSTLSEKAKPA.L	Apolipoprotein A-I	1954.92	42.4	A.EYHFRVGSEAEGYALQV.S	Fibrinogen alpha chain
3785.10	117.6	A.RLAEYHAKATEHLSTLSEKAKPALEDLRQGLLPV.L	Apolipoprotein A-I	3076.43	43	A.MDLGTLSGIGTLDGFRHRHPDEAAFFDT.A	Fibrinogen alpha chain
1497.85	93.5	A.RLEALKENGGARLA.E	Apolipoprotein A-I	1948.96	89.4	A.STGKTFPGFFSPMLGEFV.S	Fibrinogen alpha chain
1998.06	135.7	A.RLEALKENGGARLAEYHA.K	Apolipoprotein A-I	1622.74	54.8	L.RVELEDWAGNEAYA.E	Fibrinogen alpha chain
2677.38	110.5	A.RLEALKENGGARLAEYHAKATEHL.S	Apolipoprotein A-I	2622.27	68.1	S.SSHHPGIAEFPSRGKSSSYSKQFT.S	Fibrinogen alpha chain
2764.42	69.2	A.RLEALKENGGARLAEYHAKATEHLS.T	Apolipoprotein A-I	2897.35	40.5	S.SSHHPGIAEFPSRGKSSSYSKQFTSST.S	Fibrinogen alpha chain
3689.96	122.7	A.RLEALKENGGARLAEYHAKATEHLSTLSEKAKPA.L	Apolipoprotein A-I	2045.00	44.1	T.ADSGEGDFLAEGGGVRGPRVV.E	Fibrinogen alpha chain
2165.15	147.8	A.RQKLHELQEKLSPLGEEM.R	Apolipoprotein A-I	1474.68	41.4	T.ASTGKTFPGFFSPM.L	Fibrinogen alpha chain
3126.63	63.8	A.RQKLHELQEKLSPLGEEMRDRARAHV.D	Apolipoprotein A-I	1920.91	92.1	T.ASTGKTFPGFFSPMLGEF.V	Fibrinogen alpha chain
2745.47	89.2	A.TEHLSTLSEKAKPALEDLRQGLLPV.L	Apolipoprotein A-I	2020.00	109.8	T.ASTGKTFPGFFSPMLGEFV.S	Fibrinogen alpha chain
2537.28	89.3	G.SALGKQLNLKLLDNWDSVTSTFS.K	Apolipoprotein A-I	2125.00	51.8	T.KESSSHHPGIAEFPSRGKSS.S	Fibrinogen alpha chain
1483.66	56.4	L.DDFQKKWQEEM.E	Apolipoprotein A-I	2966.43	121.5	T.KESSSHHPGIAEFPSRGKSSSYSKQFT.S	Fibrinogen alpha chain
1612.77	119.8	L.KLLDNWDSVTSTFS.K	Apolipoprotein A-I	3241.52	66	T.KESSSHHPGIAEFPSRGKSSSYSKQFTSST.S	Fibrinogen alpha chain
2734.40	102.3	L.KLLDNWDSVTSTFSKLREQLGPVT.Q	Apolipoprotein A-I	2030.96	52.4	T.LDGFRHRHPDEAAFFDT.A	Fibrinogen alpha chain
1308.68	46	L.QEGARQKLHEL.Q	Apolipoprotein A-I	1294.65	53.6	T.NIMEILRGDFS.S	Fibrinogen alpha chain
2550.33	125.9	L.QEGARQKLHELQEKLSPLGEEM.R	Apolipoprotein A-I	3181.51	110.6	T.NTKESSSHHPGIAEFPSRGKSSSYSKQFT.S	Fibrinogen alpha chain
1260.60	99	L.QEKLSPLGEEM.R	Apolipoprotein A-I	3456.62	48.4	T.NTKESSSHHPGIAEFPSRGKSSSYSKQFTSST.S	Fibrinogen alpha chain
2222.16	105.6	L.QEKLSPLGEEMRDRARAHV.D	Apolipoprotein A-I	2810.17	72.8	T.SESSVSGSTGQWHSESGSFRPDSPGSGN.A	Fibrinogen alpha chain
1777.95	83.3	L.RAELQEGARQKLHEL.Q	Apolipoprotein A-I	1573.82	43	T.SLGGWLLIQQRMDG.S	Fibrinogen alpha chain
3019.54	58.9	L.RAELQEGARQKLHELQEKLSPLGEEM.R	Apolipoprotein A-I	2174.94	83.3	T.SSTSYNRGDSTFESKSYKM.A	Fibrinogen alpha chain
1524.79	91.8	L.SALEEYTKKLNTQ.-	Apolipoprotein A-I	2246.01	89.2	T.SSTSYNRGDSTFESKSYKMA.D	Fibrinogen alpha chain
1964.09	108.8	L.SEKAKPALEDLRQGLLPV.L	Apolipoprotein A-I	1899.84	68.3	T.SYNRGDSTFESKSYKM.A	Fibrinogen alpha chain
2265.25	141	L.STLSEKAKPALEDLRQGLLPV.L	Apolipoprotein A-I	1970.89	90.6	T.SYNRGDSTFESKSYKMA.D	Fibrinogen alpha chain
2968.68	48.2	L.STLSEKAKPALEDLRQGLLPVLESFKV.S	Apolipoprotein A-I	1395.70	41	T.TNIMEILRGDFS.S	Fibrinogen alpha chain
2129.11	50.8	M.ELYRQKVEPLRAELQEGA.R	Apolipoprotein A-I	1408.75	49.8	V.IGPDGHKEVTKEV.V	Fibrinogen alpha chain
2205.14	69.5	M.RDRARAHVDALRTHLAPYS.D	Apolipoprotein A-I	1608.84	57.9	V.IGPDGHKEVTKEVVT.S	Fibrinogen alpha chain
2151.07	40.3	N.WDSVTSTFSKLREQLGPVT.Q	Apolipoprotein A-I	1486.66	45.3	V.SETESRGSESGIFT.N	Fibrinogen alpha chain
1853.87	53.5	Q.DEPPQSPWDRVKDLAT.V	Apolipoprotein A-I	1701.76	75.7	V.SETESRGSESGIFTNT.K	Fibrinogen alpha chain
2215.11	64.7	Q.DEPPQSPWDRVKDLATVYV.D	Apolipoprotein A-I	2045.93	135.5	V.SETESRGSESGIFTNTKES.S	Fibrinogen alpha chain
1437.77	72.6	S.ALEEYTKKLNTQ.-	Apolipoprotein A-I	3633.75	95.1	V.SETESRGSESGIFTNTKESSSHHPGIAEFPSRGK.S	Fibrinogen alpha chain
1540.86	54.2	S.DELRQRLAARLEA.L	Apolipoprotein A-I	3807.81	153.6	V.SETESRGSESGIFTNTKESSSHHPGIAEFPSRGKSS.S	Fibrinogen alpha chain
2210.17	99.6	S.DELRQRLAARLEALKENGGA.R	Apolipoprotein A-I	4144.98	81.2	V.SETESRGSESGIFTNTKESSSHHPGIAEFPSRGKSSSYS.K	Fibrinogen alpha chain
2550.40	110.7	S.DELRQRLAARLEALKENGGARLA.E	Apolipoprotein A-I	1341.69	46.1	V.SFRGADYSLRAV.R	Fibrinogen alpha chain
3050.60	119.2	S.DELRQRLAARLEALKENGGARLAEYHA.K	Apolipoprotein A-I	2030.05	63.5	V.SGNVSPGTRREYHTEKLV.T	Fibrinogen alpha chain

1656.87	73.9	S.FLSALEEYTKKLNT.Q	Apolipoprotein A-I	2131.10	46.4	V.SGNVSPGTRREYHTEKLVT.S	Fibrinogen alpha chain
1784.94	105.1	S.FLSALEEYTKKLNTQ.-	Apolipoprotein A-I	3788.04	61.6	V.SGNVSPGTRREYHTEKLVTSKGDKELRTGKEKVT.S	Fibrinogen alpha chain
1140.68	65.1	S.KLREQLGPVT.Q	Apolipoprotein A-I	1837.98	44.6	V.TKTVIGPDGHKEVTKEV.V	Fibrinogen alpha chain
2560.28	156.8	S.KLREQLGPVTQEFWDNLEKET.E	Apolipoprotein A-I	1456.82	44.4	L.KDLWQKRQKQV.K	Fibrinogen beta chain
3403.72	56.6	S.KLREQLGPVTQEFWDNLEKETEGLRQEM.S	Apolipoprotein A-I	1936.95	79.2	M.EDWKGDKVKAHYGGFTV.Q	Fibrinogen beta chain
2178.23	112.2	S.TLSEKAKPALEDLRQGLLPV.L	Apolipoprotein A-I	1160.63	50.1	M.KIRPFFPQQ.-	Fibrinogen beta chain
1662.81	74.4	T.EGLRQEMSKDLEEV.K	Apolipoprotein A-I	1289.66	51.5	T.RMGPTELLIEM.E	Fibrinogen beta chain
2644.47	165.2	T.EHLSTLSEKAKPALEDLRQGLLPV.L	Apolipoprotein A-I	1747.75	112.2	T.WDMAKHGTDDGVVWM.N	Fibrinogen beta chain
1739.93	82.2	T.HLAPYSDELRQRLAA.R	Apolipoprotein A-I	1856.76	106.5	A.FDGFDFGDDPSDKFFT.S	Fibrinogen gamma chain
2077.20	64.7	T.LSEKAKPALEDLRQGLLPV.L	Apolipoprotein A-I	2846.14	57	A.FDGFDFGDDPSDKFFTSHNGMQFST.W	Fibrinogen gamma chain
1438.63	100.3	T.QEFWDNLEKET.E	Apolipoprotein A-I	2399.96	137.5	A.GGDAGDAFDGFDFGDDPSDKFFT.S	Fibrinogen gamma chain
3082.48	50.9	T.QEFWDNLEKETEGLRQEMSKDLEEV.K	Apolipoprotein A-I	2486.95	90.1	A.GGDAGDAFDGFDFGDDPSDKFFTS.H	Fibrinogen gamma chain
2982.48	58.6	T.STFSKLREQLGPVTQEFWDNLEKET.E	Apolipoprotein A-I	3288.30	135.3	A.GGDAGDAFDGFDFGDDPSDKFFTSHNGMQFS.T	Fibrinogen gamma chain
1243.65	61.9	V.DALRTHLAPYS.D	Apolipoprotein A-I	3389.38	135.2	A.GGDAGDAFDGFDFGDDPSDKFFTSHNGMQFST.W	Fibrinogen gamma chain
2296.22	103	V.DALRTHLAPYSDELRQRLAA.R	Apolipoprotein A-I	1515.69	113.8	A.GHLNGVYYQGGTYS.K	Fibrinogen gamma chain
1266.62	60.1	V.DVLKDSGRDYV.S	Apolipoprotein A-I	1654.86	73.7	A.MFKVGPEADKYRLT.Y	Fibrinogen gamma chain
1901.88	64.3	V.DVLKDSGRDYVSQFEGS.A	Apolipoprotein A-I	1888.97	70.1	A.MFKVGPEADKYRLTYA.Y	Fibrinogen gamma chain
2512.25	73.6	V.DVLKDSGRDYVSQFEGSALGKQL.N	Apolipoprotein A-I	2270.14	50.7	A.MFKVGPEADKYRLTYAYFA.G	Fibrinogen gamma chain
2739.36	129.6	V.DVLKDSGRDYVSQFEGSALGKQLNL.K	Apolipoprotein A-I	2781.08	175.3	A.YFAGGDAGDAFDGFDFGDDPSDKFFT.S	Fibrinogen gamma chain
2411.18	151.4	V.KAKVQPYLDDFQKKWQEEM.E	Apolipoprotein A-I	1458.68	97.8	G.HLNGVYYQGGTYS.K	Fibrinogen gamma chain
3666.91	135.8	V.KAKVQPYLDDFQKKWQEEMELYRQKVEPL.R	Apolipoprotein A-I	1922.85	46.6	I.QLTYNPDESSKPNMIDA.A	Fibrinogen gamma chain
3894.11	62	V.KAKVQPYLDDFQKKWQEEMELYRQKVEPLRA.E	Apolipoprotein A-I	1606.79	102.8	S.KASTPNGYDNGIIWA.T	Fibrinogen gamma chain
722.40	42.6	V.LESFKV.S	Apolipoprotein A-I	2309.13	91.7	T.ADYAMFKVGPEADKYRLTYA.Y	Fibrinogen gamma chain
1069.58	66.4	V.LESFKVSFL.S	Apolipoprotein A-I	2690.30	41.4	T.ADYAMFKVGPEADKYRLTYAYFA.G	Fibrinogen gamma chain
1156.62	83.3	V.LESFKVSFLS.A	Apolipoprotein A-I	2406.17	73.2	T.QSAIPYALRVELEDWNGRTST.A	Fibrinogen gamma chain
1227.66	89.3	V.LESFKVSFLSA.L	Apolipoprotein A-I	2826.34	63.4	T.QSAIPYALRVELEDWNGRTSTADYA.M	Fibrinogen gamma chain
1862.94	129.6	V.LESFKVSFLSALEEYT.K	Apolipoprotein A-I	907.36	54.3	T.SHNGMQFS.T	Fibrinogen gamma chain
2447.31	130.8	V.LESFKVSFLSALEEYTKKLNT.Q	Apolipoprotein A-I	1008.43	66.7	T.SHNGMQFST.W	Fibrinogen gamma chain
2575.36	166.9	V.LESFKVSFLSALEEYTKKLNTQ.-	Apolipoprotein A-I	1599.85	59.8	T.TEFWLGNEKIHLI.S	Fibrinogen gamma chain
2525.29	79.9	V.LKDSGRDYVSQFEGSALGKQLNL.K	Apolipoprotein A-I	2453.19	68.2	V.DFKKNWIQYKEGFGHLSPTGT.T	Fibrinogen gamma chain
1743.91	76.5	V.SFLSALEEYTKKLNT.Q	Apolipoprotein A-I	1727.76	46.7	V.ELEDWNGRTSTADYA.M	Fibrinogen gamma chain
1871.95	112.9	V.SFLSALEEYTKKLNTQ.-	Apolipoprotein A-I	1932.84	48.8	V.RPEHPAETEYDSLYPE.D	Fibrinogen gamma chain
1264.64	76.5	V.SQFEGSALGKQL.N	Apolipoprotein A-I	2276.02	102	V.RPEHPAETEYDSLYPEDDL.-	Fibrinogen gamma chain
1491.76	99.4	V.SQFEGSALGKQLNL.K	Apolipoprotein A-I	938.40	47	V.YYQGGTYS.K	Fibrinogen gamma chain
2463.22	143.4	V.SQFEGSALGKQLNLKLLDNWDS.V	Apolipoprotein A-I	2696.20	117.8	S.SYRAGFGNQESEFWLGNENLHQL.T	Ficolin-3
2663.38	101.5	V.SQFEGSALGKQLNLKLLDNWDSVT.S	Apolipoprotein A-I	1278.62	84.5	V.DHYQLALGKFS.E	Ficolin-3
3085.56	182.9	V.SQFEGSALGKQLNLKLLDNWDSVTSTFS.K	Apolipoprotein A-I	1411.75	57.6	A.NFKFTDHLKYV.M	Haptoglobin
1539.67	75.5	V.TQEFWDNLEKET.E	Apolipoprotein A-I	1388.74	72.7	A.AFRQGHNSVFLI.K	Hemopexin
2738.48	81	A.EAKSYFEKSKEQLTPLIKKAGTEL.V	Apolipoprotein A-II	1916.07	64.8	A.AFRQGHNSVFLIKGDKV.W	Hemopexin
2538.40	180.4	A.KSYFEKSKEQLTPLIKKAGTEL.V	Apolipoprotein A-II	3869.12	103.7	I.KGDKVWVYPPEKKEKGYPKLLQDEFPGIPSPLDA.A	Hemopexin
2637.47	129.6	A.KSYFEKSKEQLTPLIKKAGTELV.N	Apolipoprotein A-II	1532.74	49.6	I.SERWKNFPSPVDA.A	Hemopexin
3979.21	157.7	L.MEKVKSPELQAEAKSYFEKSKEQLTPLIKKAGTEL.V	Apolipoprotein A-II	1440.78	49.6	V.RGEVPPRYPRPDV.R	Hemopexin
3590.97	62	V.KSPELQAEAKSYFEKSKEQLTPLIKKAGTELV.N	Apolipoprotein A-II	3341.76	51.4	V.WVYPPEKKEKGYPKLLQDEFPGIPSPLDA.A	Hemopexin
2052.03	106.1	V.TDYGKDLMEKVKSPELQA.E	Apolipoprotein A-II	1194.61	61.6	V.KDYFPEPVTV.S	Ig gamma-2 chain C region
2252.10	123.7	V.TDYGKDLMEKVKSPELQAEA.K	Apolipoprotein A-II	1240.68	43.1	V.RQAPGKGLEWV.G	Ig heavy chain V-III region TIL
2607.37	123.7	A.DEFKVKIDQTVEELRRSLAPYA.Q	Apolipoprotein A-IV	1866.97	77.1	S.TLTLSKADYEKHKVYA.C	Ig kappa chain C region
2066.07	135.5	A.KEAVEHLQKSELTQQLNA.L	Apolipoprotein A-IV	1545.80	55.7	V.AWKADSSPVKAGVET.T	Ig lambda chain C regions
3310.72	66.7	A.KEAVEHLQKSELTQQLNALFQDKLGEVNT.Y	Apolipoprotein A-IV	2844.56	56.8	A.KRYIEKIQPSGGTNINEALLRAIFI.L	Inter-alpha-trypsin inhibitor heavy chain H2
1915.99	45.4	A.QRMERVLRENADSLQA.S	Apolipoprotein A-IV	1803.00	46	A.YLTINQLLAERSLAPT.A	Inter-alpha-trypsin inhibitor heavy chain H2
3191.70	100.8	A.SLRPHADELKAKIDQNVEELKGRLTPYA.D	Apolipoprotein A-IV	1159.68	40.2	I.NEALLRAIFI.L	Inter-alpha-trypsin inhibitor heavy chain H2

1737.89	122.3	A.VEHLQKSELTQQLNA.L	Apolipoprotein A-IV	3558.04	80.2	T.KTQVADAKRYIEKIQPSGGTNINEALLRAIFI.L	Inter-alpha-trypsin inhibitor heavy chain H2
2767.45	142.3	A.VEHLQKSELTQQLNALFQDKLGEV.N	Apolipoprotein A-IV	3204.56	108.1	T.LAQMDDLQDFLSKDKHADPDFTRKLWA.Y	Inter-alpha-trypsin inhibitor heavy chain H2
1287.65	46.6	V.EGHLSFLEKDL.R	Apolipoprotein A-IV	1341.69	61.9	T.SSQLKKFYNQV.S	Inter-alpha-trypsin inhibitor heavy chain H2
2368.21	74.6	V.EGHLSFLEKDLRDKVNSFFS.T	Apolipoprotein A-IV	2222.24	52.7	T.SSQLKKFYNQVSTPLLRNV.Q	Inter-alpha-trypsin inhibitor heavy chain H2
1788.91	58.9	V.NTQAEQLRRQLTPYA.Q	Apolipoprotein A-IV	3101.67	117.3	V.ADAKRYIEKIQPSGGTNINEALLRAIFI.L	Inter-alpha-trypsin inhibitor heavy chain H2
2258.17	41.4	V.SQKIGDNLRELQQRLEPYA.D	Apolipoprotein A-IV	2377.18	170	V.AGKFDPAKLDQIESVITATSANT.Q	Inter-alpha-trypsin inhibitor heavy chain H2
3098.64	71.3	V.SQKIGDNLRELQQRLEPYADQLRTQV.N	Apolipoprotein A-IV	2967.46	78.9	V.DYDFLKRLSNENHGIAQRIYGNQDT.S	Inter-alpha-trypsin inhibitor heavy chain H2
2199.40	98	A.HVALKAGKLKFIIPSPKRPV.K	Apolipoprotein B-100	1737.91	96.4	V.HFFAPDNLDPIPKNI.L	Inter-alpha-trypsin inhibitor heavy chain H2
1810.00	77.9	A.LNLPTLPEVKFPEVDV.L	Apolipoprotein B-100	2097.10	109.1	V.HFFAPDNLDPIPKNILFV.I	Inter-alpha-trypsin inhibitor heavy chain H2
2071.12	48.7	A.LRKMEPKDKDQEVLLQT.F	Apolipoprotein B-100	2076.07	41.5	V.IDFNQNIRTWRNDLISA.T	Inter-alpha-trypsin inhibitor heavy chain H2
1684.77	84	A.NDYLNSFNWERQV.S	Apolipoprotein B-100	2177.08	92.3	V.IDFNQNIRTWRNDLISAT.K	Inter-alpha-trypsin inhibitor heavy chain H2
1386.69	64.8	A.SQELQQIHQYI.M	Apolipoprotein B-100	2127.04	123.6	V.KENIQDNISLFSLGMGFDV.D	Inter-alpha-trypsin inhibitor heavy chain H2
1951.16	67.2	C.KLDFREIQIYKKLRT.S	Apolipoprotein B-100	2805.44	62.6	V.KMKQTVEAMKTILDDLRAEDHFSV.I	Inter-alpha-trypsin inhibitor heavy chain H2
2038.20	47.2	C.KLDFREIQIYKKLRTS.S	Apolipoprotein B-100	3214.47	56.2	V.QFNYPHTSVTDVTQNNFHNYFGGSEIVV.A	Inter-alpha-trypsin inhibitor heavy chain H2
1277.64	54	I.DDIDVRFQKAA.S	Apolipoprotein B-100	2028.09	122.4	V.SDGDPTVGELKLSKIQKNV.K	Inter-alpha-trypsin inhibitor heavy chain H2
1167.73	70.8	M.KLAPGELTIIL.-	Apolipoprotein B-100	2288.17	44.1	V.STPLLRNVQFNYPHTSVTDV.T	Inter-alpha-trypsin inhibitor heavy chain H2
1848.98	42	M.RDAVEKPQEFTIVAFV.K	Apolipoprotein B-100	1825.85	93	V.TQNNFHNYFGGSEIVV.A	Inter-alpha-trypsin inhibitor heavy chain H2
1185.63	76.2	M.SAFGYVFPKAV.S	Apolipoprotein B-100	1456.68	72.9	T.YQHFYDGSEIVV.A	Inter-alpha-trypsin inhibitor heavy chain H3
1558.80	41.3	T.IEMSAFGYVFPKAV.S	Apolipoprotein B-100	1952.99	80.4	T.YQHFYDGSEIVVAGRLV.D	Inter-alpha-trypsin inhibitor heavy chain H3
2081.19	82.2	T.IIVPEQTIEIPSIKFSVPA.G	Apolipoprotein B-100	1649.91	78.1	V.HFFAPQGLPVVPKNV.A	Inter-alpha-trypsin inhibitor heavy chain H3
3434.88	97	T.KIKFDKYKAEKSHDELPRTFQIPGYTVPV.V	Apolipoprotein B-100	3089.47	65.8	A.LDNGGLARRIHEDSDSALQLQDFYQEV.A	Inter-alpha-trypsin inhibitor heavy chain H4
2824.44	70.3	T.LNLNDFQVPDLHIPEFQLPHISHT.I	Apolipoprotein B-100	2589.26	70.8	A.SAENVNKARSFAAGIQALGGTNINDA.M	Inter-alpha-trypsin inhibitor heavy chain H4
2977.47	177	T.SLKDNVPKATGVLYDYVNKYHWEHT.G	Apolipoprotein B-100	2680.45	91.3	S.RQLGLPGPPDVPDHAAYHPFRRLA.I	Inter-alpha-trypsin inhibitor heavy chain H4
1254.71	41.4	T.VRTPALHFKSV.G	Apolipoprotein B-100	1640.88	93.9	V.AGKLQDRGPDVLTATV.S	Inter-alpha-trypsin inhibitor heavy chain H4
2027.12	81.3	V.ALNANTKNQKIRWKNEV.R	Apolipoprotein B-100	1704.84	103.9	V.HYFAPEGLTTMPKNV.V	Inter-alpha-trypsin inhibitor heavy chain H4
1380.73	48.7	V.ISMYRELLKDL.S	Apolipoprotein B-100	2050.04	45	V.HYFAPEGLTTMPKNVVFV.I	Inter-alpha-trypsin inhibitor heavy chain H4
1767.82	80.7	V.LYDYVNKYHWEHT.G	Apolipoprotein B-100	1783.91	46.7	V.TQNNFRLLFKGSEMV.V	Inter-alpha-trypsin inhibitor heavy chain H4
2032.05	69.8	V.NGQVPDGVSKVLVDHFGYT.K	Apolipoprotein B-100	1882.99	100.7	V.TQNNFRLLFKGSEMVV.A	Inter-alpha-trypsin inhibitor heavy chain H4
2225.02	65	V.QVHASQPSSFHDFPDLGQEV.A	Apolipoprotein B-100	1330.66	68.9	T.AVDRTAGWNIPM.G	Lactotransferrin
1797.05	100.4	V.RVPSYTLILPSLELPV.L	Apolipoprotein B-100	1259.63	66.5	T.YEKYLGPQYV.A	Lactotransferrin
2358.20	102.3	V.SDGIAALDLNAVANKIADFELPT.I	Apolipoprotein B-100	1496.81	85.5	A.AFKGLKSLEYLDL.S	Lumican
1006.56	40.5	V.SQFTLPKSV.S	Apolipoprotein B-100	2185.03	84.9	L.DNNKISNIPDEYFKRFNA.L	Lumican
1861.98	86.8	V.SQFTLPKSVSDGIAALDL.N	Apolipoprotein B-100	2702.39	52.2	L.DNNKISNIPDEYFKRFNALQYL.R	Lumican
1814.96	45.8	V.SSKLRRNLQNNAEWV.Y	Apolipoprotein B-100	1498.84	70.7	L.SFNQIARLPSGLPV.S	Lumican
2744.47	117.3	V.SSKLRRNLQNNAEWVYQGAIRQI.D	Apolipoprotein B-100	2988.55	46.1	V.SLLTLYLDNNKISNIPDEYFKRFNA.L	Lumican
1641.85	81	V.YDKSLWDFLKLDV.T	Apolipoprotein B-100	2025.88	56	I.TFRSDFSNEERFTGFDA.H	Mannan-binding lectin serine protease 1
1213.57	44.8	A.KMREWFSET.F	Apolipoprotein C-I	2670.37	51.9	A.TPLGPKWPEPVFGRLASPGFPGEYA.N	Mannan-binding lectin serine protease 2
1715.83	41.1	A.KMREWFSETFQKV.K	Apolipoprotein C-I	1547.78	59.3	E.IVGGHEAQPHSRPY.M	Myeloblastin
1462.86	72.9	T.FQKVKEKLKIDS.-	Apolipoprotein C-I	1749.86	95.9	E.IVGGHEAQPHSRPYMA.S	Myeloblastin
2945.56	68.2	A.AQNLYEKTYLPAVDEKLRDLYSKST.A	Apolipoprotein C-II	1457.69	40.2	V.RTQEPTQQHFSV.A	Myeloblastin
1553.81	69.2	A.VDEKLRDLYSKST.A	Apolipoprotein C-II	1755.87	84.5	V.RTQEPTQQHFSVAQV.F	Myeloblastin
2279.11	77.1	A.VDEKLRDLYSKSTAAMSTYT.G	Apolipoprotein C-II	1606.83	75.4	A.ILREDKDPQKMYA.T	Neutrophil gelatinase-associated lipocalin
2074.94	94.6	G.TQQPQQDEMPSPTFLTQV.K	Apolipoprotein C-II	1707.90	62	G.RTKELTSELKENFI.R	Neutrophil gelatinase-associated lipocalin
2419.19	90	G.TQQPQQDEMPSPTFLTQVKES.L	Apolipoprotein C-II	2098.12	72.4	G.RTKELTSELKENFIRFS.K	Neutrophil gelatinase-associated lipocalin
2519.30	89.4	L.YEKTYLPAVDEKLRDLYSKST.A	Apolipoprotein C-II	1431.79	47.6	L.GLPENHIVFPVPI.D	Neutrophil gelatinase-associated lipocalin
1634.84	106.8	T.GIFTDQVLSVLKGEE.-	Apolipoprotein C-II	3141.63	125.6	L.IPAPPLSKVPLQQNFQDNQFQGKWYVV.G	Neutrophil gelatinase-associated lipocalin
1586.76	85.7	V.KESLSSYWESAKTA.A	Apolipoprotein C-II	1511.76	76.9	N.YNQHAMVFFKKV.S	Neutrophil gelatinase-associated lipocalin
2012.97	137.4	V.KESLSSYWESAKTAAQNL.Y	Apolipoprotein C-II	1624.87	114.1	T.LGNIKSYPGLTSYLV.R	Neutrophil gelatinase-associated lipocalin
2534.23	59.3	V.KESLSSYWESAKTAAQNLYEKT.Y	Apolipoprotein C-II	3456.73	44.8	T.SDLIPAPPLSKVPLQQNFQDNQFQGKWYVV.G	Neutrophil gelatinase-associated lipocalin
2978.48	156.5	V.KESLSSYWESAKTAAQNLYEKTYLPA.V	Apolipoprotein C-II	1285.66	44.4	V.SQNREYFKIT.L	Neutrophil gelatinase-associated lipocalin

2187.11	127.9	A.KDALSSVQESQVAQQARGWV.T	Apolipoprotein C-III	2017.04	46	I.RENYPLPWEKDTEKLV.A	Phosphatidylinositol-glycan-specific phospholipase D
2288.16	86.3	A.KDALSSVQESQVAQQARGWVT.D	Apolipoprotein C-III	1763.94	41.7	V.LISPEASSRFGSSLITV.R	Phosphatidylinositol-glycan-specific phospholipase D
2694.27	109.4	A.KDALSSVQESQVAQQARGWVTDGFS.S	Apolipoprotein C-III	2115.04	98.1	V.TSGLIGGEDGRVYVYNGKET.T	Phosphatidylinositol-glycan-specific phospholipase D
1872.95	63.9	A.LSSVQESQVAQQARGWV.T	Apolipoprotein C-III	2071.15	106.5	V.RKGHFDTLSKGELKQLLT.K	Protein S100-A12
1974.01	51.5	A.LSSVQESQVAQQARGWVT.D	Apolipoprotein C-III	1869.04	76.5	N.FLKKENKNEKVIEHI.M	Protein S100-A9
2380.11	71.5	A.LSSVQESQVAQQARGWVTDGFS.S	Apolipoprotein C-III	2357.24	78.2	N.FLKKENKNEKVIEHIMEDL.D	Protein S100-A9
3459.74	73.3	A.LSSVQESQVAQQARGWVTDGFSSLKDYWSTV.K	Apolipoprotein C-III	2573.31	77.7	N.FLKKENKNEKVIEHIMEDLDT.N	Protein S100-A9
2104.02	89.5	A.RGWVTDGFSSLKDYWSTV.K	Apolipoprotein C-III	1825.93	98.2	V.KLGHPDTLNQGEFKEL.V	Protein S100-A9
2114.95	171	A.SEAEDASLLSFMQGYMKHA.T	Apolipoprotein C-III	1925.02	127.5	V.KLGHPDTLNQGEFKELV.R	Protein S100-A9
2445.14	111.6	A.SEAEDASLLSFMQGYMKHATKT.A	Apolipoprotein C-III	2437.28	53.6	V.KLGHPDTLNQGEFKELVRKDL.Q	Protein S100-A9
2516.17	160	A.SEAEDASLLSFMQGYMKHATKTA.K	Apolipoprotein C-III	1677.91	68.5	A.RLSQRFPKAEFAEV.S	Serum albumin
2830.35	91.1	A.SEAEDASLLSFMQGYMKHATKTAKDA.L	Apolipoprotein C-III	1473.71	69.3	L.FEQLGEYKFQNA.L	Serum albumin
1512.71	104.5	A.SLLSFMQGYMKHA.T	Apolipoprotein C-III	2541.25	109.8	R.DAHKSEVAHRFKDLGEENFKAL.V	Serum albumin
1613.78	83.2	A.SLLSFMQGYMKHAT.K	Apolipoprotein C-III	2640.36	144.1	R.DAHKSEVAHRFKDLGEENFKALV.L	Serum albumin
1842.92	102.8	A.SLLSFMQGYMKHATKT.A	Apolipoprotein C-III	2753.46	61.2	R.DAHKSEVAHRFKDLGEENFKALVL.I	Serum albumin
1913.94	89.1	A.SLLSFMQGYMKHATKTA.K	Apolipoprotein C-III	2866.53	94.5	R.DAHKSEVAHRFKDLGEENFKALVLI.A	Serum albumin
2228.13	85.3	A.SLLSFMQGYMKHATKTAKDA.L	Apolipoprotein C-III	2937.56	125.8	R.DAHKSEVAHRFKDLGEENFKALVLIA.F	Serum albumin
2090.04	158.5	A.TKTAKDALSSVQESQVAQQA.R	Apolipoprotein C-III	3155.67	109.4	R.DAHKSEVAHRFKDLGEENFKALVLIAFA.Q	Serum albumin
2588.34	157.5	A.TKTAKDALSSVQESQVAQQARGWV.T	Apolipoprotein C-III	1524.87	47.9	T.KKVPQVSTPTLVEV.S	Serum albumin
2689.40	127.3	A.TKTAKDALSSVQESQVAQQARGWVT.D	Apolipoprotein C-III	1873.99	81.6	V.AHRFKDLGEENFKALV.L	Serum albumin
1425.69	69.3	S.LLSFMQGYMKHA.T	Apolipoprotein C-III	2100.16	48.1	V.AHRFKDLGEENFKALVLI.A	Serum albumin
1098.55	66.1	S.SLKDYWSTV.K	Apolipoprotein C-III	2171.19	56.4	V.AHRFKDLGEENFKALVLIA.F	Serum albumin
1504.68	80.8	T.DGFSSLKDYWSTV.K	Apolipoprotein C-III	1945.08	83.3	V.RYTKKVPQVSTPTLVEV.S	Serum albumin
2109.03	113.4	V.KDKFSEFWDLDPEVRPT.S	Apolipoprotein C-III	1314.61	62.1	A.NYIGSDKYFHA.R	Serum amyloid A protein
2508.23	100	V.KDKFSEFWDLDPEVRPTSAVAA.-	Apolipoprotein C-III	1580.75	57.6	A.LQGVGDMGRAYWDI.M	Serum amyloid A-4 protein
1486.72	43.1	V.QESQVAQQARGWV.T	Apolipoprotein C-III	1710.81	88.2	I.MISNHQNSNRYLYA.R	Serum amyloid A-4 protein
1993.90	44.4	V.QESQVAQQARGWVTDGFS.S	Apolipoprotein C-III	1466.68	46.2	I.SNHQNSNRYLYA.R	Serum amyloid A-4 protein
3073.47	74.6	V.QESQVAQQARGWVTDGFSSLKDYWSTV.K	Apolipoprotein C-III	1286.60	50.3	S.ESWRSFFKEA.L	Serum amyloid A-4 protein
1605.72	95	V.TDGFSSLKDYWSTV.K	Apolipoprotein C-III	1683.85	70.8	S.ESWRSFFKEALQGV.G	Serum amyloid A-4 protein
2147.09	66.8	A.GLVEKVQAAVGTSAAPVPSDNH.-	Apolipoprotein E	3290.70	58.3	S.KSNEKAEEWGRSGKDPDRFRPDGLPKKY.-	Serum amyloid A-4 protein
3410.63	66.8	A.KVEQAVETEPEPELRQQTEWQSGQRWEL.A	Apolipoprotein E	2875.32	93.3	V.GDMGRAYWDIMISNHQNSNRYLYA.R	Serum amyloid A-4 protein
1762.09	48.7	A.SHLRKLRKRLLRDA.D	Apolipoprotein E	3443.74	49.4	V.LEDSKSNEKAEEWGRSGKDPDRFRPDGLPK.K	Serum amyloid A-4 protein
2328.23	83.1	V.RAKLEEQAQQIRLQAEAFQA.R	Apolipoprotein E	3734.91	73.8	V.LEDSKSNEKAEEWGRSGKDPDRFRPDGLPKKY.-	Serum amyloid A-4 protein
2633.36	117.4	A.ALKPALRSGVQQLIQYYQDQKDA.N	Apolipoprotein F	2490.31	104.2	I.RHKLLPNLNDIVAVGPEHFYGT.N	Serum paraoxonase/arylesterase 1
2335.15	43.6	V.LEFSDHPGIHEPLEPEVKYV.G	Carboxypeptidase N catalytic chain	1518.73	86.1	L.NDIVAVGPEHFYGT.N	Serum paraoxonase/arylesterase 1
1493.81	84.8	A.KEKHYYIGIIET.T	Ceruloplasmin	1657.85	46.9	L.TLLGMGLALFRNHQS.S	Serum paraoxonase/arylesterase 1
2646.18	123.7	C.SEPEKVDKDNEDFQESNRMYSV.N	Ceruloplasmin	2137.09	49.6	L.TLLGMGLALFRNHQSSYQT.R	Serum paraoxonase/arylesterase 1
2418.20	78.1	V.DVHAAFFHGQALTNKNYRIDT.I	Ceruloplasmin	2291.13	68.1	M.DLNEEDPTVLELGITGSKFDV.S	Serum paraoxonase/arylesterase 1
2204.10	112.8	V.HAAFFHGQALTNKNYRIDT.I	Ceruloplasmin	2274.25	94.6	S.GLKYPGIKSFNPNSPGKILLM.D	Serum paraoxonase/arylesterase 1
1986.95	75	V.HFHGHSFQYKHRGVYS.S	Ceruloplasmin	2589.39	52.4	S.SGLKYPGIKSFNPNSPGKILLMDL.N	Serum paraoxonase/arylesterase 1
1670.88	42.3	V.HLKNLASRPYTFHS.H	Ceruloplasmin	1556.81	52.6	T.LLGMGLALFRNHQS.S	Serum paraoxonase/arylesterase 1
1444.81	60.5	V.WLGFLGPIIKAET.G	Ceruloplasmin	1957.81	99.2	T.NDHYFLDPYLQSWEM.Y	Serum paraoxonase/arylesterase 1
2151.00	107.1	A.MDIHFHSPAFQHPPTEFI.R	Clusterin	2013.92	138.7	V.AEGFDFANGINISPDGKYV.Y	Serum paraoxonase/arylesterase 1
1492.68	73.8	A.MFQPFLEMIHEA.Q	Clusterin	1653.93	49.6	V.LRIQNILTEEPKVT.Q	Serum paraoxonase/arylesterase 1
2478.15	126.5	A.QQAMDIHFHSPAFQHPPTEFI.R	Clusterin	2368.20	156.8	V.RVVAEGFDFANGINISPDGKYV.Y	Serum paraoxonase/arylesterase 1
2272.00	87.9	G.DQTVSDNELQEMSNQGSKYV.N	Clusterin	2458.09	176.2	V.SSFNPHGISTFTDEDNAMYLLV.V	Serum paraoxonase/arylesterase 1
1791.83	106.1	I.HFHSPAFQHPPTEFI.R	Clusterin	2557.15	162.5	V.SSFNPHGISTFTDEDNAMYLLVV.N	Serum paraoxonase/arylesterase 1

Endogenous Protein/Peptides Identified from Plasma

m/z	Scores	Sequence	Protein	m/z	Scores	Sequence	Protein
1110.5730	40.2	D.IFTSCKDVVV.Q	26S proteasome non-ATPase regulatory subunit 2	1160.6756	39.2	M.KIRPFFPQQ.-	Fibrinogen beta chain
1853.9313	75.2	D.TQNIFFMSKVTNPKQA.-	Alpha-1-antichymotrypsin	1791.7288	68.9	F.FSTYDRDNDGWLTSD.P	Fibrinogen beta chain
2259.2120	101.3	M.IEQNTKSPLFMGKVVNPTQK.-	Alpha-1-antitrypsin	2047.0116	65.8	W.YSMRKMSMKIRPFFPQ.Q	Fibrinogen beta chain
2375.2026	76.8	F.LMIEQNTKSPLFMGKVVNPTQ.K	Alpha-1-antitrypsin	2175.0758	78.2	W.YSMRKMSMKIRPFFPQQ.-	Fibrinogen beta chain
2390.2274	142	L.MIEQNTKSPLFMGKVVNPTQK.-	Alpha-1-antitrypsin	1088.5715	70.8	D.WVQKTIAEN.-	Haptoglobin
2503.3005	163.3	F.LMIEQNTKSPLFMGKVVNPTQK.-	Alpha-1-antitrypsin	1959.0198	133.6	Y.VKVTSIQDWVQKTIAEN.-	Haptoglobin
1752.7861	43.7	S.APHGPGLIYRQPNCDD.P	Alpha-2-HS-glycoprotein	2122.0923	124.8	V.YVKVTSIQDWVQKTIAEN.-	Haptoglobin
2579.3122	81	D.LRHTFMGVVSLGSPSGEVSHPRKT.R	Alpha-2-HS-glycoprotein	2278.1951	161.6	Y.GVYVKVTSIQDWVQKTIAEN.-	Haptoglobin
1524.7987	75.7	L.SALEEYTKKLNTQ.-	Apolipoprotein A-I	2441.2306	48.8	E.YGVYVKVTSIQDWVQKTIAEN.-	Haptoglobin
1568.7060	48.2	Q.DEPPQSPWDRVKD.L	Apolipoprotein A-I	1699.9602	47.8	D.KFLASVSTVLTSKYR.-	Hemoglobin subunit alpha
1637.8607	96.8	F.LSALEEYTKKLNTQ.-	Apolipoprotein A-I	2910.4764	97.8	M.VLSPADKTNVKAAWGKVGAHAGEYGAEAL.E	Hemoglobin subunit alpha
1971.0246	95.9	K.VSFLSALEEYTKKLNTQ.-	Apolipoprotein A-I	3326.6948	114	M.VLSPADKTNVKAAWGKVGAHAGEYGAEALERM.F	Hemoglobin subunit alpha
2099.1040	53.2	F.KVSFLSALEEYTKKLNTQ.-	Apolipoprotein A-I	3356.7831	65.2	A.AHLPAEFTPAVHASLDKFLASVSTVLTSKYR.-	Hemoglobin subunit alpha
2115.9996	36.1	Q.DEPPQSPWDRVKDLATVY.V	Apolipoprotein A-I	3427.7758	216.8	L.AAHLPAEFTPAVHASLDKFLASVSTVLTSKYR.-	Hemoglobin subunit alpha
2118.1183	163.8	S.FKVSFLSALEEYTKKLNT.Q	Apolipoprotein A-I	3473.7329	216.5	M.VLSPADKTNVKAAWGKVGAHAGEYGAEALERMF.L	Hemoglobin subunit alpha
2246.1816	133.7	S.FKVSFLSALEEYTKKLNTQ.-	Apolipoprotein A-I	3540.8930	67.4	T.LAAHLPAEFTPAVHASLDKFLASVSTVLTSKYR.-	Hemoglobin subunit alpha
2330.1041	31.3	Q.DEPPQSPWDRVKDLATVYVD.V	Apolipoprotein A-I	3740.9833	256.8	L.VTLAAHLPAEFTPAVHASLDKFLASVSTVLTSKYR.-	Hemoglobin subunit alpha
2333.2437	94.7	E.SFKVSFLSALEEYTKKLNTQ.-	Apolipoprotein A-I	3820.9689	172.4	M.VLSPADKTNVKAAWGKVGAHAGEYGAEALERMFLSF.P	Hemoglobin subunit alpha
2334.2046	38.2	L.ESFKVSFLSALEEYTKKLNT.Q	Apolipoprotein A-I	3854.0775	100.5	L.LVTLAAHLPAEFTPAVHASLDKFLASVSTVLTSKYR.-	Hemoglobin subunit alpha
2462.2888	142.9	L.ESFKVSFLSALEEYTKKLNTQ.-	Apolipoprotein A-I	1271.6976	39	D.PENFRLLGNVL.V	Hemoglobin subunit beta
2771.4213	131.4	L.PVLESFKVSFLSALEEYTKKLNTQ.-	Apolipoprotein A-I	1494.8184	74.2	M.VHLTPEEKSAVTAL.W	Hemoglobin subunit beta
2785.3662	58.8	Q.DEPPQSPWDRVKDLATVYVDVLKD.S	Apolipoprotein A-I	1737.9038	77.4	M.VHLTPEEKSAVTALWG.K	Hemoglobin subunit beta
3200.5571	67.1	Q.DEPPQSPWDRVKDLATVYVDVLKDSGRD.Y	Apolipoprotein A-I	2293.1856	86.8	M.VHLTPEEKSAVTALWGKVNVD.E	Hemoglobin subunit beta
1462.8553	73.8	T.FQKVKEKLKIDS.-	Apolipoprotein C-I	3274.7342	233.3	M.VHLTPEEKSAVTALWGKVNVDEVGGEALGRL.L	Hemoglobin subunit beta
1606.8271	85.2	G.TPDVSSALDKLKEFG.N	Apolipoprotein C-I	3387.7989	84.4	M.VHLTPEEKSAVTALWGKVNVDEVGGEALGRLL.V	Hemoglobin subunit beta
1980.9585	106.6	P.DVSSALDKLKEFGNTLED.K	Apolipoprotein C-I	1987.9460	134.6	G.GSKGPLDQLEKGGETAQSAD.P	Heparin cofactor 2
2179.0531	171.4	G.TPDVSSALDKLKEFGNTLED.K	Apolipoprotein C-I	1296.6239	72	D.PEVQFNWYVD.G	Ig gamma-2 chain C region
1626.7848	41.9	F.WDLDPEVRPTSAVAA.-	Apolipoprotein C-III	2336.1187	57.5	C.SVMHEALHNHYTQKSLSLSPG.K	Ig gamma-2 chain C region
2271.0692	32.6	D.GFSSLKDYWSTVKDKFSEF.W	Apolipoprotein C-III	1421.7780	74.8	V.KLSLDIEIATYR.K	Keratin, type II cytoskeletal 73
2759.2609	118.9	A.SEAEDASLLSFMQGYMKHATKTAKD.A	Apolipoprotein C-III	2866.5176	41.2	E.RPPTGPALPSPYSKVTAPRRPQRYSS.G	Kinesin-like protein KIF26A
1930.8610	36.9	A.EEAGARVQQNVPSGTDTGD.P	Apolipoprotein L1	904.4656	40.8	K.RPPGFSPF.R	Kininogen-1
1389.8262	30.4	N.PRRKLEFALLF.L	Ceruloplasmin	1060.5543	47.4	K.RPPGFSPFR.S	Kininogen-1
1750.0006	41.4	K.VFNPRRKLEFALLF.L	Ceruloplasmin	1295.6089	32.6	L.SHVQSQTNGGPSP.T	Leucine-rich repeat and fibronectin type-III
1088.5535	42.7	A.GVAGAAGGGGSIGAS.K	Chromobox protein homolog 6	1083.5541	34.6	K.HWNGSGSLLL.N	Leucine-rich repeat-containing protein 36
2682.3054	163.2	D.PKKGHIYQGSEADSVFSGFLIFPSA.-	Complement C1q subcomponent subunit A	1458.7066	40.3	I.ATALNTSGAGGSRPAQ.A	Misshapen-like kinase 1
942.4601	75.6	I.HWESASLL.R	Complement C3	1690.8775	54.6	L.FVLWDQQHKFPVF.M	Plasma protease C1 inhibitor
961.4913	66.1	H.WESASLLR.S	Complement C3	2736.3733	43.9	L.FVLWDQQHKFPVFMGRVYDPRA.-	Plasma protease C1 inhibitor
1098.5728	76.4	I.HWESASLLR.S	Complement C3	1525.7972	42.8	D.PNHFRPAGLPEKY.-	Putative serum amyloid A-3 protein
1211.6388	66.7	R.IHWESASLLR.S	Complement C3	1628.8530	100.5	D.PQTFYYAVAVVKKD.S	Serotransferrin precursor
1367.7617	31.4	H.RIHWESASLLR.S	Complement C3	1157.6633	38.7	L.VEVSRNLGKVG.S	Serum albumin precursor
1504.8270	53.5	G.SPMYSIITPNILR.L	Complement C3	1232.6647	73.6	D.LGEENFKALVL.I	Serum albumin precursor)
1605.8524	48.4	I.THRIHWESASLLR.S	Complement C3	1416.8042	70.2	D.LGEENFKALVLIA.F	Serum albumin precursor
1617.8841	65	G.SPMYSIITPNILRL.E	Complement C3	1424.7592	37.4	R.DAHKSEVAHRFK.D	Serum albumin precursor

1746.9586	43.3	G.SPMYSIITPNILRLE.S	Complement C3
1865.0066	65	R.SSKITHRIHWESASLL.R	Complement C3
1934.0474	44.2	S.SKITHRIHWESASLLR.S	Complement C3
2021.0874	91.2	R.SSKITHRIHWESASLLR.S	Complement C3
2032.0160	95	D.APDHQELNLDVSLQLPSR.S	Complement C3
2092.0336	84	G.SPMYSIITPNILRLESEE.T	Complement C3
2193.0926	96.4	G.SPMYSIITPNILRLESEET.M	Complement C3
2324.1341	92.2	G.SPMYSIITPNILRLESEETM.V	Complement C3
2536.2580	85.2	G.SPMYSIITPNILRLESEETMVL.E	Complement C3
2988.4284	116.8	G.SPMYSIITPNILRLESEETMVLEAHD.A	Complement C3
3359.6068	70.3	G.SPMYSIITPNILRLESEETMVLEAHDAQGD.V	Complement C3
1449.7797	38.6	K.SHALQLNNRQIR.G	Complement C4-B
1498.7919	34.6	R.NGFKSHALQLNNR.Q	Complement C4-B
1739.9334	87.8	R.NGFKSHALQLNNRQI.R	Complement C4-B
1781.9911	39.9	N.GFKSHALQLNNRQIR.G	Complement C4-B
1891.0332	71.4	R.GLEEELQFSLGSKINVK.V	Complement C4-B
1896.0234	102.2	R.NGFKSHALQLNNRQIR.G	Complement C4-B
2378.2221	40.9	K.DDPDAPLQPVTPLQLFEGRRN.R	Complement C4-B
1830.9485	112	L.PWLKEKLQDEDLGFL.-	Complement factor B
2318.2055	126.4	L.FQVLPWLKEKLQDEDLGFL.-	Complement factor B
1959.0691	46.2	E.KKVGEKLSEGDLLAEIET.D	Dihydrolipoyllysine-residue acetyltransferase component of pyruvate dehydrogenase complex, mitochondrial
905.4795	41	D.FLAEGGGVR.G	Fibrinogen alpha chain
1020.5121	58.6	G.DFLAEGGGVR.G	Fibrinogen alpha chain
1206.5678	93.5	G.EGDFLAEGGGVR.G	Fibrinogen alpha chain
1263.5850	104.4	S.GEGDFLAEGGGVR.G	Fibrinogen alpha chain
1350.6167	87.4	D.SGEGDFLAEGGGVR.G	Fibrinogen alpha chain
1465.6812	149.4	A.DSGEGDFLAEGGGVR.G	Fibrinogen alpha chain
1536.6770	147.6	T.ADSGEGDFLAEGGGVR.G	Fibrinogen alpha chain
2284.0347	64.6	F.FDTASTGKTFPGFFSPMLGEF.V	Fibrinogen alpha chain
2931.3294	56.2	K.SSSYSKQFTSSTSYNRGDSTFESKSY.K	Fibrinogen alpha chain
3239.5287	35.4	K.SYKMADEAGSEADHEGTHSTKRGHAKSRPV.R	Fibrinogen alpha chain
1539.7601	85.9	R.DAHKSEVAHRFKD.L	Serum albumin precursor
1652.8449	75.6	R.DAHKSEVAHRFKDL.G	Serum albumin precursor
1709.8671	87.7	R.DAHKSEVAHRFKDLG.E	Serum albumin precursor
1830.0820	33.4	L.LVRYTKKVPQVSTPTL.V	Serum albumin precursor
1838.9086	53.1	R.DAHKSEVAHRFKDLGE.E	Serum albumin precursor
1967.9467	33.9	R.DAHKSEVAHRFKDLGEE.N	Serum albumin precursor)
2081.9884	87.3	R.DAHKSEVAHRFKDLGEEN.F	Serum albumin precursor
2229.0487	99.1	R.DAHKSEVAHRFKDLGEENF.K	Serum albumin precursor
2242.1180	68.2	A.HKSEVAHRFKDLGEENFKA.L	Serum albumin precursor
2302.1907	43.2	K.SEVAHRFKDLGEENFKALVL.I	Serum albumin precursor
2313.1534	44.1	D.AHKSEVAHRFKDLGEENFKA.L	Serum albumin precursor
2357.1283	80.4	R.DAHKSEVAHRFKDLGEENFK.A	Serum albumin precursor
2428.1987	133.7	R.DAHKSEVAHRFKDLGEENFKA.L	Serum albumin precursor
2430.2686	43.8	H.KSEVAHRFKDLGEENFKALVL.I	Serum albumin precursor
2541.2748	117.5	R.DAHKSEVAHRFKDLGEENFKAL.V	Serum albumin precursor
2567.3374	140.4	A.HKSEVAHRFKDLGEENFKALVL.I	Serum albumin precursor
2638.3699	142.4	D.AHKSEVAHRFKDLGEENFKALVL.I	Serum albumin precursor
2753.4069	162.8	R.DAHKSEVAHRFKDLGEENFKALVL.I	Serum albumin precursor
2822.4883	111.8	D.AHKSEVAHRFKDLGEENFKALVLIA.F	Serum albumin precursor
2866.4612	80.2	R.DAHKSEVAHRFKDLGEENFKALVLI.A	Serum albumin precursor
2898.5628	129	A.HKSEVAHRFKDLGEENFKALVLIAF.A	Serum albumin precursor
2937.5528	164.9	R.DAHKSEVAHRFKDLGEENFKALVLIA.F	Serum albumin precursor
2969.5945	78.5	D.AHKSEVAHRFKDLGEENFKALVLIAF.A	Serum albumin precursor
3084.6029	145.8	R.DAHKSEVAHRFKDLGEENFKALVLIAF.A	Serum albumin precursor
3283.7031	113.3	R.DAHKSEVAHRFKDLGEENFKALVLIAFAQ.Y	Serum albumin precursor
3446.7408	156	R.DAHKSEVAHRFKDLGEENFKALVLIAFAQY.L	Serum albumin precursor
3559.8010	46.3	R.DAHKSEVAHRFKDLGEENFKALVLIAFAQYL.Q	Serum albumin precursor
1588.8558	58.7	D.PDRFRPDGLPKKY.-	Serum amyloid A-4 protein
1437.7793	43.2	E.TPSAAALAAARVELP.G	Solute carrier family 12 member 2
1856.9203	120.6	L.LSPYSYSTTAVVTNPKE.-	Transthyretin
1969.9945	93.2	A.LLSPYSYSTTAVVTNPKE.-	Transthyretin
2041.0344	167	A.ALLSPYSYSTTAVVTNPKE.-	Transthyretin
2697.3925	50	A.GPTGTGESKCPLMVKVLDAVRGSPAIN.V	Transthyretin
3042.5575	90	D.SGPRRYTIAALLSPYSYSTTAVVTNPKE.-	Transthyretin
3443.8026	61.4	F.TANDSGPRRYTIAALLSPYSYSTTAVVTNPKE.-	Transthyretin

Peptide/Protein Identifications from Ionophore Experiments

m/z	Scores	Sequence	Protein
1286.63	36.6	G.DDAPRAVFPSIV.G	Actin, cytoplasmic 1
2215.01	58.1	K.DLYANTVLSGGTTMYPGIADR.M	Actin, cytoplasmic 1
1686.83	36.2	P.EEHPVLLTEAPLNPK.A	Actin, cytoplasmic 1
1198.68	38.5	R.AVFPSIVGRPR.H	Actin, cytoplasmic 1
1912.85	32.6	V.GMGQKDSYVGDEAQSKRG.I	Actin, cytoplasmic 1
2240.07	55.8	V.GMGQKDSYVGDEAQSKRGILT.L	Actin, cytoplasmic 1
1675.84	35.6	A.GFAGDDAPRAVFPSIVG.R	Actin, cytoplasmic 1
1275.67	47.7	N.ELRVAPEEHPV.L	Actin, cytoplasmic 1
1954.07	114.1	R.VAPEEHPVLLTEAPLNPK.A	Actin, cytoplasmic 1
1309.65	41.4	V.SLGSPSGEVSHPR.K	Alpha-2-HS-glycoprotein
1538.78	34.8	V.SLGSPSGEVSHPRKT.R	Alpha-2-HS-glycoprotein
1538.82	81.6	V.SLGSPSGEVSHPRKT.R	Alpha-2-HS-glycoprotein
2110.02	52.4	K.LHTEAQIQEEGTVVELTGR.Q	Alpha-2-macroglobulin
1661.80	54	M.HGPEGLRVGFYESDV.M	Alpha-2-macroglobulin
1047.47	33.2	E.AGDNGMEQIL.W	Alpha-actinin-4
2032.96	53.9	K.FTASAGIQVVGDDLTVTNPK.R	Alpha-enolase -
1964.12	53.5	L.SEKAKPALEDLRQGLLPV.L	Apolipoprotein A-I
1853.89	39.3	Q.DEPPQSPWDRVKDLAT.V	Apolipoprotein A-I
1555.79	35.4	S.FLSALEEYTKKLN.T	Apolipoprotein A-I
1784.88	32.8	S.FLSALEEYTKKLNTQ.-	Apolipoprotein A-I
2575.25	127.1	V.LESFKVSFLSALEEYTKKLNTQ.-	Apolipoprotein A-I
1642.80	25.8	V.SFLSALEEYTKKLN.T	Apolipoprotein A-I
1743.86	50.2	V.SFLSALEEYTKKLNT.Q	Apolipoprotein A-I
1871.92	47.3	V.SFLSALEEYTKKLNTQ.-	Apolipoprotein A-I
1871.96	80.6	V.SFLSALEEYTKKLNTQ.-	Apolipoprotein A-I
2048.01	51.7	V.LKPEEEAPAPEVGASKPEGI.D	Vitronectin
2048.02	115.4	V.LKPEEEAPAPEVGASKPEGI.D	Vitronectin
1672.83	48.8	A.NTQPRGPPASSPAPAPK.F	Zyxin
3340.64	95.5	E.EEIFPSPPPPPEEEGGPEAPIPPPPQPREKV.S	Zyxin
1760.95	39.1	F.HVQPQPQPKPQVQLH.V	Zyxin
2203.16	61.2	F.HVQPQPQPKPQVQLHVQSQ.T	Zyxin
2304.18	98	F.HVQPQPQPKPQVQLHVQSQT.Q	Zyxin
2809.36	37.9	I.DLEIDSLSSLLDDMTKNDPFKARVS.S	Zyxin
2120.01	34.3	K.FSPGAPGGSGSQPNQKLGHPEA.L	Zyxin
1704.80	30.9	K.VNPFRPGDSEPPPAPGA.Q	Zyxin
1832.87	36.7	K.VNPFRPGDSEPPPAPGAQ.R	Zyxin
2060.00	54.1	K.VNPFRPGDSEPPPAPGAQRA.Q	Zyxin
1743.87	32.7	L.ANTQPRGPPASSPAPAPK.F	Zyxin
2174.09	59.4	L.ANTQPRGPPASSPAPAPKFSPV.T	Zyxin
1989.01	45.1	N.TQPRGPPASSPAPAPKFSPV.T	Zyxin
2361.18	41.4	S.KFSPGAPGGSGSQPNQKLGHPEAL.S	Zyxin
2287.21	66.6	S.LANTQPRGPPASSPAPAPKFSPV.T	Zyxin
1921.99	32.1	V.RSPGAPGPLTLKEVEELE.Q	Zyxin
2211.01	50.2	V.GGPSLTSDLQAQSKGNPEQTPV.L	Vitronectin
2211.05	82.2	V.GGPSLTSDLQAQSKGNPEQTPV.L	Vitronectin
1611.75	31.9	S.DLQAQSKGNPEQTPV.L	Vitronectin
1843.93	49.6	V.IIEGDLERTEERAELA.E	Tropomyosin alpha-3 chain
1765.83	31.7	T.KESSSHHPGIAEFPSR.G	Fibrinogen alpha chain
1822.86	31.7	T.KESSSHHPGIAEFPSRG.K	Fibrinogen alpha chain
1822.88	101.3	T.KESSSHHPGIAEFPSRG.K	Fibrinogen alpha chain
1950.95	47	T.KESSSHHPGIAEFPSRGK.S	Fibrinogen alpha chain
1950.97	123.9	T.KESSSHHPGIAEFPSRGK.S	Fibrinogen alpha chain
2212.04	47.7	T.KESSSHHPGIAEFPSRGKSSS.Y	Fibrinogen alpha chain
2125.01	61.8	T.KESSSHHPGIAEFPSRGKSS.S	Fibrinogen alpha chain
2125.06	136.3	T.KESSSHHPGIAEFPSRGKSS.S	Fibrinogen alpha chain
1728.82	31.7	T.ESRGSESGIFTNTKES.S	Fibrinogen alpha chain
1474.72	104.8	T.FPGFFSPMLGEFV.S	Fibrinogen alpha chain
1760.79	35.7	T.GKTFPGFFSPMLGEFV.S	Fibrinogen alpha chain
2585.11	100.4	S.YKMADEAGSEADHEGTHSTKRGHA.K	Fibrinogen alpha chain
2585.15	57.2	S.YKMADEAGSEADHEGTHSTKRGHA.K	Fibrinogen alpha chain
3152.44	50.5	S.YKMADEAGSEADHEGTHSTKRGHAKSRPV.R	Fibrinogen alpha chain
1553.69	68.7	S.YNRGDSTFESKSY.K	Fibrinogen alpha chain
1812.81	71.7	S.YNRGDSTFESKSYKM.A	Fibrinogen alpha chain
1883.87	133.3	S.YNRGDSTFESKSYKMA.D	Fibrinogen alpha chain
2292.00	53.3	S.YSKQFTSSTSYNRGDSTFES.K	Fibrinogen alpha chain
2507.12	48.6	S.YSKQFTSSTSYNRGDSTFESKS.Y	Fibrinogen alpha chain
1536.65	62.9	T.ADSGEGDFLAEGGGVR.G	Fibrinogen alpha chain
1536.69	75.4	T.ADSGEGDFLAEGGGVR.G	Fibrinogen alpha chain
2158.97	92.7	S.STSYNRGDSTFESKSYKMA.D	Fibrinogen alpha chain
2507.05	56.6	S.SVSGSTGQWHSESGSFRPDSPGSGN.A	Fibrinogen alpha chain
2379.03	48.5	S.SYSKQFTSSTSYNRGDSTFES.K	Fibrinogen alpha chain
2594.18	31.2	S.SYSKQFTSSTSYNRGDSTFESKS.Y	Fibrinogen alpha chain
3016.31	55.4	S.SYSKQFTSSTSYNRGDSTFESKSYKM.A	Fibrinogen alpha chain
3087.36	55	S.SYSKQFTSSTSYNRGDSTFESKSYKMA.D	Fibrinogen alpha chain
1001.52	58.1	S.TGKTFPGFF.S	Fibrinogen alpha chain
1316.64	36.6	S.TGKTFPGFFSPM.L	Fibrinogen alpha chain
1861.91	105.2	S.TGKTFPGFFSPMLGEFV.S	Fibrinogen alpha chain
2045.01	123.7	T.ADSGEGDFLAEGGGVRGPRVV.E	Fibrinogen alpha chain
2019.98	109.5	T.ASTGKTFPGFFSPMLGEFV.S	Fibrinogen alpha chain
2466.02	97.4	S.SSYSKQFTSSTSYNRGDSTFES.K	Fibrinogen alpha chain
2681.20	51.9	S.SSYSKQFTSSTSYNRGDSTFESKS.Y	Fibrinogen alpha chain
3103.41	49.4	S.SSYSKQFTSSTSYNRGDSTFESKSYKM.A	Fibrinogen alpha chain
3174.40	47.8	S.SSYSKQFTSSTSYNRGDSTFESKSYKMA.D	Fibrinogen alpha chain
1665.74	39.6	S.STSYNRGDSTFESKS.Y	Fibrinogen alpha chain
1828.80	68.5	S.STSYNRGDSTFESKSY.K	Fibrinogen alpha chain
2087.96	73.7	S.STSYNRGDSTFESKSYKM.A	Fibrinogen alpha chain
2897.35	99.2	S.SSHHPGIAEFPSRGKSSSYSKQFTSST.S	Fibrinogen alpha chain
2622.17	102.5	S.SSHHPGIAEFPSRGKSSSYSKQFT.S	Fibrinogen alpha chain
2622.23	85	S.SSHHPGIAEFPSRGKSSSYSKQFT.S	Fibrinogen alpha chain
1780.86	33	S.SSHHPGIAEFPSRGKSS.S	Fibrinogen alpha chain
1780.90	97.2	S.SSHHPGIAEFPSRGKSS.S	Fibrinogen alpha chain
1867.85	36.5	S.SSHHPGIAEFPSRGKSSS.Y	Fibrinogen alpha chain
2117.96	71	S.SSHHPGIAEFPSRGKSSSYS.K	Fibrinogen alpha chain
2117.98	56.2	S.SSHHPGIAEFPSRGKSSSYS.K	Fibrinogen alpha chain

2380.23	60.4	E.KTIDDLEEKLAQAKEENVGLH.Q	Tropomyosin alpha-4 chain	1265.58	62.8	S.SSHHPGIAEFPS.R	Fibrinogen alpha chain
2072.02	33.5	V.ILEGELERAEERAEVSEL.K	Tropomyosin alpha-4 chain	1265.61	40.9	S.SSHHPGIAEFPS.R	Fibrinogen alpha chain
2714.20	124.4	D.AKAVLEEDEEVTEEAEMEPEDKGH.-	Tubulin beta-1 chain	1421.70	35.1	S.SSHHPGIAEFPSR.G	Fibrinogen alpha chain
2515.06	90.3	K.AVLEEDEEVTEEAEMEPEDKGH.-	Tubulin beta-1 chain	1478.68	75.5	S.SSHHPGIAEFPSRG.K	Fibrinogen alpha chain
2231.83	78.8	L.EEDEEVTEEAEMEPEDKGH.-	Tubulin beta-1 chain	1478.71	83.3	S.SSHHPGIAEFPSRG.K	Fibrinogen alpha chain
2231.88	126.1	L.EEDEEVTEEAEMEPEDKGH.-	Tubulin beta-1 chain	1693.86	63.6	S.SSHHPGIAEFPSRGKS.S	Fibrinogen alpha chain
3739.62	79.2	V.SEYQQFQDAKAVLEEDEEVTEEAEMEPEDKGH.-	Tubulin beta-1 chain	2535.20	59.2	S.SHHPGIAEFPSRGKSSSYSKQFT.S	Fibrinogen alpha chain
2040.01	86	R.EANLQALIATGGDINAAIER.L	Ubiquilin-1	2535.20	114.1	S.SHHPGIAEFPSRGKSSSYSKQFT.S	Fibrinogen alpha chain
2353.10	58.9	G.EKTPKDESANQEEPEARVPAQ.S	Vasodilator-stimulated phosphoprotein	1304.65	62.7	S.HHPGIAEFPSRG.K	Fibrinogen alpha chain
2353.11	54	G.EKTPKDESANQEEPEARVPAQ.S	Vasodilator-stimulated phosphoprotein	1943.91	47.2	S.HHPGIAEFPSRGKSSSYS.K	Fibrinogen alpha chain
2497.18	63.1	R.LLQDSVDFSLADAINTEFKNTR.T	Vimentin	1178.54	55.4	S.SHHPGIAEFPS.R	Fibrinogen alpha chain
1134.54	32	I.IESPSTSLSVD.L	Stromal interaction molecule 2	1178.57	51.5	S.SHHPGIAEFPS.R	Fibrinogen alpha chain
1398.70	31.3	A.QISPEGRAAMEPI.V	Talin-1	1391.66	52.3	S.SHHPGIAEFPSRG.K	Fibrinogen alpha chain
2846.35	32.2	E.AVDNLSAFASNPEFSSIPAQISPEGRAA.M	Talin-1	1391.68	80.5	S.SHHPGIAEFPSRG.K	Fibrinogen alpha chain
2113.04	42.8	E.KNPLPSKETIEQEKQAGES.-	Thymosin beta-4	1519.78	63.8	S.SHHPGIAEFPSRGK.S	Fibrinogen alpha chain
2701.23	54.3	K.TETQEKNPLPSKETIEQEKQAGES.-	Thymosin beta-4	2030.94	72.7	S.SHHPGIAEFPSRGKSSSYS.K	Fibrinogen alpha chain
2113.07	107.8	E.KNPLPSKETIEQEKQAGES.-	Thymosin beta-4-like protein 6	2810.31	73.7	S.SHHPGIAEFPSRGKSSSYSKQFTSST.S	Fibrinogen alpha chain
2946.65	172.5	I.EKFDKSKLKKTETQEKNPLPSKETI.E	Thymosin beta-4-like protein 6	1606.82	58.9	S.SHHPGIAEFPSRGKS.S	Fibrinogen alpha chain
3933.12	175.2	I.EKFDKSKLKKTETQEKNPLPSKETIEQEKQAGES.-	Thymosin beta-4-like protein 6	933.47	43.4	P.GIAEFPSRG.K	Fibrinogen alpha chain
2829.37	136.4	K.KTETQEKNPLPSKETIEQEKQAGES.-	Thymosin beta-4-like protein 6	1572.74	30.1	P.GIAEFPSRGKSSSYS.K	Fibrinogen alpha chain
2701.28	126	K.TETQEKNPLPSKETIEQEKQAGES.-	Thymosin beta-4-like protein 6	2076.98	55	P.GIAEFPSRGKSSSYSKQFT.S	Fibrinogen alpha chain
3198.63	132.3	S.KLKKTETQEKNPLPSKETIEQEKQAGES.-	Thymosin beta-4-like protein 6	2077.03	62.2	P.GIAEFPSRGKSSSYSKQFT.S	Fibrinogen alpha chain
1613.82	66.7	T.ETQEKNPLPSKETI.E	Thymosin beta-4-like protein 6	1450.65	30.1	R.GDSTFESKSYKMA.D	Fibrinogen alpha chain
2600.24	119	T.ETQEKNPLPSKETIEQEKQAGES.-	Thymosin beta-4-like protein 6	1870.78	86.6	R.GGSTSYGTGSETESPRNPS.S	Fibrinogen alpha chain
2098.02	93.3	K.TLFELAAESDVSTAIDLFR.Q	Transforming growth factor-beta-induced protein ig-h3	2603.11	100.6	R.GSESGIFTNTKESSSHHPGIAEFPS.R	Fibrinogen alpha chain
2121.92	59.7	G.SYALTSEEAERSDGDPVQPA.V	Serum deprivation-response protein	2816.30	37.9	R.GSESGIFTNTKESSSHHPGIAEFPSRG.K	Fibrinogen alpha chain
2121.94	42.2	G.SYALTSEEAERSDGDPVQPA.V	Serum deprivation-response protein	2944.39	42.7	R.GSESGIFTNTKESSSHHPGIAEFPSRGK.S	Fibrinogen alpha chain
2471.08	79.7	R.YEGSYALTSEEAERSDGDPVQPA.V	Serum deprivation-response protein	1220.48	33.7	R.HPDEAAFFDTA.S	Fibrinogen alpha chain
3363.55	65	R.YEGSYALTSEEAERSDGDPVQPAVLQVHQTS.-	Serum deprivation-response protein	1442.61	36.1	R.HRHPDEAAFFDT.A	Fibrinogen alpha chain
2524.24	76.4	S.GAVEGKEELPDENKSLEETLHTV.D	Serum deprivation-response protein	1442.64	36.4	R.HRHPDEAAFFDT.A	Fibrinogen alpha chain
1871.83	54.4	Y.ALTSEEAERSDGDPVQPA.V	Serum deprivation-response protein	1399.62	48.4	S.ETESRGSESGIFT.N	Fibrinogen alpha chain
1871.85	40	Y.ALTSEEAERSDGDPVQPA.V	Serum deprivation-response protein	1399.63	64.7	S.ETESRGSESGIFT.N	Fibrinogen alpha chain
1623.75	61.6	K.DVFLGMFLYEYAR.R	Serum albumin precursor	1614.70	34.2	S.ETESRGSESGIFTNT.K	Fibrinogen alpha chain
1639.88	39.3	K.KVPQVSTPTLVEVSR.N	Serum albumin precursor	1614.73	34.1	S.ETESRGSESGIFTNT.K	Fibrinogen alpha chain
2753.38	62.5	R.DAHKSEVAHRFKDLGEENFKALVL.I	Serum albumin	1958.87	30.9	S.ETESRGSESGIFTNTKES.S	Fibrinogen alpha chain
1184.68	32.2	I.LPNVATLGRMI.L	Rab GDP dissociation inhibitor beta	2646.14	47.1	S.FRPDSPGSGNARPNNPDWGTFEEV.S	Fibrinogen alpha chain
2603.11	101.4	R.SLDRNLPSDSQDLGQHGLEEDFM.L	Serglycin	1263.56	76	S.GEGDFLAEGGGVR.G	Fibrinogen alpha chain
2716.18	45	R.SLDRNLPSDSQDLGQHGLEEDFML.-	Serglycin	2233.89	78.5	S.GSTGQWHSESGSFRPDSPGSGN.A	Fibrinogen alpha chain
1359.66	31.9	E.EGIGCAARGGATPLS.Y	Serine/threonine-protein phosphatase 6 regulatory subunit 1	1091.53	44.3	S.HHPGIAEFPS.R	Fibrinogen alpha chain
1152.61	43.9	K.DDNPNLPRLV.R	Serum albumin	1304.62	66.4	S.HHPGIAEFPSRG.K	Fibrinogen alpha chain
1681.82	109.6	R.NLAKGKEESLDSDLY.A	Platelet basic protein	2031.92	57.4	M.LGEFVSETESRGSESGIFT.N	Fibrinogen alpha chain
2177.10	55.9	R.QVTITGSAASISLAQYLINAR.L	Poly(rC)-binding protein 1	2247.00	56.2	M.LGEFVSETESRGSESGIFTNT.K	Fibrinogen alpha chain
1675.84	35.6	A.GFAGDDAPRAVFPSIVG.R	P	2591.18	37.3	M.LGEFVSETESRGSESGIFTNTKES.S	Fibrinogen alpha chain
1275.67	47.7	N.ELRVAPEEHPV.L	P	2591.18	81.2	M.LGEFVSETESRGSESGIFTNTKES.S	Fibrinogen alpha chain
3611.67	42.6	T.MDDDTAVLVIDNGSGMCKAGFAGDDAPRAVFPSIVG.R	P	1193.45	32	N.NPDWGTFEEV.S	Fibrinogen alpha chain
3723.13	99.7	K.LAADEDDDDDEEDDDEDDDDDDFDDEEAEEK.A	Nucleophosmin	2945.39	34.7	M.DLGTLSGIGTLDGFRHRHPDEAAFFDT.A	Fibrinogen alpha chain
1441.76	30.3	I.DLQGPGPWGFRLV.G	PDZ and LIM domain protein 1	1370.67	30	M.ELERPGGNEITR.G	Fibrinogen alpha chain
2346.14	38.1	L.QEILESEEKGDPNKPSGFRSV.K	PDZ and LIM domain protein 1	1554.73	47.1	L.DGFRHRHPDEAAF.F	Fibrinogen alpha chain
2218.07	93.8	Q.EILESEEKGDPNKPSGFRSV.K	PDZ and LIM domain protein 1	1917.84	56.8	L.DGFRHRHPDEAAFFDT.A	Fibrinogen alpha chain
2719.35	108.1	T.SFLVLQEILESEEKGDPNKPSGFR.S	PDZ and LIM domain protein 1	1918.87	45.7	L.GEFVSETESRGSESGIFT.N	Fibrinogen alpha chain

2905.45	38.9	T.SFLVLQEILESEEKGDPNKPSGFRSV.K	PDZ and LIM domain protein 1	2162.91	94	M.ADEAGSEADHEGTHSTKRGHA.K	Fibrinogen alpha chain
2631.26	67.3	G.TEFMQDPDEEHLKKSSQVPRTE.A	PDZ and LIM domain protein 7	2730.20	84.6	M.ADEAGSEADHEGTHSTKRGHAKSRPV.R	Fibrinogen alpha chain
3045.48	54	Q.AEKKKMQQNIQELEEQLEEEESARQ.K	Myosin-9	2127.91	40.8	I.TRGGSTSYGTGSETESPRNPS.S	Fibrinogen alpha chain
3414.71	59.6	Q.AEKKKMQQNIQELEEQLEEEESARQKLQ.L	Myosin-9	1481.65	39.1	K.ESSSHHPGIAEFPS.R	Fibrinogen alpha chain
1842.90	31.5	E.KSQEDQENPLRSLNAN.E	Mitotic spindle assembly checkpoint protein MAD1	1481.68	62.8	K.ESSSHHPGIAEFPS.R	Fibrinogen alpha chain
1230.61	33.8	S.EVTWNITVPDG.F	Mannan-binding lectin serine protease 1	1637.73	41	K.ESSSHHPGIAEFPSR.G	Fibrinogen alpha chain
2212.12	70.9	V.SRIDGPTGQKTKEAQPGQSQV.S	Latent-transforming growth factor beta-binding protein 1	1637.76	48.3	K.ESSSHHPGIAEFPSR.G	Fibrinogen alpha chain
2054.04	52.9	K.ILTATVDNANVLLQIDNAR.L	Keratin, type I cytoskeletal 14	1694.79	116.5	K.ESSSHHPGIAEFPSRG.K	Fibrinogen alpha chain
2068.09	61.2	K.ILTATVDNANILLQIDNAR.L	Keratin, type I cytoskeletal 17	1909.93	68.1	K.ESSSHHPGIAEFPSRGKS.S	Fibrinogen alpha chain
2392.11	71.9	R.GLGVGFGSGGGSSSSVKFVSTTSSSR.K	Keratin, type II cytoskeletal 5	1996.92	42.7	K.ESSSHHPGIAEFPSRGKSS.S	Fibrinogen alpha chain
2520.22	110	R.GLGVGFGSGGGSSSSVKFVSTTSSSRK.S	Keratin, type II cytoskeletal 5	1996.98	64.2	K.ESSSHHPGIAEFPSRGKSS.S	Fibrinogen alpha chain
2646.26	95.7	R.QSSVSFRSGGSRSFSTASAITPSVSR.T	Keratin, type II cytoskeletal 5	2083.94	54.2	K.ESSSHHPGIAEFPSRGKSSS.Y	Fibrinogen alpha chain
2359.11	51.4	R.AEAESWYQTKYEELQVTAGR.H	Keratin, type II cytoskeletal 6C	2083.95	32.2	K.ESSSHHPGIAEFPSRGKSSS.Y	Fibrinogen alpha chain
2418.21	69.7	R.AIGGGLSSVGGGSSTIKYTTTSSSSR.K	Keratin, type II cytoskeletal 6C	1359.75	49.8	K.GDKELRTGKEKV.T	Fibrinogen alpha chain
2546.26	126.5	R.AIGGGLSSVGGGSSTIKYTTTSSSSRK.S	Keratin, type II cytoskeletal 6C	1460.79	57.6	K.GDKELRTGKEKVT.S	Fibrinogen alpha chain
1705.74	30.4	G.HGHEQQHGLGHGHKF.K	Kininogen-1	2028.85	49.1	K.MADEAGSEADHEGTHSTKR.G	Fibrinogen alpha chain
2069.94	47.7	G.HGLGHGHEQQHGLGHGHKF.K	Kininogen-1	2293.95	78.5	K.MADEAGSEADHEGTHSTKRGHA.K	Fibrinogen alpha chain
1943.83	45.4	H.NLGHGHKHERDQGHGHQ.R	Kininogen-1	2861.30	105.7	K.MADEAGSEADHEGTHSTKRGHAKSRPV.R	Fibrinogen alpha chain
904.45	44.8	K.RPPGFSPF.R	Kininogen-1	1913.82	58.3	K.QFTSSTSYNRGDSTFES.K	Fibrinogen alpha chain
1655.81	45	S.SRQLGLPGPPDVPDHA.A	Inter-alpha-trypsin inhibitor heavy chain H4	2553.05	128.7	K.SSSYSKQFTSSTSYNRGDSTFES.K	Fibrinogen alpha chain
1655.84	49.6	S.SRQLGLPGPPDVPDHA.A	Inter-alpha-trypsin inhibitor heavy chain H4	2553.10	55.1	K.SSSYSKQFTSSTSYNRGDSTFES.K	Fibrinogen alpha chain
1726.84	43.1	S.SRQLGLPGPPDVPDHAA.Y	Inter-alpha-trypsin inhibitor heavy chain H4	3190.46	36.7	K.SSSYSKQFTSSTSYNRGDSTFESKSYKM.A	Fibrinogen alpha chain
2271.07	51.4	S.SRQLGLPGPPDVPDHAAYHPF.R	Inter-alpha-trypsin inhibitor heavy chain H4	2122.83	101.4	K.SYKMADEAGSEADHEGTHST.K	Fibrinogen alpha chain
1568.78	41.4	S.RQLGLPGPPDVPDHA.A	Inter-alpha-trypsin inhibitor heavy chain H4	2122.86	145.2	K.SYKMADEAGSEADHEGTHST.K	Fibrinogen alpha chain
1639.79	34	S.RQLGLPGPPDVPDHAA.Y	Inter-alpha-trypsin inhibitor heavy chain H4	2250.92	50.2	K.SYKMADEAGSEADHEGTHSTK.R	Fibrinogen alpha chain
2184.03	37.9	S.RQLGLPGPPDVPDHAAYHPF.R	Inter-alpha-trypsin inhibitor heavy chain H4	2250.94	68.3	K.SYKMADEAGSEADHEGTHSTK.R	Fibrinogen alpha chain
2526.27	39.4	M.NFRPGVLSSRQLGLPGPPDVPDHA.A	Inter-alpha-trypsin inhibitor heavy chain H4	2464.03	70.4	K.SYKMADEAGSEADHEGTHSTKRG.H	Fibrinogen alpha chain
2012.00	40.4	P.GVLSSRQLGLPGPPDVPDHA.A	Inter-alpha-trypsin inhibitor heavy chain H4	2464.05	47.1	K.SYKMADEAGSEADHEGTHSTKRG.H	Fibrinogen alpha chain
2083.02	30.6	P.GVLSSRQLGLPGPPDVPDHAA.Y	Inter-alpha-trypsin inhibitor heavy chain H4	2601.11	80.2	K.SYKMADEAGSEADHEGTHSTKRGH.A	Fibrinogen alpha chain
2627.25	37.9	P.GVLSSRQLGLPGPPDVPDHAAYHPF.R	Inter-alpha-trypsin inhibitor heavy chain H4	2672.08	132.4	K.SYKMADEAGSEADHEGTHSTKRGHA.K	Fibrinogen alpha chain
2657.26	79.2	R.MNFRPGVLSSRQLGLPGPPDVPDHA.A	Inter-alpha-trypsin inhibitor heavy chain H4	2672.13	134	K.SYKMADEAGSEADHEGTHSTKRGHA.K	Fibrinogen alpha chain
2582.22	63.1	R.NVHSGSTFFKYYLQGAKIPKPEA.S	Inter-alpha-trypsin inhibitor heavy chain H4	1707.93	77.2	K.TVIGPDGHKEVTKEVV.T	Fibrinogen alpha chain
2109.04	40.7	R.PGVLSSRQLGLPGPPDVPDHA.A	Inter-alpha-trypsin inhibitor heavy chain H4	1336.60	38.5	L.DGFRHRHPDEA.A	Fibrinogen alpha chain
2724.30	83.7	R.PGVLSSRQLGLPGPPDVPDHAAYHPF.R	Inter-alpha-trypsin inhibitor heavy chain H4	1336.61	39.8	L.DGFRHRHPDEA.A	Fibrinogen alpha chain
1412.67	54	R.QLGLPGPPDVPDHA.A	Inter-alpha-trypsin inhibitor heavy chain H4	1550.76	35.7	G.TLDGFRHRHPDEA.A	Fibrinogen alpha chain
1483.70	31.6	R.QLGLPGPPDVPDHAA.Y	Inter-alpha-trypsin inhibitor heavy chain H4	954.45	36.2	H.HPGIAEFPS.R	Fibrinogen alpha chain
2027.92	33.1	R.QLGLPGPPDVPDHAAYHPF.R	Inter-alpha-trypsin inhibitor heavy chain H4	1110.55	33.2	H.HPGIAEFPSR.G	Fibrinogen alpha chain
1742.88	59.4	L.SSRQLGLPGPPDVPDHA.A	Inter-alpha-trypsin inhibitor heavy chain H4	1167.58	52.2	H.HPGIAEFPSRG.K	Fibrinogen alpha chain
1100.51	52.1	L.GLPGPPDVPDH.A	Inter-alpha-trypsin inhibitor heavy chain H4	1480.64	33.1	H.SESGSFRPDSPGSGN.A	Fibrinogen alpha chain
1171.56	79	L.GLPGPPDVPDHA.A	Inter-alpha-trypsin inhibitor heavy chain H4	2736.13	54.1	H.SESGSFRPDSPGSGNARPNNPDWGTF.E	Fibrinogen alpha chain
1242.59	39.2	L.GLPGPPDVPDHAA.Y	Inter-alpha-trypsin inhibitor heavy chain H4	2736.17	66.1	H.SESGSFRPDSPGSGNARPNNPDWGTF.E	Fibrinogen alpha chain
1954.99	32.8	G.VLSSRQLGLPGPPDVPDHA.A	Inter-alpha-trypsin inhibitor heavy chain H4	3093.32	57.7	H.SESGSFRPDSPGSGNARPNNPDWGTFEEV.S	Fibrinogen alpha chain
2570.23	39.1	G.VLSSRQLGLPGPPDVPDHAAYHPF.R	Inter-alpha-trypsin inhibitor heavy chain H4	1906.92	86.4	I.AEFPSRGKSSSYSKQFT.S	Fibrinogen alpha chain
3836.77	33	Q.PPVEEEDEHFDDTVVCLDTYNCDLHFKISRDR.L	Heterogeneous nuclear ribonucleoprotein U	2182.02	30.8	I.AEFPSRGKSSSYSKQFTSST.S	Fibrinogen alpha chain
3877.28	169.4	K.KKEEEEDEEDEEDEEEEEDEEDEDEEEDDDD.E	High mobility group protein B1	1077.52	49.7	E.GDFLAEGGGVR.G	Fibrinogen alpha chain
4005.35	196	K.KKKEEEEDEEDEEDEEEEEDEEDEDEEEDDDD.E	High mobility group protein B1	1352.61	45.2	E.SSSHHPGIAEFPS.R	Fibrinogen alpha chain
1946.01	81.3	A.VLEYLTAEILELAGNAAR.D	Histone H2A type 1-H	1690.80	45.7	F.DTASTGKTFPGFFSPM.L	Fibrinogen alpha chain
2431.28	30.8	A.VLEYLTAEILELAGNAARDNKK.T	Histone H2A type 1-H	1816.82	47.7	F.EEVSGNVSPGTRREYH.T	Fibrinogen alpha chain
1359.67	36.6	W.EPNKVSSNSGMLP.N	Histone-lysine N-methyltransferase MLL	2046.92	40.1	F.EEVSGNVSPGTRREYHTE.K	Fibrinogen alpha chain
1917.87	39.6	A.GEYGAEALERMFLSFPT.T	Haemoglobin subunit alpha	2488.24	39.7	F.EEVSGNVSPGTRREYHTEKLVT.S	Fibrinogen alpha chain

2125.92	43.3	A.HAGEYGAEALERMFLSFPT.T	Haemoglobin subunit alpha	2467.04	85.4	F.ESKSYKMADEAGSEADHEGTHST.K	Fibrinogen alpha chain
2015.05	60.4	A.SLDKFLASVSTVLTSKYR.-	Haemoglobin subunit alpha	3016.30	136.4	F.ESKSYKMADEAGSEADHEGTHSTKRGHA.K	Fibrinogen alpha chain
1502.68	31.9	A.WGKVGAHAGEYGAEA.L	Haemoglobin subunit alpha	3583.65	103.7	F.ESKSYKMADEAGSEADHEGTHSTKRGHAKSRPV.R	Fibrinogen alpha chain
1833.86	48.2	K.TYFPHFDLSHGSAQVK.G	Haemoglobin subunit alpha	1228.59	32.9	F.FDTASTGKTFPG.F	Fibrinogen alpha chain
1399.76	30.5	S.DLHAHKLRVDPV.N	Haemoglobin subunit alpha	2383.11	68.1	F.FDTASTGKTFPGFFSPMLGEFV.S	Fibrinogen alpha chain
1947.91	51.5	V.DDMPNALSALSDLHAHKL.R	Haemoglobin subunit alpha	2691.16	30	F.TNTKESSSHHPGIAEFPSRGKSSSY.S	Fibrinogen alpha chain
2514.23	35.3	V.DDMPNALSALSDLHAHKLRVDPV.N	Haemoglobin subunit alpha	1020.50	67.5	G.DFLAEGGGVR.G	Fibrinogen alpha chain
1437.73	41.2	V.TLAAHLPAEFTPAV.H	Haemoglobin subunit alpha	1206.55	93.9	G.EGDFLAEGGGVR.G	Fibrinogen alpha chain
1645.82	34.3	V.TLAAHLPAEFTPAVHA.S	Haemoglobin subunit alpha	1206.56	62.5	G.EGDFLAEGGGVR.G	Fibrinogen alpha chain
2606.27	52.8	V.TLAAHLPAEFTPAVHASLDKFLASV.S	Haemoglobin subunit alpha	1516.73	37.9	G.EGDFLAEGGGVRGPR.V	Fibrinogen alpha chain
1441.64	41	Y.FPHFDLSHGSAQV.K	Haemoglobin subunit alpha	1350.59	69.3	D.SGEGDFLAEGGGVR.G	Fibrinogen alpha chain
1705.78	38.8	A.FSDGLAHLDNLKGTFA.T	Haemoglobin subunit beta	1350.63	37.1	D.SGEGDFLAEGGGVR.G	Fibrinogen alpha chain
1423.69	42.7	A.HHFGKEFTPPVQ.A	Haemoglobin subunit beta	1403.67	57.4	A.STGKTFPGFFSPM.L	Fibrinogen alpha chain
1212.66	38.3	D.EVGGEALGRLLV.V	Haemoglobin subunit beta	1948.94	114.6	A.STGKTFPGFFSPMLGEFV.S	Fibrinogen alpha chain
1286.63	63.2	H.HFGKEFTPPVQ.A	Haemoglobin subunit beta	1560.67	30	A.RPNNPDWGTFEEV.S	Fibrinogen alpha chain
2178.12	38.3	M.VHLTPEEKSAVTALWGKVNV.D	Haemoglobin subunit beta	1088.54	51.6	A.STGKTFPGFF.S	Fibrinogen alpha chain
2521.24	75.8	M.VHLTPEEKSAVTALWGKVNVDEV.G	Haemoglobin subunit beta	1272.63	60.9	A.STGKTFPGFFSP.M	Fibrinogen alpha chain
1327.68	51.5	V.DEVGGEALGRLLV.V	Haemoglobin subunit beta	1883.76	46.2	A.DEAGSEADHEGTHSTKRG.H	Fibrinogen alpha chain
1328.66	42.1	V.NVDEVGGEALGRL.L	Haemoglobin subunit beta	2091.88	95.8	A.DEAGSEADHEGTHSTKRGHA.K	Fibrinogen alpha chain
1441.72	45.5	V.NVDEVGGEALGRLL.V	Haemoglobin subunit beta	2659.16	132	A.DEAGSEADHEGTHSTKRGHAKSRPV.R	Fibrinogen alpha chain
1540.78	64.1	V.NVDEVGGEALGRLLV.V	Haemoglobin subunit beta	1465.62	76.2	A.DSGEGDFLAEGGGVR.G	Fibrinogen alpha chain
2296.21	42.7	V.TALWGKVNVDEVGGEALGRLLV.V	Haemoglobin subunit beta	1465.63	133.2	A.DSGEGDFLAEGGGVR.G	Fibrinogen alpha chain
1350.70	67.4	V.VAGVANALAHKYH.-	Haemoglobin subunit beta	1619.74	61	A.DSGEGDFLAEGGGVRGP.R	Fibrinogen alpha chain
1327.73	31.4	V.DEVGGEALGRLLV.V	Haemoglobin subunit beta	1775.78	66	A.DSGEGDFLAEGGGVRGPR.V	Fibrinogen alpha chain
1540.84	59.5	V.NVDEVGGEALGRLLV.V	Haemoglobin subunit beta	1775.80	72.1	A.DSGEGDFLAEGGGVRGPR.V	Fibrinogen alpha chain
2276.96	68.2	K.WGDAGAEYVVESTGVFTTMEK.A	Glyceraldehyde-3-phosphate dehydrogenase	1973.96	122.6	A.DSGEGDFLAEGGGVRGPRVV.E	Fibrinogen alpha chain
1299.56	30.5	Y.DNEFGYSNRVV.D	Glyceraldehyde-3-phosphate dehydrogenase	1566.70	30.1	K.DQKAEGDANPVPYY.Y	Cyclin-dependent kinase-like 4
1368.67	54.4	R.DSSRLPSEGPRPA.H	Flavin reductase	2551.12	153.5	R.TLEIPGNSDPNMIPDGDFNSYVR.V	Complement C4-A
1826.70	66.2	T.DEYDGHSTYPSHQYQ.-	Flavin reductase	1896.01	81.8	R.NGFKSHALQLNNRQIR.G	Complement C4-A
1696.76	31.5	V.MPPHIGDQPLTGAYTV.T	Flavin reductase	1896.03	45.4	R.NGFKSHALQLNNRQIR.G	Complement C4-A
2079.04	33.9	K.KREEAPSLRPAPPPISGGGY.R	Fibrinogen beta chain	1739.89	71.5	R.NGFKSHALQLNNRQI.R	Complement C4-A
1950.95	45.4	K.REEAPSLRPAPPPISGGGY.R	Fibrinogen beta chain	2378.18	81.7	K.DDPDAPLQPVTPLQLFEGRRN.R	Complement C4-A
1951.00	40.1	K.REEAPSLRPAPPPISGGGY.R	Fibrinogen beta chain	1626.82	48.7	R.NGFKSHALQLNNRQ.I	Complement C4-A
2502.29	35.7	K.REEAPSLRPAPPPISGGGYRARPA.K	Fibrinogen beta chain	1865.00	44.3	R.SSKITHRIHWESASLL.R	Complement C3
1071.54	39.6	P.APPPISGGGYR.A	Fibrinogen beta chain	2021.11	42.2	R.SSKITHRIHWESASLLR.S	Complement C3
1425.77	44.2	H.RPLDKKREEAPS.L	Fibrinogen beta chain	1671.80	51	R.SYTVAIAGYALAQMGR.L	Complement C3
1776.96	48.1	V.TSKGDKELRTGKEKVT.S	Fibrinogen alpha chain	1219.65	32.2	S.KITHRIHWE.S	Complement C3
1872.71	81.5	Y.KMADEAGSEADHEGTHST.K	Fibrinogen alpha chain	1377.74	49.4	S.KITHRIHWESA.S	Complement C3
2422.04	139	Y.KMADEAGSEADHEGTHSTKRGHA.K	Fibrinogen alpha chain	1464.75	39.6	S.SKITHRIHWESA.S	Complement C3
2989.40	84	Y.KMADEAGSEADHEGTHSTKRGHAKSRPV.R	Fibrinogen alpha chain	1464.77	51.1	S.SKITHRIHWESA.S	Complement C3
1390.60	68.2	Y.NRGDSTFESKSY.K	Fibrinogen alpha chain	1855.82	32.3	R.SEETKENEGFTVTAEGK.G	Complement C3
1390.63	73.2	Y.NRGDSTFESKSY.K	Fibrinogen alpha chain	1551.80	62	R.SSKITHRIHWESA.S	Complement C3
1649.73	94.9	Y.NRGDSTFESKSYKM.A	Fibrinogen alpha chain	942.44	54.3	I.HWESASLL.R	Complement C3
1720.77	110.4	Y.NRGDSTFESKSYKMA.D	Fibrinogen alpha chain	1098.55	72.7	I.HWESASLLR.S	Complement C3
1720.78	59.2	Y.NRGDSTFESKSYKMA.D	Fibrinogen alpha chain	1098.56	57.3	I.HWESASLLR.S	Complement C3
1775.93	35	A.RGHRPLDKKREEAPS.L	Fibrinogen beta chain	1504.75	57	G.SPMYSIITPNILR.L	Complement C3
2320.93	65.4	V.SGSTGQWHSESGSFRPDSPGSGN.A	Fibrinogen alpha chain	1136.56	56.6	I.THRIHWESA.S	Complement C3
2320.98	89.3	V.SGSTGQWHSESGSFRPDSPGSGN.A	Fibrinogen alpha chain	2868.37	92.3	R.EGVQKEDIPPADLSDQVPDTESETRI.L	Complement C3
2391.99	32.4	V.SGSTGQWHSESGSFRPDSPGSGNA.R	Fibrinogen alpha chain	1914.96	39.2	V.AEKALQEYRKKHREE.-	Clusterin
3933.73	36.5	V.SGSTGQWHSESGSFRPDSPGSGNARPNNPDWGTFEEV.S	Fibrinogen alpha chain	1914.99	66.8	V.AEKALQEYRKKHREE.-	Clusterin

2218.14	46.6	V.SGNVSPGTRREYHTEKLVTS.K	Fibrinogen alpha chain
2131.10	53.4	V.SGNVSPGTRREYHTEKLVT.S	Fibrinogen alpha chain
4924.15	44.2	V.SETESRGSESGIFTNTKESSSHHPGIAEFPSRGKSSSYSKQFTSST.S	Fibrinogen alpha chain
3894.77	42.6	V.SETESRGSESGIFTNTKESSSHHPGIAEFPSRGKSSS.Y	Fibrinogen alpha chain
4057.80	66	V.SETESRGSESGIFTNTKESSSHHPGIAEFPSRGKSSSY.S	Fibrinogen alpha chain
3807.78	184.1	V.SETESRGSESGIFTNTKESSSHHPGIAEFPSRGKSS.S	Fibrinogen alpha chain
3720.70	208.5	V.SETESRGSESGIFTNTKESSSHHPGIAEFPSRGKS.S	Fibrinogen alpha chain
2132.94	75	V.SETESRGSESGIFTNTKESS.S	Fibrinogen alpha chain
2132.97	131.5	V.SETESRGSESGIFTNTKESS.S	Fibrinogen alpha chain
2761.18	39.9	V.SETESRGSESGIFTNTKESSSHHPGI.A	Fibrinogen alpha chain
2761.25	104.2	V.SETESRGSESGIFTNTKESSSHHPGI.A	Fibrinogen alpha chain
2832.34	71.4	V.SETESRGSESGIFTNTKESSSHHPGIA.E	Fibrinogen alpha chain
3505.65	187.4	V.SETESRGSESGIFTNTKESSSHHPGIAEFPSRG.K	Fibrinogen alpha chain
3633.64	153.8	V.SETESRGSESGIFTNTKESSSHHPGIAEFPSRGK.S	Fibrinogen alpha chain
1486.65	38.5	V.SETESRGSESGIFT.N	Fibrinogen alpha chain
1486.67	96.9	V.SETESRGSESGIFT.N	Fibrinogen alpha chain
1701.74	35.8	V.SETESRGSESGIFTNT.K	Fibrinogen alpha chain
1701.75	93.3	V.SETESRGSESGIFTNT.K	Fibrinogen alpha chain
2045.90	48.3	V.SETESRGSESGIFTNTKES.S	Fibrinogen alpha chain
2045.93	135.2	V.SETESRGSESGIFTNTKES.S	Fibrinogen alpha chain
1507.82	62.8	V.IGPDGHKEVTKEVV.T	Fibrinogen alpha chain
3169.31	45.4	T.SYNRGDSTFESKSYKMADEAGSEADHEGT.H	Fibrinogen alpha chain
3494.41	122.7	T.SYNRGDSTFESKSYKMADEAGSEADHEGTHST.K	Fibrinogen alpha chain
4043.66	33.2	T.SYNRGDSTFESKSYKMADEAGSEADHEGTHSTKRGHA.K	Fibrinogen alpha chain
2286.01	143.9	T.SYNRGDSTFESKSYKMADEA.G	Fibrinogen alpha chain
2561.09	67.5	T.SSTSYNRGDSTFESKSYKMADEA.G	Fibrinogen alpha chain
3769.54	67.5	T.SSTSYNRGDSTFESKSYKMADEAGSEADHEGTHST.K	Fibrinogen alpha chain
4886.25	33.4	T.SSTSYNRGDSTFESKSYKMADEAGSEADHEGTHSTKRGHAKSRPV.R	Fibrinogen alpha chain
1477.67	77.9	T.SYNRGDSTFESKS.Y	Fibrinogen alpha chain
1640.70	76.9	T.SYNRGDSTFESKSY.K	Fibrinogen alpha chain
1262.51	65.4	T.SYNRGDSTFES.K	Fibrinogen alpha chain
1899.86	94	T.SYNRGDSTFESKSYKM.A	Fibrinogen alpha chain
1970.87	121.4	T.SYNRGDSTFESKSYKMA.D	Fibrinogen alpha chain
1537.63	48.2	T.SSTSYNRGDSTFES.K	Fibrinogen alpha chain
1752.76	76.9	T.SSTSYNRGDSTFESKS.Y	Fibrinogen alpha chain
1915.83	83.5	T.SSTSYNRGDSTFESKSY.K	Fibrinogen alpha chain
2246.00	93.1	T.SSTSYNRGDSTFESKSYKMA.D	Fibrinogen alpha chain
2174.98	72.4	T.SSTSYNRGDSTFESKSYKM.A	Fibrinogen alpha chain
1574.87	40.3	T.SKGDKELRTGKEKV.T	Fibrinogen alpha chain
1675.91	36.8	T.SKGDKELRTGKEKVT.S	Fibrinogen alpha chain
2810.11	34.8	T.SESSVSGSTGQWHSESGSFRPDSPGSGN.A	Fibrinogen alpha chain
2340.10	38.2	T.NTKESSSHHPGIAEFPSRGKSS.S	Fibrinogen alpha chain
2427.18	37.9	T.NTKESSSHHPGIAEFPSRGKSSS.Y	Fibrinogen alpha chain
2590.19	107.6	T.NTKESSSHHPGIAEFPSRGKSSSY.S	Fibrinogen alpha chain
2590.21	81.6	T.NTKESSSHHPGIAEFPSRGKSSSY.S	Fibrinogen alpha chain
2677.16	125.5	T.NTKESSSHHPGIAEFPSRGKSSSYS.K	Fibrinogen alpha chain
2677.24	129.4	T.NTKESSSHHPGIAEFPSRGKSSSYS.K	Fibrinogen alpha chain
2253.07	64.6	T.NTKESSSHHPGIAEFPSRGKS.S	Fibrinogen alpha chain
2253.12	105.5	T.NTKESSSHHPGIAEFPSRGKS.S	Fibrinogen alpha chain
1075.54	32.8	R.RPHFFFPK.S	Clusterin
1069.47	35.8	I.DELFQDRF.F	Clusterin
1069.50	36.6	I.DELFQDRF.F	Clusterin
1317.58	32.2	I.DELFQDRFFT.R	Clusterin
1317.62	63.7	I.DELFQDRFFT.R	Clusterin
1791.84	82.5	I.HFHSPAFQHPPTEFI.R	Clusterin
2271.94	54.4	G.DQTVSDNELQEMSNQGSKYV.N	Clusterin
1043.59	51.6	G.VPPEVFTRV.S	Cathepsin G
932.51	30.7	S.FLPWIRT.T	Cathepsin G
1033.56	34.7	S.FLPWIRTT.M	Cathepsin G
1033.58	35.3	S.FLPWIRTT.M	Cathepsin G
2189.12	31.6	A.SEPGEAKKMEDKEKDNKLI.S	Bridging integrator 2
2170.11	99	V.DTKEAEGAPQVEAGKRLEEL.R	Caldesmon
2610.16	37.8	N.TEEVPGSLCLRKFSCMFFGAVSSD.Q	Cell cycle checkpoint control RAD9B
1426.75	33.1	A.TVGSLAGQPLQERA.Q	Apolipoprotein E
2009.99	37.8	G.SLAGQPLQERAQAWGERL.R	Apolipoprotein E
2547.17	44.7	K.SWFEPLVEDMQRQWAGLVEKV.Q	Apolipoprotein E
2111.03	52.1	A.KVEQAVETEPEPELRQQT.E	Apolipoprotein E
2108.97	49.9	V.KDKFSEFWDLDPEVRPT.S	Apolipoprotein C-III
2109.00	112	V.KDKFSEFWDLDPEVRPT.S	Apolipoprotein C-III
1504.70	81.3	T.DGFSSLKDYWSTV.K	Apolipoprotein C-III
1947.85	34.1	R.GWVTDGFSSLKDYWSTV.K	Apolipoprotein C-III
1374.63	40	E.FWDLDPEVRPT.S	Apolipoprotein C-III
1590.71	40	F.SEFWDLDPEVRPT.S	Apolipoprotein C-III
1590.75	32.6	F.SEFWDLDPEVRPT.S	Apolipoprotein C-III
1227.58	39.5	F.WDLDPEVRPT.S	Apolipoprotein C-III
2058.96	35.3	K.DALSSVQESQVAQQARGWV.T	Apolipoprotein C-III
1980.89	44.3	K.DKFSEFWDLDPEVRPT.S	Apolipoprotein C-III
1980.92	64.6	K.DKFSEFWDLDPEVRPT.S	Apolipoprotein C-III
2689.35	74.1	A.TKTAKDALSSVQESQVAQQARGWVT.D	Apolipoprotein C-III
2588.25	137.9	A.TKTAKDALSSVQESQVAQQARGWV.T	Apolipoprotein C-III
2614.23	35	A.SLLSFMQGYMKHATKTAKDALSSV.Q	Apolipoprotein C-III
1913.94	41.7	A.SLLSFMQGYMKHATKTA.K	Apolipoprotein C-III
1842.87	35.9	A.SLLSFMQGYMKHATKT.A	Apolipoprotein C-III
1512.69	35.9	A.SLLSFMQGYMKHA.T	Apolipoprotein C-III
1464.71	34.5	I.FTDQVLSVLKGEE.-	Apolipoprotein C-II
1577.78	31.4	G.IFTDQVLSVLKGEE.-	Apolipoprotein C-II
2691.33	107.9	P.DVSSALDKLKEFGNTLEDKARELI.S	Apolipoprotein C-I
1634.87	86.4	T.GIFTDQVLSVLKGEE.-	Apolipoprotein C-II
2187.05	47.3	A.KDALSSVQESQVAQQARGWV.T	Apolipoprotein C-III
2516.12	58.6	A.SEAEDASLLSFMQGYMKHATKTA.K	Apolipoprotein C-III
2114.88	62.5	A.SEAEDASLLSFMQGYMKHA.T	Apolipoprotein C-III
1919.94	66	Y.ADEFKVKIDQTVEELR.R	Apolipoprotein A-IV
2614.23	44.4	V.SQKIGDNLRELQQRLEPYADQL.R	Apolipoprotein A-IV
1838.86	44.7	R.GNTEGLQKSLAELGGHLD.Q	Apolipoprotein A-IV
2599.21	144.9	R.GNTEGLQKSLAELGGHLDQQVEEF.R	Apolipoprotein A-IV
2755.31	42.1	R.GNTEGLQKSLAELGGHLDQQVEEFR.R	Apolipoprotein A-IV
2394.20	40.8	R.LTPYADEFKVKIDQTVEELR.R	Apolipoprotein A-IV
2573.32	46.1	L.KEEIGKELEELRARLLPHANEV.S	Apolipoprotein A-IV

3181.53	135.2	T.NTKESSSHHPGIAEFPSRGKSSSYSKQFT.S	Fibrinogen alpha chain
3456.66	92.3	T.NTKESSSHHPGIAEFPSRGKSSSYSKQFTSST.S	Fibrinogen alpha chain
1824.82	47.6	T.NTKESSSHHPGIAEFPS.R	Fibrinogen alpha chain
1824.84	55.2	T.NTKESSSHHPGIAEFPS.R	Fibrinogen alpha chain
1980.92	54.9	T.NTKESSSHHPGIAEFPSR.G	Fibrinogen alpha chain
2037.94	48.6	T.NTKESSSHHPGIAEFPSRG.K	Fibrinogen alpha chain
2037.95	54	T.NTKESSSHHPGIAEFPSRG.K	Fibrinogen alpha chain
2166.05	60.6	T.NTKESSSHHPGIAEFPSRGK.S	Fibrinogen alpha chain
2166.09	117.3	T.NTKESSSHHPGIAEFPSRGK.S	Fibrinogen alpha chain
2212.11	116.1	T.KESSSHHPGIAEFPSRGKSSS.Y	Fibrinogen alpha chain
2375.13	50.4	T.KESSSHHPGIAEFPSRGKSSSY.S	Fibrinogen alpha chain
2462.16	101	T.KESSSHHPGIAEFPSRGKSSSYS.K	Fibrinogen alpha chain
2718.23	77.6	T.KESSSHHPGIAEFPSRGKSSSYSKQ.F	Fibrinogen alpha chain
2966.43	146	T.KESSSHHPGIAEFPSRGKSSSYSKQFT.S	Fibrinogen alpha chain
1954.96	41.4	I.SASAEELRQRLAPLAEDV.R	Apolipoprotein A-IV
1927.89	52.7	K.SLAELGGHLDQQVEEFR.R	Apolipoprotein A-IV
1319.64	26.3	L.EPYADQLRTQV.N	Apolipoprotein A-IV
1258.53	43.6	L.GGHLDQQVEEF.R	Apolipoprotein A-IV
1414.66	48.3	L.GGHLDQQVEEFR.R	Apolipoprotein A-IV
1848.91	66.7	A.DEFKVKIDQTVEELR.R	Apolipoprotein A-IV
2607.28	73.2	A.DEFKVKIDQTVEELRRSLAPYA.Q	Apolipoprotein A-IV
1796.88	30	A.SAEELRQRLAPLAEDV.R	Apolipoprotein A-IV
1144.48	45.9	G.HLDQQVEEF.R	Apolipoprotein A-IV
1661.83	38.5	I.DQNVEELKGRLTPY.A	Apolipoprotein A-IV

APPENDIX II

Proteins Identified and Quantitated in the ECLIPSE A1ATD Shotgun Experiments

Protein	Scores	Peptide	114_116	#114_116	114_115	#114_115	114_117	#114_117
Complement component C9	107.2	1	0.29	1	0.38	1	0.57	1
Plasma serine protease inhibitor	47.6	1	0.47	1	0.38	1	0.29	1
Alpha-1-antitrypsin	472	7	0.49	6	0.41	7	0.47	7
Apolipoprotein(a)	52.5	1	0.52	1	0.57	1	1.04	1
Afamin	135.2	2	0.94	2	0.6	2	1.1	2
Complement C1r subcomponent-like protein	141.1	2	0.52	2	0.61	2	0.56	2
Vitamin K-dependent protein S	70.2	1	1.22	1	0.61	1	1.31	1
Plasma kallikrein	50.6	1	0.61	1	0.63	1	0.84	1
Carboxypeptidase N catalytic chain	30.3	1	0.67	1	0.66	1	0.84	1
Apolipoprotein A-I	303.5	4	1.18	4	0.69	4	0.75	4
Apolipoprotein A-IV	108.7	2	0.8	2	0.7	2	0.61	2
Voltage-dependent calcium channel subunit alpha-2/delta-1	36.8	1	1.02	1	0.71	1	0.98	1
Follistatin-related protein 1	47.8	1	0.82	1	0.73	1	0.79	1
CD5 antigen-like	572.7	7	0.58	6	0.78	7	0.79	6
Extracellular matrix protein 1	56.1	1	1.08	1	0.78	1	1.12	1
C-Myc-binding protein	34.9	1	1.09	1	0.79	1	0.85	1
Carboxypeptidase N subunit 2	215	3	0.82	3	0.81	3	1	3
Vascular cell adhesion protein 1	74.9	1	2.29	1	0.82	1	1.28	1
Lumican	152.6	3	0.93	3	0.84	3	1.16	3
Serotransferrin	4802.5	58	0.77	48	0.85	50	0.93	49
Coagulation factor XIII B chain	95.2	1	0.84	1	0.88	1	0.91	1
Alpha-2-macroglobulin	2153.9	28	1.37	22	0.9	22	1.91	22
ATP-binding cassette sub-family G member 2	33.6	1	0.73	1	0.9	1	0.98	1
Leucine-rich alpha-2-glycoprotein	136.3	2	1.55	2	0.9	2	2.01	2
Carboxypeptidase B2	210.7	2	1.4	2	0.91	2	1.44	2
CD44 antigen	46.4	1	0.59	1	0.93	1	1.05	1
Target of Nesh-SH3	31	1	1.79	1	0.96	1	1.55	1
Insulin-like growth factor-binding protein 3	162.6	2	1.57	2	0.99	2	1.62	2
Complement factor D	38.3	1	0.59	1	1.03	1	0.67	1
Hyaluronan-binding protein 2	57.3	1	1.6	1	1.04	1	1.84	1
Alpha-1-acid glycoprotein 2	382.5	7	0.77	6	1.05	7	0.83	6

Tetraspanin-14	31.1	1	2.46	1	1.05	1	1.56	1
Vitamin D-binding protein	119.9	2	1.41	2	1.06	2	1.26	2
Fibrinogen gamma chain	47.2	1	1.08	1	1.09	1	0.71	1
Fibulin-1	59.3	1	2.57	1	1.12	1	1.77	1
Clusterin	130	2	1.27	1	1.13	1	1.42	1
Attractin	102.1	2	3.02	2	1.14	2	2.49	2
Protein Z-dependent protease inhibitor	57.7	1	1.83	1	1.14	1	1.59	1
Protein AMBP	489.7	7	1.75	6	1.15	6	1.79	6
Neuronal growth regulator 1	75.7	1	1.85	1	1.16	1	1.96	1
Inter-alpha-trypsin inhibitor heavy chain H4	283.5	5	2.08	4	1.18	4	1.83	4
Syntaxin-12	37.8	1	1.39	1	1.19	1	1.78	1
Plastin-2	44.2	1	3.45	1	1.21	1	1.41	1
Apolipoprotein E	49	1	1.68	1	1.22	1	1.52	1
Lymphatic vessel endothelial hyaluronic acid receptor 1	73.6	1	1.88	1	1.22	1	1.43	1
Apolipoprotein B-100	345.7	5	2.36	4	1.23	4	2.26	4
Complement C3	92.4	1	1.45	1	1.24	1	1.42	1
Hepatocyte growth factor activator	231	4	2.16	4	1.26	4	2.23	4
Interleukin-1 receptor accessory protein	42	1	1.71	1	1.26	1	1.69	1
Sex hormone-binding globulin	77.9	1	2.29	1	1.27	1	2.27	1
Angiotensinogen	218.2	3	0.64	2	1.28	3	0.66	2
Dopamine beta-hydroxylase	31	1	0.89	1	1.3	1	2.22	1
Selenoprotein P	135.8	2	1.85	2	1.3	2	2.14	2
Kallistatin	105.1	2	4.11	2	1.31	2	4.21	2
Thyroxine-binding globulin	360.1	4	2.04	3	1.34	4	2.19	3
Vascular non-inflammatory molecule 3	42.2	1	1.31	1	1.35	1	1.28	1
Complement C1r subcomponent	90.6	1	2.36	1	1.39	1	1.96	1
L-selectin	54.9	1	3.85	1	1.4	1	3.29	1
Phosphatidylinositol-glycan-specific phospholipase D	84.4	1	1.38	1	1.44	1	1.22	1
Hepatocyte growth factor-like protein	188.5	3	2.26	3	1.47	3	2.31	3
Cell surface glycoprotein MUC18	78.2	1	1.17	1	1.5	1	2.2	1
Zinc-alpha-2-glycoprotein	173.8	3	1.85	3	1.55	3	1.48	3
Serum paraoxonase/arylesterase 2	36.6	1	0.79	1	1.58	1	0.52	1
Thrombospondin-4	68.2	1	1.44	1	1.58	1	1.62	1
Bone marrow proteoglycan	47.7	1	1.58	1	1.6	1	1.44	1

Tetranectin	237.4	2	2.33	2	1.6	2	2.08	2
Fibrinogen alpha chain	142.3	1	2.91	1	1.69	1	4.37	1
Alpha-1-acid glycoprotein 1	277.3	5	1.37	5	1.77	5	0.78	4
Complement C1s subcomponent	111.4	1	2.93	1	1.92	1	3.34	1
Galectin-3-binding protein	59.5	1	1.83	1	2.03	1	3.87	1
Complement C2	277.1	4	2.9	4	2.22	4	4.43	4
Coagulation factor V	55.6	1	3.64	1	2.34	1	3.33	1
Laminin subunit alpha-2	54.1	1	1.98	1	2.35	1	2.18	1
Corticosteroid-binding globulin	218.5	3	6.27	3	2.43	3	5.54	3
Pigment epithelium-derived factor	106.2	1	8.62	1	3.38	1	9.29	1
Serum albumin	9759.6	120	0.59	100	0.78	109	0.59	102
Haptoglobin	755	11	0.66	11	1.05	11	0.82	11

Proteins Identified and Quantitated in the EXACTLE Shotgun Experiments

Protein	Scores	Peptides	114_116	#114_116	114_115	#114_115	114_117	#114_117
Complement C2	185.8	3	1.07	3	1.51	3	2.55	3
Pigment epithelium-derived factor	197	4	1.23	4	1.12	4	2.45	4
Insulin-like growth factor-binding protein complex	81.3	2	1.13	2	1.14	2	2.03	2
Cystatin-A	55.2	1	1.31	1	4.22	1	2.28	1
Zinc-alpha-2-glycoprotein	595.8	10	1.95	8	1.63	8	2.98	8
Clusterin	206.6	3	1.31	2	1.34	2	1.85	2
Neural cell adhesion molecule L1	42.4	1	1.22	1	1.32	1	1.72	1
Insulin-like growth factor-binding protein 2	108.4	2	1.2	2	1.45	2	1.63	2
Receptor-type tyrosine-protein phosphatase eta	103.3	1	1.32	1	1.03	1	1.79	1
Neurogenic locus notch homolog protein 2	89.8	1	1.16	1	0.97	1	1.5	1
Glutathione peroxidase 3	34.8	1	1.44	1	1.67	1	1.79	1
Biotinidase	84.6	1	0.97	1	1.24	1	1.2	1
Fibrinogen gamma chain	35.2	1	1.08	1	1.49	1	1.31	1
Di-N-acetylchitobiase	43.5	1	0.99	1	1.04	1	1.2	1
Tetranectin	147.2	2	1.33	1	0.55	1	1.53	1
Insulin-like growth factor-binding protein 3	36.3	1	1.41	1	1.59	1	1.58	1
Angiotensinogen	257.5	3	0.87	3	0.5	3	0.97	3
Aminopeptidase N	32.6	1	1.31	1	1.38	1	1.44	1
Protein S100-A14	79.7	1	1.47	1	1.32	1	1.61	1
Apolipoprotein B-100	40.2	1	0.93	1	1.26	1	1	1
Insulin-like growth factor II	61.4	1	1.34	1	1.13	1	1.42	1
Platelet basic protein	197.2	3	1.13	3	1.35	3	1.19	3

Hepatocyte growth factor activator	268.4	4	1.58	4	1.62	4	1.65	4
Inositol polyphosphate 5-phosphatase CRL-1	67.8	2	1.54	1	1.93	1	1.59	1
Interleukin-1 receptor accessory protein	39.4	1	1.38	1	1.18	1	1.4	1
Vasorin	38.1	1	1.12	1	1.51	1	1.13	1
Leucine-rich alpha-2-glycoprotein	355	8	1.27	8	1.27	7	1.28	7
L-selectin	280	4	1.32	4	1.97	4	1.33	4
Alpha-2-macroglobulin	323.4	5	1.08	5	0.95	5	1.07	5
Alpha-1-acid glycoprotein 1	120.9	3	1.07	2	1.51	2	1.05	2
Actin, cytoplasmic 1	38.1	1	1.14	1	1.15	1	1.1	1
Pregnancy zone protein	116.1	2	1.63	2	1.18	2	1.57	2
Protein EMSY	35.4	1	1.4	1	1.76	1	1.32	1
Protein AMBP	509.9	7	1.47	5	1.25	5	1.37	5
Cholinesterase	90.8	2	1.28	2	1.71	2	1.18	2
Vascular cell adhesion protein 1	41.9	1	1.52	1	1.12	1	1.39	1
Pantetheinase	122.6	3	1.66	2	1.73	2	1.51	2
Tigger transposable element-derived protein 6	32.4	1	3.42	1	3.07	1	3.1	1
Ig delta chain C region	105.6	2	0.8	2	1.09	2	0.7	2
Immunoglobulin J chain	173.4	2	0.99	1	1.02	1	0.86	1
Lactotransferrin	37.3	1	1.49	1	1.18	1	1.28	1
Thyroxine-binding globulin	578.1	8	1.08	7	0.93	7	1.09	7
Dynein heavy chain 12, axonemal	32.1	1	1.75	1	1.23	1	1.44	1
Ig alpha-2 chain C region	72.5	2	1.06	2	1.45	2	0.85	2
DnaJ homolog subfamily C member 7	30.6	1	1.61	1	1.3	1	1.28	1
Serum albumin	1643.2	23	1.11	13	1.23	14	1.14	15

Extracellular matrix protein 1	116.8	3	1.97	3	1.41	3	1.51	3
Complement C1r subcomponent-like protein	69.4	2	1.4	2	1.42	2	1.02	2
Catalase	112.6	2	1.25	1	1.83	1	0.91	1
C-Myc-binding protein	34.3	1	5.08	1	3.59	1	3.65	1
Ig mu chain C region	227.2	4	0.85	4	1.06	4	0.61	4
Peptidase inhibitor 16	109.8	2	2.05	2	2.1	2	1.42	2
Attractin	127.5	2	1.16	2	1.4	2	0.79	2
Putative macrophage-stimulating protein MSTP9	32.8	1	1.38	1	1.41	1	0.93	1
Corticosteroid-binding globulin	132	2	1.56	2	1.1	2	1.04	2
Serotransferrin	609.2	9	1.11	9	1.03	9	0.74	9
Alpha-1-antitrypsin	121.8	2	1.6	2	1.95	2	0.46	2